Cross-Immunity in Multi-Strain Infectious Diseases

Chamchod, Farida

Award date:
2010

Awarding institution:
University of Bath

Cross-immunity in multi-strain infectious diseases

submitted by

Farida Chamchod

for the degree of Doctor of Philosophy

of the

University of Bath

2010

Cross-immunity in multi-strain infectious diseases

Farida Chamchod

SUMMARY

The goal of this study is to try to understand multi-strain diseases with the presence of cross-immunity by using mathematical models and other mathematical tools. Cross-immunity occurs when a host who is exposed to one disease, or one strain of a disease, develops resistance or partial resistance to related diseases or strains. It is an important factor in the epidemiology of diseases prone to mutation. This work includes modelling influenza in both presence and absence of controls. It also includes modelling malaria when cross-species immunity is present. In addition, vector-bias of mosquitoes to infected humans is also studied in the single-strain malaria model.

Contents

Chapter 1

Introduction

Public health has been challenged by the reemergence of infectious diseases for decades. The pathogens mutate to evade host immunity which is acquired from previous infection, vaccination or in response to antiviral drugs. Pathogen mutations are found commonly in many reemerging infectious diseases such as: 1) measles (Cattaneo et al., 1988), 2) hepatitis B (Carman et al., 1990; Sato et al., 1995; Chen and Oon, 2000), 3) HIV (Eron et al., 1998), 4) West Nile virus (Ebel et al., 2001), 5) pertussis (Cassiday et al., 2000; Weber et al., 2001), 6) malaria (Gupta, Trenholme, Anderson and Day, 1994), and 7) influenza (Palese and Young, 1982; Webster, 1998).

A determinant of epidemic behaviour relates to time scale of infection dynamics and replenishment of susceptible hosts so that the epidemiological distinction is between fast infections and persistent infections (Gog and Grenfell, 2002). Conversely, phylogenic patterns are affected by natural selection arising from cross-immunity and neutral epidemiology processes such as spatial population separation. Pathogen strains and phylogenic lineages are produced by mutation, and their survival depends upon the epidemiological and immunological forces (Grenfell et al., 2004). Consequently, RNA viruses are categorized as follows: 1) short infections with strong cross-immunity (e.g. measles), 2) short infections with partial cross-immunity (e.g.influenza A), 3) infections with immune enhancement (e.g. dengue), and 4) persistent infections (e.g. HIV, HCV).

There are three types of influenza viruses A, B, and C. Influenza A is additionally classified by subtype on the basis of the two main surface glycoproteins haemagglutinin (HA) and neuraminidase (NA). Subtypes currently circulating in the human population include H1N1, H2N2, and H3N2 viruses. Subtypes are further classified by strains.

Antigenic variation in influenza A is driven by two important mechanisms called antigenic shift and drift. Antigenic shift generates a new subtype; antigenic binding sites are very different in different subtypes, so that immunity gained to strains of one sub-

type is virtually useless against strains of another (Webster et al., 1992). The major shift is frequently contributed by genetic reassortment or the mixing between genetic material between different strains (Holmes et al., 2005; Nelson and Holmes, 2007; Carrat and Flahault, 2007). The new viral subtype is normally associated with pandemics. The pandemic influenza viruses of 1957 (H2N2) and 1968 (H3N2) arose through reassortment between human and avian viruses, while the Spanish flu virus of 1918 (H1N1) appears to be entirely derived from an avian source (Belshe, 2005). The pandemic flu virus of 2009 (H1N1) contains genes from diverse strains of influenza originating in humans, birds, and pigs (Smith et al., 2009). On the other hand, we shall concern with antigenic drift, which generates a new strain by gradually changing the composition of the antigenic sites by point mutations. The new virus is normally responsible for an annual epidemic. Gupta et al. (1996, 1998) give the concept of a cluster of strains as a collection of independently transmitted strains with nonoverlapping repertoires of dominant polymorphic determinants that organize themselves. Although a point mutation always produces a new strain that has the same distance away in genotype space, the distance in antigenic space is variable (Smith et al., 2004; Koelle et al., 2006). Moreover, there is higher rate of antigenic evolution between clusters than within clusters. Antigenic evolution is punctuated while genetic evolution is more continuous. Because the new strain from antigenic drift process is not very different from the ancestor, host immune system might recognize it via the mechanism called cross-immunity. Some evidences show that cross-immunity plays an important roles between getting infected with the different strain from previous infection(s) (Larson et al., 1978; Davies et al., 1984). However, cross-immunity between subtypes has no clear pattern and is low (Frank et al., 1983; Sonoguchi et al., 1985).

Cross-immunity occurs when a host who is exposed to one disease, or one strain of a disease, develops resistance or partial resistance to related diseases or strains. It is an important factor in the epidemiology of diseases prone to mutation (Larson et al., 1978; Davies et al., 1984). It can act in many ways such as: 1) reducing susceptibility when hosts get infected with one strain and become less susceptible to other similar strains, 2) reducing infectivity during subsequent infections with similar strains from previous infection, and 3) polarizing immunity when only some individuals acquire complete immunity to certain strains from previous infection while others gain no immunity. Cross-immunity is high between different strains in the same subtype while it is very low if they are from different subtypes (Frank et al., 1983; Sonoguchi et al., 1985). In influenza A, cross-immunity between different strains can be estimated by the distance between them on the antigenic space.

Mathematical epidemiological models have often been used to study the dynamics of microparasites in a host population (Kermack and McKendrick, 1927; Becker, 1978;

Anderson and May, 1991; Herbert, 2000; Grenfell et al., 2001). It is now known that in some infectious diseases modelling a single pathogen strain that reduces lifelong immunity is not enough to explain their epidemics. Hence, several types of models have been developed to account for multi-strain diseases: for instance, models under a competitive exclusion where the strain with a maximum basic reproductive ratio outcompete others and survive in the host population (Bremermann and Thieme, 1989), models for superinfection in which one strain of a pathogen displaces another in an infected host (Nowak and May, 1994), models for coinfection which coexistence of different strains in the same host is possible (May and Nowak, 1995) , and cross-immunity models in which getting infected with one strain may protect the host from certain related strains (Castillo-Chavez et al., 1989; Gupta et al., 1996; Andreasen et al., 1997; Feng and Velasco-Hernandez, 1997; Gupta et al., 1998; Lin et al., 1999; Gog and Swinton, 2002; Gog and Grenfell, 2002; Kamo and Sasaki, 2002; Lin et al., 2003; Restif and Grenfell, 2006*a*; Adams and Sasaki, 2007). In this work, we are particularly interested in modelling multi-strain diseases with cross-immunity. Models of cross-immunity can be separated into at least two types: 1) history-based models in which hosts are categorized by their immune memory (Gupta, Trenholme, Anderson and Day, 1994; Andreasen et al., 1997; Gupta et al., 1998), and 2) status-based models in which hosts are categorized by their current immune status (Gog and Swinton, 2002; Gog and Grenfell, 2002). Many models in this work are based on the latter.

Controlling diseases is important for public health, to reduce the loss from infections and try to stop the the spread of the diseases. Several methods are used in controlling infectious diseases, such as vaccination, isolation, applying drugs and treatment. In this work, we concentrate on only the first two strategies and the combination between them. Vaccination is one of the most efficient ways to control infectious diseases. The most successful example is smallpox which has been completely eradicated in all countries. The aim of vaccination is to reduce the prevalence of the diseases and decrease susceptibility of a population. However, vaccines against highly mutable viruses such as influenza have to be reformulated annually to control the disease. Some examples of modelling multi-strain diseases with vaccination are as follows: Gupta et al. (1998); Restif and Grenfell (2006*b*); Raimundo et al. (2007); Gandon and Day (2007); Martcheva et al. (2008); Billings et al. (2008). Isolation is used to prevent infected individuals from further contacts and subsequent transmissions to other individuals. It is normally primarily used to control the disease when it suddenly emerges or reemerges. However, the disadvantages of isolation are the difficulty of detecting infected individuals and the cost of isolation and treatment. Although multi-strain models have been developed frequently, models including isolation are still scant (Nuno et al., 2005, 2007).

According to the characteristics of the diseases, we separate the studies of modelling

multi-strain diseases into two different chapters (2&3), modelling directly transmitted multi-strain diseases and modelling vector-borne diseases. Other types of multi-strain diseases such as sexually transmitted diseases will be roughly mentioned in the literature review part, which is mainly divided into two parts, modelling multi-strain diseases with and without controls. The studies of control strategies in multi-strains models can be found in Chapter 4. Lastly, we summarize all this work in Chapter 5.

1.1 Literature review

1.1.1 Modelling multi-strain diseases

Modelling cross-immunity

In this part, we introduce several models of cross-immunity from previous authors. Our work is developed from some models we mention here.

Gupta et al. (1996) created a model for genetic exchange of a sexually reproducing pathogen population, *Neisseria meningitidis*, in the human hosts. It is assumed that a locus encodes a set of dominant immunogens. A strain is defined by its alleles at a small number of loci instead of by its entire genotype. Each locus consists of alleles and each combination of alleles generates a particular antigenic type. The model is more general than this, but let us assume that there are two dominant loci each with two alleles, four possible types of strains are ay, ax, bx, by, ranged as strain 1-4, where a and b are alleles of the first locus, and x and y are alleles of the second locus and a set of nonoverlapping variants such as $\{ax, by\}$ is called a discordant set. Immunity is rendered not only to a given strain but also partially to other strains sharing any of the relevant determinants. Hence, infection with strain ax will limit the transmission of strains ay and bx, but will not affect the transmission of by. Transmission of these strains is reduced by a factor γ for individuals who have been exposed to strains sharing alleles with i but not i itself. Strains that do not share alleles are assumed not to interfere with each other's transmission. Hence, cross-immunity acts through reduced transmission. For simplicity, in the model the authors assume that an individual enters the immune and infectious classes simultaneously upon infection and the immunity is lifelong, so that losses from the immune categories occur at the same rate as mortality. The model is described by the following equations

$$\begin{aligned} \dot{z_i}(t) &= \lambda_i(1 - z_i) - \mu z_i, \\ \dot{y_i}(t) &= \lambda_i(1 - z_i)(1 - \gamma(1 - \phi_i)) - \sigma y_i \end{aligned}$$

for $i \in \{1,2,3,4\}$ and where z_i and y_i denote the proportion of the hosts who are immune to strain i and are infectious with strain i respectively. Note that class y_i is a subset of class z_i and classes y_i and y_j, z_i and z_j may overlap. Parameters $1/\mu$ and $1/\sigma$ denote, respectively, the life expectancy and the average duration of infectiousness of the host. The per capita force of infection for strain i is denoted by λ_i and can be explicitly formulated as a linear combination of the probability of a set of strains coinfecting a host multiplied by the fraction of the reluctant progeny that is likely to be of genotype i. The factor γ represents the degree of cross-protection which reduces the transmission of strains. Note that $\phi_i = \prod_{j\sim i}(1-z_j)$ with j denoting any strain that shares alleles with i. This is an SIR model with the S class omitted. It is a history-based model in which the partial protection affects all individuals with a given history equally. However, it can be adjusted to a status-based approach by assuming the set of epitopes that the host immune system can recognize. If $\gamma = 1$, one set of discordant strains will dominate against other strains. By assuming that four strains are circulating and have the same reproductive number, an asymmetric equilibrium is obtained. On the other hand, when cross-protection is absent, a symmetric equilibrium arises. A critical value of γ where the symmetric equilibrium becomes unstable when γ exceeds it is found in terms of the basic reproductive ratio (β_i/σ). Also, their result demonstrate that antigens that elicit the strongest immune response (so having a strongest impact on transmission success) are organized by immune selection acting within the host population into sets of nonoverlapping variants.

In a later paper, Gupta et al. (1998) adjusted their model in order to show that pathogens with antigens that do not elicit an immune response that is strong enough to induce a discrete stable strain structure may exist as a set of strains exhibiting cyclical or chaotic fluctuations in frequency over time. A new compartment w_i which is the proportion of individuals immune to any strain j that shares alleles with strain i is introduced. Previously, their model compartments are individually separated according to the strain from the combination of alleles between loci. In this work, all the strains that share alleles with strain i are grouped together. Cross-immunity only reduces transmission to the nondiscordant strain j. The model is with respect to strain i from a set of pathogen strains defined by n loci, each of which consists of m alleles, and it is as follows

$$\begin{aligned}
\dot{z}_i(t) &= (1-z_i)\lambda_i - \mu z_i, \\
\dot{w}_i(t) &= (1-w_i)\textstyle\sum_{j\sim i}\lambda_i - \mu w_i, \\
\dot{y}_i(t) &= [(1-w_i)+(1-\gamma)(w_i-z_i)]\lambda_i - \sigma y_i
\end{aligned}$$

Again, $j \sim i$ means that j shares alleles with i, i.e. j and i are non-discordant. In the model, immunity to a strain i reduces the probability of transmission of a nondiscordant strain j by a factor $(1-\gamma)$. The system with different value of γ gives three types of dynamical behaviours; 1) all strains coexist in the host population with

stable abundance when γ is low 2) one discordant set of strains dominates the other when γ is high and 3) cyclical or chaotic strain structure arises for an intermediate value of γ.

In both models, an assumption that the concordance is independent of the number of loci that have identical alleles is made. Consequently, genotypes sharing only one variant are assumed to compete to the same extent as genotypes sharing several variants. Recker and Gupta (2005) construct a model that captures the chances of a pathogen achieving transmission depending on the number of variants that the host has already encountered. Cross-immunity is now dependent on the extent to which strains share alleles or epitope regions with each other. From the study, it results that immune selection cause pathogen populations to self-organize into sets with a minimum degree of overlap between their members.

According to the pattern of influenza epidemics and many experiments in vitro and vivo supporting the idea of partial immunity, Andreasen et al. (1997) created a model that describes the effect of a change in the prevalence of the strains and the selective forces. The model includes the immunological history by dividing the population into classes, so this is the history-based model. It is an SIR-model of n interacting strains. Let $\mathcal{K} = \{1, 2, 3, \ldots, n\}$ be the set of all possible strains and let $S_{\mathcal{L}}$ denote the number of individuals that are currently uninfected but have previously been infected by the strains in the set $\mathcal{L} \subseteq \mathcal{K}$. Similarly, $I^i_{\mathcal{L}}$ represents the number of individuals currently infected by strain i who have previously recovered from infection with a strain in $\mathcal{L}$. The force of infection of virus type i is modelled by

$$\Lambda^i = \beta_i \sum_{\mathcal{L} \subseteq \mathcal{K} \setminus i} I^i_{\mathcal{L}},$$

where β_i is the transmission rate of viral type i. Cross-immunity acts to reduce susceptibility in the model. Also it is assumed that infection by strain i confers perfect and permanent immunity to strain i itself. Susceptibility to strain i of individuals with immune history $\mathcal{L}$ is reduced by a cross-immunity factor $\sigma^i_{\mathcal{L}}$ which depends on the distance between i and the set $\mathcal{L}$, to be defined later. For the class $S_{\emptyset}$,

$$\dot{S}_{\emptyset} = b - \mu S_{\emptyset} - \sum_{j \in \mathcal{K}} \Lambda^j S_{\emptyset},$$

and for $S_{\mathcal{L}}$ where $\mathcal{L} \neq \emptyset$

$$\dot{S}_{\mathcal{L}} = \sum_{j \in \mathcal{L}} \nu I^j_{\mathcal{L} \setminus j} - \sum_{i \notin \mathcal{L}} \sigma^i_{\mathcal{L}} \Lambda^i S_{\mathcal{L}} - \mu S_{\mathcal{L}}.$$

Similarly, for the class $I^i_{\mathcal{L}}, \mathcal{L} \subset \mathcal{K}, i \notin \mathcal{L}$

$$\dot{I^i_{\mathcal{L}}} = \sigma^i_{\mathcal{L}} \Lambda^i S_{\mathcal{L}} - (\mu + \nu) I^i_{\mathcal{L}}.$$

Note that b is the overall birth rate, μ is the per capita death rate, and ν is the recovery rate. Since the simultaneous infection with more than one strain is rare in influenza, coinfection is not allowed to occur in the model.

The system may have many boundary equilibria. Only the disease-free equilibrium is easy enough to study by linearisation. It is found that the disease-free equilibrium changes its stability when the largest r_i, where $r_i = \beta_i N/(\mu + \nu)$, is equal to 1. A threshold above which a new strain i can invade other prevalent strains is

$$r_i \sum_{\mathcal{L} \subseteq \mathcal{K} \setminus i} \sigma^i_{\mathcal{L}} S^\dagger_{\mathcal{L}} > 1$$

where $(S^\dagger_{\mathcal{L}}, I^\dagger_{\mathcal{L}})$ is an equilibrium with the strain i being absent. The authors assume that the viral strains can be ordered around the circle so as to indicate their degree of relatedness. For simplicity, it is assumed that $\sigma^i_{\mathcal{L}} = 0$ if $i \in \mathcal{J}$, $\sigma^i_{\mathcal{L}} = \sigma$ if $i + 1 \in \mathcal{L}$ or $i - 1 \in \mathcal{L}$ and $\sigma^i_{\mathcal{L}} = 1$ elsewhere. In addition, strain 1 and strain n are assumed to be neighbours so that the relatedness of strain i and j can be defined by the distance $|i-j| \mathrm{mod} n$. To do bifurcation analysis additional assumptions are made by focusing on a symmetric cross-protection and a symmetric transmission rate. For example, in the latter case, when $n = 4$, it is assumed that strain 1 and 3 have the same transmission rate and the transmission rate of strain 2 and 4 are the same. The result is that sustained oscillations can occur when $n \geq 4$.

Since the model generally represents the population based on immune history, it may be adjusted to model the effect of cross-immunity in other ways. Firstly, if cross-immunity only induces cross-protection to related strains for some people while others acquire nothing from the infections (polarised immunity), denote $C(\mathcal{L}, \mathcal{J}, i)$ to be a probability distribution that gives the probability that an individual who has immune history $\mathcal{L}$ and recovers from infection with strain i will acquire complete immunity to the strains in $\mathcal{J}$. Then, the flow out of the class $I^i_{\mathcal{L}}$ is distributed among $\mathcal{S}_{\mathcal{J}}$ and is determined by

$$\sum_{j \in \mathcal{L}, i \notin \mathcal{L}} C(\mathcal{L}, \mathcal{J}, i) I^i_{\mathcal{L}}$$

where $\sigma^i_{\mathcal{L}} = 1$ for all i and $\mathcal{L}$. Secondly, when cross-immunity reduces infectivity during subsequent infections with related strains, the force of infection can be determined by

$$\Lambda^i = \sum_{\mathcal{L} \subseteq \mathcal{K} \setminus i} \beta^i_{\mathcal{L}} I^i_{\mathcal{L}},$$

where $\beta^i_{\mathcal{L}}$ is the infectivity of individuals who are infected with strain i and have immune history $\mathcal{L}$.

Following Andreasen's work, Lin et al. (1999) suggested that a Hopf bifurcation is even possible with only three strains in a linear chain configuration. They assume that there is no reciprocal cross-immunity between the strain 1 and 3, and both of them confer the same immunity to strain 2. Besides, they assume that there is no additional protection from having been infected by both strains. It is assumed that getting infected with strain 2 gives full protection against strains 1 and 3. Although the system is similar to the previous work, the analysis is done in a different way. It is done by folding subclasses into plus-minus variables and reducing variables by making the assumption of the complete immunity to strains 1 and 3 of individuals previously infected with strain 2 ($\sigma^1_{\{2\}} = \sigma^3_{\{2\}} = 0$).

Gog and Swinton (2002) introduced a status-based model with polarized immunity which susceptible individuals are categorized by their immune status to explain the dynamics of the host population. In their model, $S_{\mathcal{J}}$ represents the proportion of hosts that are completely immune to the strains in the set $\mathcal{J}$, whether they are infected or susceptible to all other strains. Multiple infections are allowed. The birth rate and death rate are defined by μ. A parameter $C(\mathcal{L}, \mathcal{J}, i)$ is introduced to represent the proportion of hosts that recover to a state $\mathcal{J}$, having started in state $\mathcal{L}$ and been infected by strain i. Also in the model, I_i is the proportion of individuals infected with strain i; β_i is a transmission rate for strain i; and ν_i is a recovery rate from infection with strain i. The model is shown below

$$\begin{aligned} \dot{I}_i &= \beta_i I_i \textstyle\sum_{\mathcal{J}: i \notin \mathcal{J}} S_{\mathcal{J}} - \nu_i I_i - \mu I_i, \\ \dot{S_{\mathcal{J}}} &= \textstyle\sum_{i,\mathcal{L}} C(\mathcal{L}, \mathcal{J}, i) \beta_i I_i S_{\mathcal{L}} - \sum_{i \notin \mathcal{J}} \beta_i I_i S_{\mathcal{J}} - \mu S_{\mathcal{J}} + \mu \delta_{\mathcal{J},\emptyset}, \end{aligned}$$

where $i = 1, 2, 3, \ldots, n$, $\mathcal{J} \subset \{1, 2, \ldots, n\}$ and the function $\delta_{\mathcal{J},\emptyset}$ is 1 if $\mathcal{J} = \emptyset$ and zero otherwise. The model shows contrasting results from Andreasen's model. Hopf bifurcation and oscillations cannot occur in this model. Dawes and Gog (2002) had shown why the status-based model does not contain oscillatory dynamics and concluded that polarized immunity and implicit assumptions may be an important cause.

When the number of strains is increased, the number of dynamic variables grows rapidly. That situation is the main obstacle to study the dynamics of diseases. Hence, Gog and Grenfell (2002) developed a simple model based on the status-based formulation. The model is more tractable than previous one when the number of antigenic types is large. Rather than considering complex immune history, they consider the current immune status of the host. By integrating the assumption that cross-immunity is conferred by exposure even if immunity prevents the full disease from developing and the status-based formation with polarized immunity, only one variable is needed

to explain the host with respect to each strain. The model is described by the following equations for $i = 1, 2, 3, \ldots, n$

$$\begin{aligned} \dot{I}_i &= \beta_i S_i I_i - \nu_i I_i - \mu I_i, \\ \dot{S}_i &= \mu - \textstyle\sum_j \beta_j S_i \sigma_{ij} I_j - \mu S_i, \end{aligned}$$

where μ denotes birth and death rate; β_i is the transmission rate; ν_i is the rate of recovery; and lastly σ_{ij} denotes the chance an infection by strain j will give immunity to strain i. A single strain is considered as being located at each point in a strain space. Full details of how to derive this model from the Gog & Swinton model can be found in the next chapter. The authors considered two types of strain spaces, a linear strain space and a two-dimensional strain space in rectangular shape. It is found that the relative length of host lifetime and the host immunity can affect the patterns of coexistence. In the linear strain space, two patterns of infections are observed: a prolonged infection in which clusters are built up and distributed across the strain space; and a short infection which is seen as a series of jumps, hopping along the space. In two-dimensional strain space, the dominant strain move along the axis as a jumping series though it is not clearly seen like the linear strain space.

Kamo and Sasaki (2002) introduced the effect of seasonal forcing and the effect of cross immunity to an SIR model with two strains of pathogens. In particular, they investigated the pattern of period-doubling in the host density in echovirus disease. In the model, seasonality is introduced in terms of transmission rate:

$$\beta_i = \beta_i^0(1 + \delta \sin 2\pi t), \ i = 1, 2$$

where β_i^0 is the base transmission rate of strain i, and δ $(0 \leq \delta \leq 1)$ is the degree of seasonality. When the seasonality is small enough, the population shows an annual cycle. If it exceeds a certain threshold, 2-year, 4-year, etc. cycles will emerge. If the seasonality is sufficiently strong, the population shows chaotic behaviour. Moreover, the authors also found that in the two-strain model, the bifurcation diagrams shift more rapidly to chaos than in the single strain model if they increase the degree of seasonality.

Since a system of multiple strains with cross-immunity has a tendency to self-organise into groups or clusters, Calvez et al. (2005) investigated formation of clusters in ordered multi-strain systems. A three-compartment model is modified from Gupta et al. (1998) by considering several levels of cross-protection. Clusters can behave mainly in three different ways. First, the system may remain in homogeneous equilibrium if no structure is observed. Second, one cluster may dominate the others. Third, oscillation may arise when the clusters alternate recurrently in succession. Basically, the forma-

tion of clusters of discordant strains is expected. In an eight-strain system of three loci with two alleles, they found that it is possible to have at least two different clusters of nonoverlapping strains. Furthermore, they also found that the same cluster can arise in other models. For instance, both the Gog & Grenfell model (Gog and Grenfell, 2002) and the more complex Gog and Swinton model (Gog and Swinton, 2002) generate the same cluster formation which is in the same pattern as one of those in the Gupta model (Gupta et al., 1998).

Life-history variation and cross-immunity appear to be two important factors of pathogen evolution. Restif and Grenfell (2006*a*) integrated both factors together to study the dynamics of pertussis. If an endemic strain is already present, how those two factors affect the ability of a novel strain to invade and persist was studied. They found that if an invading strain has a much higher basic reproductive ratio than the prevalent one, competitive exclusion occurs. Otherwise, the system converges to a stable coexistence equilibrium.

Adams and Sasaki (2007) examine invasion of the third strain when first two strains are identical and coexist in the host population and how the emergence of the new strain is influenced by partial cross-immunity. Antigenic structure in cross-immunity function (linear, concave, convex) in term of antigenic distance on a one dimensional continuous antigenic space is investigated. A discontinuous cross-immunity function is further investigated in Adams and Sasaki (2009).

The other frameworks in modelling cross-immunity are a moving frame in immunity space (Pease, 1987; Casagrandi et al., 2006) in which immunity is waning with time according to the change of a new strain, the season-to-season drift (Andreasen, 2003; Boni et al., 2004), and the SIR with a one-dimensional drift model and mutation as a diffusion process (Lin et al., 2003).

Modelling multi-strain pathogens in vector-borne and sexually transmitted diseases

Vector-borne diseases are caused by viruses, bacteria, or protozoa and transmitted by biological agents or vectors. Mosquitoes are one of the most important vectors and carry infectious diseases such as malaria, dengue, yellow fever, and West Nile Fever. Other vectors include assassin bugs carrying Chagas disease and ticks carrying Lyme disease.

Modelling vector-borne diseases began with Ross (1911, 1916), followed by Macdonald (1952, 1957). In the Ross-Macdonald model, a host is assumed to be immune to further infection during the infection period only (SIS). Following it, models includ-

ing acquired immunity in hosts (SIR) were proposed by Dietz et al. (1974); Bailey (1975); Aron (1988). Some evidence shows that vector-borne diseases like malaria are antigenically diverse (Gupta, Trenholme, Anderson and Day, 1994). Gupta, Swinton and Anderson (1994) proposed a model encapsulating cross-immunity for two strains of malaria pathogens. Hosts are structured into four states: 1) x_0, immune to neither strain, 2) x_1, immune to strain 1, 3) x_2, immune to strain 2, and 4) x_3, immune to both strains. The symbols x_{I1} and x_{I2} represent infectious proportions to strains 1 and 2, respectively. Infectious states are nested within the immune compartments. Hence, x_{I1} and x_{I2} are subsets of x_1 and x_2, respectively. It is assumed that infected mosquitoes cannot be reinfected with a different strain of virus and do not recover, so mosquitoes are structured into three states: 1) y_0, susceptible to both strains, 2) y_1, infectious to strain 1, and 3) y_2, infectious to strain 2. With constant populations in both humans and mosquitoes, the model is described as follows

$$\begin{aligned}
\frac{dx_1}{dt} &= \lambda_1(1 - x_1 - x_3) - (c\lambda_2 + \mu)x_1, \\
\frac{dx_2}{dt} &= \lambda_2(1 - x_2 - x_3) - (c\lambda_1 + \mu)x_2, \\
\frac{dx_3}{dt} &= c(\lambda_1 x_2 + \lambda_2 x_1) - \mu x_3, \\
\frac{dx_{I1}}{dt} &= \lambda_1(1 - \Sigma_i x_i + cx_2) - sx_{I1}, \\
\frac{dx_{I2}}{dt} &= \lambda_2(1 - \Sigma_i x_i + cx_1) - sx_{I2}, \\
\frac{dy_1}{dt} &= ax_{I1}(1 - \Sigma_i y_i) - \mu_M y_1, \\
\frac{dy_2}{dt} &= ax_{I2}(1 - \Sigma_i y_i) - \mu_M y_2
\end{aligned}$$

where $\lambda_i = mab_i y_i$, and x_0 and y_0 may be found from $x_0 = 1 - x_1 - x_2 - x_3$, and $y_0 = 1 - y_1 - y_2$. In the model, μ is the natural death rate of the host population, m is the number of female mosquitoes per human host, a is the biting rate, b is the proportion of infected bites on the host that produces an infection, s is the rate of losing the capacity to produce infective gametocytes, and μ_M is the death rate of the vectors. The proportion c is the degree of cross-protection afforded by immunity to one strain; when c is unity, there is no cross-immunity; when c is zero, there is full cross-protection. As c decreases, the behaviour of independent strain transmission and coexistence increasingly changes to coupled behaviours. The strain with a lower transmissibility is taken over by the strain with a higher one. Oscillation is increased if cross-immunity between strains is strong and it is reduced by large differences in the transmission probabilities. From the result, the absence of cross-immunity tends to support a variety of strains which corresponds to the strain-specific immunity that an individual acquires to malaria parasites and malaria strains that have evolved mechanisms that act to reduce the degree of cross-immunity to avoid interactions with other strains that may lead to their elimination.

In the malaria models, cross-immunity may act to reduce the probability of the host

being infected by the related strains. However, for dengue virus, some evidences show that cross-reactive antibodies may act to enhance the severity of a subsequent infection by another strain and so lead to dengue shock syndrome and dengue hemorrhagic fever. Modelling antibody-dependent enhancement in dengue can be found in Feng and Velasco-Hernandez (1997); Ferguson et al. (1999); Esteva and Vargas (2003); Adams et al. (2006), for instance.

Sexually transmitted diseases such as gonorrhoea, chlamydia, genital warts, herpes, syphilis, and AIDS are transmitted via sexual contact. It has been suggested that males and females should be divided separately in modelling the diseases that are transmitted through sexual activity. Castillo-Chavez et al. (1996) introduced a heterosexual model to study a human population who get exposed to two different strains of gonorrhoea. A two-sex SIS model is used. Superscripts m and f denote the male and female populations, respectively. There are two groups of infectives: those infected with strain 1 and those infected with strain 2. The model is described as follows

$$\begin{aligned}
\dot{S^m} &= \tilde{\mu}^m - B^m - \mu^m S^m + \textstyle\sum_{i=1}^{2} \gamma_i^m I_i^m, \\
\dot{I_i^m} &= B_i^m - (\mu^m + \gamma_i^m) I_i^m, i = 1, 2, \\
\dot{S^f} &= \tilde{\mu}^f - B^f - \mu^f S^f + \textstyle\sum_{i=1}^{2} \gamma_i^f I_i^f, \\
\dot{I_i^f} &= B_i^f - (\mu^f + \gamma_i^f) I_i^f, i = 1, 2,
\end{aligned}$$

where

$$B_i^m = r^m(T^m, T^f) S^m \beta_i^f \frac{I_i^f}{T^f}, B_i^f = r^f(T^m, T^f) S^f \beta_i^m \frac{I_i^m}{T^m},$$

$$B^m = \frac{r^m(T^m, T^f) S^m}{T^f} \sum_{j=1}^{2} \beta_j^f I_j^f, B^f = \frac{r^m(T^m, T^f) S^m}{T^f} \sum_{j=1}^{2} \beta_j^m I_j^m.$$

In the model, $\tilde{\mu}^k, k = m, f$ represents the birth rate; μ^k denotes the natural death rate; γ_i^k is the recovery rate from strain i; β_i^k is the transmission rate of infection to strain i; and r^k as a function of T^m and T^f is the average rates of partner acquisition per male and female. With a behaviourally and genetically homogeneous population, coexistence is not possible unless certain assumptions are made. In contrast, in heterosexually mixing hosts coexistence is observed in many situations. A question whether a large proportion of women who are asymptomatic to gonorrhoea is a sufficient condition for coexistence was pointed out. Some example of other work in this area can be found in Castillo-Chavez et al. (1997, 1999); Li et al. (2003).

Superinfection and coinfection

Without considering transmission efficiency, hosts favour the lowest virulence strain of pathogen. When both virulence and transmission efficiency are linked, a trade-off

between host mortality and transmission efficiency exists. Consequently, hosts may support coexistence of multiple strains. By interaction between strains, there are two different patterns of coexistence; coinfection when hosts harbour infections of multiple strains of pathogen at one time, and superinfection when one strain with more virulence takes over a less virulent strain.

Superinfection is one strain of a pathogen displaces another in an infected host. Nowak and May (1994) developed a superinfection model such that a heterogeneous parasite population with a range of different virulences is considered. Under the assumptions that the more virulent strains can drive out less virulent strains and the infection of a host is dominated by a single parasite, a more virulent strain takes over a host infected by a less virulent strain. The model takes the form

$$\begin{aligned} \dot{x}(t) &= b - \mu x - x\sum_{i=1}^{n}\beta_i y_i, \\ \dot{y_i}(t) &= y_i(\beta_i x - \mu - \delta_i + s\beta_i \sum_{j=1}^{i-1} y_j - s\sum_{j=i+1}^{n}\beta_j y_j) \end{aligned}$$

where $i = 1, \ldots, n$; x represents uninfected hosts; y_i denotes infected individuals to strain i; b is the birth rate of uninfected hosts; μ is the natural death rate; s is the rate at which superinfection occurs; β_i is the transmission rate of strain i; and δ_i is the virulence of strain i. They conclude that: 1) superinfection shifts virulence of the pathogen to higher levels that are beyond the level that would maximize the basic reproductive ratio; and 2) it leads to a polymorphism of strains with several levels of virulence.

Coinfection is a term that indicates a stable coexistence of different strains of pathogens in the same host. Under the circumstance that there is no competition among different strains in the same host, host can harbour infection of multiple strains at one time. Mosquera and Adler (1998) proposed a coinfection model for two strains of pathogens with superinfection and single infection as limits. The coinfection model is described by

$$\begin{aligned} \dot{S}(t) &= (b-\mu)S - c_1 I_1 S - c_2 I_2 S - \epsilon_1 c_1 I_{12} S \epsilon_2 c_2 I_{12} S + \gamma_1 I_1 + \gamma_2 I_2, \\ \dot{I_1}(t) &= c_1 I_1 S - (k + \beta_1 + \gamma_1) I_1 + \epsilon_1 c_1 I_{12} S - a_2 c_2 I_1 I_2 + \gamma_{12} I_{12} - \epsilon_2 a_2 c_2 I_1 I_{12}, \\ \dot{I_2}(t) &= c_2 I_2 S - (k + \beta_2 + \gamma_2) I_2 + \epsilon_2 c_2 I_{12} S - a_1 c_1 I_1 I_2 + \gamma_{21} I_{12} - \epsilon_1 a_1 c_1 I_2 I_{12}, \\ \dot{I_{12}}(t) &= (a_1 c_1 + a_2 c_2) I_1 I_2 + (\epsilon_2 a_2 c_2 I_1 + \epsilon_1 a_1 c_1 I_2) I_{12} - (\gamma_{12} + \gamma_{21} + k + \beta_{12}) I_{12} \end{aligned}$$

For notations, S represents susceptible individuals; I_1, I_2, I_{12} denote infected individuals to strain 1, strain 2, and both strains, respectively; b is a birth rate; μ is a natural death rate; β_i denotes disease-induced mortality rate of strain i; γ_i denotes a recovery rate to strain i; c_i denotes transmission rate depending on the parasite's virulence; ϵ_i is a proportion to reduce infectiousness of doubly-infected individuals acting as strain i; and a_i is a proportion to reduce susceptibility to the other strain when infected with

strain i. The coinfection function is examined in three different shapes, discontinuous, piecewise continuous, and differentiable cases. A single infection model is derived by setting $a_1 = a_2 = 0$. From the model, to derive the superinfection model, it is assumed that the absence of doubly infected individuals is due to the rapid removal through recovery class or through enhanced mortality caused by the double infection itself. The equations becomes

$$\begin{aligned}
\dot{S}(t) &= -c_1 I_1 S - c_2 I_2 S + (r-k)S + \gamma_1 I_1 + \gamma_2 I_2, \\
\dot{I}_1(t) &= c_1 I_1 S - (k + \beta_1 + \gamma_1) I_1 - \delta I_1 I_2 - \sigma_{12} I_1 I_2, \\
\dot{I}_2(t) &= c_2 I_2 S - (k + \beta_2 + \gamma_2) I_2 - \delta I_1 I_2 - \sigma_{21} I_1 I_2.
\end{aligned}$$

The new parameters are δ, which is the difference between the per contact rate of transfer from I_1 to I_2 and the per contact rate of transfer from I_2 to I_1 and σ_{ij}, which is the mortality rate incurred when I_i individuals are infected with strain j. Conditions under which the coinfection and superinfection models allow more than one strain of parasites are studied. The authors found that the coinfection model has a propensity to favour more virulence and coexistence than the single infection, depending on two factors: 1) how close one is to the superinfection limit and 2) the shape of coinfection function. Other examples of the study of superinfection and coinfection are Gandon et al. (2001, 2002); Saldana et al. (2003); Iannelli et al. (2005); Boldin and Diekmann (2008).

1.1.2 Modelling multi-strain diseases with controls

Several management strategies have been used to control diseases, depending on the epidemiological characteristics of the pathogens. The aim is often to minimize the prevalence of the disease and ideally to reduce it to zero. Mathematical models provide a means to study the effectiveness of different strategies so as to understand the epidemiology of the disease and perhaps consequently help us to avoid the loss from its presence in the population.

Vaccinating newborns is an effective way to control many harmful diseases. For example, a vaccination model for a multi-strain disease is developed by Restif and Grenfell (2006*b*). The model is for studying immune evasion as a dynamic process for two strains of pertussis. Initially a single strain is present, controlled at a low endemic level by vaccination. A novel mutant strain is then introduced to which the vaccine offers limited protection, so as to investigate the circumstances under which the mutant strain can invade and persist. Both deterministic and stochastic frameworks were studied and the latter is highlighted in their work as it includes the possibility of extinctions of either strain. The vaccination programme is paediatric. The vaccine confers full protection

against strain 1 but partial protection against strain 2. The model is described as follows:

$$
\begin{aligned}
dS/dt &= \mu(1-p-S) - \beta S(I_1 + J_1 + I_2 + J_2 + I_{v2}) + \sigma(R_1 + R_2 + R) + \sigma_v V, \\
dI_1/dt &= \beta S(I_1 + J_1) - (\gamma + \mu) I_1, \\
dI_2/dt &= \beta S(I_2 + J_2 + I_{v2}) - (\gamma + \mu) I_2, \\
dR_1/dt &= \gamma I_1 - \beta(1-\theta) R_1(I_2 + J_2 + I_{v2}) - (\mu + \sigma) R_1, \\
dR_2/dt &= \gamma I_2 - \beta(1-\theta) R_2(I_1 + J_1) - (\mu + \sigma) R_2, \\
dV/dt &= \mu(p - V) - \beta(1-\tau) V(I_2 + J_2 + I_{v2}) - \sigma_v V, \\
dJ_1/dt &= \beta(1-\theta) R_2(I_1 + J_1) - \left(\tfrac{\gamma}{1-\nu} + \mu\right) J_1, \\
dJ_2/dt &= \beta(1-\theta) R_1(I_2 + J_2 + I_{v2}) - \left(\tfrac{\gamma}{1-\nu} + \mu\right) J_2, \\
dI_{v2}/dt &= \beta(1-\theta) V(I_2 + J_2 + I_{v2}) - \left(\tfrac{\gamma}{1-\eta} + \mu\right) I_{v2}, \\
dR/dt &= \gamma\left(\tfrac{J_1 + J_2}{1-\nu} + \tfrac{I_{v2}}{1-\eta}\right) - (\mu + \sigma) R,
\end{aligned}
$$

where S is the proportion of susceptible individuals to both strains, I_i is the proportion of primarily infected individuals with strain i, R_i is the proportion of immune individuals to strain i only, J_i is the proportion of secondarily infected individuals with strain i, V is the proportion of vaccinated individuals who are still immune to strain 1, I_{v2} is the proportion of vaccinated individuals who are infected by strain 2, and R is the proportion of immune individuals to both strains. Other parameters the model are as follows: β is the transmission rate, γ the recovery rate, μ the birth and death rate, p the vaccine coverage, σ the rate of loss natural immunity, σ_v the rate of loss vaccine immunity, θ the cross-protection conferred by primary infection (reduction in susceptibility), ν the cross-protection conferred by primary infection (reduction in infectious period), τ the cross-protection conferred by vaccination (reduction in susceptibility), and η the cross-protection conferred by vaccination (reduction in infectious period). Two conclusions are made: 1) the probability of persistence of a novel strain can be minimized by an intermediate level of cross-protection conferred by vaccination, and 2) it is lower in case cross-immunity acts to reduce the infectious period instead of susceptibility.

Isolation is one of the most effective ways to control diseases. It is focused only on infected individuals, not a large pool of susceptible individuals like vaccination. It can be applied instantaneously, while a vaccine against an emerging disease such as influenza may need at least six months to produce. However the disadvantage of isolation is to detect infectious individuals when symptoms are ambiguous. Isolation might be made more efficient by tracing and quarantining contacts of infected individuals.

An example of an isolation model of a multi-strain disease is given here is by Nuno et al. (2005), who introduced host isolation into a two-strain model of influenza under

various levels of cross-immunity between strains. In the model, individuals are separated into classes as follows; susceptible individuals (S); primarily infected individuals (I_i); isolated individuals with strain i (Q_i); recovered individuals from strain i (R_i); secondarily infected individuals (V_i); recovered individuals from both strains (W). The model takes the form

$$\begin{aligned}
\frac{dS}{dt} &= b - \sum_{i=1}^{2} \beta_i S \frac{(I_i+V_i)}{A} - \mu S, \\
\frac{dI_i}{dt} &= \beta_i S \frac{(I_i+V_i)}{A} - (\mu + \gamma_i + \delta_i) I_i, \\
\frac{dQ_i}{dt} &= \delta_i I_i - (\mu + \alpha_i) Q_i, \\
\frac{dR_i}{dt} &= \gamma_i I_i + \alpha_i Q_i - \beta_j \sigma_{ij} R_i \frac{(I_j+V_j)}{A} - \mu R_i, j \neq i, \\
\frac{dV_i}{dt} &= \beta_i \sigma_{ij} R_j \frac{(I_i+V_i)}{A} - (\mu + \gamma_i) V_i, j \neq i \\
\frac{dW}{dt} &= \sum_{i=1}^{2} \gamma_i V_i - \mu W \\
A &= S + W + \sum_{i=1}^{2} (I_i + V_i + R_i)
\end{aligned}$$

where A denotes the non-isolated individuals and σ_{ij} is the measure of the cross-immunity of a prior infection with strain i to an exposure with strain j. Other parameters are described as follows: b is the recruitment rate; β_i is the transmission rate of strain i; μ is the natural death rate; δ_i is the per capita isolation rate for strain i; γ_i is the per capita recovery rate from strain i; and α_i is the per capita rate at which an individual leaves the isolation class resulting from infection with strain i. Nuno et al. (2005) conclude that cross-immunity and isolation leads to sustained oscillations or periodic epidemic outbreaks. Moreover, the threshold condition for coexistence is possible even though the isolation basic reproductive ratio of one of the strains is below 1, resulting from the backward bifurcation.

In certain diseases like vector-borne diseases, control strategies can be applied not only to the host population but also to the vector population. For example, in malaria and dengue, the vectors are mosquitoes which transmit the diseases to hosts, so reducing the number of them by destroying their habitats, releasing sterile mosquitoes, using larvicide, and using insecticide are possible ways to control the disease. Larvicide is used to reduce the number of larvae while insecticide is used to eliminate adult mosquitoes (e.g. Yang and Ferreira (2008)).

Chapter 2

Modelling directly transmitted multi-strain diseases

In this chapter, we develop a model with host cross-immunity to a continuum of strains of influenza. The model is based on a status-based framework with polarized immunity assumption by Gog and Grenfell (2002). We first show how to derive the Gog and Grenfell model from the Gog and Swinton model (Gog and Swinton, 2002) to understand the concepts of the model we develop from. The status-based framework where hosts are described by their current immune status is applied to both models but, with an additional assumption that cross-immunity is conferred by exposure even if immunity prevents the full disease from developing, the number of equations in the Gog and Grenfell model is reduced drastically comparing with the Gog and Swinton model, and so the system becomes more tractable. To be precise, it is reduced from $2^n + n - 1$ to $2n$ for the system of n co-circulating strains of influenza. Second we introduce our model based on the Gog and Grenfell model, but where a strain is assumed to be a point on a real line instead of a point in a discrete space. The dynamics of multi-strain influenza can then be described by two integro-differential equations. In the presence of three different types of cross-immunity functions, we study a travelling wave of the disease propagation from the infected population to the uninfected population due to mutation, calculate the minimum wave speed, and compare the results.

To study the human disease such as influenza, the dynamics at a large geographical scale should be considered. In section 2.3, we study spatial heterogeneity (differences between populations in different locations) by a metapopulation model with a status-based framework. Metapopulations are one of the simplest spatial models applicable to modeling many human diseases (Ruan et al., 2006; Sani and Kroese, 2008). The idea is to subdivide the total population into distinct subpopulations, each of which

has its own dynamics, together with limited interaction between subgroups (Keeling and Rohani, 2008).

2.1 The derivation of the Gog and Grenfell model

We consider two-strain models of influenza for simplicity of exposition. Note however that our derivation is still valid for n co-circulating strains. From the Gog and Swinton model, we have

$$\begin{aligned}
\dot{S}_\phi &= \mu N - \mu S_\phi - C(\phi,\{1\},1)\Lambda_1 S_\phi - C(\phi,\{1,2\},1)\Lambda_1 S_\phi - \\
&\quad C(\phi,\{2\},2)\Lambda_2 S_\phi - C(\phi,\{1,2\},2)\Lambda_2 S_\phi, \\
\dot{S}_{\{1\}} &= C(\phi,\{1\},1)\Lambda_1 S_\phi - C(\{1\},\{1,2\},2)\Lambda_2 S_{\{1\}} - \\
&\quad C(\{1\},\{1,2\},1)\Lambda_1 S_{\{1\}} - \mu S_{\{1\}}, \\
\dot{S}_{\{2\}} &= C(\phi,\{2\},2)\Lambda_2 S_\phi - C(\{2\},\{1,2\},1)\Lambda_1 S_{\{2\}} - \\
&\quad C(\{2\},\{1,2\},2)\Lambda_2 S_{\{2\}} - \mu S_{\{2\}}, \\
\dot{S}_{\{1,2\}} &= C(\phi,\{1,2\},1)\Lambda_1 S_\phi + C(\phi,\{1,2\},2)\Lambda_2 S_\phi + \\
&\quad C(\{1\},\{1,2\},2)\Lambda_2 S_{\{1\}} + C(\{2\},\{1,2\},1)\Lambda_1 S_{\{2\}} - \mu S_{\{1,2\}}, \\
\dot{I}_1 &= \Lambda_1(S_\phi + S_{\{2\}}) - \nu_1 I_1 - \mu I_1, \\
\dot{I}_2 &= \Lambda_2(S_\phi + S_{\{1\}}) - \nu_2 I_2 - \mu I_2,
\end{aligned} \tag{2.1.1}$$

where $\mathcal{J} \subseteq \{1,2\}$, $\Lambda_i = \beta_i I_i$, $S_\mathcal{J}$ represents the number of hosts that are completely immune to the strains in the set $\mathcal{J}$, I_i the number of infectious individuals to strain i, and $C(\mathcal{L},\mathcal{J},i)$ the probability that hosts recover to a state $\mathcal{J}$, having started in state $\mathcal{L}$ and been infected by strain i. The polarized immunity is assumed which means that cross-immunity acts to render some hosts totally immune while other hosts gain nothing from infections. Also, the reduced-transmission of cross-immunity is assumed. By assuming that cross-immunity is conferred by exposure even if immunity prevents the full disease from developing, this allows all hosts to have the same chance of gaining immunity to a strain whatever their current immune status is. Besides, $S_{\{1,2\}}$ does not appear in other equations, so it can be omitted from the system. Let $S_1 = S_\phi + S_{\{2\}}$ and $S_2 = S_\phi + S_{\{1\}}$. Hence, by the fact that $\sum_\mathcal{J} C(\mathcal{K},\mathcal{J},i) = 1$:

$$\dot{S}_1 = \mu N - \mu S_1 - \Lambda_1 S_1 - C(\phi,\{1,2\},2)\Lambda_2 S_\phi - C(\{2\},\{1,2\},2)\Lambda_2 S_{\{2\}}$$

Define $C(\phi,\{1,2\},2) = C(\{2\},\{1,2\},2) = \sigma_{12}$, which is the chance that an infection by strain 2 gives immunity to strain 1. The differential equation of I_1 in the Gog and Grenfell model is obviously gained from the Gog and Swinton model. The equations for S_2 and I_2 are obtained in the similar way. Therefore, by those assumptions, the

system (2.1.1) becomes

$$\begin{aligned} \dot{S}_1 &= \mu - \mu S_1 - \beta_1 S_1 I_1 - \sigma_{12}\beta_2 S_1 I_2, \\ \dot{I}_1 &= \beta_1 S_1 I_1 - (\mu + \nu_1) I_1, \\ \dot{S}_2 &= \mu - \mu S_2 - \beta_2 S_2 I_2 - \sigma_{21}\beta_1 S_2 I_1, \\ \dot{I}_2 &= \beta_2 S_2 I_2 - (\mu + \nu_2) I_2, \end{aligned} \tag{2.1.2}$$

in terms of proportion of individuals. Note that these classes are not mutually exclusive, and that some individuals do not belong to any of them. For example, an individual susceptible to both strains is in both S_1 and S_2, while an individual who has recovered from both is in none of theses classes.

2.2 An epidemic model with host cross-immunity to a continuum of strains

For n co-circulating strains in a host population, the Gog and Grenfell model is described as follows

$$\begin{aligned} \dot{S}_i &= \mu N - \textstyle\sum_j \frac{\beta_j}{N} S_i \sigma_{ij} I_j - \mu S_i, \\ \dot{I}_i &= \frac{\beta_i}{N} S_i I_i - \nu_i I_i - \mu I_i, \end{aligned} \tag{2.2.1}$$

for $i = 1, 2, 3, \ldots, n$, where S_i and I_i are the proportions of susceptible and infectious individuals to strain i, respectively. Also in the model, $1/\mu$ is an average lifetime of hosts and for the total population size to be constant μ is assumed to be both the birth and death rate of hosts. For each strain i, β_i is a transmission rate and ν_i is a recovery rate so that $1/\nu_i$ is the infectious period to strain i. The cross-immunity between strains is described by σ_{ij}, the probability that infected by strain j will give immunity to strain i. Note that the system is with frequency-dependent transmission. It can be written in terms of proportions of individuals by reusing the previous symbols as follows

$$\begin{aligned} \dot{S}_i &= \mu - \textstyle\sum_j \beta_j S_i \sigma_{ij} I_j - \mu S_i, \\ \dot{I}_i &= \beta_i S_i I_i - \nu_i I_i - \mu I_i, \end{aligned} \tag{2.2.2}$$

2.2.1 Formulation of the model

First we introduce the mutation term into the system (2.2.2) by assuming that a virus in an infectious individual may mutate to a neighbouring strain. Hence, the model incorporating mutation is

$$\begin{aligned} \dot{S}_i &= \mu - \textstyle\sum_j \beta_j S_i \sigma_{ij} I_j - \mu S_i, \\ \dot{I}_i &= \beta_i S_i I_i - \nu_i I_i - \mu I_i + d(I_{i+1} - 2I_i + I_{i-1}), \end{aligned} \tag{2.2.3}$$

where d is the mutation rate on the antigenic space. Second, we introduce a continuum approximation to the system so that strains take values in $\Re$. It means that S_i and I_i can be approximated by $S(x,t)$ and $I(x,t)$; $S_{i\pm1}$ and $I_{i\pm1}$ can be approximated by $S(x\pm\delta x)$ and $I(x\pm\delta x)$; d can be approximated by $\hat{D}/\delta^2$; finally σ_{ij} can be estimated by $\sigma(x,y)\delta y$. The system (2.2.3) becomes

$$\begin{array}{rcl} \frac{\partial S(x,t)}{\partial t} & = & \mu - \sum_y \beta(y)S(x,t)\sigma(x,y)I(y,t)\delta y - \mu S(x,t), \\ \frac{\partial I(x,t)}{\partial t} & = & \beta(x)S(x,t)I(x,t) - \nu(x)I(x,t) - \mu I(x,t) + \hat{D}\frac{(I(x+\delta x)-2I(x,t)+I(x-\delta x)}{\delta x^2}. \end{array} \tag{2.2.4}$$

As $\delta x \to 0$ and $\delta y \to 0$, we now propose the system with host cross-immune to a continuum of strains

$$\begin{array}{rcl} \frac{\partial S(x,t)}{\partial t} & = & \mu - \int_{-\infty}^{\infty} \beta(y)S(x,t)\sigma(x,y)I(y,t)dy - \mu S(x,t), \\ \frac{\partial I(x,t)}{\partial t} & = & \beta(x)S(x,t)I(x,t) - \nu(x)I(x,t) - \mu I(x,t) + \hat{D}\frac{\partial^2 I(x,t)}{\partial x^2}. \end{array} \tag{2.2.5}$$

In the model, x represents a strain positioned as a point on a real line so the other position on a line represents the other strain. Consequently, for example, $I(x,t)$ is the proportion of infectious individuals to a strain at the position x at time t. Moreover, a cross-immunity term in the model can be expressed as the function of the distance between two positions and the distance exhibits the antigenic difference between the strains.

2.2.2 Analysis

Spatially uniform steady states

For simplicity, we assume a constant transmission rate and recovery rate for each strain in the model (2.2.5). Hence, every strain shares the same general character. Cross-immunity between two strains $\sigma(x,y)$ at the position x and y is assumed to be a function of the distance between them $|x-y|$, so $\sigma(x,y) = K(|x-y|)$ for some function K. The function reduces more susceptibility to infections when y approaches x or in other words two strains are similar. By these assumptions, we can find the spatially uniform steady states of the system explicitly as follows:

1. the disease-free steady state

$$(S(x,t), I(x,t)) = (S^0, I^0) = (1, 0) \tag{2.2.6}$$

2. the disease-present steady state

$$(S(x,t), I(x,t)) = (S^*, I^*) = \left(\frac{1}{R_0}, \frac{\mu(R_0-1)}{\beta\sum}\right) \tag{2.2.7}$$

where $R_0 = \beta/(\mu+\nu)$ represents the basic reproductive ratio of the influenza strain and $\Sigma = \int_{-\infty}^{\infty} \sigma(x,y)dy$, both of which are independent of x.

Spatially uniform linearised perturbation near the steady states

Let S^* and I^* be spatially uniform steady state solutions, and let $\hat{S}$ and $\hat{I}$ be spatially uniform perturbations from them. Then,

$$\hat{S}(t) = S(t) - S^*$$

$$\hat{I}(t) = I(t) - I^*$$

so we have the linearised equations

$$\begin{array}{rcl} \frac{\partial \hat{S}}{\partial t} & = & -\beta \hat{S}(t) I^* \int_{-\infty}^{\infty} \sigma(x,y)dy - \beta S^* \int_{-\infty}^{\infty} \sigma(x,y)\hat{I}(t)dy - \mu \hat{S}(t), \\ \frac{\partial \hat{I}}{\partial t} & = & \beta(\hat{S}(t)I^* + S^*\hat{I}(t)) - \nu \hat{I}(t) - \mu \hat{I}(t) \end{array} \tag{2.2.8}$$

which implies the Jacobian matrix of the system (2.2.5) as follows:

$$J = \begin{bmatrix} -\beta\Sigma I^* - \mu & -\beta\Sigma S^* \\ \beta I^* & \beta S^* - \nu - \mu \end{bmatrix}. \tag{2.2.9}$$

The Jacobian matrix at the disease-free steady state $(S^0, I^0) = (1, 0)$ is

$$J^0 = \begin{bmatrix} -\mu & -\beta\Sigma \\ 0 & (\nu+\mu)(R_0 - 1) \end{bmatrix}. \tag{2.2.10}$$

The eigenvalues of J^0 are $-\mu$ and $(\nu+\mu)(R_0-1)$. Hence, (S^0, I^0) is stable if and only if $R_0 < 1$. We next consider the stability of the disease-present steady state when $R_0 > 1$. For the disease-present steady state, we have

$$J^* = \begin{bmatrix} -\mu R_0 & -\beta\Sigma/R_0 \\ \mu(R_0-1)/\Sigma & 0 \end{bmatrix}. \tag{2.2.11}$$

Whenever $R_0 > 1$, tr $J^* < 0$ and $\det J^* > 0$. By the Routh-Hurwitz criteria, (S^*, I^*) is stable if and only if $R_0 > 1$.

Spatially non-uniform linearised perturbation near the steady states

We now look at spatially non-uniform perturbations in the form

$$\begin{array}{rcccl} \hat{S}(x,t) & = & S(x,t) - S^* & = & s(t)e^{ikx}, \\ \hat{I}(x,t) & = & I(x,t) - I^* & = & i(t)e^{ikx}. \end{array} \tag{2.2.12}$$

This perturbation includes both positive and negative perturbations from the steady state. For example, at the disease-free steady state ($I^* = 0$), a small perturbation $\hat{I}$ may take positive and negative values, and hence include biologically infeasible values of $I(x,t)$. However, if the steady state is stable to a general sign-indefinite perturbation, it is *a fortiori* stable to a positive perturbation as well. We shall therefore proceed to analyse stability to a general perturbation. Note that at k=0 the perturbation corresponds to the spatially uniform linearised perturbation in the previous subsection. Here, we consider $k \geq 0$.

The linearised equations of (2.2.5) are

$$\begin{array}{rcl} \frac{ds}{dt} & = & -\beta I^* \Sigma s - e^{-ikx} K^*(k) \beta S^* i - \mu s, \\ \frac{di}{dt} & = & \beta I^* s + \beta S^* i - \nu i - \mu i - \hat{D} k^2 i, \end{array} \tag{2.2.13}$$

where

$$K^*(k) = \int_{-\infty}^{\infty} K(x-y) e^{iky} dy.$$

Note that K^* relates to the cross-immunity function $\sigma(x,y) = K(x-y)$. By substituting $z = x - y$, we obtain

$$K^*(k) = \int_{-\infty}^{\infty} K(z) e^{-ikz} e^{ikx} dz = e^{ikx} \tilde{K}(k) \tag{2.2.14}$$

where $\tilde{K}$ is the Fourier transform of K. By the equation (2.2.13), the Jacobian matrix of the governed system (2.2.5) is

$$J(k) = \begin{bmatrix} -\beta \Sigma I^* - \mu & -\beta S^* \tilde{K}(k) \\ \beta I^* & \beta S^* - \nu - \mu - \hat{D} k^2 \end{bmatrix} \tag{2.2.15}$$

At the disease-free steady state, we obtain

$$J^0(k) = \begin{bmatrix} -\mu & -\beta \tilde{K}(k) \\ 0 & (\nu + \mu)(R_0 - 1) - \hat{D} k^2 \end{bmatrix} \tag{2.2.16}$$

The eigenvalues are $-\mu$ and $(\nu+\mu)(R_0-1) - \hat{D}k^2$. Hence, the disease-free steady state is stable to spatially non-uniform linearised perturbation if $R_0 < 1$. In conclusion, the disease-free steady state is linearly stable to all perturbations whenever $R_0 < 1$. Let us

now consider the Jacobian matrix at the disease-present steady state. It is as follows

$$J^*(k) = \begin{bmatrix} -\mu R_0 & -\beta\tilde{K}(k)/R_0 \\ \mu(R_0-1)/\Sigma & -\hat{D}k^2 \end{bmatrix} \tag{2.2.17}$$

Whenever $R_0 > 1$, we have tr $J^*(k) < 0$ and $\det J^*(k) = (\mu(R_0-1)+\mu)\hat{D}k^2 + \mu\beta S^*(R_0-1)\tilde{K}(k)/\Sigma$ which its sign depends on the value of $\tilde{K}(k)$. For example, in one of our case studies which will be mentioned in detail later, $K(x-y) = e^{-(\frac{x-y}{l})^2}$, we have

$$\tilde{K}(k) = e^{-l^2k^2/4}\Sigma$$

so that

$$\det J^*(K) > 0$$

for all values of l. The spatially uniform disease-present steady state in this case is stable to both uniform and non-uniform linearised perturbations when $R_0 > 1$.

2.2.3 Numerical Results

Table 2.1: Lists of parameters for influenza

Parameter	Description	Value	References
μ	birth and death rate	1/70 (year^{-1})	estimated
ν	recovery rate	365/7 (year^{-1})	Gog and Grenfell (2002)
R_0	the basic reproductive ratio	3-7	Casagrandi et al. (2006)
β	transmission rate	$R_0(\mu+\nu)$	

We first rescale the system (2.2.5) by introducing $T = (\mu+\nu)t$. Hence, with the constant transmission rate and recover rate of each strain, the system (2.2.5) becomes

$$\begin{array}{rcl} \frac{\partial S(x,T)}{\partial T} & = & \frac{\mu}{(\mu+\nu)} - \frac{\beta}{(\mu+\nu)}S(x,T)\int_{-\infty}^{\infty}\sigma(x,y)I(y,T)dy - \frac{\mu}{(\mu+\nu)}S(x,T), \\ \frac{\partial I(x,T)}{\partial T} & = & \frac{\beta}{(\mu+\nu))}S(x,T)I(x,T) - I(x,T) + D\frac{\partial^2 I(x,T)}{\partial x^2}. \end{array} \tag{2.2.18}$$

To study the propagation of influenza due to mutation from the infected population to the uninfected population, we shall introduce initial conditions as heaviside step functions on a one-dimensional antigenic domain $[x_1, x_2]$ with the equal proportions of infectious individuals of I^* to a strain on the antigenic space $[x_1, \bar{x}]$ and the uninfected individuals to the influenza strain on the antigenic space $[\bar{x}, x_2]$, where $\bar{x} = \frac{1}{2}(x_1 + x_2)$.

Thus initial conditions are given by

$$\begin{aligned} S(x,0) &= S^* + (1-S^*)H(x-\bar{x}) \quad x_1 \le x \le x_2, \\ I(x,0) &= I^* - I^* H(x-\bar{x}) \qquad\quad x_1 \le x \le x_2, \end{aligned}$$

where S^* and I^* correspond to (2.2.7), $\bar{x} = (x_1 + x_2)/2$, and H represents a heaviside step function. An example of the initial condition $I(x,0)$ is shown in Figure 2-1(a). The boundary conditions are assumed as zero fluxes:

$$\frac{\partial I}{\partial x}(x_1, T) = 0 = \frac{\partial I}{\partial x}(x_2, T), \;\; T_1 \le T \le T_2.$$

Note that parameter values can be found in Table 2.1.

The model (2.2.18) is solved with the initial conditions and the boundary conditions relating to types of cross-immunity functions $\sigma(x,y)$ as follows

1. $\sigma(x,y) = Ae^{-(\frac{x-y}{l})^2}$ where A is a constant, and l is a typical length scale involved in cross-immunity. It is a form that cross-immunity varies smoothly and symmetrically about each strain and tails off with distance.

2. $\sigma(x,y) = \delta(x-y)$, a dirac-delta function. There is no cross-immunity to neighbouring strains; strain x gives target immunity to itself only.

3. $\int \sigma(x,y)I(y,t)dy \approx \sigma I(x-h,t) + I(x,t) + \sigma I(x+h,t)$ where σ is a constant and $0 < \sigma < 1$. We essentially return to the discrete-strain space with each strain giving perfect immunity to itself and partial immunity to the two neighbouring strains.

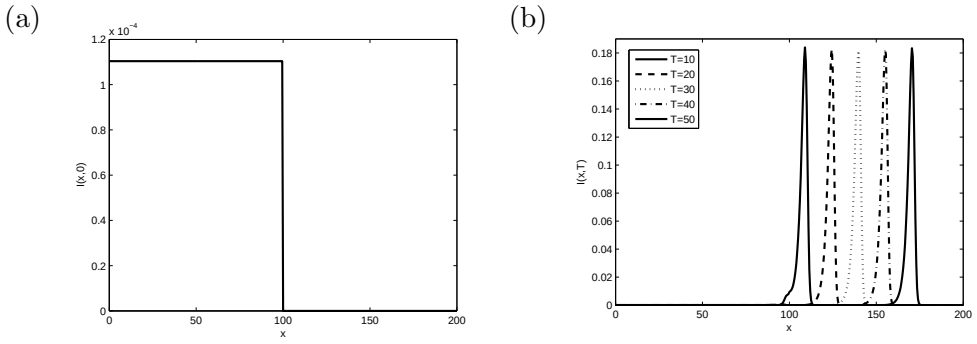

Figure 2-1: (a) An initial condition for the $I(x,T)$ on the domain $[0,200]$ when $\sigma(x,y) = Ae^{-(\frac{x-y}{l})^2}$ ($A = 1$, $l = 1$, $S^* = 0.2857$, $I^0 = 0$, and $I^* = 0.0001$) (Note that S^0 and S^* are in different scale.) (b) For type 1 of $\sigma(x,y)$, a travelling wave occurs in the infectious population and it is driven by mutation on the antigenic space with $c_1 = 161.7$ space units per year ($A = 1$, $l = 1$, $D = 0.25$ or $d = 1$)

(a) (b)

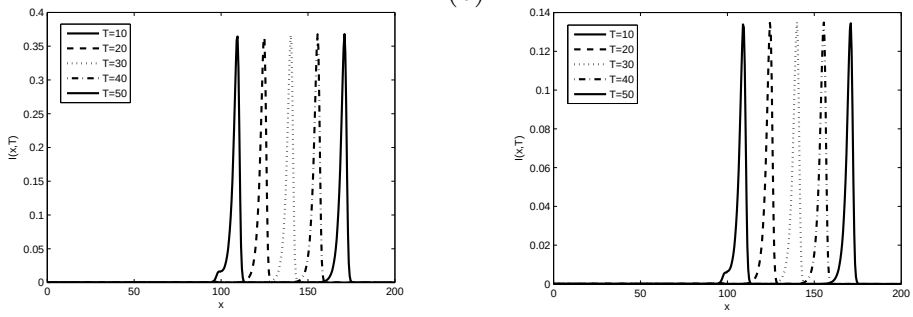

Figure 2-2: (a) For type 2 of $\sigma(x, y)$, this graph shows a travelling wave of the disease mutation in the infectious population with $c_2 = 156.5$ space units per year ($D = 0.25$ or $d = 1$, $S^* = 0.2857$, $I^* = 0.0002$) (b) For type 3 of $\sigma(x, y)$, this graph shows a travelling wave of the disease mutation in the infectious population with $c_3 = 161.7$ space units per year ($\sigma = 0.8$, $D = 0.25$ or $d = 1$, $S^* = 0.2857$, $I^* = 0.0001$)

Figure 2-1(b) and Figure 2-2(a)-(b) show a travelling wave from the infectious population to the susceptible population to strains on the antigenic space x. The travelling wave represents an antigenic drift process with strains present in the population dying out and being replaced by new ones at new points in the antigenic space. Each peak represents a cluster of influenza, building up and dying out. Hence, each strain is transient. The process repeats over the rest of the strain space. In long term, the proportion of infectious individuals tends to the spatially uniform disease-present steady state. By calculating a wave speed from the formula

$$c = \frac{x_2 - x_1}{t_2 - t_1},$$

where x_1 is one position on the antigenic space of a wave at time t_1 and x_2 is the same position on the antigenic space of the wave but at time t_2, we find that without cross-immunity to neighbouring strains the wave speed of the infectious population changes due to the mutation on the antigenic space (for example, $c_2 = 88.7$ space units per year when $D = 0.2$ or $c_2 = 156.5$ space units per year when $D = 1$). It is also true when cross-immunity is present ($c_1 = c_3 = 156.5$ space units per year when $D = 1$). In conclusion, cross-immunity might not alter the wave speed and the speed might be influenced by how fast the virus mutates (mutation rate). We further study the system (2.2.18) with type 3 of cross-immunity functions for the relation of cross-immunity, the mutation rate, and a wave speed, a minimum wave speed, and spatially non-uniform steady states in the next section.

2.2.4 Additional analysis

We study the following system in details

$$\begin{array}{rcl} \frac{\partial S}{\partial T} & = & \frac{\mu}{(\mu+\nu)} - \frac{\beta}{(\mu+\nu)} S(\sigma I(x-h,T) + I + \sigma I(x+h,T)) - \frac{\mu}{(\mu+\nu)} S, \\ \frac{\partial I}{\partial T} & = & \frac{\beta}{(\mu+\nu)} SI - I + d(I(x-h,T) - 2I + I(x+h,T)), \end{array} \tag{2.2.19}$$

where individuals acquire a perfect immunity to a strain they get infected with and a partial immunity to two neighbouring strains. The mutation term is approximated by a central difference and d is a function of step size.

Spatially uniform steady states

Two spatially uniform steady states are

$$(S, I) = (S^0, I^0) = (1, 0), \text{ and } (S, I) = (S^*, I^*) = \left(\frac{1}{R_0}, \frac{\mu(R_0 - 1)}{\beta(1 + 2\sigma)} \right).$$

Clearly, if influenza is endemic, the prevalence of it is reduced by the presence of cross-immunity.

Spatially non-uniform steady states

Let $I_{i-1} = I(x-h), I_i = I(x), \text{ and } I_{i+1} = I(x+h)$. Given that

$$\begin{array}{rcl} \frac{\partial S_i}{\partial t} & = & \mu - \mu S_i - \beta S_i(\sigma I_{i-1} + I_i + \sigma I_{i+1}), \\ \frac{\partial I_i}{\partial t} & = & \beta S_i I_i - \nu I_i - \mu I_i + d(I_{i-1} - 2I_i + I_{i+1}), \end{array} \tag{2.2.20}$$

travelling waves in such systems are often blocked, or prevented from occurring, by homoclinic or heteroclinic orbits of the steady state equations. The steady state equations of the system (2.2.20) are

$$\begin{array}{rcl} \mu - \mu S_i - \beta S_i(\sigma I_{i-1} + I_i + \sigma I_{i+1}) & = & 0, \\ \beta S_i I_i - \nu I_i - \mu I_i + d(I_{i-1} - 2I_i + I_{i+1}) & = & 0. \end{array} \tag{2.2.21}$$

A doubly infinite sequence,

$$\{(S_i, I_i)\}_{i \in \mathcal{Z}} = \ldots, (S_{-1}, I_{-1}), (S_0, I_0), (S_1, I_1), \ldots,$$

is an orbit of (2.2.21) if it satisfies (2.2.21) for each i. It is heteroclinic from (S^0, I^0) to

(S^*, I^*) if

$$S_i \to S^0, I_i \to I^0 \text{ as } i \to -\infty, \text{ and } S_i \to S^*, I_i \to I^* \text{ as } i \to \infty.$$

It is homoclinic if the sequence tends to the same steady state as $i \to \pm\infty$.

We separate values of d and σ into 4 cases: 1) $d = \sigma = 0$, 2) $d = 0, \sigma > 0$, 3) $d > 0, \sigma = 0$, and 4) $d > 0, \sigma > 0$.

1. When $d = \sigma = 0$,
   for each i, either $(S_i, I_i) = (1, 0)$ or $(S_i, I_i) = (S^*, I^*)$. Hence there is a heteroclinic orbit with a sequence

   $$\ldots, (S_{-1}, I_{-1}), (S_0, I_0), (S_1, I_1), \ldots := \ldots, (1, 0), (S^*, I^*), (S^*, I^*), \ldots, \quad (2.2.22)$$

   for instance.

2. When $d = 0, \sigma > 0$,
   either $I_i = 0$ or $S_i = 1/R_0$. Let $I_i = 0$ for $i \leq 0$, $S_i = 1$ for $i \leq -1$, and $S_i = 1/R_0$ for $i \geq 1$. Then the second equation of (2.2.21) is satisfied for all i, and the first is satisfied for all $i \leq -1$. For $i \geq 0$ the first of (2.2.21) gives

   $$\sigma I_{i-1} + I_i + \sigma I_{i+1} = \frac{\mu(1 - S_i)}{\beta S_i}.$$

   With $i = 0$ this gives

   $$\sigma I_1 = \frac{\mu(1 - S_0)}{\beta S_0}, \quad (2.2.23)$$

   or alternatively

   $$S_0 = \frac{\mu}{\mu + \sigma\beta I_1}, \quad (2.2.24)$$

   and with $i > 0$ we obtain

   $$\sigma I_{i-1} + I_i + \sigma I_{i+1} = \frac{\mu(1 - S_i)}{\beta S_i} = (2\sigma + 1)I^*. \quad (2.2.25)$$

   We may choose I_1 arbitrarily, determining S_0 by (2.2.24), and the problem for I_i with $i \geq 2$ is given by the second-order linear difference equation (2.2.25) with $I_0 = 0$, I_1 chosen. The general solution is $I_i = I^* + A\lambda_1^i + B\lambda_2^i$, where λ_1 and λ_2 are solutions of the auxiliary equation

   $$\sigma\lambda^2 + \lambda + \sigma = 0.$$

   For $\sigma < \frac{1}{2}$ the roots of this quadratic are real, and satisfy $\lambda_2 < -1 < \lambda_1 < 0$. The solution tending to I^* as $i \to \infty$ (obtained by choosing $I_1 = I^*(1 - \lambda_1)$) is

given by

$$I_i = I^*(1 - \lambda_1^i).$$

This completes the description of the heteroclinic orbit in this case. For $\sigma > \frac{1}{2}$ the roots of the quadratic are complex, and lie on the unit circle. In this case I_i does not tend to I^* as $i \to \infty$, but the solution circles about (I^*, I^*) in (I_i, I_{i+1}) space. Although this is no longer a heteroclinic orbit, it appears from the numerical results of the last section, shown in Figure 2-3(a), that it is nevertheless sufficient to preclude the existence of a travelling wave with non-zero wave speed.

3. When $d > 0, \sigma = 0$,
we show that any solution of the system is concave near $I = 0$ so that neither a heteroclinic nor a homoclinic orbit can occur. Define $M_i = I_{i+1} - 2I_i + I_{i-1}$. The steady state equations are

$$\begin{aligned} \mu - \mu S_i - \beta S_i I_i &= 0, \\ \beta S_i I_i - \nu I_i - \mu I_i + dM_i &= 0. \end{aligned}$$

By eliminating S_i between these equations, we have

$$\frac{\mu\beta I_i}{\mu + \beta I_i} - (\mu + \nu)I_i + dM_i = 0.$$

Given $I_i = I$, $M_i = M$ is given by

$$M = -\frac{\mu(\beta - \mu - \nu)I - \beta(\mu + \nu)I^2}{d(\mu + \beta I)}.$$

Hence $M = 0$ when $I = 0$ or when $I = \mu(R_0 - 1)/\beta = I^*$, and $M < 0$ for $0 < I < I^*$. Any solution is concave near $I = 0$, so cannot tend to $I = 0$ from above, no heteroclinic or homoclinic orbit can exist, and we expect to see a travelling wave with positive wave speed.

4. When $d > 0, \sigma > 0$,
we again use convexity and concavity to show that neither a heteroclinic nor a homoclinic orbit can occur. Define $M_i = I_{i+1} - 2I_i + I_{i-1}$. Note that for a biologically realistic solution, $M_i \geq -2I_i$. Then,

$$\sigma I_{i+1} + I_i + \sigma I_{i-1} = \sigma M_i + (1 + 2\sigma)I_i.$$

The steady state equations (2.2.21) become

$$\begin{aligned} \mu - \mu S_i - \beta S_i \sigma M_i - \beta(1 + 2\sigma)S_i I_i &= 0, \\ \beta S_i I_i - \nu I_i - \mu I_i + dM_i &= 0. \end{aligned}$$

Eliminating S_i between these two equations,

$$\frac{\mu\beta I_i}{\mu+\beta\sigma M_i+\beta(1+2\sigma)I_i}-(\mu+\nu)I_i+dM_i=0.$$

Given $I_i=I$, we can find $M_i=M$ by solving

$$Q(M):=\beta\sigma dM^2+a_1(I)M+a_2(I)=0,$$

where

$$\begin{aligned} a_1(I) &= \mu d+\beta d(1+2\sigma)I-\beta\sigma(\mu+\nu)I, \\ a_2(I) &= -\mu(\mu+\nu+\beta)I-\beta(1+2\sigma)(\mu+\nu)I^2. \end{aligned}$$

Note that for fixed $I>0$, Q is convex with $Q(0)<0$ and

$$Q(-2I)=-2\mu dI-2\beta dI^2-\mu(\mu+\nu+\beta)I-\beta(\mu+\nu)I^2<0.$$

Hence, the biologically realistic root M_i ($M\geq -2I$) of $Q(M)=0$ satisfies $M_i>0$, or $I_{i+1}-2I_i+I_{i-1}>0$. Consequently the function I_i is convex, and there is no heteroclinic orbit or homoclinic orbit, which must have both convex and concave regions. Therefore, from Cases 3 & 4, we expect a travelling wave with a positive wave speed, as shown numerically in Figure 2-3(a), to exist whenever $d>0$. This corresponds to sets of strains of influenza emerging and then dying out, as new mutant strains emerge to take their place.

The study of wave speed

By varying σ and d between 0 and 1, it can be seen from Figure 2-3(a) that a travelling wave is a pulled wave which speed is determined by its leading edge. Thus, the stable wave speed should be the minimum wave speed that we get from the linearisation at (1,0). We linearise the system (2.2.19) about $(S,I)=(1,0)$ by defining $u=1-S$ and neglect terms of higher orders of u and I. We obtain

$$\begin{aligned} \tfrac{\partial u}{\partial T} &= -\tfrac{\mu}{\mu+\nu}u+\tfrac{\beta}{\mu+\nu}(\sigma I(x-h,T)+I+\sigma I(x+h,T)), \\ \tfrac{\partial I}{\partial T} &= \tfrac{\beta}{\mu+\nu}I-I+d(I(x-h,T)-2I+I(x+h,T)). \end{aligned} \tag{2.2.26}$$

The second equation of (2.2.26) is a linear equation for I. We look for a solution in the form

$$I=w(z),$$

where $z=x+c_3T$. Thus the equation $\partial I/\partial T$ becomes

$$c_3\frac{\partial w}{\partial z}=(R_0-1)w+d(w(z-h)-2w+w(z+h)).$$

(a) (b)

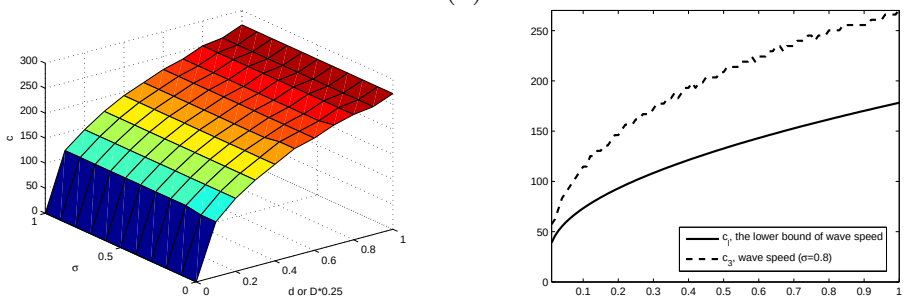

Figure 2-3: (a) This graph shows a relation of a diffusion rate (d), a cross-immunity value (σ), and a wave speed (c) (b) Wave speeds and their lower bound as d varies ($\sigma = 0.8$)

Now let us look for a solution of w in the form of an exponential term

$$w = e^{\lambda z}.$$

We obtain the following characteristic equation

$$c_3 = \frac{(R_0 - 1)}{\lambda} + \frac{2d(\cosh \lambda h - 1)}{\lambda}$$

In order to find a minimum of wave speed, we differentiate through the equation with respect to λ to get

$$-\frac{(R_0 - 1)}{\lambda^2} + \frac{2d(h\lambda \sinh \lambda h - \cosh \lambda h + 1)}{\lambda^2} = 0 \tag{2.2.27}$$

Note that obviously the wave speed (c_3) does not depend on the parameter σ. Figure 2-3(b) shows the wave speeds when d varies but σ is fixed at 0.8, and their lower bound.

2.2.5 Conclusions and discussion

Under the assumption that a strain is positioned as a point on a real line instead of a point in a discrete space, the number of differential equations in the status-based model, with an additional assumption that cross-immunity is conferred by exposure even if immunity prevents the full disease from developing, is reduced from $2n$ to 2, where n is the number of co-circulating strains of influenza. The system becomes more tractable although the number of strains increases. Mutation to neighbouring strains in an infectious individual is incorporated as a diffusion term in the model. Consequently, we can study stability of the system for threshold conditions.

In the model, there are two spatially uniform steady states: the disease-free steady and

the disease-present steady state. The model is uniformly perturbed and non-uniformly perturbed near each steady state. We find that the disease-free steady state is stable if $R_0 < 1$ while the disease-present steady state is stable if $R_0 > 1$.

To study the propagation of influenza driven by mutation from infectious population to susceptible population, we introduce initial conditions as heaviside step functions on a one-dimensional antigenic domain and a boundary condition as a zero flux. Three types of cross-immunity functions are considered for wave speed calculation; 1) when cross-immunity varies smoothly and symmetrically about each strain and tails off with distance, 2) when cross-immunity is absent, and 3) when cross-immunity is only given to two neighbouring strains on the discrete space. We find that a travelling wave occurs from the infectious population to the susceptible population to a new strain on the antigenic space. The travelling wave represents an antigenic drift process with strains present in the population dying out and being replaced by new ones at new points in the antigenic space. Each strain is transient. A cluster of influenza builds up and dies out. This process repeats over the rest of the strain space in the numerical results. In long term, the proportion of infectious individuals tends to the spatially uniform disease-present steady state finally and the prevalence of infectious population to a strain is reduced when cross-immunity is present. The stronger the cross-immunity, the lower prevalence of infectious individuals to strains of influenza. From the numerical results, the presence of cross-immunity may not influence the uninfected population to be infected with a new strain on the antigenic space. So it does not influence the wave speed of travelling waves. This result corresponds to Gog and Grenfell (2002).

We further study the model with type 3 of cross-immunity functions. We show that there are heteroclinic orbits preventing a travelling wave to occur when mutation is absent. When cross-immunity is absent, there are no heteroclinic orbits. By investigating the relation of d (mutation rate), σ (cross-immunity coefficient), and c (the wave speed), we find that a travelling wave is a pulled wave. Hence, the minimum wave speed can be calculated by linearising the system near the spatially uniform disease-free steady state and it does not depend on cross-immunity coefficient. Note that this minimum wave speed is also the minimum wave speed of the system for other types of cross-immunity functions, $\sigma(x, y)$. Therefore, with this type of cross-immunity, we not only show that cross-immunity does not influence the wave speed by comparing the numerical results with other type of cross-immunity and considering the minimum wave speed formula, but also by analyzing the presence of heteroclinic orbits. The latter shows mathematical support with the conclusion so that the conclusion is not just from the numerical results.

All in all, the model with host cross-immunity to a continuum of strains is proposed. There are only two integro-differential equations although the number of strains in-

creases so that the system is tractable and its mathematical analysis becomes approachable. By studying the propagation of strains driven by mutation in infected individuals, we find that a travelling wave represents an antigenic drift process that each strain finally dies out and is replaced by new ones at new points in the antigenic space. Also, a cluster of influenza strains emerges, building up and dying out.

2.3 A metapopultion model to study influenza

We assume that a human population is divided into subpopulations such as cities or communities. For simplicity, we assume that there are only 2 subpopulations in our model. Each subpopulation is divided into compartments of susceptible to strain i (S_i^j), infected with strain i (I_i^j), for $i = 1, 2$, and $j = 1, 2$. The total number of individuals in each subpopulation is represented by N_j and $\sum_j N_j = N$. We assume that the spread of influenza is due to migration or permanent movement of individuals such that individuals move randomly between subpopulations. Also, for simplicity, we assume that a travelling rate between subpopulations is not different between infectious and susceptible individuals for each strain. Let m_{lk} denote the per capita rate of travel from subgroup k to subgroup l with $m_{ll} = 0$, for $l = 1, 2$ and $k = 1, 2$.

The model in this chapter is based on the status-based framework by Gog and Grenfell (2002). However, we assume density dependence in the model. Hence we start with introducing movements of individuals to the metapopulation model extended from the Gog and Swinton model and then reduce it by the additional assumption made in the similar way in the Gog and Grenfell model in Section 2.1. The model takes the following form:

$$\begin{aligned}
\frac{dS_1^1}{dt} &= \mu N_1 - \mu S_1^1 - \beta_{11} I_1^1 S_1^1 - \sigma\beta_{21} I_2^1 S_1^1 + m_{12} S_1^2 - m_{21} S_1^1, \\
\frac{dI_1^1}{dt} &= \beta_{11} I_1^1 S_1^1 - (\mu + \nu) I_1^1 + m_{12} I_1^2 - m_{21} I_1^1, \\
\frac{dS_2^1}{dt} &= \mu N_1 - \mu S_2^1 - \beta_{21} I_2^1 S_2^1 - \sigma\beta_{11} I_1^1 S_2^1 + m_{12} S_2^2 - m_{21} S_2^1, \\
\frac{dI_2^1}{dt} &= \beta_{21} I_2^1 S_2^1 - (\mu + \nu) I_2^1 + m_{12} I_2^2 - m_{21} I_2^1, \\
\frac{dS_1^2}{dt} &= \mu N_2 - \mu S_1^2 - \beta_{12} I_1^2 S_1^2 - \sigma\beta_{22} I_2^2 S_1^2 + m_{21} S_1^1 - m_{12} S_1^2, \\
\frac{dI_1^2}{dt} &= \beta_{12} I_1^2 S_1^2 - (\mu + \nu) I_1^2 + m_{21} I_1^1 - m_{12} I_1^2, \\
\frac{dS_2^2}{dt} &= \mu N_2 - \mu S_2^2 - \beta_{22} I_2^2 S_2^2 - \sigma\beta_{12} I_1^2 S_2^2 + m_{21} S_2^1 - m_{12} S_2^2, \\
\frac{dI_2^2}{dt} &= \beta_{22} I_2^2 S_2^2 - (\mu + \nu) I_2^2 + m_{21} I_2^1 - m_{12} I_2^2,
\end{aligned} \tag{2.3.1}$$

for subpopulation 1 and 2, expressed as superscripts, respectively. In the model, we assume that the life span of human, and recovery time from strain 1 and 2 are equal in both subpopulations. Since we have movements of individuals in infected classes, we only have the same type of the steady state in both populations, for example, the

disease dies out in both subpopulations and there is no situation that both strains die out in subpopulation 1 while only strain 2 persists in subpopulation 2.

From the system (2.3.1), the disease-free steady state is

$$(S_1^1, I_1^1, S_2^1, I_2^1, S_1^2, I_1^2, S_2^2, I_2^2) = (S_1^{10}, 0, S_2^{10}, 0, S_1^{20}, 0, S_2^{20}, 0),$$

where

$$S_1^{10} = \frac{\mu(\mu + m_{12})N_1 + \mu m_{12}N_2}{[(\mu + m_{21})(\mu + m_{12}) - m_{12}m_{21}]} = S_2^{10},$$

and

$$S_1^{20} = \frac{\mu(\mu + m_{21})N_2 + \mu m_{21}N_1}{[(\mu + m_{21})(\mu + m_{12}) - m_{12}m_{21}]} = S_2^{20}.$$

Linear stability of the disease-free steady state of the system can be investigated by using the next-generation matrix (van den Driessche and Watmough, 2002). By ordering the infected variables as $I_1^1, I_1^2, I_2^1, I_2^2$, the matrix of new infections F is given by

$$F = \begin{bmatrix} F_1 & \underline{0} \\ \underline{0} & F_2 \end{bmatrix},$$

where

$$F_1 = \begin{bmatrix} \beta_{11}S_1^{10} & 0 \\ 0 & \beta_{12}S_1^{20} \end{bmatrix},\ F_2 = \begin{bmatrix} \beta_{21}S_2^{10} & 0 \\ 0 & \beta_{22}S_2^{20} \end{bmatrix},\ \text{and } \underline{0} = [0]_{2\times 2}.$$

The matrix of transfer between classes is

$$V = \begin{bmatrix} V_1 & \underline{0} \\ \underline{0} & V_2 \end{bmatrix},$$

where

$$V_1 = \begin{bmatrix} (m_{21} + \nu + \mu) & -m_{12} \\ -m_{21} & (m_{12} + \nu + \mu) \end{bmatrix},\ V_2 = \begin{bmatrix} (m_{21} + \nu + \mu) & -m_{12} \\ -m_{21} & (m_{12} + \nu + \mu) \end{bmatrix},$$

Hence, we obtain

$$FV^{-1} = \begin{bmatrix} F_1V_1^{-1} & 0 \\ 0 & F_2V_2^{-1} \end{bmatrix},$$

and the basic reproductive ratio is the spectrum of FV^{-1}, thus,

$$\text{Spec}(FV^{-1}) = \max\{\text{eigenvalues of } F_1V_1^{-1}, \text{eigenvalues of } F_2V_2^{-1}\}.$$

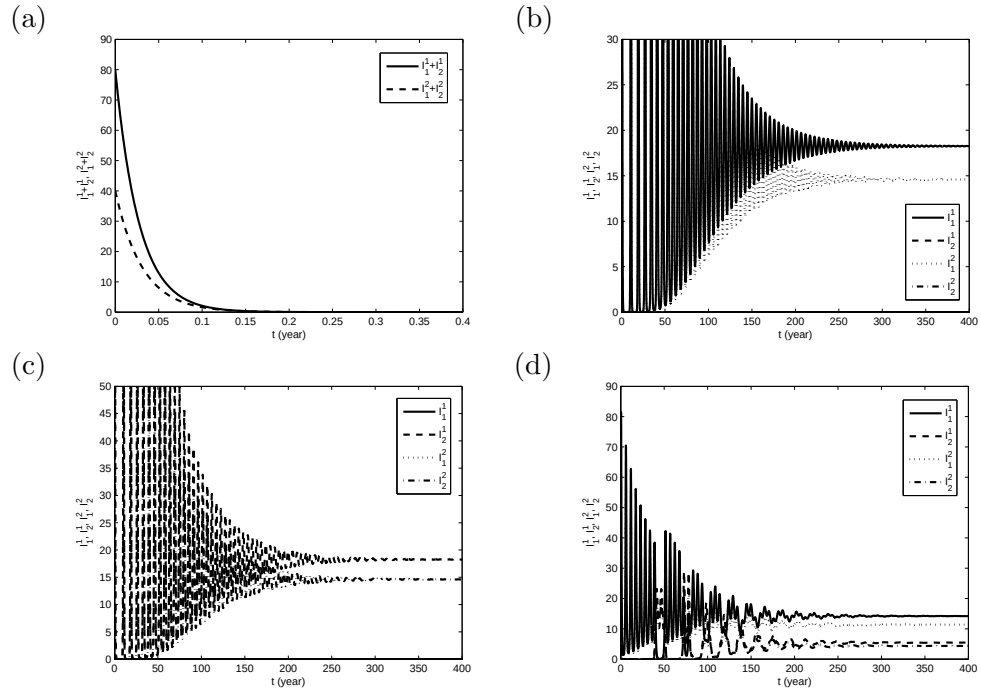

Figure 2-4: (a) Both strains die out in both subpopulations when $R_{01} = 0.9$ and $R_{02} = 0.8$ ($m_{12} = 0.2, m_{21} = 0.16, \sigma = 0.8, N_1 = 100000, N_2 = 80000$). (b) Only strain 1 persists in both subpopulations when $R_{01} = 3$ and $R_{02} = 0.8$ (c) Strain 2 persists when $R_{01} = 0.8$ and $R_{02} = 3$. (d) Both strains coexist when $R_{01} = 3$ and $R_{02} = 2$.

or

$$\begin{aligned} R_0 &= \max\{R_{01}, R_{02}\} \\ &= \max\{\frac{\mathrm{tr}(F_1V_1^{-1})+\sqrt{\mathrm{tr}(F_1V_1^{-1})^2-4\det(F_1V_1^{-1})}}{2}, \frac{\mathrm{tr}(F_2V_2^{-1})+\sqrt{\mathrm{tr}(F_2V_2^{-1})^2-4\det(F_2V_2^{-1})}}{2}\}, \end{aligned}$$

where R_{01} and R_{02} represent the basic reproductive ration of strain 1 and 2, respectively.

We show that; 1) both strains die out when $R_{01} < 1$ and $R_{02} < 1$, 2) stain 1 persists in both subpopulations when $R_{01} > 1$ and $R_{02} < 1$, 3) strain 2 persists in both subpopulations when $R_{01} < 1$ and $R_{02} > 1$, and 4) both strains coexist when $R_{01} > 1$ and $R_{02} > 1$ (see Figure 2-4).

2.4 Conclusions and discussion

In this chapter, we propose a mathematical model of continuum strains of influenza. The goal of this study is to use a real line to represent a strain space so that the number of equations from the Gog and Grenfell models from $2n$ is reduced to 2 and to study what can be derived from this approachable system. The system of equations becomes tractable although the number of strains increases. Consequently, we can study stability of the system for threshold conditions. We study three types of cross-immunity and show that a travelling wave occurs and represents antigenic drift process

with strains dying out and being replaced by new ones at new point on the strain space. Clusters emerge and die out. In case, cross-immunity acts to reduce individuals from getting infected with two neighbouring strains (Type 3), we not only show that cross-immunity does not influence the wave speed by comparing the numerical results with other type of cross-immunity and considering the minimum wave speed formula, but also by analyzing the presence of heteroclinic orbits. The latter shows mathematical support with the conclusion so that the conclusion is not just from the numerical results.

We next propose a metapopulation model for two communities. This model is based on a status-based framework by Gog and Grenfell (2002). We investigate stability of the disease-free steady state by the next-generation matrix and numerical results from the simulations. This work should be further investigated to include controls such as isolation or vaccination, or stochastic process that strains die out locally.

Chapter 3

Modelling vector-borne diseases

We devote this chapter to study the transmission dynamics of malaria which is a vector-borne disease. Each year, malaria kills over a million people, infects more than a billion people worldwide, and dampens the economics of its endemic regions (Snow et al., 2005; Guerra et al., 2006). Malaria is a mosquito-borne infectious disease caused by protozoan parasites in the genus *Plasmodium*. There are over 120 species of the parasite but only four of them commonly infect humans: *P. falciparum*, *P. vivax*, *P. malariae*, and *P. ovale*. Recent study shows that *P. knowlesi* can also infect humans although it is mainly transmitted in monkeys (Cox-Singh et al., 2008; Cox-Singh and Singh, 2008) so it might be counted as the fifth species that infects human (White, 2008). Clinically, *P. falciparum* is the deadliest one while *P. vivax* is the most widespread. The malaria parasites are endemic in Africa, tropical and sub-tropical regions of Asia, North and South America, and the Middle East, for instance. Over 300 million people suffer from malaria every year. *P. falciparum* is common in Africa and is the main cause of malaria deaths. Some evidences show that *P. vivax* causes up to 65 % of malaria in India and more people were at risk from it in 2005 than any other species (Mendis et al., 2001; Guerra et al., 2006). The symptoms of *P. vivax* is excruciating but not fatal. It involves cyclical fever and chills, headache, vomiting, diarrhea, and the enlargement of the spleen. However, in *P. falciparum*, there might be complications including acute anaemia and cerebral malaria.

The life cycle of malaria parasites begins with female *Anopheles* mosquitoes inoculating sporozoites of the parasites from their salivary gland either into the skin (Yamauchi et al., 2007) or into the peripheral circulation (Rosenberg et al., 1990) during their blood meal. The sporozoites then travel in the bloodstream to the liver to infect the hepatocytes and undergo asexual multiplication to produce schizonts in approximately 2-10 days (Mota et al., 2002). Each schizont, containing over 30000 merozoites, ruptures and releases the merozoites into the human bloodstream (Doolan et al., 2009). After

the merozoites are introduced, they infect red blood cells (Cowman and Crabb, 2006). The malaria symptoms appear when they burst these cells. Some of the merozoites are transformed into male and female gametocytes, which are ingested by mosquitoes during their blood meal (Drakeley et al., 2006). The gametocytes multiply themselves to produce sporozoites that make their way to the salivary gland of mosquitoes (Doolan et al., 2009). The cycle is perpetuated by inoculation of the sporozoites into new hosts.

It has been known that acquired immunity for malaria is achievable after a single infection, but especially in *P. falciparum* it often requires repeated infections (Day and Marsh, 1991; Gupta et al., 1999; Hviid, 2005). Children in endemic areas become infected early in life and experience more severe symptoms during the first five years in life. As the immunity develops the disease becomes less severe and the number of parasites circulating in blood declines (Doolan et al., 2009). This immunity is not fully acquired and declines with time (Collins et al., 1968). Without new exposures, individuals may lose their immune memory gained from previous infections. Also, individuals lose immunity easily by moving out of the endemic area.

A mathematical model of malaria was introduced by Ross and extended by MacDonald (Ross, 1916; Macdonald, 1952, 1957). In the Ross-McDonald model, hosts are assumed to be immune to further infection during the infection period only. The model with acquired immunity was proposed later by Dietz et al. (1974) and extended by Bailey (1975); Aron (1988). In those models, the immunity is boosted by additional infections. After that several authors have attempted to study the dynamics of malaria by considering many key factors such as the latent period in hosts (Yang, 2000; Ngwa, 2004), partial immunity (Chiyaka et al., 2007*b*), and incubation time in mosquitoes (Wei et al., 2008), for instance. It has been shown that vector-borne diseases like malaria are antigenically diverse (Contacos et al., 1972; Gupta, Trenholme, Anderson and Day, 1994). Hence, modelling a single strain might not be enough to explain the dynamics of the diseases. Although models of multi-strain diseases have been fruitfully introduced, (Castillo-Chavez et al., 1989; Gupta et al., 1996; Andreasen et al., 1997; Gupta et al., 1998; Lin et al., 1999; Gog and Swinton, 2002; Gog and Grenfell, 2002; Lin et al., 2003; Restif and Grenfell, 2006*a*; Adams and Sasaki, 2007) models of malaria transmission with cross-immunity are not numerous (Gupta, Swinton and Anderson, 1994; Abu-Raddad and Ferguson, 2004). Multi-strain models of vector-borne diseases have concentrated more in dengue transmission (Feng and Velasco-Hernandez, 1997; Ferguson et al., 1999; Esteva and Vargas, 2003; Adams et al., 2006).

In this chapter, we propose models to explain the dynamics of multi-strain malaria. We do not include the disease-induced death rate in hosts in the models, assuming that either the mortality due to the disease is small enough not to affect the host demography or the disease is not fatal. In the first model, we apply a status-based framework in a

host population to describe hosts according to their current immune status to a strain of malaria. For simplicity, we only study either two co-circulating strains of malaria in the same species or two different species. In the second model, we study the dynamics of two different species of malaria by considering the different types of cross-species immunity between them. We assume that cross-species immunity acts in the similar way with suppression during coinfection of both species. Hence, the coinfection model is first introduced and then reduced to another model that encapsulates partial cross-immunity between different species. The model is particularly used for studying *P. falciparum* and *P. vivax* in the endemic area. Controlling vector-borne diseases based on the models will be introduced later in Chapter 4.

In addition, we study two single-strain models of *P. falciparum* in the last two sections. We concentrate on life-histories of mosquitoes in both of the SIS and SIRS models for hosts while the SI model is used for mosquitoes. These studies are to emphasize that certain factors in mosquitoes might influence the dynamical behaviours of the system. Those factors are such as seasonality, incubation time, and attractiveness of infectious individuals to mosquitoes.

3.1 Mathematical model of host's immune status to malaria

We propose the model that can be used to describe the dynamics of either two co-circulating strains of *P. falciparum* or two co-circulating species of *P. falciparum* and *P. vivax*, for instance. By applying the status-based framework with polarized immunity and the reduced-transmission assumption (Gog and Grenfell, 2002), only one immune class is needed to describe hosts with respect to each strain or species. We introduce the status-based model (Gog and Swinton, 2002) for the interactions of humans and mosquitoes with two strains or species of the disease. For the rest of this work, we refer to an interaction between two different strains although the interaction between two species is similar.

3.1.1 Formulation of the model

We start with introducing a status-based model with polarized immunity in a vector-borne disease with two co-circulating strains and then we reduce the number of equations by an additional assumption of partial cross-immunity acting as reduced transmission. A status-based model with polarized immunity is introduced by Gog and Swinton (2002) for describing a different form of cross-immunity from a history-based model with cross-immunity acting as reduced susceptibility (Andreasen et al., 1997). The idea is by categorizing a susceptible population according to their current immune

status. With the polarized-immunity assumption, an individual is either entirely susceptible to a strain, or totally immune to it. A partial cross-immunity parameter in the model determines the destination category of immunity after the exposure to the pathogen strain. Each host is in one of immune classes although it is currently infectious. It is assumed that there is no removal of infected so that infectious individuals move to their susceptible state directly. Our model is based on the same idea, but with two populations interacting. Our notation follows that of Gog and Swinton. We only apply a status-based framework with a human population, so we divide it into four immune classes which are non-immune ($S_\emptyset$), immune to strain 1 but susceptible to strain 2 ($S_{\{1\}}$), immune to strain 2 but susceptible to strain 1 ($S_{\{2\}}$), and immune to both strains ($S_{\{1,2\}}$). Infectious individuals are divided into two classes which are infectious with strain 1 (I_1) and infectious with strain 2 (I_2). So each infectious individual is counted twice corresponding to the immune state and the infectious class. We assume that a total size of the human population (N) is at equilibrium with μ as the per capita birth and death rate and

$$\sum_J S_J = N. \tag{3.1.1}$$

In the model, ν_i is a recovery rate from strain i. Cross-immunity is described through a parameter $C(K, J, i)$ which represents the probability of hosts having started with state K, been exposed to strain i, and entered to state J. Note that C is not defined unless $i \in J$, $K \subset J$, and since there is no death due to the disease,

$$\sum_J C(K, J, i) = 1 \tag{3.1.2}$$

where the sum is taken over all subsets $J \subset L = 1, 2$ such that $K \subset J$, $i \in J$, and $K \cup \{i\} \subset J$. In this work, we do not include the latent period in humans.

We assume 1) that the parasites are not harmful to the mosquitoes 2) that once a mosquito has ingested a particular strain of malaria, it carries that strain, and that strain only for the rest of its life (Gupta, Swinton and Anderson, 1994; Feng and Velasco-Hernandez, 1997; Esteva and Vargas, 2003; Supriatna et al., 2008). We do not consider incubation time of P. vivax in mosquitoes in the model. The vector population is separated into three classes which are susceptible (U), infectious with strain 1 (V_1), and infectious with strain 2 (V_2). The transmission rate from infectious mosquitoes with strain i to susceptible humans is described by β_i which implicitly depends on the biting rate of mosquitoes (b) and the probability of successful infection with strain i in human (p_{h_i}). The transmission rate from infectious human with strain i to susceptible mosquitoes is denoted by α_i which is a function of the biting rate of mosquitoes and the probability of successful infection with strain i in mosquito (p_{m_i}). The total population size of mosquitoes (M) is assumed to be at equilibrium. With the recruitment rate of

mosquitoes equal to B and the death rate equal to η, M is B/η. The model takes the form

$$\begin{aligned}
\dot{S}_{\emptyset}(t) &= \mu N - \mu S_{\emptyset} - C(\emptyset,\{1\},1)\beta_1 V_1 S_{\emptyset} - C(\emptyset,\{1,2\},1)\beta_1 V_1 S_{\emptyset} - \\
&\quad C(\emptyset,\{2\},2)\beta_2 V_2 S_{\emptyset} - C(\emptyset,\{1,2\},2)\beta_2 V_2 S_{\emptyset}, \\
\dot{S}_{\{1\}}(t) &= C(\emptyset,\{1\},1)\beta_1 V_1 S_{\emptyset} - C(\{1\},\{1,2\},2)\beta_2 V_2 S_{\{1\}} - \\
&\quad C(\{1\},\{1,2\},1)\beta_1 V_1 S_{\{1\}} - \mu S_{\{1\}}, \\
\dot{S}_{\{2\}}(t) &= C(\emptyset,\{2\},2)\beta_2 V_2 S_{\emptyset} - C(\{2\},\{1,2\},1)\beta_1 V_1 S_{\{2\}} - \\
&\quad C(\{2\},\{1,2\},2)\beta_2 V_2 S_{\{2\}} - \mu S_{\{2\}}, \\
\dot{S}_{\{1,2\}}(t) &= C(\emptyset,\{1,2\},1)\beta_1 V_1 S_{\emptyset} + C(\emptyset,\{1,2\},2)\beta_2 V_2 S_{\emptyset} + \\
&\quad C(\{1\},\{1,2\},2)\beta_2 V_2 S_{\{1\}} + C(\{2\},\{1,2\},1)\beta_1 V_1 S_{\{2\}} - \mu S_{\{1,2\}}, \\
\dot{I}_1(t) &= \beta_1 V_1 (S_{\emptyset} + S_{\{2\}}) - (\mu + \nu_1) I_{\{1\}}, \\
\dot{I}_2(t) &= \beta_2 V_2 (S_{\emptyset} + S_{\{1\}}) - (\mu + \nu_2) I_{\{2\}}, \\
\dot{U}(t) &= B - \eta U - \alpha_1 I_1 U - \alpha_2 I_2 U, \\
\dot{V}_1(t) &= \alpha_1 I_1 U - \eta V_1, \\
\dot{V}_2(t) &= \alpha_2 I_2 U - \eta V_2.
\end{aligned} \tag{3.1.3}$$

In the model, we have : $C(\emptyset,\{1\},1) + C(\emptyset,\{1,2\},1) = 1$, $C(\{2\},\{1,2\},1) = 1$, $C(\emptyset,\{2\},2) + C(\emptyset,\{1,2\},2) = 1$, and $C(\{1\},\{1,2\},2) = 1$. Because $S_{\{1,2\}}$ does not appear in the other equations, its derivative equation can be omitted from the system. By the additional assumption of reduced transmission in a status-based framework with polarized immunity (Gog and Grenfell, 2002) and that the probability of acquiring further immune memory to the other strain of the naive individual and the infectious individual with the current strain is equal ($C(\emptyset,\{1,2\},2) = C(\{2\},\{1,2\},2) = \sigma_{12}$ and $C(\emptyset,\{1,2\},1) = C(\{1\},\{1,2\},1) = \sigma_{21}$), all hosts have the same chance of acquiring immunity to a strain so that only one variable is enough to describe host's immunity to each strain. Consequently, we introduce two new variables, $S_1 = S_{\emptyset} + S_{\{2\}}$ and $S_2 = S_{\emptyset} + S_{\{1\}}$, which represent the number of susceptible individuals to strain 1 and the number of susceptible individuals to strain 2 respectively. Hence, for example, by the assumption that $C(\emptyset,\{1\},1) + C(\emptyset,\{1,2\},1) = 1$ and $C(\{2\},\{1,2\},1) = 1$, we have

$$\dot{S}_1 = \mu N - \mu S_1 - \beta_1 V_1 S_1 - C(\emptyset,\{1,2\},2)\beta_2 V_2 S_{\emptyset} - C(2,\{1,2\},2)\beta_2 V_2 S_{\{2\}}.$$

Because we assume that ($C(\emptyset,\{1,2\},2) = C(\{2\},\{1,2\},2) = \sigma_{12}$,

$$\dot{S}_1 = \mu N - \mu S_1 - \beta_1 V_1 S_1 - \sigma_{12}\beta_2 V_2 S_1.$$

The differential equation of S_2 can also be derived in the similar way. For simplicity, we further assume that $\sigma_{12} = \sigma_{21} = \sigma$. Also, the differential equation for U in the system (3.1.3) can be removed by substituting $U = M - V_1 - V_2$ in the other equations.

The system (3.1.3) is reduced to

$$\begin{aligned}
\dot{S}_1(t) &= \mu N - \mu S_1 - \beta_1 V_1 S_1 - \sigma\beta_2 V_2 S_1, \\
\dot{I}_1(t) &= \beta_1 V_1 S_1 - (\mu+\nu) I_1, \\
\dot{S}_2(t) &= \mu N_h - \mu S_2 - \beta_2 V_2 S_2 - \sigma\beta_1 V_1 S_2, \\
\dot{I}_2(t) &= \beta_2 V_2 S_2 - (\mu+\nu) I_2, \\
\dot{V}_1(t) &= \alpha_1 I_1 (M - V_1 - V_2) - \eta V_1, \\
\dot{V}_2(t) &= \alpha_2 I_2 (M - V_1 - V_2) - \eta V_2
\end{aligned} \tag{3.1.4}$$

with strains assumed to have the different transmission rate but share the same recovery rate.

For strain i, the number of vectors that become infectious when we introduce an infectious host into the susceptible population of vectors is $\alpha_i M(1/(\mu+\nu))$. The number of hosts who become infectious when we introduce an infectious mosquito into the susceptible pool of hosts is $\beta_i N(1/\eta)$. Hence, the basic reproductive ratio of strain i in the system (3.1.4) is

$$R_{0i} = \frac{\alpha_i \beta_i N M}{(\mu+\nu)\eta}.$$

where $M = B/\eta$.

3.1.2 Analysis

The steady states

There are four types of steady states of the system (3.1.4):

1. the disease-free steady state

$$P^0 = (S_1, I_1, S_2, I_2, V_1, V_2) = (S_1^0, I_1^0, S_2^0, I_2^0, V_1^0, V_2^0) = (N, 0, M, 0, 0, 0),$$

2. the single-strain steady state of strain i for $i = 1, 2$

$$P^i = (S_1, I_1, S_2, I_2, V_1, V_2) = (S_1^i, I_1^i, S_2^i, I_2^i, V_1^i, V_2^i)$$

where

$$\begin{aligned} S_i &= \frac{\mu N-(\mu+\nu)I_i}{\mu}, \\ I_i &= \frac{\mu[\alpha_i\beta_i NM-(\mu+\nu)\eta]}{\alpha_i(\mu+\nu)[\beta_i M+\mu]}, \\ S_j &= \frac{\mu N(\alpha_i I_i+\eta)}{\mu(\alpha_i I_i+\eta)+\sigma\beta_i\alpha_i MI_i}, \\ I_j &= 0 \\ V_i &= \frac{\alpha_i I_i M}{(\alpha_i I_i+\eta)} \\ V_j &= 0 \end{aligned}$$

where $i \neq j$,

3. the coexistent steady state

$$P^* = (S_1, I_1, S_2, I_2, V_1, V_2) = (S_1^*, I_1^*, S_2^*, I_2^*, V_1^*, V_2^*)$$

where

$$\begin{aligned} S_1^* &= \frac{\mu(\alpha_1 I_1+\alpha_2 I_2+\eta)N}{\mu(\alpha_1 I_1+\alpha_2 I_2+\eta)+\beta_1\alpha_1 MI_1+\sigma\beta_2\alpha_2 MI_2} \\ I_1^* &= \frac{\mu\eta[(R_1-1)(\mu\alpha_2+\beta_2\alpha_2 M)-(R_2-1)(\mu\alpha_2+\sigma\beta_2\alpha_2 M)]}{(\mu\alpha_1+\beta_1\alpha_1 M)(\mu\alpha_2+\beta_2\alpha_2 M)-(\mu\alpha_1+\sigma\beta_1\alpha_1 M)(\mu\alpha_2+\sigma\beta_2\alpha_2 M)} \\ S_2^* &= \frac{\mu(\alpha_1 I_1+\alpha_2 I_2+\eta)N}{\mu(\alpha_1 I_1+\alpha_2 I_2+\eta)+\beta_2\alpha_2 MI_2+\sigma\beta_1\alpha_1 MI_1} \\ I_2^* &= \frac{\mu\eta(R_2-1)-(\mu\alpha_1+\sigma\beta_1\alpha_1 M)I_1}{(\mu\alpha_2+\beta_2\alpha_2 M)} \\ V_1^* &= \frac{\alpha_1 MI_1}{(\alpha_1 I_1+\alpha_2 I_2+\eta)} \\ V_2^* &= \frac{\alpha_2 MI_2}{(\alpha_1 I_1+\alpha_2 I_2+\eta).} \end{aligned}$$

Stability analysis

Stability conditions of each steady state can be found by considering signs of eigenvalues of the Jacobian matrix of the system at the steady state or applying the Routh-Hurwitz criteria. The Jacobian matrix of the system (3.1.4) is

$$J = \begin{bmatrix} -\mu-\beta_1 V_1-\sigma\beta_2 V_2 & 0 & 0 & 0 & -\beta_1 S_1 & -\sigma\beta_2 S_1 \\ \beta_1 V_1 & -(\mu+\nu) & 0 & 0 & \beta_1 S_1 & 0 \\ 0 & 0 & -\mu-\beta_2 V_2-\sigma\beta_1 V_1 & 0 & -\sigma\beta_1 S_2 & -\beta_2 S_2 \\ 0 & 0 & \beta_2 V_2 & -(\mu+\nu) & 0 & \beta_2 S_2 \\ 0 & \alpha_1(M-V_1-V_2) & 0 & 0 & -\alpha_1 I_1-\eta & -\alpha_1 I_1 \\ 0 & 0 & 0 & \alpha_2(M-V_1-V_2) & -\alpha_2 I_2 & -\alpha_2 I_2-\eta \end{bmatrix}. \tag{3.1.5}$$

At the disease-free steady state, two eigenvalues of the Jacobian matrix are $-\mu$, $-\mu$, and the rests are those of of the characteristic equation

$$(\lambda^2+(\mu+\nu+\eta)\lambda+\eta(\mu+\nu)-\alpha_1\beta_1 NM)(\lambda^2+(\mu+\nu+\eta)\lambda+\eta(\mu+\nu)-\alpha_2\beta_2 NM)=0$$

The first polynomial has two negative real roots (the increment is always positive) if and only if

$$R_{01} = \frac{\alpha_1\beta_1 NM}{\eta(\mu+\nu)} < 1$$

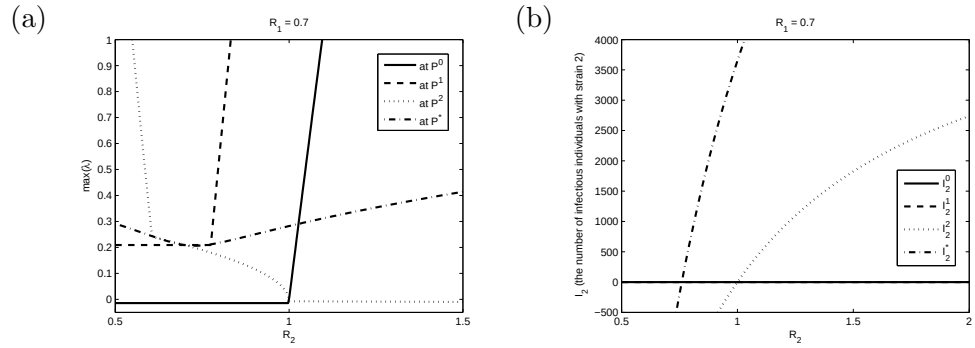

Figure 3-1: (a) A bifurcation graph when $R_{01} = 0.7$ of R_{02} against $\max(\lambda)$ (b) A graph when $R_{01} = 7$ of R_{02} against I_2 at the steady states

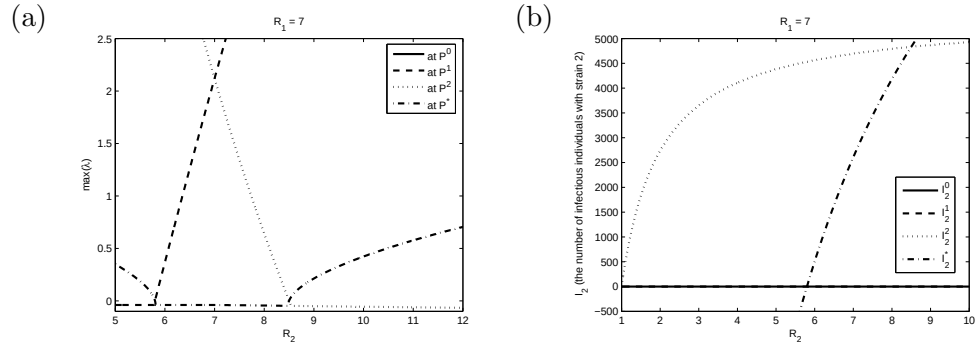

Figure 3-2: (a) A bifurcation graph when $R_{01} = 7$ of R_{02} against $\max(\lambda)$ (b) A graph when $R_{01} = 0.7$ of R_{02} against I_2 at the steady states

and the second polynomial has two negative real roots (the increment is always positive) if and only if

$$R_{02} = \frac{\alpha_2 \beta_2 NM}{\eta(\mu + \nu)} < 1.$$

Hence, the disease-free steady state is stable if and only if $R_{01} < 1$ and $R_{02} < 1$. Similarly, the stability conditions of the other steady states can be found by considering the signs of eigenvalues of the Jacobian matrix or using the Routh-Hurwitz criteria. Because the non disease-free steady states and their characteristic equations are unwieldy to deal with, we instead study them numerically.

Numerical Analysis

We assume that a human lifetime $(1/\mu)$ is 70 years and a mosquito lifetime $(1/\eta)$ is 20/365 years. An infectious period of malaria in human $(1/\nu)$ is assumed to be 14/365 years. The total size of human population (N) is 10,000,000 and the total size of mosquito population (M) is 50,000,000. The transmission probability of infection

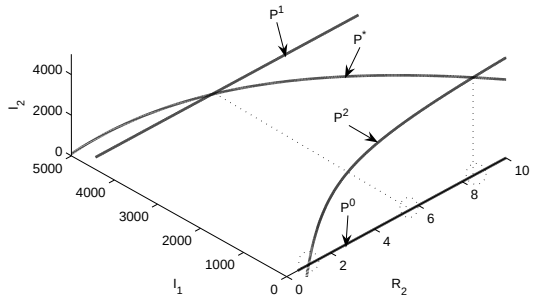

Figure 3-3: A three dimensional bifurcation graph of R_2, I_1, and I_2 at the steady states

to mosquitoes (α_1, α_2) is $1.5e-5$ for both strains. The transmission probability of infection to humans (β_1, β_2) of each strain depends on its basic reproductive ratio. The cross-immunity parameter (σ) is fixed at 0.7, otherwise it is as stated.

We choose the basic reproductive ratio of strain 2 (R_{02}) to be a bifurcation parameter and separate the basic reproductive ratio of strain 1 (R_{01}) into two cases: 1) $R_{01} < 1$, and 2) $R_{01} > 1$. R_{02} is varied by varying β_2 while other parameters are fixed. We consider the maximum of the eigenvalues $(\max(\lambda))$ of the Jacobian matrix at each steady state. If it is less than zero, all the eigenvalues of the Jacobian matrix at that steady state are negative, which implies that the steady state we consider is stable. If it is greater than zero, it is enough to say that the steady state is unstable even though the other eigenvalues are all negative. A point where two steady states exchange their stabilities ($\max(\lambda)$ of one steady state changes sign from negative to positive and the other changes sign from positive to negative) is where transcritical bifurcation occurs. We also show a cross-section graph from a three dimensional plot of the number of infectious individuals with strain 1 and strain 2 at the steady states against R_{02} along with bifurcation graphs. We note here that points, where 1) the number of infectious individuals with strain 2 at the single-strain steady steady state of strain 2 (I_2^2) changes its value from negative to positive when $R_{01} < 1$, 2) the number of infectious individuals with strain 2 at the coexistent steady state (I_2^*) changes its value from negative to positive when $R_{01} > 1$, 3) the intersection of the number of infectious individuals with strain 2 at the coexistent steady state (I_2^*) and the single-strain steady state of strain 2 (I_2^2) when $R_{01} > 1$, should be compared with the bifurcation graphs where bifurcation occurs in both cases (See Figure 3-1,3-2, and 3-3).

1. Case I: $R_{01} < 1$

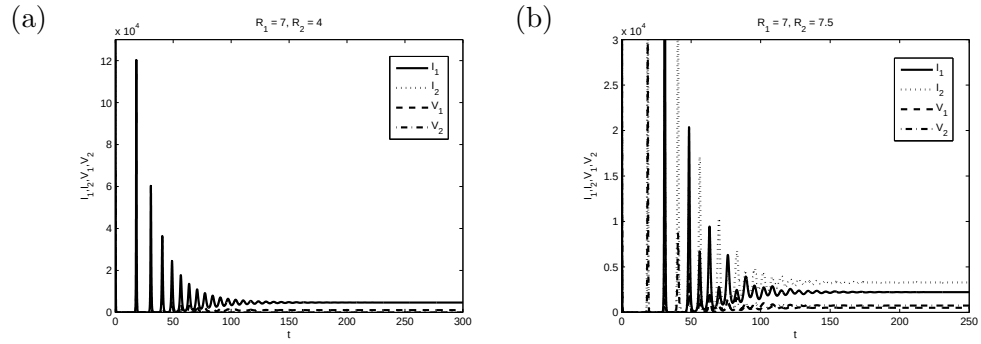

Figure 3-4: (a) A numerical result when $R_{01} = 7$ and $R_{02} = 4$ (strain 1 persists) (b) A numerical result when $R_{01} = 7$ and $R_{02} = 7.5$ (both strains coexist)

We choose $R_{01} = 0.7$. In Figure 3-1(a), the $\max(\lambda)$ of the Jacobian matrix at the disease-free steady state changes sign at $R_{02} = 1$ from negative to the positive while the $\max(\lambda)$ of the Jacobian matrix at the single-strain steady state of strain 2 changes sign from positive to the negative. Hence we have the interchange of stability of two steady states at $R_{02} = 1$. Therefore, $R_{02} = 1$ is a transcritical bifurcation value. In long term, both strains die out when $R_{02} < 1$ and strain 2 persists when $R_{02} > 1$. Also $R_{02} = 1$ is where the value of I_2^2 changes its value from negative to positive (See Figure 3-1(b)).

2. Case II: $R_{01} > 1$

   We choose $R_{01} = 7$. In this case, the $\max(\lambda)$ of the Jacobian matrix at the single-strain steady state of strain 1 changes the value from negative to positive while the $\max(\lambda)$ of the Jacobian matrix at the coexistent steady state changes sign form positive to negative at $R_{02} \approx 5.8$ (See Figure 3-2(a)). So $R_{02} \approx 5.8$ is where a first transcritical bifurcation occurs. Also $R_{02} = 5.8$ is where the value of I_2^* changes its value from negative to positive (See Figure 3-2(b)). A second transcritical bifurcation occurs when $R_{02} \approx 8.5$, which is where the $\max(\lambda)$ of the Jacobian matrix at the coexistent steady state changes its sign from negative to positive and the $\max(\lambda)$ of the Jacobian matrix at the single-strain steady state of strain 2 changes its sign from positive to negative (See Figure 3-2 (a)) and at the same bifurcation point, the coexistent steady state intersects the single-strain steady state of strain 2 (See Figure 3-2(b)). In conclusion, we have that; 1) strain 1 only persists whenever $R_{02} < 5.8$; 2) both strains coexist whenever $5.8 < R_{02} < 8.5$; and 3) strain 2 persists if and only if $R_{02} > 8.5$. We show examples of numerical results when $R_{01} = 7$ and $R_{02} = 4$ in Figure 3-4(a) such that strain 1 persists and when $R_{01} = 7$ and $R_{02} = 7.5$ in Figure 3-4(b) such that both strain coexist.

(a)

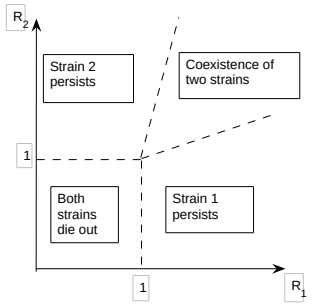

(b)

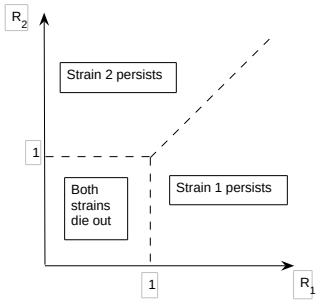

Figure 3-5: (a) A bifurcation diagram of R_{01} and R_{02} when $0 < \sigma < 1$ (b) A bifurcation diagram of R_{01} and R_{02} when $\sigma = 1$

Similarly, we can consider the case when R_{01} is vary while R_{02} is fixed for the bifurcation graphs on $R_{01} - \max(\lambda)$ plane. All in all, by considering the effect of cross-immunity in the model, the bifurcation diagrams on $R_{01} - R_{02}$ plane can be described by Figure 3-5(a)-(b). In Figure 3-5(a), the bigger the cross-immunity is, the smaller the area of the coexistence. When cross-immunity gives full protection to the other strain coexistence of the two strains is impossible (See Figure 3-5(b)).

3.1.3 Conclusion and discussion

A model of host-immune status is developed for transmission of two strains or species of malaria in which cross-immunity plays an important role. By the status-based framework with polarised immunity and the assumption that cross-immunity is conferred by exposure to the disease via an infective mosquito, rather than developing the full infection itself, the model becomes tractable with only one immune variable to describe host immunity to each strain. We study the system analytically and numerically for bifurcation analysis. We propose the threshold condition that can be used to predict

the dynamics of the strains, such that the first strain of malaria dies out whenever

$$R_{01} = \frac{\alpha_1 \beta_1 NM}{\eta(\mu + \nu)} < 1$$

and the second whenever

$$R_{02} = \frac{\alpha_2 \beta_2 NM}{\eta(\mu + \nu)} < 1.$$

Also, we investigate the system numerically when cross-immunity is present and one strain has the basic reproductive ratio greater than 1, whether another strain dies out, coexists, or drives out the other (see Figure 3-5(a)). For example, when strain 1 has the basic reproductive ratio (R_{01}), 7, only strain 1 persists whenever $R_{02} < 5.8$; both strains coexist whenever $5.8 < R_{02} < 8.5$; and only strain 2 persists whenever $R_{02} > 8.5$.

3.2 From suppression during coinfection to cross-species immunity:can it happen on malaria transmission?

Maitland et al. (1997) find that although the prevalence of *P. falciparum* and *P. vivax* in Vanuatu fluctuates, the burden of malaria remains constant. This suggests that there is direct interaction between *P. falciparum* and *vivax*. In this study, we propose a novel model that captures the presence of both malaria species, *P. falciparum* and *P. vivax*, suppression between them, and possible cross-species immunity. We introduce the single-species models, the coinfection model, and the cross-immunity model adjusted from the coinfection model by omitting mixed infection of both species. We then investigate the relations between these two species and their dynamical behaviours.

3.2.1 Single-species models

Malaria transmission occurs through interactions between two populations, human and mosquito. Each species has different characteristics such as a transmission rate, a recovery rate, relapse, and incubation time. In this section, we study single-species models of *P. falciparum* and *P. vivax*.

A malaria transmission model for *P. falciparum*

A human population is divided into three categories: susceptible (S), infectious to *P. falciparum* (I_1), and recovered from *P. falciparum* (R_1), under the assumption that a recovered individual acquires immunity from recovering (Koella and Antia, 2003;

Koella and Boete, 2003; Smith et al., 2005; Keeling and Rohani, 2008; Gaudart et al., 2009) but that immunity wanes with time (Collins et al., 1968; Burattini et al., 1993). It is often assumed that immunity depends on exposure and it is boosted by additional infections (Koella and Antia, 2003; Koella and Boete, 2003). Here, for simplicity, an individual is assumed to acquire immunity within a single infection (Gupta et al., 1999). Also, we assume that immune individuals can be reinfected with the parasites but they cannot transmit the disease (Doolan et al., 2009) due to low densities of parasitaemia or protection during curative treatment (Gaudart et al., 2009).

A mosquito population is divided into two categories: susceptible (U), and infectious to *P. falciparum* (V_1). It is assumed that infectious mosquitoes do not recover. Once infected, they remain infected for life. The model for malaria transmission caused by *P. falciparum* takes the forms:

$$\begin{aligned} \dot{S}(t) &= \mu N - \tfrac{\beta_1}{N} V_1 S - \mu S + \gamma_1 R_1, \\ \dot{I}_1(t) &= \tfrac{\beta_1}{N} V_1 S - (\mu + \nu_1) I_1, \\ \dot{R}_1(t) &= \nu_1 I_1 - (\mu + \gamma_1) R_1, \\ \dot{U}(t) &= \eta M - \tfrac{\alpha_1}{N} I_1 U - \eta U, \\ \dot{V}_1(t) &= \tfrac{\alpha_1}{N} I_1 U - \eta V_1, \end{aligned} \tag{3.2.1}$$

where $\beta_1 = bp_h$, $\alpha_1 = bp_m$, b is the biting rate, p_h is the probability of successful infection in humans, p_m is the probability of successful infection in mosquitoes. A study of this model in details can be found in the section 3.3.1.

A malaria transmission model for *P. vivax*

It has been known that relapses often occur in individuals who are infected with *P. vivax* or *P. ovale* (Cogswell, 1992). Clinically, relapse means a return of disease symptoms after its apparent cessation. During a primary attack, some hypnozoites might remain dormant in the liver instead of transforming into schizonts, and hence later cause a relapse or another attack of parasitemia (Ishikawa et al., 2003). Natural relapse malaria might be induced by *Anopheles* mosquitoes (Hulden et al., 2008). Mathematical models for studying *P. vivax* are not numerous (Ishikawa et al., 2003; Pongsumpun and Tang, 2007). Here, we propose a basic model for simplistic use when coinfection occurs in the

next study in Section 3.2.3 as follows

$$\begin{aligned}
\dot{S}(t) &= \mu N - \tfrac{\beta_2}{N} V_2 S - \mu S + \gamma_2 R_2, \\
\dot{I}_2(t) &= \tfrac{\beta_2}{N} V_2 S - (\mu + \nu_2 + \omega_{21}) I_2 + \omega_{22} D_2, \\
\dot{D}_2(t) &= \omega_{21} I_2 - (\mu + \omega_{22}) D_2, \\
\dot{R}_2(t) &= \nu_2 I_2 - (\mu + \gamma_2) R_2, \\
\dot{U}(t) &= \eta M - \tfrac{\alpha_2}{N} I_2 U - \eta U, \\
\dot{V}_2(t) &= \tfrac{\alpha_2}{N} I_2 U - \eta V_2,
\end{aligned} \tag{3.2.2}$$

where some infectious individuals from the compartment I_2 enter the compartment D_2 when some of their hypnozoites remain dormant and they do not acquire immunity from their primary infection. Under the assumption that individuals in the D_2 compartment do not acquire the immunity, they either die due to the natural causes or reenter the I_2 compartment from relapse. The detail of flows of other compartments is similar to the model (3.2.1) in the previous section in describing the dynamics of *P. falciparum*. A flow diagram of (3.2.2) is shown in Figure 3-6. It is important to understand when an epidemic can take place, hence to calculate the basic reproductive ratio. We use the next-generation matrix $K = [k_{ij}]$ (Diekmann and Heesterbeek, 2000). We define the three infected types-at-birth; I_2: type 1; D_2 : type 2; V_2 : type 3; where type-at-birth refers to the birth of the infection in the individual rather than the individual. We define $k_{ij} = \mathbb{E}\{\#$ of type-at-birth i that a type-at-birth j gives rise to in its life time (as a type-at-birth $j)\}$. So,

$$\begin{aligned}
k_{11} &= 0, \\
k_{21} &= \tfrac{\omega_{21}}{\mu+\nu_2+\omega_{21}}, \\
k_{31} &= \tfrac{\alpha_2 q}{\mu+\nu_2+\omega_{21}}, \\
k_{12} &= \tfrac{\omega_{22}}{\mu+\omega_{22}}, \\
k_{22} &= 0, \\
k_{32} &= 0, \\
k_{13} &= \tfrac{\beta_2}{\eta}, \\
k_{23} &= 0, \\
k_{33} &= 0.
\end{aligned}$$

Hence,

$$K = \begin{bmatrix} 0 & \frac{\omega_{22}}{\mu+\omega_{22}} & \frac{\beta_2}{\eta} \\ \frac{\omega_{21}}{\mu+\nu_2+\omega_{21}} & 0 & 0 \\ \frac{\alpha_2 q}{\mu+\nu_2+\omega_{21}} & 0 & 0 \end{bmatrix},$$

whose principal eigenvalue λ is easily calculated. Here, we define the basic reproductive ratio of the system (3.2.2) as the square of the maximum eigenvalue of K. Therefore,

the basic reproductive ratio is

$$R_0^2 = \frac{\beta_2 \alpha_2 q}{\eta(\mu + \nu_2 + \omega_{21})} + \frac{\omega_{21}}{(\mu + \nu_2 + \omega_{21})} \frac{\omega_{22}}{(\mu + \omega_{22})}.$$

From the formula, R_0^2 has two components: one is from infectious individuals; the other one comes from infections due to relapses. The latter takes into account the infectious individuals that do not die in the infectious class and become inactive with the parasites. Note that some authors define R_0^2 to be a square root of this term. The study of the system (3.2.2) in detail can be found in the next section.

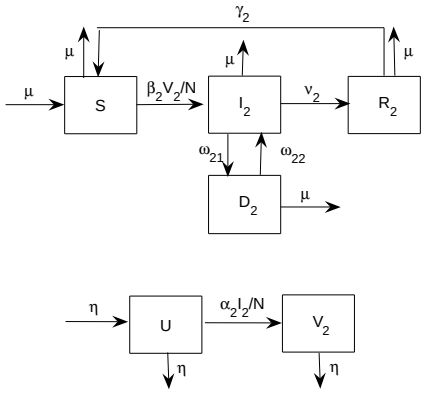

Figure 3-6: A flow diagram for malaria transmission by *P. vivax*

3.2.2 A study of the mathematical model for transmission of *P.vivax*

We introduce the new variables as follows

$$s = \frac{S}{N},\ i_2 = \frac{I_2}{N},\ d_2 = \frac{D_2}{N},\ r_2 = \frac{R_2}{N},\ u = \frac{U}{M},\ v_2 = \frac{V_2}{M}.$$

Hence, the system (3.2.2) can be rewritten by

$$\begin{aligned} \dot{s}(t) &= \mu - \beta_2 q v_2 s - \mu s + \gamma_2(1 - s - i_2 - d_2), \\ \dot{i}_2(t) &= \beta_2 q v_2 s - (\mu + \nu_2 + \omega_{21}) i_2 + \omega_{22} d_2, \\ \dot{d}_2(t) &= \omega_{21} i_2 - (\mu + \omega_{22}) d_2, \\ \dot{v}_2(t) &= \alpha_2 i_2 (1 - v_2) - \eta v_2, \end{aligned} \tag{3.2.3}$$

where $q = M/N$, $\beta_2 = b p_{h_2}$, $\alpha_2 = b p_{m_2}$, b is the biting rate of mosquitoes, p_{h_2} is the probability of successful infection of *P. vivax* in humans, and p_{m_2} is the probability of

successful infection of *P. vivax* in mosquitoes. The differential equations for r_2 and u are omitted and they can be found from $r_2 = 1 - s - i_2 - d_2$ and $u = 1 - v_2$, directly. The system (3.2.3) has two steady states:

1. the disease-free steady state

$$P^0 = (s^0, i_2^0, d_2^0, v_2^0) = (1, 0, 0, 0)$$

2. the disease-present steady state

$$P^* = (s^*, i_2^*, d_2^*, v_2^*)$$

where

$$\begin{aligned} s^* &= \frac{\mu(\mu+\omega_{22})+\gamma_2(\mu+\omega_{22})-[\gamma_2(\mu+\omega_{21}+\omega_{22})+(\mu+\nu_2)(\mu+\omega_{22})+\mu\omega_{21}]i_2^*}{(\mu+\gamma_2)(\mu+\omega_{22})}, \\ d_2^* &= \frac{\omega_{21} i_2^*}{(\mu+\omega_{22})}, \\ v_2^* &= \frac{\alpha_2 i_2^*}{(\eta+\alpha_2 i_2^*)}, \end{aligned}$$

and i_2^* is in the following form:

$$i_2^* = \frac{\beta_2\alpha_2 q(\mu+\gamma_2)(\mu+\omega_{22}) - \eta(\mu+\gamma_2)[(\mu+\nu_2)(\mu+\omega_{22})+\mu\omega_{21}]}{\beta_2\alpha_2 q[\gamma_2(\mu+\omega_{21}+\omega_{22})+(\mu+\nu_2)(\mu+\omega_{22})+\mu\omega_{21}]+\alpha_2(\mu+\gamma_2)[(\mu+\nu_2)(\mu+\omega_{22})+\mu\omega_{21}]}.$$

Since the system is unwieldy to deal with, we numerically show that vivax malaria dies out when $R_0^2 < 1$ and is endemic when $R_0^2 > 1$. Parameters in the model can be found in Table 3.1. Otherwise, they are stated. Figure 3-7 shows that *P. vivax* dies

Table 3.1: Lists of parameters for malaria transmission

Parameter	Description	Value	References
β_2	transmission rate in humans	bp_{h_2}	-
α_2	transmission rate in mosquitoes	bp_{m_2}	-
μ	birth and death rate	1/70 (year^{-1})	estimated
b	biting rate	100-182 (year^{-1})	Gupta, Swinton and Anderson (1994)
p_{h_2}	probability of successful infection in humans	0.1	Gupta, Swinton and Anderson (1994)
p_{m_2}	probability of successful infection in mosquitoes	0.2	estimated
ν_2	recovery rate	2.34 (year^{-1})	Ishikawa et al. (2003)
γ_2	rate of losing immunity	1/16 (year^{-1})	Ishikawa et al. (2003)
ω_{21}	rate of entering hypnozoite stage	0.51 (year^{-1})	Ishikawa et al. (2003)
ω_{22}	rate of relapse	365/42 (year^{-1})	Anstey et al. (2009)
η	natural death rate of mosquitoes	365/20 (year^{-1})	Anderson and May (1991)
q	the number of mosquitoes per individual	1-2	Gupta, Swinton and Anderson (1994)

Note that for estimation of ν_2 and ω_{21}, it is assumed that rate of losing infectiousness per year (ν) is 365/128 and the probability that an individual injected with sporozoites develops the hypnozoites (ξ) is approximately 0.18 (Ishikawa et al., 2003). Hence, $\nu i_2 = (1-\xi)\nu i_2 + \xi\nu i_2$, so that $\nu_2 = (1-\xi)\nu$ and $\omega_{21} = \xi\nu$. We also assume that the probability of successful infection in humans is equal in both *P. falciparum* and *P. vivax*. Due to the limited reproductive capacity from the preference of infecting young RBCs only, the fewer merozoites produced, and low level of parasitemias in vivax malaria (Anstey et al., 2009), we assume that the probability of successful infection in mosquitoes is less than one in falciparum malaria, which is approximately 0.3 (Drakeley et al., 2006).

out when the basic reproductive ratio (R_0^2) is less than 1 and it is endemic when the basic reproductive ratio is greater than 1.

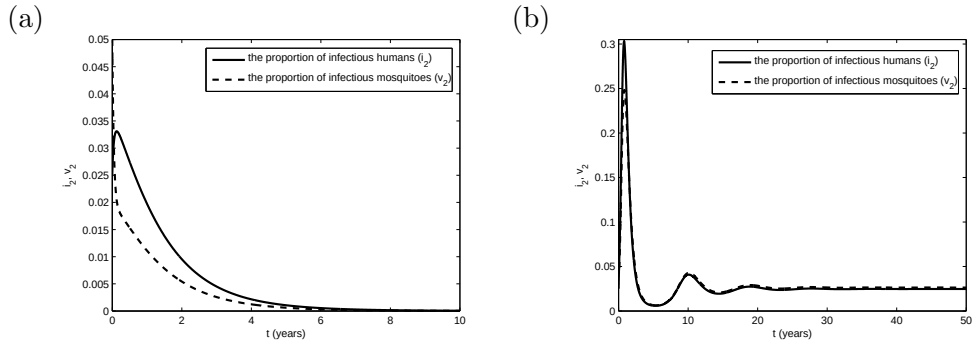

Figure 3-7: (a) *P. vivax* dies out when $R_0^2 = 0.94 < 1$ ($b = 100, q = 1, p_{h_2} = 0.06, p_{m_2} = 0.1, \nu_2 = 3.5$) (b) *P. vivax* is endemic in the host population when $R_0^2 = 4$ (from data) > 1.

3.2.3 Formulation of the coinfection model and its study

In several malaria endemic areas such as Asia, or South America, there are normally more than two species coexisting, in particular *P. falciparum* and *P. vivax* (Snounou and White, 2004). Many studies in the past have only concentrated on the transmission of *P. falciparum* due to its malignancy, although *P. vivax* is the most wide-spread and they often coexist. Here, we propose a mathematical model for studying the spread of malaria in an endemic area where both *P. falciparum* and *P. vivax* are present. We first propose a coinfection model that accounts for a host who harbours two different species at the same period. In the model, cross-species immunity is absent. A flow diagram of the model is shown in Figure 3-8.

Susceptible individuals are recruited to the host population by birth or immigration and by loss of acquired immunity to the species they previously infected with. The naive population is diminished by infection to *P. falciparum* and *P. vivax*, or natural death.

The infectious population to *P. falciparum* is increased by infection of the susceptible population and it is reduced by recovery, natural death, or coinfection with *P. vivax*. Similarly, the infectious population to *P. vivax* is increased by infection of susceptible individuals to *P. vivax*. Individuals move out from this class by recovery, natural death, relapse, or coinfection with *P. falciparum*.

Individuals infected with *P. vivax* move into the relapse class when some of their hypnozoites remain dormant in their livers instead of transforming into schizonts. They move

out from the relapse class by natural death, when another attack of parasitemia occurs so that they become infectious again, or when they get infected with *P. falciparum* while they still remain dormant with *P. vivax*.

Individuals acquire immunity to *P. falciparum* or *P. vivax* after recovering. They move out of immune classes by natural death, waning of immunity, infection with the other species.

The movement into the coinfection class is by becoming infected with both species at the same period. Individuals move out from this class by natural death, and when they recover and acquire the immunity from the parasites, either immune to *P. falciparum* or *P. vivax*. They also move out from this class because *P. vivax* becomes dormant.

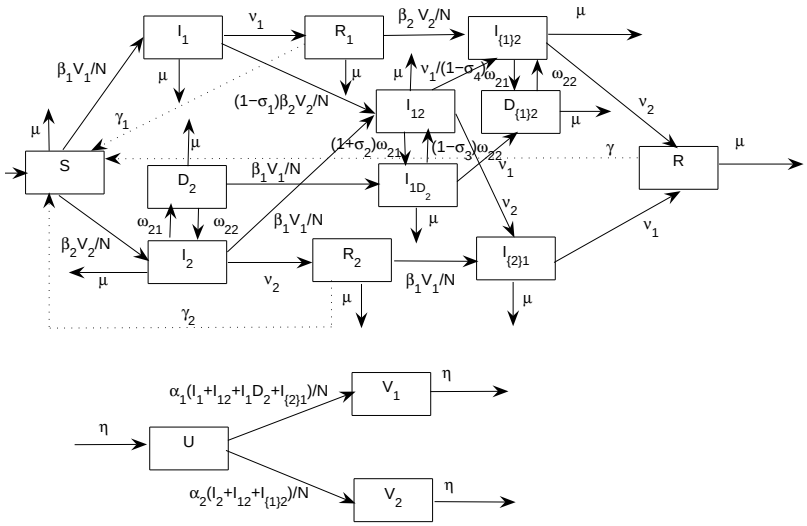

Figure 3-8: A flow diagram for a malaria transmission coinfection model

Individuals who were primarily infected with *P. falciparum* and became immune to it may become infected with *P. vivax* and enter the $I_{\{1\}2}$ class. Individuals who were previously infected with both species might become immune to *P. falciparum* and also enter this class. They move out from it when they die due to natural death, acquire immunity to *P. vivax*, or become dormant with *P. vivax*. Similarly, individuals immune to *P. vivax* may get infected with *P. falciparum* or ones who are infected with both species may become immune to *P. vivax*, so that they enter the $I_{\{2\}1}$ class. The movement out of this class is either from natural death or recovery.

For the I_{1D_2} class, which represents individuals who are infectious to *P. falciparum* but dormant with *P. vivax*, the movement into this class is from individuals who remain dormant with *P. vivax* getting infected with *P. falciparum* or individuals coinfected

with both species becoming dormant with *P. vivax*. The individuals move out this class by natural death, relapse, or recovering from *P. falciparum*.

Another dormant class relating to secondary infection is $D_{\{1\}_2}$, representing individuals who successfully acquired immunity to *P. falciparum* and infected with *P. vivax* but become dormant with it. Individuals who enter this class are either previously dormant with *P. vivax* and then infected and immune with *P. falciparum*, or primarily infected and acquired immunity to *P. falciparum* and secondarily infected with *P. vivax* and become dormant with it. The flow out of this class is from relapse and natural death.

Individuals in the class R are immune to both *P. falciparum* and *P. vivax* but the immunity wanes with time and they become completely susceptible from losing it.

Mosquitoes become infectious with *P. falciparum* or *P. vivax* when they bite infectious humans and get infected with the parasites.

In the presence of active infection with *P. falciparum*, the emergence of *P. vivax* blood-stages may be prevented by cross-species regulation and suppression (William et al., 1996; Maitland et al., 1997; Bruce et al., 2000; Bruce and Day, 2002). Hence, we assume that the number of individual infected with *P. falciparum* to become infected with *P. vivax* in the subsequent infection is reduced and *P. vivax* becomes more inactive when individuals coinfect with both species. On the other hand, infection with *P. vivax* may not protect individuals from developing subsequent infection with *P. falciparum* (Maitland et al., 1997). However, complications and clinical symptoms may be reduced comparing with those who had not suffered *P. vivax* infection (Looareesuwan et al., 1987). Here, we assume that infection with *P. vivax* helps individuals to recover from *P. falciparum* more quickly than individuals who had not experienced with *P. vivax*. Furthermore, it has been observed that infection with *P. falciparum* might suppress subsequent infection with *P. vivax* that emerges from the liver (Maitland et al., 1997; Ord et al., 2008). Consequently, we assume that relapses are reduced in individuals actively infected with *P. falciparum* but remaining inactive with *P. vivax*.

The model takes the following form:

$$
\begin{aligned}
\dot{S}(t) &= \mu(N-S) - \tfrac{\beta_1}{N}V_1 S - \tfrac{\beta_2}{N}V_2 S + \gamma_1 R_1 + \gamma_2 R_2 + \gamma R,\\
\dot{I}_1(t) &= \tfrac{\beta_1}{N}V_1 S - (1-\sigma_1)\tfrac{\beta_2}{N}V_2 I_1 - (\mu+\nu_1)I_1,\\
\dot{I}_2(t) &= \tfrac{\beta_2}{N}V_2 S - \tfrac{\beta_1}{N}V_1 I_2 - (\mu+\nu_2+\omega_{21})I_2 + \omega_{22}D_2,\\
\dot{D}_2(t) &= \omega_{21}I_2 - \tfrac{\beta_1}{N}V_1 D_2 - (\mu+\omega_{22})D_2,\\
\dot{R}_1(t) &= \nu_1 I_1 - \tfrac{\beta_2}{N}V_2 R_1 - (\mu+\gamma_1)R_1,\\
\dot{R}_2(t) &= \nu_2 I_2 - \tfrac{\beta_1}{N}V_1 R_2 - (\mu+\gamma_2)R_2,\\
\dot{I}_{12}(t) &= (1-\sigma_1)\tfrac{\beta_2}{N}V_2 I_1 + \tfrac{\beta_1}{N}V_1 I_2 + (1-\sigma_3)\omega_{22}I_{1D_2} - (\mu + \tfrac{\nu_1}{(1-\sigma_4)} + \nu_2 + (1+\sigma_2)\omega_{21})I_{12},\\
\dot{I}_{1D_2}(t) &= \tfrac{\beta_1}{N}V_1 D_2 + (1+\sigma_2)\omega_{21}I_{12} - (\mu+\nu_1+(1-\sigma_3)\omega_{22})I_{1D_2},\\
\dot{I}_{\{1\}2}(t) &= \tfrac{\beta_2}{N}V_2 R_1 + \tfrac{\nu_1}{(1-\sigma_4)}I_{12} + \omega_{22}D_{\{1\}2} - (\mu+\nu_2+\omega_{21})I_{\{1\}2},\\
\dot{I}_{\{2\}1}(t) &= \tfrac{\beta_1}{N}V_1 R_2 + \nu_2 I_{12} - (\mu+\nu_1)I_{\{2\}1},\\
\dot{D}_{\{1\}2}(t) &= \omega_{21}I_{\{1\}2} + \nu_1 I_{1D_2} - (\mu+\omega_{22})D_{\{1\}2},\\
\dot{R}(t) &= \nu_2 I_{\{1\}2} + \nu_1 I_{\{2\}1} - (\mu+\gamma)R,\\
\dot{U}(t) &= \eta M - \tfrac{\alpha_1}{N}(I_1 + I_{12} + I_{1D_2} + I_{\{2\}1})U - \tfrac{\alpha_2}{N}(I_2 + I_{12} + I_{\{1\}2})U - \eta U,\\
\dot{V}_1(t) &= \tfrac{\alpha_1}{N}(I_1 + I_{12} + I_{1D_2} + I_{\{2\}1})U - \eta V_1,\\
\dot{V}_2(t) &= \tfrac{\alpha_2}{N}(I_2 + I_{12} + I_{\{1\}2})U - \eta V_2,
\end{aligned}
\tag{3.2.4}
$$

where $0 < \sigma_1, \sigma_2, \sigma_3, \sigma_4 < 1$. The basic reproductive ratio of each species is similar to the single-species model in the previous section. Hence,

$$R_0^1 = \frac{\beta_1\alpha_1 q}{\eta(\mu+\nu_1)}, \text{ and } R_0^2 = \frac{\beta_2\alpha_2 q}{\eta(\mu+\nu_2+\omega_{21})} + \frac{\omega_{21}}{(\mu+\nu_2+\omega_{21})}\frac{\omega_{22}}{(\mu+\omega_{22})}.$$

The system is unwieldy to deal with, so we study it numerically. In addition, *P. falciparum* parasites replicate better in the warmer climate while *P. vivax* has ability in completing its sporogonic cycle so that it can be multiplied in lower temperature (Cui et al., 2003; Hoshen and Morse, 2004). Some studies support that *P. vivax* parasites tend to turn into inactive state during the highly transmission of *P. falciparum* (Maitland et al., 1997; Ord et al., 2008). Also mosquitoes tend to feed more often when the weather is warmer (Githeko et al., 2000). Here, we first introduce seasonality as a sinusoidal function in transmission rates of humans and mosquitoes of *P. falciparum* under the assumption that there is a season in each year that *P. falciparum* is highly transmitted. Hence,

$$\beta_1 = \beta_1^0(1-\beta_1^1 cos2\pi t), \text{ and } \alpha_1 = \alpha_1^0(1-\alpha_1^1 cos2\pi t).$$

Figure 3-9(a) shows the transmission rates of *P. falciparum* depending on time. The transmission of *P. falciparum* is assumed to be highest in the middle of each year. Figure 3-9(b) and Figure 3-10 show the synchronization of the prevalence of *P. falciparum* in the human population with the sinusoidal transmission rates of *P. falciparum*. How-

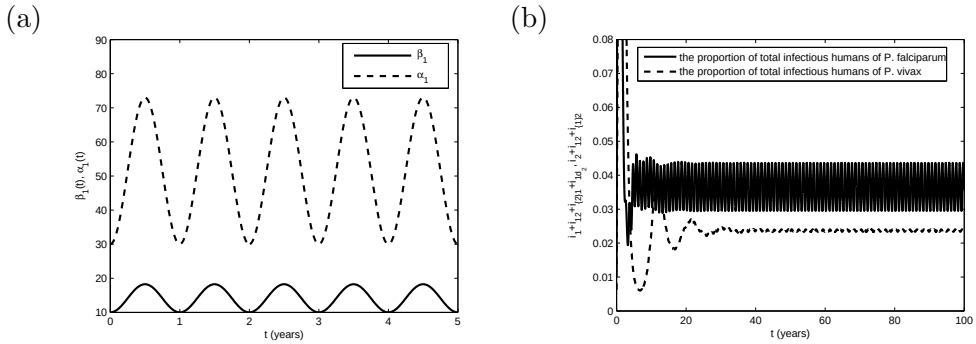

Figure 3-9: (a) Transmission rates of humans and mosquitoes in sinusoidal functions $(\min(\beta_1) = 10, \max(\beta_1 = 18.25), \min(\alpha_1) = 30, \max(\alpha_1) = 73)$ (b) This graph shows the number of infectious individuals with *P. falciparum* and *P. vivax* when transmission rates in both humans and mosquitoes of *P. falciparum* is in term of the sinusoidal function

ever, the prevalence of *P. vivax* is high between every two peaks of *P. falciparum*. This result suggests that during high transmission of *P. falciparum*, *P. vivax* might maintain lower transmission (relating to relapse mechanism) and it may highly been transmitted later when the prevalence of *P. falciparum* is low. This result corresponds to some real data of malaria transmission from other literatures (Syafruddin et al. (2009), for instance). In conclusion, by our results, the prevalence and incidences of *P. falciparum* and *P. vivax*, that seem to vary in each season in many parts of the world, may relate to mechanisms driven by malaria parasites and seasonality in mosquitoes.

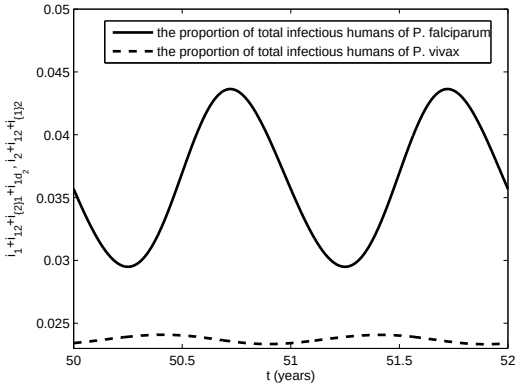

Figure 3-10: The proportions of infectious humans and mosquitoes with seasonality in *P. falciparum*

We incorporate the increase of rate of becoming inactive and the reduction of rate of relapsing of *P. vivax* of individuals infected with *P. vivax* in the presence of *P. falciparum* (William et al., 1996; Maitland et al., 1997) by introducing both of them in

terms of sinusoidal functions such that in each year during the time that *P. falciparum* is highly present, *P. vivax* is suppressed and becomes less present. Note that from above we also introduce transmission rates of *P. vivax* as sinusoidal functions. Consequently, in *P. vivax*, we have

$$\beta_2 = \beta_2^0(1+\beta_2^1 cos2\pi t), \alpha_2 = \alpha_2^0(1+\alpha_2^1 cos2\pi t), \omega_{21} = \omega_{21}^0(1-\omega_{21}^1 cos2\pi t), \omega_{22} = \omega_{22}^0(1+\omega_{22}^1)cos2\pi t.$$

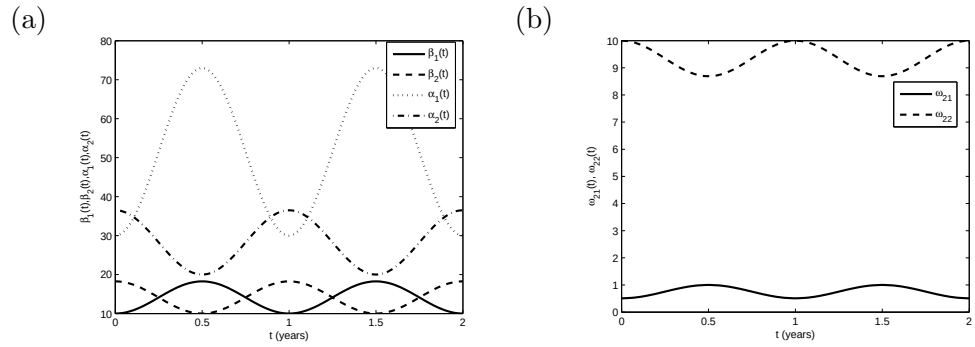

Figure 3-11: (a) Comparison of transmission rates of *P. falciparum* and *P. vivax* ($\min(\beta_1) = \min(\beta_2) = 10, \max(\beta_1) = \max(\beta_2) = 18.25, \min(\alpha_1) = 30, \max(\alpha_1) = 73, \min(\alpha_2) = 20, \max(\alpha_2) = 36.5$) (b) Rate of becoming inactive with *P. vivax* and rate of its relapsing ($\min(\omega_{21}) = 0.51, \max(\omega_{22}) = 1, \min(\omega_{22}) = 8.69, \max(\omega_{22}) = 10$)

Comparison of transmission rates between *P. falciparum* and *P. vivax* in terms of sinusoidal functions can be found in Figure 3-11(a). Rate of becoming inactive with *P. vivax* and rate of relapsing with seasonal fluctuation are shown in 3-11(b). By incorporating all those terms into the model (3.2.4), the numerical result is shown in Figure 3-12(a). We find that the prevalence of *P. falciparum* is synchronized with its transmission rate which is peak at the middle of each year and the prevalence of *P. vivax* is also synchronized with its transmission rate which is peak between every two peaks of transmission rate of *P. falciparum*. By comparing the proportion of infectious individuals in Figure 3-10 and 3-12, without including seasonality in *P. vivax*, the prevalence of *P. vivax* is high slightly before the highly transmitted season of *P. falciparum* while including seasonality in *P. vivax*, its prevalence is high in the middle of every highly transmitted season of *P. falciparum*. We introduce a simple version of this model and study the relation between two cross-immunity values, σ_1 and σ_4 in the next section. Comparing proportions of the number of infectious individuals to *P. vivax* from Figure 3-10 and Figure 3-12(a), we see that an outbreak (a jump) happens first in each year in the second case where rate of relapsing and rate of becoming inactive are sinusoidal (see Figure 3-12(b)).

(a)

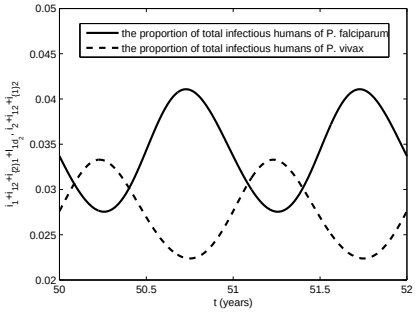

(b)

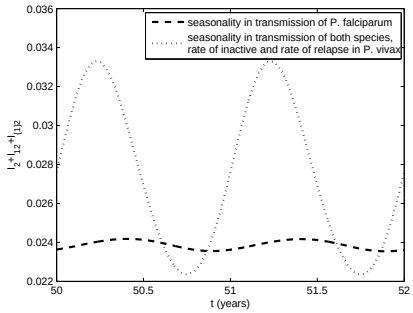

Figure 3-12: (a) The proportions of infectious humans and mosquitoes with seasonality in *P. falciparum* and *P. vivax* (b) Comparison of proportions of infectious humans with *P. vivax* from Figure 3-10 and Figure 3-12(a)

3.2.4 Formulation of the cross-species immunity model and its study

The cross-species immunity model in this section is a simplistic version of the coinfection model (3.2.4) that coinfection between *P. falciparum* and *P. vivax* is omitted. We assume that cross-species immunity is present and acts in the similar way with suppression during subsequent infection in the coinfection model. Hence, individuals immune to *P. falciparum* may have cross-species immunity that reduces transmission of *P. vivax* while individuals immune to *P. vivax* may have cross-species immunity that reduces complications and recovery time to *P. falciparum*. The flow diagram is shown in Figure 3-13. The governing equations can be described by

$$
\begin{aligned}
\dot{S}(t) &= \mu(N-S) - \tfrac{\beta_1}{N}V_1 S - \tfrac{\beta_2}{N}V_2 S + \gamma_1 R_1 + \gamma_2 R_2 + \gamma R,\\
\dot{I}_1(t) &= \tfrac{\beta_1}{N}V_1 S - (\mu+\nu_1)I_1,\\
\dot{I}_2(t) &= \tfrac{\beta_2}{N}V_2 S - (\mu+\nu_2+\omega_{21})I_2 + \omega_{22}D_2,\\
\dot{D}_2(t) &= \omega_{21}I_2 - (\mu+\omega_{22})D_2,\\
\dot{R}_1(t) &= \nu_1 I_1 - (1-\sigma_1)\tfrac{\beta_2}{N}V_2 R_1 - (\mu+\gamma_1)R_1,\\
\dot{R}_2(t) &= \nu_2 I_2 - \tfrac{\beta_1}{N}V_1 R_2 - (\mu+\gamma_2)R_2,\\
\dot{I}_{\{1\}2}(t) &= (1-\sigma_1)\tfrac{\beta_2}{N}V_2 R_1 + \omega_{22}D_{\{1\}2} - (\mu+\nu_2+\omega_{21})I_{\{1\}2},\\
\dot{I}_{\{2\}1}(t) &= \tfrac{\beta_1}{N}V_1 R_2 - (\mu+\tfrac{\nu_1}{(1-\sigma_4)})I_{\{2\}1},\\
\dot{D}_{\{1\}2}(t) &= \omega_{21}I_{\{1\}2} - (\mu+\omega_{22})D_{\{1\}2},\\
\dot{R}(t) &= \nu_2 I_{\{1\}2} + \tfrac{\nu_1}{(1-\sigma_4)}I_{\{2\}1} - (\mu+\gamma)R,\\
\dot{U}(t) &= \eta M - \tfrac{\alpha_1}{N}(I_1+I_{\{2\}1})U - \tfrac{\alpha_2}{N}(I_2+I_{\{1\}2})U - \eta U,\\
\dot{V}_1(t) &= \tfrac{\alpha_1}{N}(I_1+I_{\{2\}1})U - \eta V_1,\\
\dot{V}_2(t) &= \tfrac{\alpha_2}{N}(I_2+I_{\{1\}2})U - \eta V_2,
\end{aligned}
\tag{3.2.5}
$$

We study asymptotic solutions of the system (3.2.5) numerically. By fixing σ_4 at 0.2 and varying σ_1, we find that both species coexist when $\sigma_1 < 0.9$ and *P. vivax* dies out

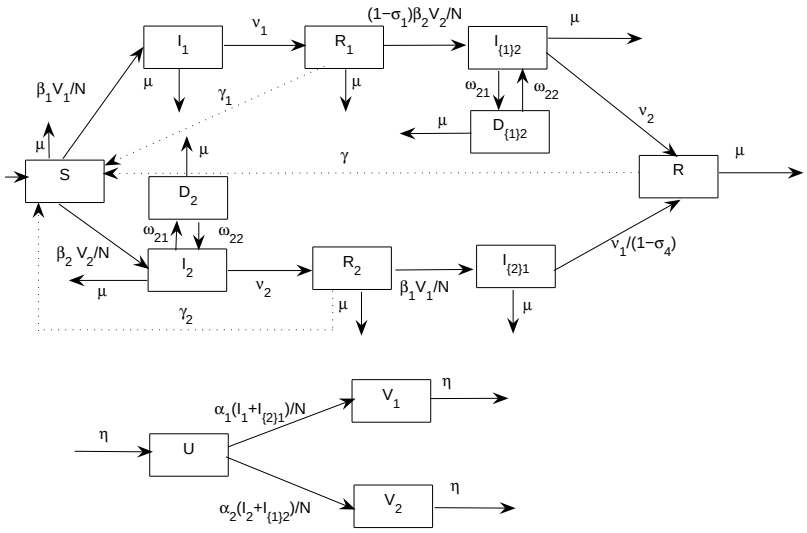

Figure 3-13: A flow diagram for a malaria transmission cross-species immunity model

when $\sigma_1 \geq 0.9$ (see Figure 3-14(a)). This is also true when σ_4 is 0 or when there is no cross-species immunity to *P. falciparum*. Hence, when cross-species immunity that acts to reduce transmission of *P. vivax* is very high (> 0.9), *P. vivax* may die out. Figure 3-14(b) shows that both species coexist for all the possible range of σ_4 ($0 \leq \sigma_4 < 1$) while σ_1 is fixed at 0.5. This is also true when $0 \leq \sigma_1 < 0.9$. Thus, both species of malaria still coexist although cross-species immunity that acts to reduce complications and recovery time of *P. falciparum* is very high. However, when cross-immunity of *P. falciparum* becomes very large (> 0.9), both species die out. The proportions of infectious humans to *P. falciparum* and *P. vivax* when both σ_1 and σ_2 vary are shown in Figure 3-15. Note that $R_0^1 = 8$ and $R_0^2 = 4$ for all cases.

(a) (b)

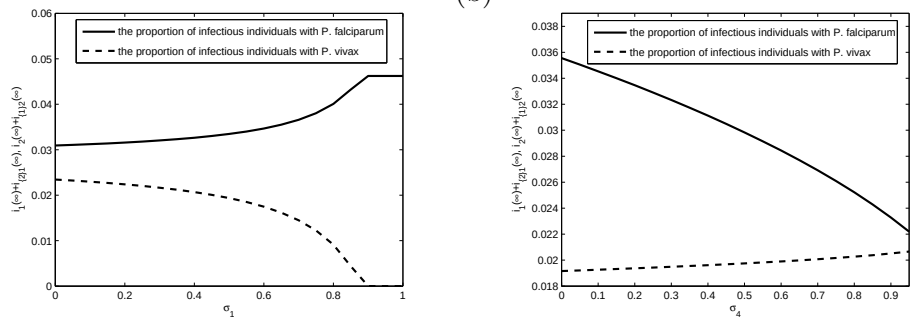

Figure 3-14: (a) Asymptotic solutions of infectious humans with *P. falciparum* and *P. vivax* when σ_1 varies between 0 and 1 ($R_0^1 = 8, R_0^2 = 4, \sigma_4 = 0.2$) (b) Asymptotic solutions of infectious humans when σ_4 varies between 0 and 0.95 ($\sigma_1 = 0.5$)

We next study the mean age at infection of humans. We calculate it by considering the mean time an individual remains susceptible to each species (Keeling and Rohani, 2008). By ignoring the small natural mortality term, the mean age at infection of *P. falciparum* is approximated by

$$A_1 = \frac{1}{\beta_1 V_1^*/N} = \frac{1}{\beta_1 q v_1^*},$$

where V_1^*, v_1^*, q are the number of mosquitoes infected with *P. falciparum* at the steady state, its proportion, and the number of mosquitoes per human, respectively. Note that in this case there are two possible steady states of the system (3.2.5), the single-species steady state of *P. falciparum* and the coexistence steady state. Similarly, the mean age at infection of *P. vivax* is approximated by

$$A_2 = \frac{1}{\beta_2 V_2^*/N} = \frac{1}{\beta_2 q v_2^*},$$

where V_2^* and v_2^* are the number of mosquitoes infected with *P. vivax* at the steady state and its proportion. In Figure 3-16(a), we show that the mean age at infection of *P. falciparum* relates to cross-species immunity. In the presence of both cross-species immunities ($\sigma_1 > 0, \sigma_4 > 0$), the mean age at infection of *P. falciparum* is increased so that susceptible individuals averagely become infected after when the cross-species immunities are both absent. The mean age at infection of *P. falciparum* is shortest when cross-immunity of *P.falciparum* to *P. vivax* is present but cross-immunity of *P. vivax* to reduce complications of *P. falciparum* is absent ($\sigma_1 > 0, \sigma_4 = 0$). On the other hand, when the later is present and the former is absent ($\sigma_1 = 0, \sigma_4 > 0$), the mean age at infection is longest. Consequently, the presence of cross-species immunity of *P. vivax* that reduces the complications of *P. falciparum* helps with the longer mean age at infection of *P. falciparum* but the presence of cross-species immunity of *P. falciparum* to reduce transmission of *P. vivax* reduces it to be shorter. Figure 3-16(b) shows the mean age at infection of *P. vivax*. When both of the cross-species immunities are present, the mean age at infection of *P. vivax* is increased. It is shortest when cross-immunity that reduces the *falciparum* complication in term the recovery time is present while cross-immunity of *P. falciparum* to reduce transmission of *P. vivax* is absent ($\sigma_1 = 0, \sigma_4 > 0$). In contrast, it is longest when the latter is absent while the former is present. In conclusion, the presence of cross-species immunity of *P. falciparum* to *P. vivax* lengthens the mean age at infection of *P. vivax* while the presence of cross-species immunity of *P. vivax* to *P. falciparum* alone shortens it. This conclusion only clearly occurs when the basic reproductive ratios of *P. falciparum* and *P. vivax* are quite small ($R_0^1 < 4, R_0^2 < 2.5$). Whenever the basic reproductive ratios of the malaria species become much bigger, the presence of cross-immunity does not help much with reducing the mean age at infection.

We note here that in hyperendemic areas, people become infected with malaria in an early age (< 5 year old) (Gupta and Day, 1994). In our simulation, from real data in Table 3.1 and 3.2, we have $R_0^1 \approx 8$ and $R_0^2 \approx 4$. Our estimation for the mean age at infection of *P. falciparum* is 2 year old and it is 4 year old for *P. vivax*. In contrast, if we know the mean age at infection of the population, we can approximate the basic reproductive ratio of each species of malaria. From our model, if the mean age at infection is approximately less than 5 year old, the basic reproductive ratio for *P. falciparum* should be greater than 4 while the basic reproductive ratio for *P. vivax* should be greater than 3.5.

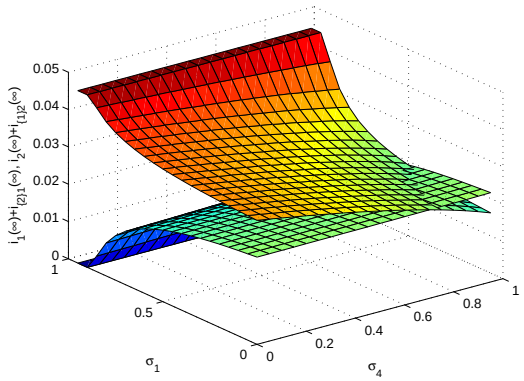

Figure 3-15: The proportion of infectious humans when σ_1 and σ_4 vary ($R_0^1 = 8, R_0^2 = 4$)

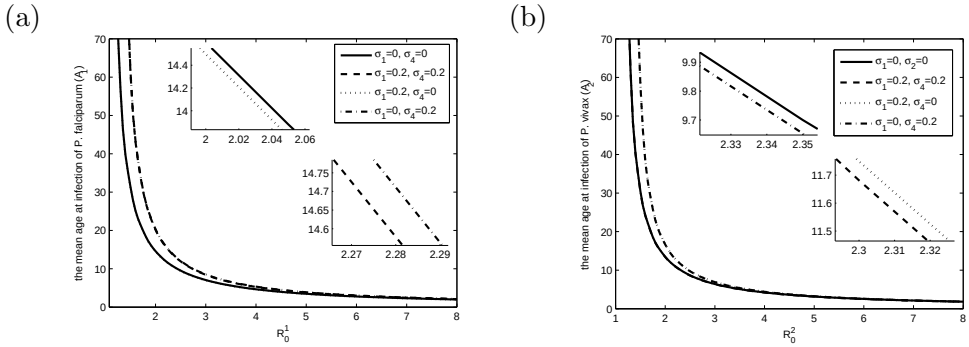

Figure 3-16: (a) A relation of mean age at infection of *P. falciparum* (A_1), the basic reproductive ratio (R_0^1), σ_1, and σ_4 (b) A relation of mean age at infection of *P. vivax* (A_2), the basic reproductive ratio (R_0^2), σ_1, and σ_4

3.2.5 Conclusion and discussion

In this work, we propose two single-species models for *P. falciparum* and *P. vivax*. We study the model for *P. falciparum* transmission in detail in the next section. For

the transmission model of *P. vivax*, there are two steady-states, the disease-free steady state and the disease-present steady state. We introduce the basic reproductive ratio of the system and show that *P. vivax* dies out when it is less than 1 and endemic when it is greater than 1 numerically.

We next introduce a novel model that accounts for coinfection of both species and suppression during their subsequent infection. Under the assumption that transmission of *P. falciparum* is seasonal and can be described by a sinusoidal function such that the highest transmission occurs in the middle of each year, we find that the prevalence of *P. falciparum* is synchronized with its transmission so that it is peak in the middle of every year. Moreover, we find that the highest prevalence of *P. vivax* takes place between every two peaks of *P. falciparum* and slightly before where the highest prevalence of *P. falciparum*. Next, we introduce sinusoidal functions in transmission of *P. falciparum* and *P. vivax*, rate of becoming inactive to *P. vivax*, and rate of relapsing to capture interactions and suppressions between these two species. In this case, the highest prevalence of *P. vivax* occurs in the middle of every highly transmitted season of *P. falciparum*. Let us assume that *P. falciparum* is highly transmitted in wet season. Hence, without including seasonality in *P. vivax*, the prevalence of *P. vivax* is high slightly before the wet season while including seasonality in *P. vivax*, its prevalence is high in dry season (in the middle of every wet season). In each area, *P. vivax* may interact with *P. falciparum* differently. For example, in where hot season is short and winter is long, it may try to avoid interaction with *P. faciparum* via relapse mechanism, suppression during infections, and capability of multiplying in cold weather. In this case, the model including seasonality in transmission and relapse rate might be suitable for using. In contrast, where hot and wet seasons are long and winter is short, *P. vivax* may not be able to avoid encountering with *P. falciparum*. Hence, the high prevalence of *P. vivax* might occur close the same season with *P. falciparum* which is when the environments are most suitable for the parasites for multiplying and surviving. In this case, the model including only the seasonality in *P. falciparum* might be enough to describe the dynamical behaviours of the system and the prevalence of malaria.

We further investigate the relation between cross-immunity values σ_1 and σ_4, cross-immunity of *P. falciparum* to reduce transmission of *P. vivax* and cross-immunity of *P. vivax* to reduce complication of *P. falciparum* (a shorter recovery time in this case), in a cross-immunity species model that the presence of cross-species immunity is assumed and acts in the similar way with suppression during subsequent infection. We find that when σ_1 is very high, *P. vivax* may die out from the population while both coexist no matter how large σ_4 is unless σ_1 is very high (> 0.9). Cross-immunity of *P. falciparum* to reduce transmission of *P. vivax* may be an important mechanism in reducing the number of infectious individuals to *P. vivax*.

In the study of the mean age at infection in the cross-species immunity model, cross-immunity of *P. vivax* to reduce the recovery time in *P. falciparum* increases the mean age at infection of *P. falciparum* (as more humans become immune to *P. falciparum*) while cross-immunity of *P. falciparum* to reduce transmission of *P. vivax* reduces it to be shorter (as humans become immune to *P. vivax* but still susceptible to *P. falciparum*). On the other hand, cross-immunity of *P. falciparum* to *P. vivax* increases the mean age at infection of *P. vivax* (as individuals become immune to *P. vivax*) while cross-immunity of *P. vivax* to *P. falciparum* reduces it (as individuals become immune to *P. falciparum* quickly but still susceptible to *P. vivax*). This obviously occurs when the basic reproductive ratios of *P. falciparum* and *P. vivax* are quite small. However, if the basic reproductive ratios of the malaria species become much bigger, the presence of cross-immunity does not much alter the mean age at infection. From this study, we can also estimate the mean ages at infection for *P. falciparum* and *P. vivax* as 2 year old and 4 year old. The formula can also be adjusted to find the basic reproductive ratios of both species when the mean age at infection of each species is known.

All in all, our goal for this work is to try to understand the interactions and suppression between *P. falciparum* and *P. vivax* when they are commonly present in the endemic area. The models we proposed capture suppression during subsequent infection and the presence of cross-species immunity. They help us to understand more about the seasonal prevalence of each species, relations between cross-species immunity, and the mean age at infection of each species. This work can be extended to cover disease controls, or incubation time of each species, for example.

3.3 Additional work on a single-strain/species model

Anopheles mosquitoes were identified as malaria vectors over 100 years ago. In one endemic area, many species of them might be present. For example, in Africa, *An. gambiae* Giles *sensu stricto*, *An. funestus* Giles *sensu stricto*, and *An. arabiensis* Patton play major roles in malaria transmission in human (Coetzee et al., 2000; Okello et al., 2006; Kent et al., 2007). The first two species are strikingly anthropophilic while the latter is more zoophilic (Githeko et al., 1994). It has been known that several blood-seeking mosquitoes search for their meal by making use of host odours (Takken and Knols, 1999). Moreover, carbon dioxide from a vertebrate's exhalation also acts as a kairomone for the mosquito recipients (Costantini et al., 1996; Mukabana et al., 2004). A recent study shows that malaria parasites manipulate a host to be more attractive to mosquitoes (Lacroix et al., 2005). In many endemic regions, seasonal variation in temperature and rainfall affects the abundance of mosquitoes, rainfall increases the numbers of mosquitoes and the incubation time of the malaria parasites in mosquitoes

is reduced when the temperature is warmer (Hoshen and Morse, 2004).

Several mathematical models have been created to study the dynamics of malaria transmission. Many are focused on mechanisms in human such as immunity, waning of immunity, symptomatic and asymptotic infection, and incubation time. In this work, we concentrate on the dynamical behaviour of malaria transmission driven by various factors in mosquitoes including seasonality, incubation time, and attractiveness to infectious humans. In this section, we discuss two different single-strain models. In the first model, we use the $SIRS$ model for describing the dynamics of hosts while the SI model is used in mosquitoes (Koella and Antia, 2003; Koella and Boete, 2003; Smith et al., 2005; Gaudart et al., 2009). Then we introduce each factor that might affect mosquitoes into the model (seasonality, incubation time, and attractiveness to infectious individuals, respectively) to study the dynamical behaviours due to the presence of each factor to the system. In many malaria transmission model with the presence of immunity in hosts, it is known that the duration of immunity depends on exposure, so that immunity is boosted by additional infections (Koella and Antia, 2003; Koella and Boete, 2003). Immune individuals can be reinfected with the parasites but they only carry low densities of parasitaemia so that they cannot transmit the disease (Doolan et al., 2009). Also, it can be thought that immune individuals are those who are resistant to the disease during curative treatment (Gaudart et al., 2009). For simplicity, in this work, we assume that an individual can acquire immunity from high-density parasitaemia after a single infection, and immunity acts against high-density parasitaemia but it wanes with time (Collins et al., 1968; Burattini et al., 1993). In the second model, we introduce a vector-bias term in the SIS and SI framework to model the host population and the mosquito population. In this case, infectious hosts are assumed to be susceptible immediately after recovering. Hence, infections can repeatedly occurs in the same individual. Then, we introduce incubation time in mosquitoes into the vector-bias model, and discuss a travelling wave of malaria propagation.

3.3.1 Modelling complex life-histories of mosquitoes on the effect of malaria transmission

This work is organized as follows. First, we introduce the basic model, that hosts acquire immunity but that it wanes with time (SIRS). We keep the model for hosts quite simple so as to concentrate on the biology of mosquitoes. Mosquitoes are assumed to be either susceptible or infected with malaria (SI). Once infected, they remain infected for life. Second, we incorporate the seasonal forcing into the mosquito population to study the effects of it on malaria transmission, when the size of mosquito population and the transmission rate depend on seasonality. Third, since an extrinsic incubation period in

mosquitoes is important to the parasites in determining whether the mosquitoes can transmit the parasites during their lifetime, a time delay due to incubation is introduced into the mosquito population, and the delay system is studied. Fourth, behaviours of mosquitoes are translated into mathematical terms and encapsulated into the model to study the spread of malaria. Fifth, we discuss the system when controls in mosquitoes are present. Finally, we close this work by commenting on the role of immunity, the behaviours of mosquitoes, and controls on mosquitoes, on the dynamics of malaria.

Formulation of the model

Malaria transmission consists of interactions between two populations, human and mosquito. A human population is categorized into three compartments: susceptible (S), infectious (I), and recovered (R), while a mosquito population is divided into two compartments: susceptible (U) and infectious (V), under the assumption that the parasites are not harmful to mosquitoes and mosquitoes do not recover from them. Individuals are protected from further infections while they are infectious. Recovered individuals acquire immunity, but the immunity wanes with time. To be precise, we define recovered individuals as persons who can be reinfected with the parasites but only carry low densities of parasitaemia (Doolan et al., 2009), and for simplicity in this work, the level of parasitaemia in blood is assumed to be low enough not to transmit the disease. We also assume that humans and mosquitoes are born disease-free, so there is no vertical transmission in either population. The flow diagram is shown in Figure 3-17. The model takes the form:

$$\begin{aligned} \dot{S}(t) &= \mu N - f_1(V)S - \mu S + \gamma R, \\ \dot{I}(t) &= f_1(V)S - (\mu + \nu)I, \\ \dot{R}(t) &= \nu I - (\mu + \gamma)R, \\ \dot{U}(t) &= B - f_2(I)U - \eta U, \\ \dot{V}(t) &= f_2(I)U - \eta V, \end{aligned} \tag{3.3.1}$$

where N is the total size of the human population and we denote M here as the total size of the mosquito population. In the model, $f_1(V)$ and $f_2(I)$ represent forces of infection in human and mosquito, respectively, which we define in the next section.

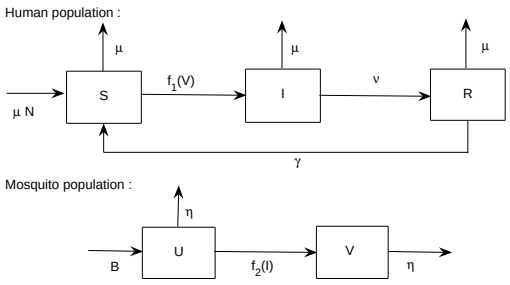

Figure 3-17: A flow diagram for the SIRS-SI model

Analysis and numerical results of a basic model

For simplicity, we treat forces of infections in human and mosquito to be frequency dependent as follows:

$$f_1(V) = \frac{\beta V}{N} = \frac{bp_h V}{N}, \tag{3.3.2}$$

$$f_2(I) = \frac{\alpha I}{N} = \frac{bp_m I}{N} \tag{3.3.3}$$

where β, α, b, p_h, and p_m represents transmission rate in human and mosquito, the biting rate, and the probability of successful infection in human and mosquito, respectively. Since the total size of each population is constant, we may introduce new variables,

$$s = \frac{S}{N},\ i = \frac{I}{N},\ r = \frac{R}{N},\ u = \frac{U}{M},\ v = \frac{V}{M},$$

and a parameter $q = M/N$. The system (3.3.1) becomes

$$\begin{aligned} \dot{s}(t) &= \mu - \beta q v s - \mu s + \gamma(1 - s - i), \\ \dot{i}(t) &= \beta q v s - (\mu + \nu) i, \\ \dot{v}(t) &= \alpha i(1 - v) - \eta v. \end{aligned} \tag{3.3.4}$$

Note that the derivative equations of r and u are omitted as the solutions can be found directly from $r = 1 - s - i$ and $u = 1 - v$. The basic reproductive ratio of the system is

$$R_0 = \frac{\beta \alpha q}{\eta(\mu + \nu)} = \frac{b^2 p_h p_m q}{\eta(\mu + \nu)}$$

(Note: some authors define R_0 to be the square root of this expression.). Parameter values can be found in Table 3.2 The system has two steady states:

1. the disease-free steady state:

$$P^0 = (s^0, i^0, v^0) = (1, 0, 0),$$

2. the disease-present steady state:

$$P^* = (s^*, i^*, v^*)$$

where

$$i^* = \frac{\eta(\mu+\gamma)(R_0-1)}{(\mu+\gamma)\alpha + (\mu+\gamma+\nu)\eta R_0}, \text{ and } s^* = \frac{(\mu+\gamma)-(\mu+\gamma+\nu)i^*}{(\mu+\gamma)}, \; v^* = \frac{\alpha i^*}{\alpha i^* + \eta}.$$

By considering the eigenvalues of the jacobian matrix of the system (3.3.4), it may be shown that the disease-free steady state is stable if and only if $R_0 < 1$. Moreover, whenever $R_0 > 1$, the disease-present steady state exists and is stable. The proof uses the Routh-Hurwitz criteria, but it is omitted here. A transcritical bifurcation, where two steady states exchange their stability, occurs at $R_0 = 1$ (see Figure 3-18). From the expression for i^* above or Figure 3-18, we can see that the proportion of infectious humans (i^*) is an increasing function of γ and hence a decreasing function of the period of immunity $1/\gamma$.

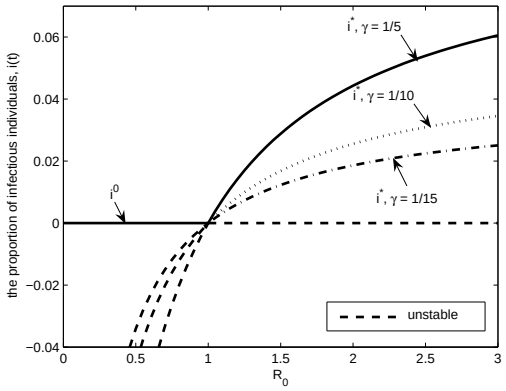

Figure 3-18: A transcritical bifurcation diagram

Seasonality

Because the abundance of mosquitoes can be increased due to rainfall, we incorporate a sinusoidal function into the basic recruitment rate to describe the high number of mosquitoes during the wet season (Muir, 1988; Anderson and May, 1991). We assume

Table 3.2: Lists of parameters for malaria transmission

Parameter	Description	Value	References
B	recruitment rate of mosquitoes	$\eta q N$	-
β	transmission rate in humans	bp_h	-
α	transmission rate in mosquitoes	bp_m	-
N	the total size of human population	200000	estimated
μ	birth and death rate	1/70 (year^{-1})	estimated
b	biting rate	100-182 (year^{-1})	Gupta, Swinton and Anderson (1994)
p_h	probability of successful infection in humans	0.1	Gupta, Swinton and Anderson (1994)
p_m	probability of successful infection in mosquitoes	0.3-0.4	Drakeley et al. (2006)
ν	recovery rate	365/180 (year^{-1})	Fillipe et al. (2007)
γ	rate of losing immunity	1/10 (year^{-1})	Collins et al. (1968)
η	natural death rate of mosquitoes	365/20 (year^{-1})	Anderson and May (1991)
q	the number of mosquitoes per individual	1-2	Gupta, Swinton and Anderson (1994)
τ	the incubation time in mosquitoes	10 (days)	Collins et al. (1968)

that the mosquito recruitment is low at the beginning and the end but peaks at the middle of every year. For this section, the system we consider is formally the same as in section 3.3.1, namely (3.3.1) with forces of infection given by (3.3.2) and (3.3.3). However, a seasonal fluctuation in the mosquito recruitment rate is in the following form:

$$B(t) = B_0(1 - B_1 \cos 2\pi t). \tag{3.3.5}$$

where the period of the forcing is 1 year (see Figure 3-19(a)). The transmission rate is assumed to be a constant. The total size of the mosquito population is now not constant but time-dependent, and can be found from the following formula:

$$M(t) = B_0 \left[\frac{1}{\gamma} - \frac{B_1}{\gamma(1 + (2\pi/\gamma)^2)} \left(\cos 2\pi t + \frac{2\pi}{\gamma} \sin 2\pi t \right) - e^{-\gamma t} \left(\frac{1}{\gamma} - \frac{B_1}{\gamma(1 + (2\pi/\gamma)^2)} \right) \right].$$

The seasonal fluctuation in the recruitment rate results in annual dynamics of malaria, with high prevalence during the rainy season each year according to the abundance of mosquitoes (see Figure 3-19(b)). Note that there is a transient outbreak which is then followed by the synchronicity of infectious human and mosquito populations relating to the recruitment number of mosquitoes.

In addition, mosquitoes tend to feed more frequently in warmer climates (Githeko et al., 2000). This might affect malaria transmission by inducing the higher biting rate of mosquitoes (b) during the hot season in the model. Consequently, transmission rates in humans and mosquitoes are increased. Moreover, the replication of malaria parasites in mosquitoes also increases in warmer temperatures (Hoshen and Morse, 2004) which might be represented in the model in term of increasing the probability of successful infection in mosquitoes (p_m). Hence, the transmission rate in mosquitoes is increased. The force of infection in humans is now described by

$$f_1(V) = \frac{\beta(t)V}{N} = \frac{\beta_0(1 - \beta_1 cos 2\pi t)V}{N} \tag{3.3.6}$$

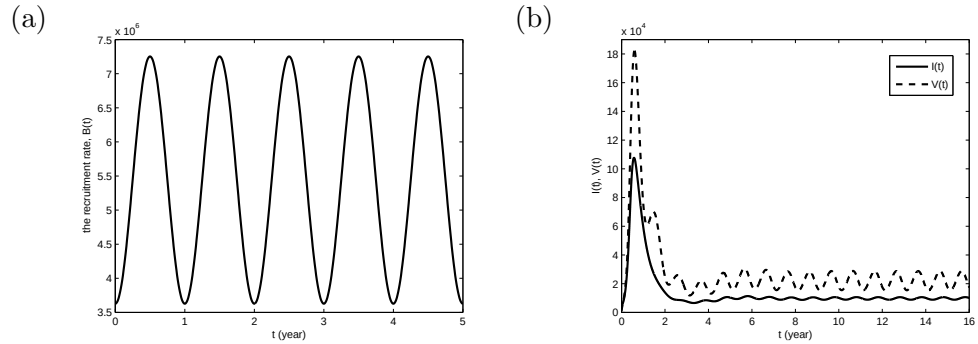

Figure 3-19: (a) A seasonal fluctuation in the recruitment rate ($\gamma = 1/10, b = 100, p_h = 0.1, p_m = 0.3, N = 200,000, B_0 \approx 5,400,000, B_1 \approx 0.33$. Note that B_0 and B_1 are approximated from the function $B(t)$ that at $\min(B(t))$, $R_0 = 8$ and $q \approx 1$ while at $\max(B(t))$, $R_0 = 16$ and $q \approx 2$ (b) The annually dynamical results from varying the recruitment rate while the transmission rate is fixed.

where the transmission rate in humans depends on time and it is a sinusoid with the period of the forcing 1 year. The force of infection in mosquitoes is:

$$f_2(I) = \frac{\alpha(t)I}{N} = \frac{\alpha_0(1 - \alpha_1 cos 2\pi t)I}{N} \tag{3.3.7}$$

where the transmission rate in mosquitoes is time-dependent and sinusoidal. The total sizes of both populations become time-dependent. By fixing the recruitment rate B as a constant, the seasonal fluctuation in the transmission rate for both humans and mosquitoes is shown in Figure 3-20(a). In Figure 3-20(b), a big outbreak occurs in the first two years. After that, the prevalence is synchronized in both populations and occurs annually corresponding to the transmission rate that is high in hot season and low in the other seasons in each year.

Assuming that we have higher transmission rate in the hot season, higher numbers of mosquitoes in the rainy season, and both of them are described by sinusoidal functions, we introduce the fraction 1/3 year to represent a time-gap from the middle of one season to another season in each year (such as Thailand that each year consists of 3 seasons; hot, rainy, and winter) into the time variable in the equations (3.3.6)-(3.3.7) so that $\cos(2\pi t)$ is changed to $\cos(2\pi(t + 1/3))$ for the hot season (see Figure 3-21(a)). Hence, the peak of transmission rate is 4 months before the peak of the recruitment rate in the sinusoidal fluctuations. By comparing the dynamical results of $I(t)$ and $V(t)$ from those when $B = B(t)$, β=const (high numbers of mosquitoes in the rainy season) and B=const, $\beta = \beta(t + 1/3)$ (high transmission in the hot season), and $B = B(t)$, $\beta = \beta(t + 1/3)$ (high numbers of mosquitoes in the rainy season and high transmission in the hot season), the prevalence of malaria in both populations of the later case peaks between the hot and the wet season (see Figure 3-21(b)).

(a) (b)

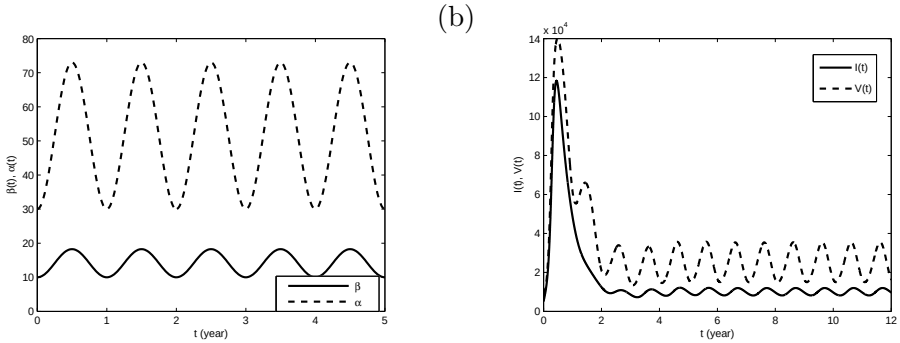

Figure 3-20: (a) A seasonal fluctuation in the transmission rate ($N = 200,000, \min(\beta) = b*p_h = 100*0.1, \max(\beta) = (182)*0.1, \min(\alpha) = b*p_m = (100)*0.3$, and $\min(\alpha) = (182)*0.4$. Note that $\min(b) = 100, \max(b) = 182, \min(p_m) = 0.3$, and $\max(p_m) = 0.4$. (b) The annually dynamical results from varying the transmission rate while the recruitment rate is fixed.

From our study, we conclude that the prevalence of malaria is high in the wet season due to the abundance of mosquitoes and it is high in the hot season due to the higher biting rate of mosquitoes and the preferable time of the parasite replications. Furthermore, for a country such as Thailand where there is a cool season, a hot season, and a wet season, each of roughly equal length, the number of mosquitoes varies between seasons. There might be more mosquitoes during the rainy season than in winter and summer, malaria parasites multiply better in the hot season, and the mosquitoes then tend to bite more often. These factors are taken into account in the model, and it suggests that the peak of prevalence is between the hot and the wet season.

(a) (b)

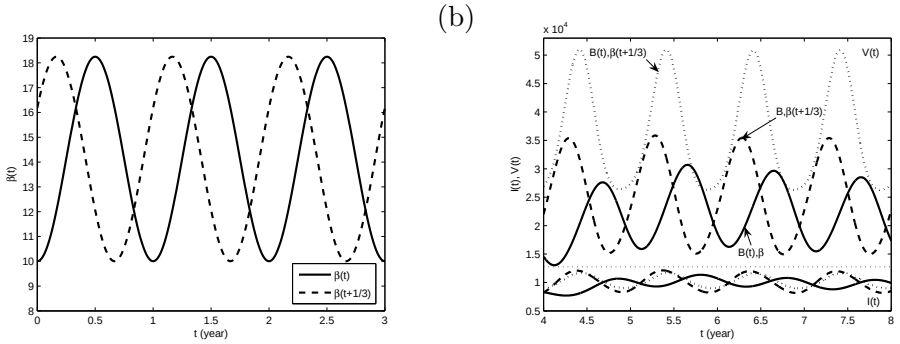

Figure 3-21: (a) A seasonal fluctuation in the transmission rate in humans when an increment between seasons (1/3 year) is added (b) A comparison of the prevalence of the disease affected by different seasons.

Incubation time in mosquitoes

Incubation time of the parasites in mosquitoes is one of crucial factors for malaria transmission due to the short lifespan of mosquitoes. It approximately takes $\tau = 10$ days after blood feeding for the sporozoites to appear in the mosquito salivary gland (Beier, 1998). During those 10 days the mosquito is infected but not infectious, and is in a latent state. For simplicity, we omit the incubation time in humans ($\approx 5.5 - 15$ days) and introduce only incubation time for mosquitoes in the model (3.3.4) (Koella, 1991; Wei et al., 2008). We make the following assumptions. On biting an infected human and successfully acquiring the malaria parasite, an initially uninfected mosquito (U) immediately enters a latent compartment (W). It leaves this latent compartment a fixed time τ later, and enters the infectious compartment (V), as long as it does not die first. Since the death rate for all mosquitoes, including those in the latent compartment, is η, the probability that it survives long enough to enter the infectious compartment is $e^{-\eta\tau}$. Hence if the flux onto the latent compartment W at time t is $\frac{\alpha}{N}I(t)U(t)$, the flux out at time t is $\frac{\alpha}{N}I(t-\tau)U(t-\tau)e^{-\eta\tau}$. The equations in terms of proportions become

$$\begin{aligned} \dot{s}(t) &= \mu - \beta q v(t) s(t) - \mu s(t) + \gamma(1 - s(t) - i(t)), \\ \dot{i}(t) &= \beta q v(t) s(t) - (\mu + \nu) i(t), \\ \dot{u}(t) &= \eta - \alpha i(t) u(t) - \eta u(t), \\ \dot{v}(t) &= \alpha i(t-\tau) u(t-\tau) e^{-\eta\tau} - \eta v(t) \end{aligned} \tag{3.3.8}$$

where $B = \eta M$ (see Figure 3-22).

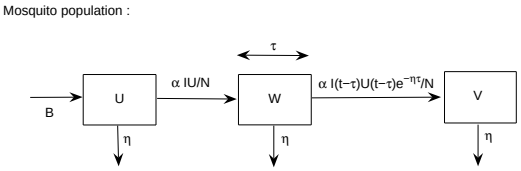

Figure 3-22: A flow diagram for the model including incubation time in mosquitoes

The basic reproductive ratio of the system is

$$R_0^\tau = \frac{\beta\alpha q e^{-\eta\tau}}{\eta(\mu + \nu)} = \frac{b^2 p_h p_m q e^{-\eta\tau}}{\eta(\mu + \nu)}.$$

The disease-free steady state is

$$P_\tau^0 = (s_\tau^0, i_\tau^0, u_\tau^0, v_\tau^0) = (1, 0, 1, 0),$$

and the disease-present steady state is as follows

$$P_\tau^* = (s_\tau^*, i_\tau^*, u_\tau^*, v_\tau^*),$$

where

$$\begin{array}{rcl} s_\tau^* & = & \frac{(\mu+\gamma)-(\mu+\nu+\gamma)i_\tau^*}{(\mu+\gamma)}, \\ i_\tau^* & = & \frac{\eta(\mu+\gamma)(R_0^\tau-1)}{R_0{*}\tau\eta(\mu+\nu+\gamma)-\alpha(\mu+\gamma)}, \\ u_\tau^* & = & \frac{\eta}{(\alpha i_\tau^*+\eta)}, \\ v_\tau^* & = & \frac{\alpha i_\tau^* e^{-\eta\tau}}{(\alpha i_\tau^*+\eta)} \end{array}$$

By considering the properties of the the characteristic equation from the linearised system at the disease-free steady state, we can prove that the disease-free steady state is stable if and only if $R_0^\tau < 1$. The linearised system at the disease-free steady state of the system (3.3.8) is

$$\begin{array}{rcl} \dot{s}(t) & = & -\beta q v(t) - (\mu+\gamma)s(t) - \gamma i(t), \\ \dot{i}(t) & = & \beta q v(t) - (\mu+\nu)i(t), \\ \dot{u}(t) & = & -\alpha i(t) - \eta u(t), \\ \dot{v}(t) & = & \alpha i(t-\tau)e^{-\eta\tau} - \eta v(t). \end{array} \tag{3.3.9}$$

This system can be rewritten in the following form:

$$\frac{dx}{dt} = J_0 x + J_1 x(t-\tau)$$

where $x(t) = (s(t), i(t), u(t), v(t))^T$,

$$J_0 = \begin{bmatrix} -(\mu+\gamma) & -\gamma & 0 & -\beta q \\ 0 & -(\mu+\nu) & 0 & \beta q \\ 0 & -\alpha & -\eta & 0 \\ 0 & 0 & 0 & -\eta \end{bmatrix}, \text{ and } J_1 = \begin{bmatrix} 0 & 0 & 0 & 0 \\ 0 & 0 & 0 & 0 \\ 0 & 0 & 0 & 0 \\ 0 & \alpha e^{-\eta\tau} & 0 & 0 \end{bmatrix}.$$

Assuming that $x = e^{\lambda t}\hat{v}$, we obtain

$$\lambda\hat{v} = (J_0 + e^{-\lambda\tau}J_1)\hat{v}.$$

The characteristic equation is

$$|J_0 + e^{-\lambda\tau}J_1 - \lambda I| = 0$$

or

$$(\lambda+\mu+\gamma)(\lambda+\eta)(\lambda^2+(\mu+\nu+\eta)\lambda+\eta(\mu+\nu)-\beta\alpha q e^{-(\eta+\lambda)\tau})=0.$$

Obviously, two of the eigenvalues are $\lambda_1 = -(\mu+\gamma)$ and $\lambda_2 = -\eta$ which always give stable manifolds. Hence stability of the disease-free steady state depends on the following function

$$F(\lambda,\tau)=\lambda^2+(\mu+\nu+\eta)\lambda+\eta(\mu+\nu)(1-R_0^\tau e^{-\lambda\tau})=0. \tag{3.3.10}$$

We consider the properties of this function so as to prove that the disease-free steady state is stable if and only if $R_0 < 1$ by following the steps of proof from Ruan et al. (2008) and Wei et al. (2008). We separate τ into two cases:A) $\tau = 0$, and B) $\tau > 0$.

A) For $\tau = 0$, we have

$$F(\lambda,0)=\lambda^2+(\mu+\nu+\eta)\lambda+\eta(\mu+\nu)(1-R_0^0)=0.$$

By the Routh-Hurwitz criteria, the disease-free steady state is stable if $R_0^0 < 1$ and unstable if $R_0^0 > 1$. Moreover, when $R_0^0 < 1$, we have two real and negative eigenvalues, which are

$$\lambda_\pm=\frac{-(\mu+\nu+\eta)\pm\sqrt{(\mu+\nu+\eta)^2-4\eta(\mu+\nu)(1-R_0^0)}}{2}.$$

B) For $\tau > 0$, we consider three cases of R_0^τ: 1) $R_0^\tau < 1$, 2) $R_0^\tau = 1$, and 3) $R_0^\tau > 1$. We also rearrange $F(\lambda,\tau)$ in the following form:

$$\lambda^2+(\mu+\nu+\eta)\lambda=\eta(\mu+\nu)(R_0^\tau e^{-\lambda\tau}-1). \tag{3.3.11}$$

We define

$$K(\lambda)=\lambda^2+(\mu+\nu+\eta)\lambda, \text{ and}$$

$$G(\lambda,\tau)=\eta(\mu+\nu)(R_0^\tau e^{-\lambda\tau}-1).$$

1. $R_0^\tau < 1$.
   Suppose λ is real. Because $K(\lambda)$ is an increasing function for $\lambda \geq 0$ ($K(0) = 0, \frac{\partial K}{\partial\lambda} = 2\lambda+(\mu+\nu+\eta) > 0, \forall\lambda \geq 0$) and $G(\lambda,\tau)$ is a decreasing function for $\lambda \geq 0$ ($G(0,\tau) = \eta(\mu+\nu)(R_0^\tau-1) < 0, \frac{\partial G}{\partial\lambda} = \eta(\mu+\nu)(-\tau R_0^\tau e^{-\lambda\tau}-1) < 0, \forall\lambda \geq 0$). These two functions do not intersect for any non-negative λ. Hence, there is no real and non-negative solution, λ, of $F(\lambda,\tau) = 0$. Consequently, if (3.3.10) has two roots with non-negative real parts, they must be complex conjugates crossing the imaginary axis. Figure 3-23(a) shows that there are two negative and real

eigenvalues at $\tau = 0$. When $0 < \tau << 1$, two eigenvalues are a pair of conjugates with negative real parts as shown in Figure 3-23(b). For (3.3.10) to have a pair of conjugates with positive real parts changed from the complex conjugates with negative real parts (as we know each τ leads to different λ), there must have a pair of imaginary solution satisfying (3.3.10). Hence, for some $\tau > 0$, (3.3.10) must have the purely imaginary solutions. Without loss of generality, we assume that one of that purely imaginary solutions is $\lambda = i\omega$ and

$$\omega^4 + [(\mu+\nu)^2 + \eta^2]\omega^2 + (\mu+\nu)^2\eta^2(1 - R_0^{\tau 2}) = 0.$$

Let $z = \omega^2$. We have

$$z^2 + ((\mu+\nu)^2 + \eta^2)z + (\mu+\nu)^2\eta^2(1 - R_0^{\tau 2}) = 0. \tag{3.3.12}$$

Since $R_0^\tau < 1$, both of the coefficients of this quadratic equation are positive. Both roots are either real and negative or complex conjugates with negative real parts. Hence, (3.3.12) does not have positive real roots that leads to a positive ω. Consequently,there is no ω such that $i\omega$ is a solution of (3.3.10). By Rouche's theorem, the real parts of all the eigenvalues at $F(\lambda, \tau) = 0$ are negative for all values of $\tau > 0$ (Theorem 9.17.4 in **?**).

2. $R_0^\tau = 1$
   Clearly, zero is a root of (3.3.10). Because $F(0, \tau) = 0$ and $dF(\lambda, \tau)/d\lambda > 0$ for all $\lambda \geq 0$ and $\tau > 0$, zero is a simple root and there is no positive root. Hence, the disease-free steady state is degenerate.

3. $R_0^\tau > 1$ In this case, we expect (3.3.10) to have a positive root and the disease-free steady state to be unstable. Suppose λ is real. We have that K is increasing with $K(0) = 0$ and G is decreasing with $G(0, \tau) = \eta(\mu+\nu)(R_0^\tau - 1) > 0$. The two functions must intersect for $\lambda^* > 0$. We see that every $\tau \geq 0$, we can always find a positive real λ^* that is one of the roots of (3.3.11). Hence, (3.3.10) has a positive real solution and it is enough to say that the disease-free steady state is unstable.

In conclusion, from all three cases, the disease-free steady state is stable if and only if $R_0^\tau < 1$, $\forall \tau \geq 0$. The linearised system at the disease-present steady state of the system (3.3.8) is

$$\begin{aligned}
\dot{s}(t) &= -\beta q s^* v(t) - \beta q v^* s(t) - (\mu+\gamma)s(t) - \gamma i(t), \\
\dot{i}(t) &= \beta q v^* s(t) + \beta q s^* v(t) - (\mu+\nu)i(t), \\
\dot{u}(t) &= -\alpha u^* i(t) - \alpha i^* u(t) - \eta u(t), \\
\dot{v}(t) &= \alpha u^* i(t-\tau)e^{-\eta\tau} + \alpha i^* u(t-\tau)e^{-\eta\tau} - \eta v(t).
\end{aligned} \tag{3.3.13}$$

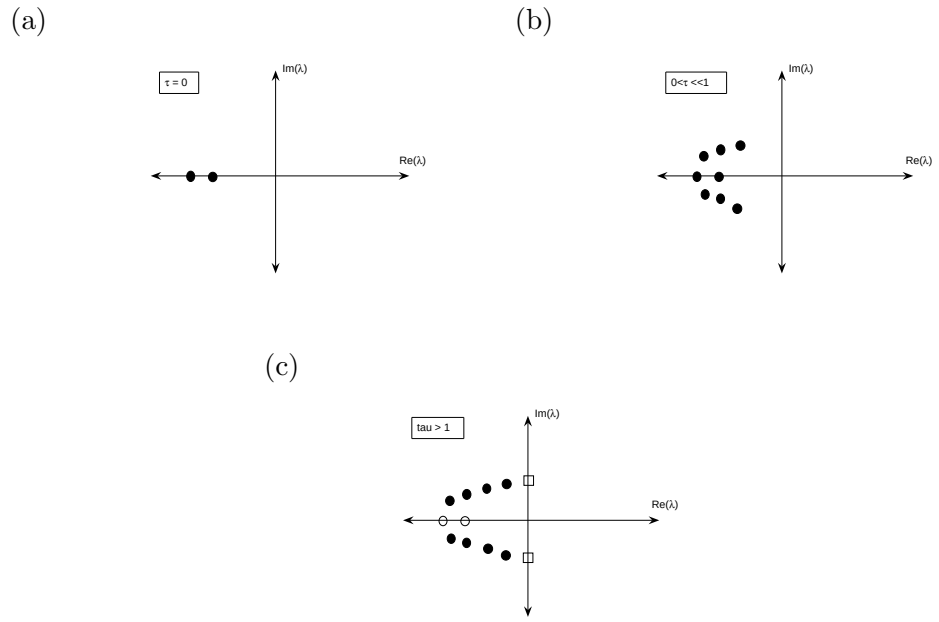

Figure 3-23: (a) Two eigenvalues are real and negative when $\tau = 0$. (b) The eigenvalues are a pair of conjugates with negative real parts and they are very close to those two real and negative when $0 < \tau << 1$. (c) The eigenvalues are a pair of conjugates when $\tau > 0$ and for them to change from complex conjugates with negative real parts to positive real parts, the roots must cross the imaginary axis.

The characteristic equation can be derived in the similar way with the linear system at the disease-free steady state and it is of order 4. In case we use τ as a bifurcation parameter and let $\lambda(\tau) = \rho(\tau)+i\omega(\tau)$ be the eigenvalue of the characteristic equation at the disease present-steady state, we might be able to find τ^* such that a Hopf bifurcation occurs (a family of periodic solutions bifurcates from the disease-present steady state as τ passes the value τ^* such that it loses its stability as a pair of conjugates eigenvalues crosses the imaginary axis. However, our characteristic equation at the disease-present steady state is in a complicated form and it is beyond the scope of this work. Hence, we instead study the dynamical behaviours of the system numerically.

With the effect of incubation time on the the dynamics of the system, the basic reproductive ratio is reduced exponentially when the incubation time in mosquitoes increases (see Figure 3-24(a)). Consequently, in Figure 3-24(b), the numbers of infectious humans and mosquitoes at the steady state decrease when the incubation time in mosquitoes increases. Note that the incubation time in mosquitoes does affect both populations due to the contacts between them. By plotting the asymptotic solutions $(i(\infty), v(\infty))$ of the system (3.3.8) against τ or incubation time which is allowed to vary while other parameters are fixed as Table 3.2, we obtain the bifurcation diagram shown in Figure 3-

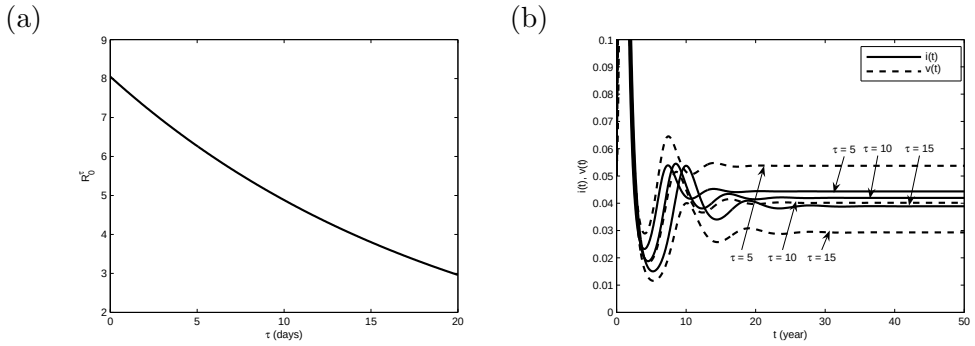

Figure 3-24: (a) An incubation effect from mosquitoes on the basic reproductive ratio (b) An incubation effect from mosquitoes on the number of infectious humans and mosquitoes (τ is in days)

25. In long-term dynamics, malaria would die out for an incubation time of 42 days. For realistic incubation times, the disease is endemic. However, longer incubation time in mosquitoes does decrease the prevalence of malaria.

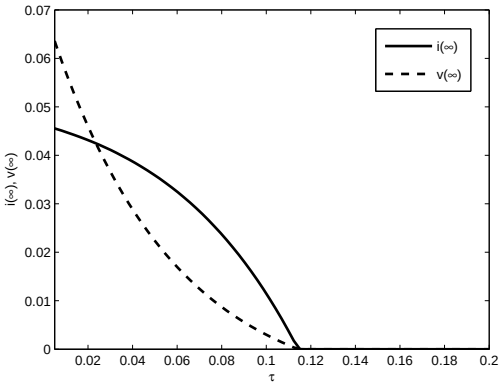

Figure 3-25: The bifurcation diagram between τ and i^* and v^*

Behaviours of mosquitoes driven by the malaria parasites

Lacroix et al. (2005) showed that attractiveness might be different for individuals who carry the parasite's gametocytes and both uninfected and recovered individuals, due to the manipulation of the malaria parasites in hosts. So, we incorporate the bias term of vectors into the model to describe this manipulation (Kingsolver, 1987; Chamchod, 2006; Hosack et al., 2008). We assume that a mosquito arrives at a human at random and let it pick a human with the probability p if the human is infectious, l_1 if the human is susceptible, and l_2 if the human is recovered ($p > l_1, l_2$). Otherwise, the mosquito

arrives at another human at random. Note that recovered humans are assumed to have the same chance of getting bitten by the mosquitoes as susceptible humans ($l_1 = l_2 = l$) but after the exposure, those show no symptoms and are assumed to carry very low number of gametocytes so that they are not infectious. Hence, the probability that a mosquito picks the first human and the first human is infectious is $(I/N)p$. The probability that a mosquito picks the first human and the first human is susceptible is $(S/N)l$ and the probability that a mosquito picks the first human and the first human is recovered is $(R/N)l$. Hence the probability that the first human is infectious under the condition that a mosquito picks him is $pI/(pI+l(S+R))$. The probability that the first human is susceptible and recovered respectively under the condition that a mosquito picks him is $lS/(pI + l(S + R))$ and $lR/(pI + l(S + R))$. Also, the diffusion term is introduced in the model to represent the mosquito's movement as a random walk. Attractiveness in humans can expressed in several chemical forms such as sweat, body odour, and breath (Skinner et al., 1965; Takken and Knols, 1999; Mukabana et al., 2004). Hence, we incorporate a chemotaxis term to explain the chemically directed movement to humans driven by the malaria parasites (Murray, 1993). With a constant population size in humans, $R = N - S - I$ and the system in terms of proportions of densities of individuals in each compartment is given by

$$\begin{aligned}
\frac{\partial s}{\partial T} &= \frac{\mu}{(\mu+\nu)} - \frac{\beta q}{(\mu+\nu)}\frac{ls}{(p-l)i+l}v - \frac{\mu}{(\mu+\nu)}s + \frac{\gamma}{(\mu+\nu)}(1-s-i),\\
\frac{\partial i}{\partial T} &= \frac{\beta q}{(\mu+\nu)}\frac{ls}{(p-l)i+l}v - i,\\
\frac{\partial u}{\partial T} &= \frac{\eta}{(\mu+\nu)}(u+v) - \frac{\alpha}{(\mu+\nu)}\frac{pi}{(p-l)i+l}u - \frac{\eta}{(\mu+\nu)}u + d\frac{\partial^2 u}{\partial x^2} - \chi\frac{\partial}{\partial x}u\frac{\partial i}{\partial x},\\
\frac{\partial v}{\partial T} &= \frac{\alpha}{(\mu+\nu)}\frac{pi}{(p-l)i+l}u - \frac{\eta}{(\mu+\nu)}v + d\frac{\partial^2 v}{\partial x^2} - \chi\frac{\partial}{\partial x}v\frac{\partial i}{\partial x}
\end{aligned} \tag{3.3.14}$$

where $T = (\mu+\nu)t$, $B = \eta(U+V)$, x is a space variable, d is a diffusion coefficient which is positive, and χ represents a chemotaxis coefficient which is positive. Note that the total density of the human population (N) is constant in time and space while the total density of the mosquito population (M) depends on time and space variables. Also, $u = U/M^0$, $v = V/M^0$, and $q = M^0/N$, where M^0 is the total density of the mosquito population at the spatially uniform disease-free steady state. Because malaria parasites manipulate hosts to be more affective in terms of sweat or breath, for instance,

$$\begin{aligned}
-\chi_1\frac{\partial}{\partial x}u\frac{\partial s}{\partial x} - \chi_2\frac{\partial}{\partial x}u\frac{\partial i}{\partial x} - \chi_3\frac{\partial}{\partial x}u\frac{\partial r}{\partial x} &= -\chi_1\frac{\partial}{\partial x}u\frac{\partial(1-i)}{\partial x} - \chi_2\frac{\partial}{\partial x}u\frac{\partial i}{\partial x}\\
&= -(\chi_2-\chi_1)\frac{\partial}{\partial x}u\frac{\partial i}{\partial x}\\
&= -\chi\frac{\partial}{\partial x}u\frac{\partial i}{\partial x},
\end{aligned}$$

where $\chi_2 > \chi_1, \chi_3 > 0, \chi_1 = \chi_3, s + r = 1 - i$. The chemotaxis term in the $\frac{\partial v}{\partial T}$ equation can be derived in a similar way. Moreover, we allow the biting rate of susceptible and infectious mosquitoes to be different due to the manipulation of malaria parasites in mosquitoes that increases the biting frequency (Lacroix et al., 2005). Thus, $\beta = b_v p_h$

and $\alpha = b_u p_m$ where $b_v > b_u$. It can be seen that a primary case in the human population makes infectious contacts with mosquitoes at rate $\alpha p M \frac{1}{lN}$ for an expected time $1/(\mu+\nu)$ and a primary case in the mosquito population makes infectious contacts with humans at rate $\beta \frac{lN}{lN}$ for an expected time $1/\eta$. Hence, the basic reproductive ratio of the system can be derived from the system (3.3.14) and given by

$$R_0^b = \frac{\beta \alpha q p}{\eta(\mu+\nu)l}.$$

Note that by fixing the parameter in R_0^b to be the same values with R_0 and $b_u = b_v$, $R_0 < R_0^b$ because $p > l$. The spatially uniform disease-free steady state of the system (3.3.14) is

$$P^0 = (s^0, i^0, u^0, v^0) = (1, 0, 1, 0)$$

and the spatially uniform disease-present steady state is

$$P^* = (s^*, i^*, u^*, v^*)$$

where

$$\begin{aligned} s^* &= \tfrac{(\mu+\gamma)-(\mu+\nu+\gamma)i^*}{(\mu+\gamma)}, \\ u^* &= 1 - \tfrac{\alpha p i^*}{\eta[(p-l)i^*+l]+\alpha p i^*}, \\ v^* &= \tfrac{\alpha p i^*}{\eta[(p-l)i^*+l]+\alpha p i^*}, \end{aligned}$$

and i^* satisfies the equation

$$c_1 i^{*2} + c_2 i^* + c_3 = 0$$

with

$$\begin{aligned} c_1 &= (\mu+\gamma)(\mu+\nu)(p-l)[\eta(p-l)+\alpha p], \\ c_2 &= \beta\alpha(\mu+\nu+\gamma)pl + (\mu+\gamma)(\mu+\nu)[\eta l(p-l) + l(\eta(p-l)+\alpha p)], \\ c_3 &= -(\mu+\gamma)(\mu+\nu)\eta l^2(R_0^b - 1). \end{aligned}$$

Obviously, c_1 and c_2 are positive and c_3 is negative when $R_0^b > 1$. Hence, the spatially uniform disease-present steady state exists (takes a positive real value) if and only if $R_0^b > 1$. Moreover, i^* is the biggest root of the polynomial equation. The stability condition of each steady state can be obtained by considering the Routh-Hurwitz criteria. We found that the disease-free steady state is stable if and only if $R_0^b < 1$ while the disease-present steady state is stable if and only if $R_0^b > 1$. The proof is omitted here. Without including the mosquito movement and the chemotaxis terms, the prevalence of malaria is increased when p is increased (see Figure 3-26(a)). Moreover, in Figure 3-26(b), when $R_0^b > 1$, the number of infectious humans and mosquitoes tend to the steady states in long term dynamics.

We further study the propagation of malaria from infected populations to uninfected

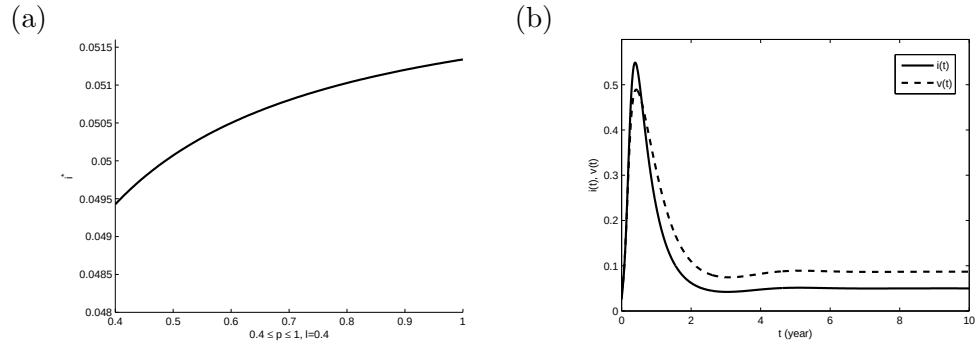

Figure 3-26: (a) A relation between p and I^* ($0.4 \leq p \leq 1$,l=0.4) (b) A numerical result of $I(t)$ and $V(t)$ ($b_v = 0.5 * 365, b_u = 100, p_h = 0.1, p_m = 0.3, p = 0.7, l = 0.6$)

populations (infected mosquito population to uninfected human population and infected human population to uninfected mosquito population) when the mosquito movement and the chemotaxis terms are taken into account. As an example, we shall consider a one-dimensional domain $[x_1, x_2]$ with malaria initially present at its steady state in $[x_1, \bar{x}]$ and absent in $[\bar{x}, x_2]$, where $\bar{x} = \frac{1}{2}(x_1 + x_2)$. Thus initial conditions are given by

$$\begin{aligned} s(x,0) &= s^* + (1-s^*)H(x-\bar{x}), & x_1 \leq x \leq x_2, \\ i(x,0) &= i^* - i^* H(x-\bar{x}), & x_1 \leq x \leq x_2, \\ u(x,0) &= u^* + (1-u^*)H(x-\bar{x}), & x_1 \leq x \leq x_2, \\ v(x,0) &= v^* - v^* H(x-\bar{x}), & x_1 \leq x \leq x_2, \end{aligned}$$

where $H(x)$ is a heaviside step function (see Figure 3-27(a)). The following boundary conditions are assumed as zero fluxes:

$$\begin{aligned} d\frac{\partial u}{\partial x}(x_1,T) - \chi u(x_1,T)\frac{\partial i}{\partial x}(x_1,T) &= 0 = d\frac{\partial u}{\partial x}(x_2,T) - \chi u(x_2,T)\frac{\partial i}{\partial x}(x_2,T), \\ d\frac{\partial v}{\partial x}(x_1,T) - \chi v(x_1,T)\frac{\partial i}{\partial x}(x_1,T) &= 0 = d\frac{\partial v}{\partial x}(x_2,T) - \chi v(x_2,T)\frac{\partial i}{\partial x}(x_2,T), \end{aligned}$$

where $T_1 \leq T \leq T_2$. From Figure 3-27(b), we can see that malaria propagates from the infected population to the uninfected population like a travelling wave. The wave speed (c) can be calculated from the graph by the formula

$$c = \frac{x_2 - x_1}{t_2 - t_1}$$

where $x_2 - x_1$ is the distance on the space and $t_2 - t_1$ is the time difference corresponding to the wave. For example, when $p = 0.7$ and $l = 0.4$, the wave speed is 14.5 space units per year. Other variables also share the same wave speed with v or V. Although we do not know exactly what p and l are, by varying the parameter p but keeping the diffusion coefficient, the chemotactic coefficient, and other parameters fixed, we can show that attractiveness of infectious individuals to mosquitoes influences

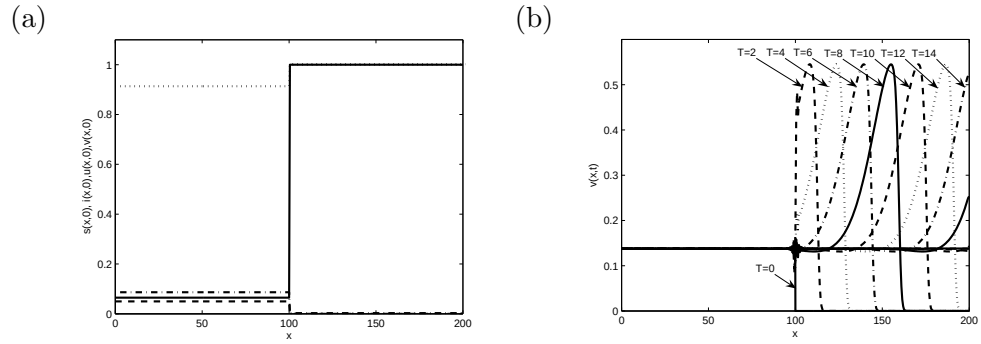

Figure 3-27: (a) Initial conditions on the domain $[0, 200]$ (b) This graph shows the travelling waves of infectious mosquitoes to susceptible humans ($T = (\mu + \nu)t, p = 0.7, l = 0.4, c = 14.5, d = 1, \psi = 1, l < p$)

the wave speed of malaria infection. Figure 3-28(a) shows that when p and l increase but the difference between them is fixed at 0.1, and $l, p \to 1$, the wave speed of malaria propagation decreases. Figure 3-28(b) suggests that the wave speed increases when p increases from l which is fixed at 0.4. In conclusion, both results suggest that the wave speed of malaria propagation depends on the difference between p and l or how attractive an infectious human is to the mosquito compared with a susceptible human.

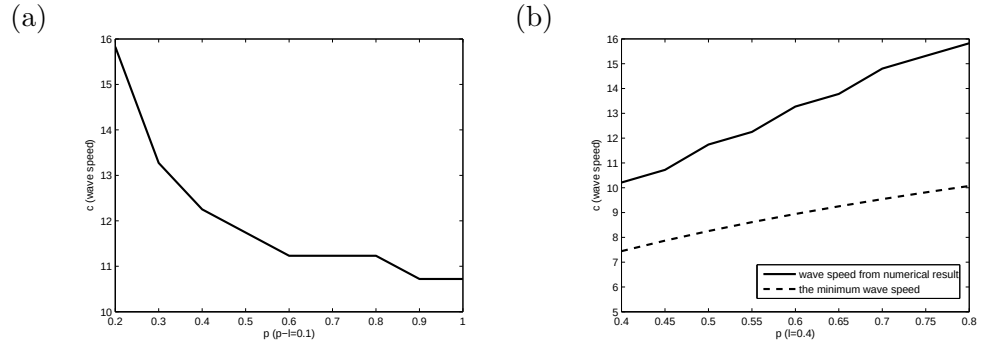

Figure 3-28: (a) A relation between the probability that a mosquito picks an infectious human (p) and the wave speed (c), when $p-l = 0.1$ and p varies (b) A relation between p and c when l is fixed at 0.4 and p varies (from the numerical result comparing with the minimum of the wave speed)

By introducing solutions of the system (3.3.14) in the travelling wave form and linearising it at the spatially uniform disease-free steady state, we can calculate the minimum wave speed of the disease propagation. We calculate this minimum wave speed by employing the method in Murray (1993). We look at travelling wave solutions as follows

$$s(x,T) = s(z),\ i(x,T) = i(z),\ u(x,T) = u(z),\ v(x,T) = v(z),\ z = x - cT.$$

Substituting them into (3.3.14), we obtain the system of ordinary differential equations

$$\begin{array}{rcl} cs' + \frac{\mu}{(\mu+\nu)} - \frac{\beta q}{(\mu+\nu)}\frac{ls}{[(p-l)i+l]}v - \frac{\mu}{(\mu+\nu)}s + \frac{\gamma}{(\mu+\nu)}(1-s-i) & = & 0, \\ ci' + \frac{\beta q}{(\mu+\nu)}\frac{ls}{[(p-l)i+l]}v - i & = & 0, \\ du'' - \chi(ui')' + cu' + \frac{\eta}{(\mu+\nu)}(u+v) - \frac{\alpha}{(\mu+\nu)}\frac{pi}{[(p-l)i+l]}u - \frac{\eta}{(\mu+\nu)}u & = & 0, \\ dv'' - \chi(vi')' + cv' + \frac{\alpha}{(\mu+\nu)}\frac{pi}{[(p-l)i+l]}u - \frac{\eta}{(\mu+\nu)}v & = & 0, \end{array} \tag{3.3.15}$$

where the prime denotes differentiation with respect to z. The system is solved with the following conditions

$$0 \leq s(-\infty) < s(\infty) = 1,\ i(-\infty) = i(\infty) = 0,\ 0 \leq u(-\infty) < u(\infty) = 1,\ v(-\infty) = v(\infty) = 0,$$

to find solutions with positive wave speed c and non-negative $s,\ i,\ u$, and v of the eigenvalue problem.

The condition on i and v lead to a pulse wave of infection propagating from infected population to uninfected population. We linearise the system (3.3.15) near the leading edge of the wave where $s \to 1,\ i \to 0,\ u \to 1$, and $v \to 0$ to obtain

$$\begin{array}{rcl} cs' - \frac{\beta q}{(\mu+\nu)}v - \frac{\mu}{(\mu+\nu)}s - \frac{\gamma}{(\mu+\nu)}(s+i) & \approx & 0, \\ ci' + \frac{\beta q}{(\mu+\nu)}v - i & \approx & 0, \\ du'' - \chi i'' + cu' + \frac{\eta}{(\mu+\nu)}v - \frac{\alpha p}{(\mu+\nu)l}i & \approx & 0, \\ dv'' + cv' + \frac{\alpha p}{(\mu+\nu)l}i - \frac{\eta}{(\mu+\nu)}v & \approx & 0. \end{array} \tag{3.3.16}$$

Because the variables s and u do not appear other equations apart from the differential equation corresponding to themselves, the differential equations of s and u are decoupled and the dynamics of the system can be described by the differential equations of i and v. By introducing a new variable w as v', we can rewrite the system (3.3.16) in the system of first-order ordinary differential equations as follows

$$\begin{array}{rcl} \frac{di}{dz} & = & \frac{1}{c}i - \frac{\beta q}{c(\mu+\nu)}v, \\ \frac{dv}{dz} & = & w, \\ \frac{dw}{dz} & = & -\frac{\alpha p}{dl(\mu+\nu)}i + \frac{\eta}{d(\mu+\nu)}v - \frac{c}{d}w. \end{array} \tag{3.3.17}$$

Consequently, the characteristic equation of the system (3.3.17) is

$$\lambda\left(\lambda + \frac{c}{d}\right)\left(\lambda - \frac{1}{c}\right) - \frac{\eta}{d(\mu+\nu)}\left(\lambda - \frac{1}{c}\right) - \frac{\beta\alpha qp}{cdl(\mu+\nu)^2} = 0. \tag{3.3.18}$$

To find the minimum wave speed, we differentiate through out (3.3.18) with respect to λ to find λ that minimize c. Hence, we have

$$3\lambda^2 + \left(\frac{2c}{d} - \frac{2}{c}\right)\lambda - \left(\frac{1}{d} + \frac{\eta}{d(\mu+\nu)}\right) = 0 \tag{3.3.19}$$

By solving (3.3.18) and (3.3.19) for c, we can find the minimum wave speed of the system (3.3.14). The minimum wave speed at some values of p while l is fixed at 0.4 is shown in Figure 3-28(b). Note that the time unit is interpreted in years.

Conclusion and discussion

Our study shows that some mechanisms in mosquitoes may play an important role in malaria transmission. By first setting up a general SIRS-SI model for vector-borne diseases with acquired immunity in hosts waning with time, we then introduce seasonality, incubation time in mosquitoes, and attractiveness to infectious individuals, respectively, in order to study the dynamics of the malaria transmission driven by each factor. Without including those factors, the number of infectious humans are increased when the protection time from acquired immunity is shortened.

Firstly, by considering seasonality in mosquitoes, a sinusoidal function is introduced in the recruitment rate to explain the high number of mosquitoes during the wet season. We found that the number of infectious humans and mosquitoes are synchronized with the number of mosquitoes, so malaria is highly transmitted during the rainy season. Similarly, by considering that mosquitoes bite more often and malaria parasites are replicated better during the hot season, we incorporate a sinusoidal function into the transmission rate in both humans and mosquitoes. In this case, the malaria transmission is high during the hot season. In case there are three seasons in each year (hot, rainy, winter), we combine those two seasonal forcing and arrive at the conclusion that malaria might be highly transmitted between hot and rainy season.

Secondly, the mosquito's lifespan is short so that incubation time of the malaria parasites might take more than half of their lifetime. Hence, it may be important to include incubation time in the study to understand the dynamic behaviours of malaria. By assuming that mosquitoes takes a fixed duration τ to be infectious after getting infected, the governed system is described by the delay differential equations with time lag τ. The prevalence of malaria is reduced when the incubation time takes longer.

Thirdly, due to the manipulation of the malaria parasite, infectious humans might be more attractive to mosquitoes than others in terms of breath and sweat. Hence, we introduce the vector-bias term into the model to account for this mechanism. Without including spatial terms, malaria is highly prevalent if infectious individuals are more attractive to the mosquitoes. Since mosquitoes move spatially toward the chemicals, diffusion term and chemotactic term are included in the model. We study the propagation of malaria from infected populations to uninfected populations. It results in the travelling wave of the disease propagation. Moreover, the speed of the waves de-

pends on the attractiveness of infectious individuals. The more attractive they are, the faster the disease travels and spreads. We also calculate the minimum of wave speed analytically and compare it with the numerical results. A vector-bias model based on SIS (susceptible-infectious-susceptible) in humans and SI in mosquitoes on malaria transmission and its full analysis is investigated in the next section. Note that the SIS-SI model is another type of models that has been used to study malaria. It is in more simplistic form that the SIRS-SI framework by omitting the presence of acquired immunity completely.

3.3.2 Analysis of a vector-bias model on malaria transmission

In this section, we incorporate a vector-bias term into a malaria-transmission model to account for the greater attractiveness of infectious humans to mosquitoes in terms of differing probabilities that a mosquito arriving at a human at random picks that human depending on whether he is infectious or susceptible. We prove that transcritical bifurcation occurs at the basic reproductive ratio equaling 1 by projecting the flow onto the extended centre manifold. Consequently, we can conclude that the disease-free steady state is stable if and only if $R_0 < 1$ and the disease-present steady state is stable if and only if $R_0 > 1$ (although the linearised system at the disease-present steady state is unwieldy to analyse for stability conditions). We next study the dynamics of the system when incubation time of malaria parasites in mosquitoes is included, and find that the longer incubation time reduces the prevalence of malaria. Also, we incorporate a random movement of mosquitoes as a diffusion term and a chemically directed movement of mosquitoes to humans expressed in terms of sweat and body odour as a chemotaxis term to study the propagation of infected population to uninfected population. We find that a travelling wave occurs; its speed is calculated numerically and estimated for the lower bound analytically.

A vector-bias model

A vector-bias model in malaria was first introduced by Kingsolver (1987). The model is extended from the Ross-Macdonald model to account for the greater attractiveness of infectious humans to mosquitoes (Macdonald, 1952, 1957). Following Kingsolver's work, Hosack et al. (2008) incorporate an extrinsic incubation time in mosquitoes to study the dynamics of the disease in term of a reproduction number. Here we include the recruitment rate and the natural death rate and define the attractiveness in a different way. In the model, hosts might get repeatedly infected due to not acquiring complete immunity so the population is assumed to be described by the SIS model. Mosquitoes are assumed not to recover from the parasites and the parasites are not

harmful to them so the mosquito population can be described by the SI model. The model takes the form:

$$\begin{aligned}
\dot{S}(t) &= \mu N - \beta \tfrac{lS}{pI+lS} V - \mu S + \nu I, \\
\dot{I}(t) &= \beta \tfrac{lS}{pI+lS} V - (\mu + \nu) I, \\
\dot{U}(t) &= \eta M - \alpha \tfrac{pI}{pI+lS} U - \eta U, \\
\dot{V}(t) &= \alpha \tfrac{pI}{pI+lS} U - \eta V,
\end{aligned} \tag{3.3.20}$$

where S, I, U, V, N and M represent the number of susceptible humans, infectious humans, susceptible mosquitoes, infectious mosquitoes, the total size of the human population and the total size of the mosquito population, respectively, $\beta = bp_h$ and $\alpha = bp_v$. The description of the parameters can be found in Table 3.2 (in the previous section). From the model, we assume that searching for a blood meal is equally likely to arrive at any human in the population, but bites that human with probability p if the human is infectious, l if the human is susceptible. Otherwise, the mosquito arrives at another human at random. Hence, the probability that a mosquito picks the first human and the first human is infectious is (pI/N). The probability that a mosquito picks the first human and the first human is susceptible is (lS/N). Hence the probability that the first human is infectious under the condition that a mosquito picks him is $pI/(pI+lS)$. The probability that the first human is susceptible under the condition that a mosquito picks him is $lS/(pI + lS)$. Similarly arguments hold for all subsequent humans. At $l = p$, the model is without vector-bias. Since infectious individuals are more attractive to the mosquitoes (Lacroix et al., 2005), $p > l$. The basic reproductive ratio is similar to the previous model,

$$R_0^b = \frac{\beta \alpha p q}{l \eta (\mu + \nu)}.$$

Stability analysis

We introduce the new variables in term of proportions as follows

$$s = \frac{S}{N},\ i = \frac{I}{N},\ u = \frac{U}{M},\ v = \frac{V}{M}.$$

Since $s + i = 1$, $u + v = 1$, the system (3.3.20) is reduced to

$$\begin{aligned}
\tfrac{di}{dt} &= \beta q \tfrac{l(1-i)}{pi+l(1-i)} v - (\mu + \nu) i \\
\tfrac{dv}{dt} &= \alpha \tfrac{pi}{pi+l(1-i)} (1 - v) - \eta v
\end{aligned} \tag{3.3.21}$$

The system consists of two steady states which are

1. the disease-free steady state

$$(i, v) = (i^0, v^0) = (0, 0), \tag{3.3.22}$$

2. the disease-present steady state

$$(i, v) = (i^*, v^*) = \left(i^*, \frac{\alpha p i^*}{\eta(pi + l(1 - i^*)) + \alpha p i^*} \right), \tag{3.3.23}$$

where i^* satisfies the equation

$$a_2 i^{*2} + a_1 i^* + a_0 = 0 \tag{3.3.24}$$

with

$$\begin{aligned} a_2 &= (\mu + \nu)(p - l)[\alpha p + \eta(p - l)], \\ a_1 &= (\mu + \nu) l[\alpha p + 2\eta l(p - l)] + \beta\alpha q p l, \\ a_0 &= (\mu + \nu)\eta l^2 - \beta\alpha q p l = l^2 \eta(\mu + \nu)(1 - R_0^b). \end{aligned}$$

Because $p > l$, a_1 and a_2 are always positive and a_0 is positive when $R_0^b < 1$, negative when $R_0^b > 1$. Hence, if $R_0^b < 1$ there is no positive root of (3.3.24), while if $R_0^b > 1$ there is one positive and one negative root. If $R_0^b > 1$, we define i^* to be the positive root of (3.3.24).

The linearised system at the disease-free steady state is given by

$$\begin{aligned} \frac{di}{dt} &= \beta q v - (\mu + \nu) i \\ \frac{dv}{dt} &= \alpha \frac{p}{l} i - \eta v \end{aligned} \tag{3.3.25}$$

Therefore, the characteristic equation is

$$\lambda^2 + (\mu + \nu + \eta)\lambda + \eta(\mu + \nu)(1 - R_0^b) = 0.$$

Two eigenvalues are given by

$$\lambda_{1,2} = \frac{-(\mu + \nu + \eta) \pm \sqrt{(\mu + \nu + \eta)^2 - 4\eta(\mu + \nu)(1 - R_0)}}{2}.$$

Both of them are negative whenever $R_0 < 1$. One is positive and one is negative when $R_0 > 1$. Hence, the disease-free steady state is stable if and only if $R_0 < 1$. The linearised system at the disease-present steady state is given by

$$\begin{aligned} \frac{di}{dt} &= -\left[\frac{\beta q l v^*}{(pi^* + l(1 - i^*))} + \frac{\beta q l (p - l)(1 - i^*) v^*}{(pi^* + l(1 - i^*))^2} + (\mu + \nu) \right] i + \frac{\beta q l (1 - i^*)}{(pi^* + l(1 - i^*))} v \\ \frac{dv}{dt} &= \left[\frac{\alpha p (1 - v^*)}{(pi^* + l(1 - i^*))} - \frac{\alpha p (p - l)(1 - v^*) i^*}{(pi^* + l(1 - i^*))^2} \right] i - \left[\frac{\alpha p i^*}{(pi^* + l(1 - i^*))} + \eta \right] v. \end{aligned} \tag{3.3.26}$$

The system is unwieldy for finding explicit eigenvalues or stability conditions by the Routh-Hurwitz condition. However, at $R_0 = 1$, at the disease-free steady state, the system has two eigenvalues $\lambda_1 = -(\mu+\nu+\eta)$ and $\lambda_2 = 0$ and hence is non-hyperbolic, so that $R_0 = 1$ may be a bifurcation value. Next, we prove that a transcritical bifurcation occurs when $R_0 = 1$ by projecting the flow onto the extended centre manifold. This is one of the important techniques for studying bifurcations of nonlinear systems. From the proof, we can consequently conclude that the disease-present steady state is stable if and only if $R_0 > 1$.

Bifurcation analysis

In order to prove that the transcritical bifurcation occurs at $(R_0^b, (i, v)) = (1, (0, 0))$, we write βq in terms of R_0^b and other parameters. So, the linearised system (3.3.25) is now

$$\begin{array}{rcl} \frac{di}{dt} & = & \frac{R_0^b \eta(\mu+\nu)l}{\alpha p} v - (\mu+\nu)i \\ \frac{dv}{dt} & = & \alpha \frac{p}{l} i - \eta v \end{array} \tag{3.3.27}$$

The proof is done by projecting the flow onto the extended centre manifold. It follows the similar steps with Glendinning (1999). The eigenvectors corresponding the eigenvalues $\lambda_1 = -(\mu+\nu+\eta)$ and $\lambda_2 = 0$ when $R_0^b = 1$ are

$$\bar{e}_1 = \begin{bmatrix} -l(\mu+\nu) \\ \alpha p \end{bmatrix}, \text{ and } \bar{e}_2 = \begin{bmatrix} l\eta \\ \alpha p \end{bmatrix}, \text{ respectively.}$$

The matrix P with its column vector as the eigenvector is

$$P = \begin{bmatrix} -l(\mu+\nu) & l\eta \\ \alpha p & \alpha p \end{bmatrix},$$

so that

$$\begin{bmatrix} -(\mu+\nu) & \frac{l\eta(\mu+\nu)}{\alpha p} \\ \frac{\alpha p}{l} & -\eta \end{bmatrix} P = P \begin{bmatrix} -(\mu+\nu+\eta) & 0 \\ 0 & 0 \end{bmatrix}.$$

By setting

$$\begin{bmatrix} z \\ w \end{bmatrix} = P^{-1} \begin{bmatrix} i \\ v \end{bmatrix},$$

we obtain the linear part of the equation in terms of z and w as follows:

$$\begin{bmatrix} \dot{z} \\ \dot{w} \end{bmatrix} = \begin{bmatrix} -(\mu+\nu+\eta) & 0 \\ 0 & 0 \end{bmatrix} \begin{bmatrix} z \\ w \end{bmatrix}.$$

The inverse matrix of P is

$$P^{-1} = \frac{-1}{\alpha pl(\mu+\nu+\eta)} \begin{bmatrix} \alpha p & -l\eta \\ -\alpha p & -l(\mu+\nu) \end{bmatrix}.$$

Hence,

$$\begin{bmatrix} z \\ w \end{bmatrix} = P^{-1} \begin{bmatrix} i \\ v \end{bmatrix} = \frac{1}{\alpha pl(\mu+\nu+\eta)} \begin{bmatrix} -\alpha pi + l\eta v \\ \alpha pi + l(\mu+\nu)v \end{bmatrix}, \tag{3.3.28}$$

and

$$\begin{bmatrix} i \\ v \end{bmatrix} = P \begin{bmatrix} z \\ w \end{bmatrix} = \begin{bmatrix} -l(\mu+\nu)z + l\eta w \\ \alpha pz + \alpha pw \end{bmatrix}. \tag{3.3.29}$$

We define a new parameter r that $R_0^b = 1 + r$ so that investigating the bifurcation at $R_0^b = 1$ is equivalent to investigating it at $r = 0$. Hence r can be treated as small as we want in the local investigation. By substituting di/dt and dv/dt from the system (3.3.21) (where βq is substituted by $R_0^b(1-p)\eta(\mu+\nu)/(\alpha p)$) and then i and v in terms of z and w into finding dz/dt and dw/dt obtained from the equation (3.3.28), consequently, the extended system is

$$\begin{aligned}
\tfrac{dz}{dt} &= \tfrac{1}{(\mu+\nu+\eta)}\{-(\mu+\nu+\eta)^2 z + \eta(\mu+\nu)[\alpha p - (2p-l)(\mu+\nu)]z^2 + \\
&\quad \eta[p(\mu+\nu)(\eta-\mu-\nu) - \alpha p\eta + \alpha p(\mu+\nu) + 2(p-l)\eta(\mu+\nu)]zw + \\
&\quad \eta^2[p(\mu+\nu) - \alpha p - (p-l)\eta]w^2 - \eta(\mu+\nu)zr - \eta(\mu+\nu)wr\}, \\
\tfrac{dw}{dt} &= \tfrac{1}{(\mu+\nu+\eta)}\{(\mu+\nu)^2[p\eta + \alpha p - (p-l)(\mu+\nu)]z^2 + \\
&\quad (\mu+\nu)[-\alpha p\eta + \alpha p(\mu+\nu) + 2(p-l)\eta(\mu+\nu) - p\eta(\eta-\mu-\nu)]zw - \\
&\quad \eta(\mu+\nu)[p\eta + \alpha p + (p-l)\eta]w^2 + \eta(\mu+\nu)zr + \eta(\mu+\nu)wr\}, \\
\tfrac{dr}{dt} &= 0.
\end{aligned} \tag{3.3.30}$$

Note that in finding di/dt and dv/dt in terms of z and w, we make an approximation as follows

$$\frac{1}{l + (p-l)i} \approx \frac{1}{l}\left(1 - \frac{(p-l)}{l}i + \text{ h.o.t}\right)$$

where $0 < (p-l)/l < 1$, $i < 1$, and i is in terms of z and w in the equation (3.3.29). Because r is treated in the similar way with z and w, there is only a linear term in the equation dz/dt. The linear centre manifold is

$$E^c(0) = \{(z, w, r) | z = 0\}$$

and the linear stable manifold is

$$E^s(0) = \{(z, w, r) | w = r = 0.\}$$

An approximation of the nonlinear centre manifold is in the following form

$$z = h(w, r) \text{ with } \frac{\partial h}{\partial w}(0,0) = \frac{\partial h}{\partial r}(0,0) = 0$$

and that

$$h(w, r) = aw^2 + bwr + r^2 + \ldots.$$

Thus,

$$\frac{dz}{dt} = \frac{dh}{dw}\frac{dw}{dt} + \frac{dh}{dr}\frac{dr}{dt}$$

By substituting h, dw/dt, dr/dt in terms of w and r and then comparing the coefficients of w^2, wr, and r^2 with those from the equation dz/dt in (3.3.30) after the substitution, we obtain

$$\begin{aligned} a &= \tfrac{\eta^2}{(\mu+\nu+\eta)^2}[p(\mu+\nu) - (\alpha p + (p-l)\eta)] \\ b &= -\tfrac{\eta(\mu+\nu)}{(\mu+\nu+\eta)^2} \\ c &= 0. \end{aligned}$$

Therefore, the centre manifold is

$$z = \frac{\eta^2}{(\mu+\nu+\eta)^2}[p(\mu+\nu) - (\alpha p + (p-l)\eta)]w^2 - \frac{\eta(\mu+\nu)}{(\mu+\nu+\eta)^2}wr + \text{ cubic terms.}$$

We substitute z back into the equation of dw/dt to get the projection of the motion on the centre manifold onto the w axis:

$$\frac{dw}{dt} = \frac{\eta(\mu+\nu)}{(\mu+\nu+\eta)}[-(p\eta + \alpha p + (p-l)\eta)w^2 + wr] + \text{ cubic terms.}$$

Note here that the expression for the centre manifold does not contribute any quadratic terms so the calculation of the centre manifold is not exactly required. On the centre manifold, we have

$$\frac{dw}{dt} = G(w, r)$$

with

$$G(0,0) = G_w(0,0) = G_r(0,0) = 0,$$

$$G_{ww} = -\frac{2\eta(\mu+\nu)}{(\mu+\nu+\eta}[p\eta + \alpha p + (p-l)\eta],\ G_{wr} = \frac{\eta(\mu+\nu)}{(\mu+\nu+\eta)},\ G_{rr} = 0.$$

Since $p > l$ and all of the parameters are positive, G_{ww} is negative while G_{wr} is positive. By the centre manifold theorem and the transcritical bifurcation theorem, the disease-free steady state is stable when $R_0^b < 1 (r < 0)$ and there is a separate unstable branch (from the disease-present steady state), and when $R_0^b > 1 (r > 0)$ the disease-free steady state becomes unstable while the separating branch becomes stable (Glendinning, 1999). Note that when $R_0^b = 1 (r = 0)$, the centre manifold is

approximated by

$$\frac{dw}{dt} \approx -\frac{\eta(\mu+\nu)}{(\mu+\nu+\eta)}[p\eta + \alpha p + (p-l)\eta]$$

so that the disease-free steady state is stable if it is approached from $w > 0$ and unstable when it is approached from $w < 0$. The proof is completed. Hence, we conclude that there is a transcritical bifurcation occurring at the bifurcation value $R_0^b = 1$. Therefore, the disease-free steady state is stable if and only if $R_0^b < 1$ and the disease-present steady state is stable if and only if $R_0^b > 1$.

Incubation time in mosquitoes

Because mosquitoes have a short lifespan, including the incubation time of malaria parasites in the model might be important in studying dynamic behaviours of the disease. It approximately takes $\tau = 10$ days after blood feeding for the sporozoites to appear in the mosquito salivary gland (Beier, 1998) and for those 10 days the mosquito is infected but not infectious, and so it is in a latent state. For simplicity, we omit the incubation time in humans ($\approx 5.5-15$ days, a negligible fraction of a human lifetime) to study only incubation time for mosquitoes in the model. We assume that the mosquito that has just bitten the infectious human moves immediately to the latent compartment (W). As long as it still survives, it becomes infectious after duration τ and enters the infectious compartment (V). Hence, at time t, the flux into the latent compartment is $\alpha p i(t)u(t)/[l+(p-l)i(t)]$ and the flux out is $\alpha p i(t-\tau)u(t-\tau)e^{-\eta\tau}/[l+(p-l)i(t-\tau)]$. The equations can be described by the following system:

$$\begin{aligned} \frac{di}{dt} &= \beta q \frac{l(1-i)}{(p-l)i+l} v - (\mu+\nu)i, \\ \frac{du}{dt} &= \eta - \alpha \frac{pi}{(p-l)i+l} u - \eta u, \\ \frac{dv}{dt} &= \alpha \frac{pi(t-\tau)}{(p-l)i(t-\tau)+l} u(t-\tau)e^{-\eta\tau} - \eta v(t), \end{aligned} \tag{3.3.31}$$

Consequently, the basic reproductive ratio of the system is

$$R_0^\tau = \frac{\beta\alpha q p e^{-\eta\tau}}{\eta(\mu+\nu)l}.$$

Note that by including incubation time of malaria parasites in humans (ω), the system leads to the basic reproductive ratio into the following form

$$R_0^{\omega\tau} = \frac{\beta\alpha q p e^{-\mu\omega} e^{-\eta\tau}}{\eta(\mu+\nu)l}.$$

Since human life span is long comparing with incubation time of the parasites, $e^{-\mu\omega}$ is close to 1. Hence, the incubation time in humans does not much alter the basic reproductive ratio which helps to determine whether the disease spreads. Consequently,

we can omit the incubation time in human in the model for simplicity in the analysis. The system (3.3.31) has two steady states, which are

1. the disease-free steady state

$$(i, u, v) = (0, 1, 0)$$

2. the disease-present steady state

$$(i, u, v) = (i^*, u^*, v^*)$$

with

$$\begin{aligned} u^* &= \frac{\eta[(p-l)i^*+l]}{\eta[(p-l)i^*+l]+\alpha p i^*}, \\ v^* &= \frac{\alpha p i^* e^{-\eta\tau}}{\eta[(p-l)i^*+l]+\alpha p i^*} \end{aligned}$$

where i^* satisfies

$$(\mu+\nu)(p-l)[\eta(p-l)+\alpha p]i^{*2}+\{\beta\alpha q p l e^{-\eta\tau}+(\mu+\nu)[\alpha p l+2\eta l(p-l)]\}i^*+(\mu+\nu)\eta l^2-\beta\alpha q p l e^{-\eta\tau}=0.$$

The linearised system of (3.3.31) at the disease-free steady state is

$$\begin{aligned} \frac{di}{dt} &= \beta q v - (\mu+\nu)i, \\ \frac{du}{dt} &= -\alpha\frac{p}{l}i - \eta u, \\ \frac{dv}{dt} &= \alpha\frac{p}{l}i(t-\tau)e^{-\eta\tau} - \eta v. \end{aligned} \tag{3.3.32}$$

The system can be written in matrix form as follows:

$$\frac{dx}{dt} = J_0 x(t) + J_1 x(t-\tau),$$

where $x(t) = (i(t), u(t), v(t))^T$,

$$J_0 = \begin{bmatrix} -(\mu+\nu) & 0 & \beta q \\ -\alpha\frac{p}{l} & -\eta & 0 \\ 0 & 0 & -\eta \end{bmatrix}, \text{ and } J_1 = \begin{bmatrix} 0 & 0 & 0 \\ 0 & 0 & 0 \\ \alpha\frac{p}{l}e^{-\eta\tau} & 0 & \end{bmatrix}.$$

By assuming that the solution of the system is $x = e^{-\lambda t}\hat{v}$, we obtain

$$\lambda\hat{v} = (J_0 + e^{-\lambda\tau}J_1)\hat{v}$$

and the characteristic equation is

$$|J_0 + e^{-\lambda\tau}J_1 - \lambda I| = 0$$

or

$$(\lambda+\eta)[\lambda^2+(\mu+\nu+\eta)\lambda+\eta(\mu+\nu)-\beta\alpha q\frac{p}{l}pe^{-(\lambda+\eta)\tau}].$$

Clearly, one of the eigenvalues is $\lambda_1=-\eta$, that always give a stable manifold. Hence, the stability of the disease-free steady state depends upon the following function

$$F(\lambda,\tau)=\lambda^2+(\mu+\nu+\eta)\lambda+\eta(\mu+\nu)(1-R_0^\tau e^{-\lambda\tau})=0. \tag{3.3.33}$$

In order to prove that the disease-free steady state is stable if and only if $R_0^\tau<1$, we consider the properties of the function F and follows the steps of proof by Ruan et al. (2008) and Wei et al. (2008). The function F is analytic with $F(0,\tau)=\eta(\mu+\nu)(1-R_0^\tau)$ and $F(\lambda,0)=\lambda^2+(\mu+\nu+\eta)\lambda+\eta(\mu+\nu)(1-R_0^0)$. We separate the proof into three cases according to the basic reproductive ratio:

1. $R_0^\tau<1$ For all positive λ and τ, $F(0,\tau)>0$ and $\partial F(\lambda,\tau)/\partial\lambda>0$ so that F is an increasing function for $\lambda>0$. Consequently, there is no zero root and no positive root for any positive τ. In the similar way with the previous section, we show that F has no imaginary roots by assuming that $\pm i\omega$ are imaginary roots of F. This follows the start of the real and negative eigenvalues on the complex plane that become a pair of complex conjugates with negative real parts when $0<\tau<<1$. For the eigenvalues to become a pair of complex conjugates with positive real parts, there must be a pair of purely imaginary eigenvalues as a solution of (3.3.33). So, ω must be a positive root of the following equation:

   $$\omega^4+[(\mu+\nu)^2+\eta^2]\omega^2+(\mu+\nu)^2\eta^2(1-R_0^{\tau 2})=0.$$

   Obviously, this equation does not have nonnegative real roots. A contradiction is found and hence F does not have purely imaginary roots. Moreover, $F(\lambda,0)$ has two negative real roots which are

   $$\lambda_\pm=\frac{-(\mu+\nu+\eta)\pm\sqrt{(\mu+\nu+\eta)^2-4\eta(\mu+\nu)(1-R_0^\tau)}}{2}$$

   and $\partial F(\lambda_\pm,0)/\partial\lambda\neq 0$. By the implicit theorem and the continuity of F, we conclude that $F(\lambda,\tau)$ has no root with positive real parts for positive τ. The disease-free steady state is stable if $R_0^\tau<1$.

2. $R_0^\tau=1$ Because $F(0,\tau)=0$ and $dF(\lambda,\tau)/d\lambda>0$ for all $\lambda\geq 0$ and $\tau>0$, zero is a simple root and there is no positive root. In the similar way with 1), we can show that there is no positive root. Hence, the disease-free steady state is degenerate.

3. $R_0^\tau>1$ Since $F(0,\tau)<0$ and $\partial F(\lambda,\tau)/\partial\lambda>0$, for all $\lambda\geq 0$ and $\tau>0$, F has a

positive root. Thus, the disease-free steady state is unstable.

The proof is completed. Therefore, the disease-free steady state is stable if and only if $R_0^\tau < 1$.

The linearised system at the disease-present steady state is

$$\begin{array}{rcl} \frac{di}{dt} & = & \frac{\beta ql(v-i^*v-v^*i)}{[(p-l)i^*+l]} - \frac{\beta ql(p-l)(v^*+i^*v^*)i}{[(p-l)i^*+l]^2]} - (\mu+\nu)i, \\ \frac{du}{dt} & = & -\frac{\alpha p(u^*i+i^*u)}{[(p-l)i^*+l]} + \frac{\alpha p(p-l)i^*u^*i}{[(p-l)i^*+l]^2} - \eta u, \\ \frac{dv}{dt} & = & \frac{\alpha p e^{-\eta\tau}(u^*i(t-\tau)+i^*u(t-\tau))}{[(p-l)i^*+l]} - \frac{\alpha p(p-l)e^{-\eta\tau}i^*u^*i}{[(p-l)i^*+l]^2} - \eta v. \end{array} \tag{3.3.34}$$

The characteristic equation can be derived in the similar way with the linear system at the disease-free steady state and it is of order 3. Here, we study the dynamics of the disease-present steady state numerically. In Figure 3-29(a), the basic reproductive

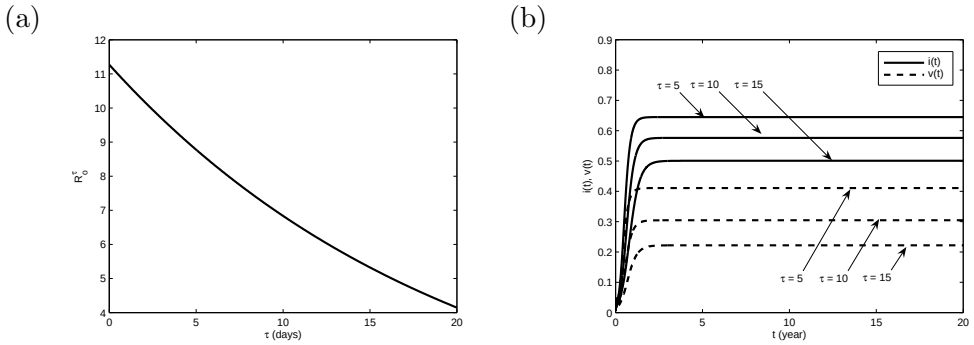

Figure 3-29: (a) An incubation effect from mosquitoes on the basic reproductive ratio ($p = 0.7, l = 0.6$) (b) An incubation effect from mosquitoes on the number of infectious humans and mosquitoes (τ is in days, $p = 0.7, l = 0.6$)

ratio is plotted against the incubation time in mosquitoes. It is decreased when the incubation time is increased. In other words, when parasites need longer time to appear in bloodstream, the disease transmission is reduced. In Figure 3-29(b), we study the solution of the system (3.3.31) at some values of τ. As we can see, the proportions of infectious humans and mosquitoes decrease when the incubation time of the malaria parasites in mosquitoes increases. The solution tends to the disease-present steady state finally. By studying the asymptotic solutions, we have found that with $p = 0.7, q = 1, R_0^\tau = 9.4$, the incubation time τ that two steady states exchanging the stability is approximately 45 days which is normally longer than the lifespan of mosquitoes (see Figure 3-30). Hence, the disease is endemic no matter what the incubation time in mosquitoes is

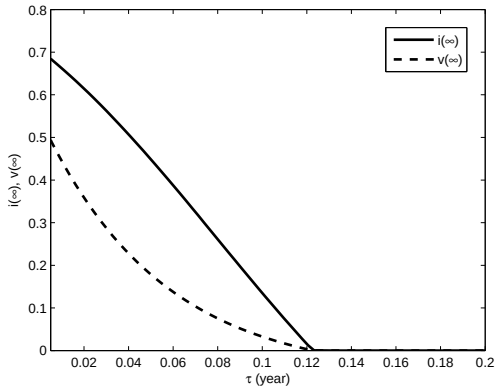

Figure 3-30: The bifurcation diagram between τ and $i(\infty)$ and $v(\infty)$ ($q = 1, p = 0.7, l = 0.6, R_0^\tau = 9.4$)

The study of travelling waves

In this section, we introduce the diffusion term to represent the mosquito's movement as a random walk. Also, because attractiveness of humans to mosquitoes is expressed in chemical forms such as sweat, body odour, and breath (Skinner et al., 1965; Takken and Knols, 1999; Mukabana et al., 2004), we incorporate a chemotaxis term to explain the chemically directed movement to humans (Murray, 1993). The governed system after rescaling becomes

$$\begin{aligned} \frac{\partial i}{\partial T} &= \frac{\beta q l(1-i)}{(\mu+\nu)[(p-l)i+l]} v - i, \\ \frac{\partial u}{\partial T} &= \frac{\eta(u+v)}{\mu+\nu} - \frac{\alpha p i}{(\mu+\nu)[(p-l)i+l]} u - \frac{\eta}{\mu+\nu} u + d\frac{\partial^2 u}{\partial x^2} - \chi \frac{\partial}{\partial x} u \frac{\partial i}{\partial x}, \\ \frac{\partial v}{\partial T} &= \frac{\alpha p i}{(\mu+\nu)[(p-l)i+l]} u - \frac{\eta}{\mu+\nu} v + d\frac{\partial^2 v}{\partial x^2} - \chi \frac{\partial}{\partial x} v \frac{\partial i}{\partial x} \end{aligned} \tag{3.3.35}$$

where the total density of the human population (N) is constant in time and space and the total density of the mosquito population (M) depends on the time and space variables, $T = (\mu + \nu)t$, x is the space variable, d is the diffusion coefficient ($d > 0$), and χ is the chemotaxis coefficient ($\chi > 0$). Note that $u = U/M^0$, $v = V/M^0$, and $q = M^0/N$ where M^0 is the total density of the mosquito population at the spatially uniform disease-free steady state. Also note that

$$\begin{aligned} -\chi_1 \frac{\partial}{\partial x} u \frac{\partial s}{\partial x} - \chi_2 \frac{\partial}{\partial x} u \frac{\partial i}{\partial x} &= -(\chi_2 - \chi_1) \frac{\partial}{\partial x} u \frac{\partial i}{\partial x} \\ &= -\chi \frac{\partial}{\partial x} u \frac{\partial i}{\partial x} \end{aligned}$$

where $s = 1 - i$, and $\chi_2 > \chi_1 > 0$ because malaria parasites manipulate hosts to be more attractive to mosquitoes via sweat and body odour, for instance.

We study the propagation of malaria from the infected population into the uninfected

population (infected human population to uninfected mosquito population and infected mosquito population to uninfected human population) by introducing the initial conditions as step functions in one-dimensional domain $[x_1, x_2]$ with malaria initially present at its spatially uniform steady state in $[x_1, \bar{x}]$) and absent in $[\bar{x}, x_2]$, where $\bar{x} = (x_1 + x_2)/2$. This the initial conditions are given by

$$\begin{aligned} i(x,0) &= i^* - i^* H(x - \bar{x}), & x_1 \le x \le x_2, \\ u(x,0) &= u^* + (1 - u^*) H(x - \bar{x}), & x_1 \le x \le x_2, \\ v(x,0) &= v^* - v^* H(x - \bar{x}), & x_1 \le x \le x_2, \end{aligned}$$

where $H(x)$ is a heaviside step function, $u^* = 1 - v^*$, i^* and v^* correspond to (3.3.23) and it is shown in Figure 3-31(a). The boundary conditions are assumed as zero fluxes:

$$\begin{aligned} d\frac{\partial u}{\partial x}(x_1,T) - \chi u(x_1,T)\frac{\partial i}{\partial x}(x_1,T) &= 0 = d\frac{\partial u}{\partial x}(x_2,T) - \chi u(x_2,T)\frac{\partial i}{\partial x}(x_2,T), \\ d\frac{\partial v}{\partial x}(x_1,T) - \chi v(x_1,T)\frac{\partial i}{\partial x}(x_1,T) &= 0 = d\frac{\partial v}{\partial x}(x_2,T) - \chi v(x_2,T)\frac{\partial i}{\partial x}(x_2,T), \end{aligned}$$

where $T_1 \le T \le T_2$.

(a) (b)

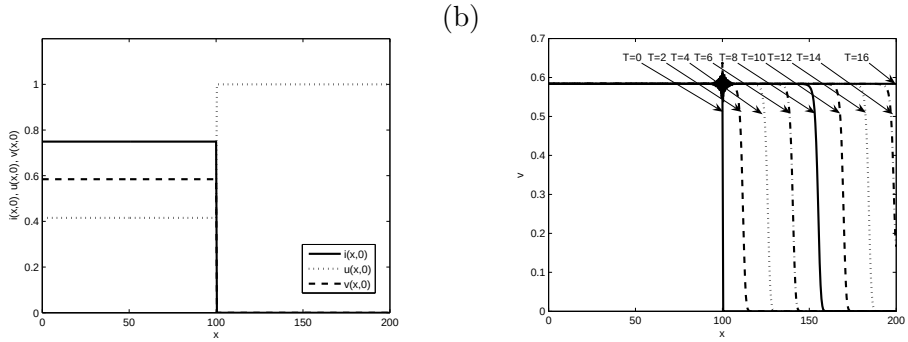

Figure 3-31: (a) Initial conditions in the one-dimensional domain $[0, 200]$ (b) This graph shows the travelling waves of infectious mosquitoes from the endemic area to the disease-free area ($T = (\mu + \nu)t, p = 0.7, l = 0.6, c = 11.23, d = 1, \chi = 1$)

In Figure 3-31(b), we can see that malaria spreads from infected population to uninfected population like travelling waves. The wave speed (c) can be calculated from the graph by the formula

$$c = \frac{x_2 - x_1}{t_2 - t_1}$$

where $x_2 - x_1$ is the distance on the space and $t_2 - t_1$ is the time difference corresponding to the wave. When $p = 0.7$ and $l = 0.4$, the wave speed is 14.5 space unit per year, for example. Other variables also share the same wave speed with v or V (see Figure 3-31). When p is larger, for example, $p = 0.8$, the speed of travelling waves becomes bigger, which is 15.7. Hence, it suggests that the more the infectious hosts become attractive to the mosquitoes, the faster of the propagation of the disease from the

infected population to the uninfected population is.

(a) (b)

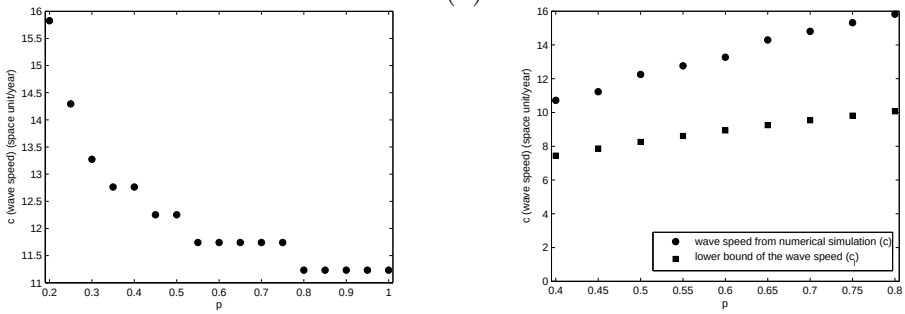

Figure 3-32: (a) A relation between the probability that a mosquito picks an infectious human (p) and the wave speed (c) when $p-l=0.1$ and p varies (b) A relation between p and c, when l is fixed at 0.4 while p varies, from a numerical simulation comparing with the minimum wave speed

We further study the wave speed c numerically by considering the relation between p and l. Note that the wave speed is expressed in space unit per year. In Figure 3-32(a), when p and l increase but the difference between them is fixed at 0.1, or in other words when l/p becomes larger ($l/p \to 1$), the wave speed of malaria propagation decreases. Figure 3-32(b) shows that wave speed of the disease increases when p increases while l is fixed at 0.4. Both results also suggest that wave speed depends on how different between p and l or how attractive the infectious human to the mosquito comparing with the susceptible human is.

Next, we calculate the lower bound of wavespeed by employing the method in Murray (1993). We look for travelling wave solutions by setting

$$i(x,T)=i(z),\ u(x,T)=u(z),\ v(x,T)=v(z),\ z=x-cT. \tag{3.3.36}$$

By substituting them into (3.3.35), we obtain the ordinary differential equation system

$$\begin{aligned} ci' + \tfrac{\beta q l(1-i)v}{(\mu+\nu)[(p-l)i+l]} - i &= 0, \\ du'' - \chi(ui')' + cu' + \tfrac{\eta}{(\mu+\nu)}(u+v) - \tfrac{\alpha p i u}{(\mu+\nu)[(p-l)i+l]} - \tfrac{\eta u}{(\mu+\nu)} &= 0, \\ dv'' - \chi(vi')' + cv' + \tfrac{\alpha p i u}{(\mu+\nu)[(p-l)i+l]} - \tfrac{\eta v}{(\mu+\nu)} &= 0, \end{aligned} \tag{3.3.37}$$

where the prime denotes differentiation with respect to z. Our goal is to find solutions with positive wave speed c and nonnegative i, u and v of the eigenvalue problem such that

$$i(-\infty)=i(\infty)=0,\ 0\le u(-\infty)<u(\infty)=1,\ v(-\infty)=v(\infty)=0.$$

The conditions on i and v lead to a pulse wave of infection that propagates into the uninfected population. We linearise the system (3.3.37) near the leading edge of the

wave where $i \to 0$, $u \to 1$, and $v \to 0$ to have

$$\begin{aligned} ci' + \tfrac{\beta q}{(\mu+\nu)} v - i &\approx 0, \\ du'' - \chi i'' + cu' + \tfrac{\eta}{(\mu+\nu)} v - \tfrac{\alpha p}{(\mu+\nu)l} i &\approx 0, \\ dv'' + cv' + \tfrac{\alpha p}{(\mu+\nu)l} i - \tfrac{\eta}{(\mu+\nu)} v &\approx 0. \end{aligned} \tag{3.3.38}$$

Since the variable u does not appear in the other two equations (decoupled), we can omit the differential equation of u and hence the dynamics of the system are governed by the differential equations of i and v, the dynamics of the wave solutions of the system (3.3.38) can be described by the following first-order ordinary differential equation system

$$\begin{aligned} \tfrac{di}{dz} &= \tfrac{1}{c} i - \tfrac{\beta q}{c(\mu+\nu)} v, \\ \tfrac{dv}{dz} &= w, \\ \tfrac{dw}{dz} &= -\tfrac{\alpha p}{dl(\mu+\nu)} i + \tfrac{\eta}{d(\mu+\nu)} v - \tfrac{c}{d} w. \end{aligned} \tag{3.3.39}$$

The characteristic equation of the system (3.3.39) is

$$\lambda \left(\lambda + \frac{c}{d}\right) \left(\lambda - \frac{1}{c}\right) - \frac{\eta}{d(\mu+\nu)} \left(\lambda - \frac{1}{c}\right) - \frac{\beta \alpha q p}{cdl(\mu+\nu)^2} = 0. \tag{3.3.40}$$

In order to find the minimum value of the wave speed (c_l), we differentiate through out the equation (3.3.40) with respect to λ to find λ that minimize c and the equation is given by

$$3\lambda^2 + \left(\frac{2c}{d} - \frac{2}{c}\right) \lambda - \left(\frac{1}{d} + \frac{\eta}{d(\mu+\nu)}\right) = 0 \tag{3.3.41}$$

By solving the equations (3.3.40) and (3.3.41) for c, we can find the minimum value of the wave speed of the system (3.3.35). The minimum value of the wave speed at some values of p and l is shown in Figure 3-32(b) in space units per year. Note that this minimum wave speed for a travelling wave shares the same value with our previous study when immunity is present.

Conclusion and discussion

Lacroix et al. (2005) suggest that infectious humans may be more attractive to mosquitoes than susceptible humans due to the manipulation of the malaria parasites in them. Previously, Kingsolver (1987) introduce a model that takes account for this manipulation. Here, we introduce the model in a different way from previous authors and analyse it relating to certain factors in mosquitoes to the spread of malaria such as incubation time, random movement, and chemically directed movement to humans.

First, we introduce the model with the dynamics of malaria in humans and mosquitoes described by SIS (susceptible-infectious-susceptible) and SI (susceptible-infectious) com-

partment models, respectively. The vector-bias term is expressed in terms of different probabilities that a mosquito arriving at a human at random and picks that human depending on whether that person is infectious, or susceptible.

Second, we prove that a transcritical bifurcation occurs at the basic reproductive ratio equaling 1 ($R_0 = 1$) by projecting the flow onto the extended centre manifold. Consequently, the disease-free steady state is stable if and only if $R_0 < 1$ and the disease-present steady state is stable if and only if $R_0 > 1$. The greater attractiveness of infectious humans to mosquitoes affects malaria transmission that the populations favor high prevalence of the parasites.

Due to short the lifespan of mosquitoes, we incorporate the incubation of malaria parasites that might play an important role in studying the dynamics behaviours of the disease. From our study, it suggests that the malaria transmission, the proportion of infectious humans and mosquitoes, decreases when incubation time of malaria parasites in mosquitoes increases. We show that the disease-free steady state is stable if $R_0^\tau < 1$ analytically and the disease-present steady state is stable if $R_0^\tau > 1$ numerically. Also, for our parameter ranges, we show that malaria is endemic no matter how long the incubation time is.

Finally, we include the random movement of mosquitoes in term of a diffusion term and attractiveness of humans to mosquitoes in chemical forms such as sweat and body odour in term of chemotaxis term into the model. We then study the propagation of the infected population to the uninfected population. We show that travelling waves occurs as a pulse wave and the wave speed can be calculated from the numerical results. We also approximate the minimum wave speed analytically and compare it with the numerical result. By comparing this minimum wave speed with one from the vector-bias model based on SIRS (susceptible-infectious-recovered-susceptible) in humans and SI in mosquitoes on malaria transmission in the previous section, we find that it shares the same minimum wave speed.

All in all, this work should be further studied by approximating the values of p and l from real data from a malaria endemic area, or including control measures into the model.

3.4 Conclusions and Discussion

In this chapter, we study mathematical models for malaria. In Section 3.1, we propose a mathematical model based on a status-based framework for two strains of malaria in the same species or two strains from different species. By the status-based framework, the

model becomes more tractable (comparing with the model in Section 3.2, for example). We then study the long-term dynamical behaviours by stability analysis and bifurcation analysis. The goal of this study is to introduce a model that can be used to study malaria transmission when controls are available in Chapter 4.

In Section 3.2, we propose two novel models, the coinfection and cross-immunity models, for studying two different species of malaria, *P. falciparum* and *P. vivax*. The coinfection model takes into account of suppression during coinfection of both species, that infection with *P. falciparum* reduces susceptibility to *P. vivax* and infection with *P. vivax* helps to reduce complications to infection with *P. falciparum*. In many parts of the world, malaria incidences and prevalence are different between species in each season. We investigate this matter by considering seasonality in each species. Due to certain factors in mosquitoes and parasites, it suggests that there is seasonality in transmission of *P. falciparum*. Hence, we introduce the transmission rate of *P. falciparum* as a sinusoidal function. We find that the prevalence of *P. falciparum* is very high in one season of each year while the prevalence of *P. vivax* is high before that season of *P. falciparum*. This result is corresponding to the data in some literature (Syafruddin et al., 2009). By considering the relapse mechanism of *P. vivax* such that rate of becoming inactive increases while rate of relapsing decreases in individuals previously infected with *P. falciparum* and currently infected with *P. vivax* and by considering the ability of *P. vivax* that can multiply better in colder weather than *P. falciparum*, we introduce seasonality in both *P. vivax* and *P.falciparum* with highly transmission happening in different seasons. In this case, the prevalence of *P. vivax* is peak in the middle of every highly transmitted season of *P. falciparum* in each year.

By omitting coinfection between *P. falciparum* and *P. vivax* and assuming that cross-species immunity exists and acts in the similar way with suppression during coinfection, we can derive the cross-immunity model that can be used to study relations between cross-species immunities σ_1 and σ_4, cross-immunity that acts to reduce susceptibility to *P. vivax* and cross-immunity that acts to reduce complications to *P. falciparum*. In this study, we show that when σ_1 is very high, *P. vivax* may die out. However no matter how high σ_4 is (unless σ_1 is high), both species still coexist. Consequently, cross-immunity of *P. falciparum* to *P. vivax* may benefit human population more than cross-immunity of *P. vivax* to *P. falciparum*. We further investigate mean ages at infection to both species of malaria from this model. We find that cross-immunity of *P. vivax* to reduce the recovery time in *P. falciparum* increases the mean age at infection of *P. falciparum* while cross-immunity of *P. falciparum* to reduce transmission of *P. vivax* reduces the mean age to be shorter. On the other hand, cross-immunity of *P. falciparum* to *P. vivax* increases the mean age at infection of *P. vivax* while cross-immunity of *P. vivax* to *P. falciparum* reduces it. This result is clearly observed when the basic reproductive

ratio is small. However, when it becomes much bigger, cross-immunity does not much help reducing the mean age at infection. In our study, we can also estimate the mean age at infection for *P. falciparum* as 2 year old and for *P. vivax* as 4 year old. This result is based estimations of the basic reproductive ratios from real data. In case the mean age at infection of each species is known, we can estimate the basic reproductive ratio, which is an important quantity in studying disease dynamics, from the formula.

In Section 3.3 and 3.4, we additionally study two single-strain models of malaria transmission. In the first model, we use the SIRS framework for describing a human population while we use the SIS framework for hosts in the second model. In the first model, we introduce each factor driven by mosquitoes one by one to study the disease dynamics relating to mosquito's behaviours. These factors are seasonality, incubation time in mosquitoes, the greater attractiveness of infectious humans, the random movement of mosquitoes, and the chemically directed movement toward humans. Differently, by assuming that rate of waning immunity is very big ($\gamma \to \infty$), the SIRS model for humans can be approximated by the SIS model. The second model becomes more tractable so that we can analyse the system analytically. Consequently, we can introduce a model that takes into account the greater attractiveness of infectious humans since the beginning of the study and then study the system when incubation time and random movement of mosquitoes, and the chemically directed movement toward humans, are taken into account.

For the first model in Section 3.3, we find that the proportion of infectious individuals is increased when rate of waning immunity becomes bigger. By incorporating seasonality in the recruitment rate of mosquitoes due to their abundance during rainy season, seasonality in the transmission rates due to the higher bitting rate of mosquitoes and parasite replications in warmer weather, malaria can be highly transmitted in every hot and wet season (in case there are three seasons in each year:hot, rainy, and winter). This corresponds to some malaria data that it is highly endemic in hot and rainy season. This work can be further investigated when controls are present. For example, when should sterlise mosquitoes and genetically modified mosquitoes be released to effectively control malaria transmission. We then introduce the incubation time in mosquitoes. The basic reproductive ratio and the prevalence of malaria are reduced when the incubation time in mosquitoes increases. Since it may take longer for malaria parasites to appear in salivary glands of mosquitoes when the weather is cold (τ is big when the temperature is cold) (Pascual et al., 2006; Patz and Olson, 2006), our result suggests that malaria in temperate regions may be less transmitted and less prevalent than tropical regions. Next, we incorporate the greater attractiveness of infectious individuals to mosquitoes. By including a random movement of mosquitoes as a diffusion term and a chemically directed movement as a chemotaxis term, we

find that travelling waves occur and their speed can be approximated. Hence, malaria propagates from the disease-present areas to the disease-free areas. We are also able to calculate the minimum wave speed and compare it with our numerical results. We can also find that the more attractive the infectious humans are, the faster malaria travels and spreads.

In Section 3.4, we first introduce an SIS-SI model by incorporating the greater attractiveness of infectious humans to mosquitoes. We then prove that the disease-free steady state is stable if and only if $R_0 < 1$ by Routh-Hurwitz criteria and the disease-present steady state is stable if and only if $R_0 > 1$ by the proof of transcritical bifurcation. Next, incubation time in mosquitoes is taken into account. We show that the disease-free steady state is stable if and only if $R_0^\tau < 1$. Numerically, we show that when $R_0^\tau > 1$ the solutions tend to the disease-present steady state. We study propagation of malaria by including a diffusion term and a chemotaxis term to represent a random movement and a chemically directed movement of mosquitoes. Travelling waves occur and we can calculate the wave speed of malaria dissemination and it lower bound.

By comparing the wave speed calculated from numerical solutions when p and l are varied in Figure 3-28 & 3-32, we see that both models lead to the same wave speed of malaria propagation and so do the minimum wave speed. However, when time passes and malaria becomes endemic (hence solutions tend to the disease-present steady state), the first model predicts significantly less numbers of infectious individuals than the second model. Hence, the presence of immunity helps to reduce the prevalence of malaria but does not alter malaria dissemination (see Figure 3-27(b) & 3-31(b)).

Chapter 4

Controls in multi-strain diseases

In this chapter, we study multi-strain models in the presence of controls. The aim of control application is generally to reduce the spread of the disease and minimize the loss. For influenza, we consider a two-strain model with a status-based framework in the presence of isolation and vaccination. In the first model, infected individuals are isolated to prevent further transmission to others. Vaccination is assumed to be given to newborns with the objective to reduce the prevalence of influenza. In the second model, we study influenza based on the waning of immunity in cross-immune individuals when vaccination is launched. Vaccination is assumed to be given to susceptible pool. We investigate both constant and time-dependent rate of vaccination in the model.

For malaria, control in hosts can be achieved by applying drugs and treatments. Since 2002 scientists can access genome sequences of *Plasmodium* freely (Gardner et al., 2002; Carlton, 2003), and vaccination research has been improved significantly. In the future, a malaria vaccination might be available. Hence the study of malaria in terms of population dynamics in the presence of vaccination might provide public health a future insight into the use of a vaccine efficiently to eradicate malaria. Vaccination models in malaria (Chiyaka et al., 2007*a*, 2008) are still scant, especially multi-strain ones. Here we consider the two-strain host-vector model with status-based framework in both with and without age classes. The model is previously introduced in Chapter 3. We propose threshold conditions for eradicating the disease. Another effective way of controlling malaria is by controlling mosquitoes (Takken and Knols, 2005). Several means affect mosquitoes differently. For example, destroying the mosquito's habitat and breeding sites, the use of larvicide, and introducing sterile mosquitoes help to reduce the number of new coming mosquitoes (Fillinger and Lindsay, 2006; Fillinger et al., 2009; Scott et al., 2002). The use of repellents and bed nets does not kill mosquitoes but helps to decrease the biting rate (Bradley et al., 1986). By spraying the walls and ceilings of the house with insecticide, the survival of adult mosquitoes resting indoors is reduced

(Pates et al., 2005). Recent reports show improvement of the study that could lead to introducing genetically modified mosquitoes, that could kill 100 per cent of parasites in their guts, to replace wild mosquitoes (Ito et al., 2002; Povelones et al., 2009) so that the transmission of malaria to humans is reduced by reducing the probability of successful infection in a human who gets bitten by an infectious mosquito. Hence, we finally end this chapter by discussing the use of these controlling methods via the basic reproductive ratio in the malaria transmission model.

4.1 Modelling isolation and vaccination in influenza

Isolation and vaccination are two of the most effective means to control a disease. Vaccination is targeted to susceptible individuals while isolation is focused on the infective individuals. Since both means are currently widely used, the study of them in detail might clarify the advantages and disadvantages between them and hopefully benefit us to use them efficiently. In this section, we introduce isolation and vaccination into a multi-strain model for influenza. We then study the stability analysis and the bifurcation analysis in each strategy. We propose criteria that might be useful for public health in terms of the parameters of the disease. We illustrate some of the results by numerical simulations. Moreover, we study the dynamics of the systems numerically when there is a delay in isolation. The impact of cross-immunity is also mentioned in some parts of this work. In terms of comparison of the models, we compare the reproductive ratio of the strain in the absence of interventions, the isolation reproductive ratio, and the vaccination reproductive ratio. Furthermore, we compare the host's mean age at infection, rate of invasion of the novel strain, and the results in terms of economic points of view. Additionally, we combine those two means into the model and then study it numerically.

4.1.1 Model formulation

Three models are mentioned in this section. The first model is the basic model before introducing an intervention. The second model is developed by considering the presence of isolation. The third model is formulated for describing the dynamics of the host population when vaccination is present.

Without intervention

The model before introducing the intervention is formulated by Gog and Grenfell (2002). The model assumes polarized susceptibility, i.e. each individual is either com-

pletely immune or completely susceptible to each strain of a disease. Immediately on infection with a strain of a disease, an individual is assumed to become immune to that strain with probability 1 and immune to related strains with reduced probabilities. For a disease with two co-circulating strains, each individual, whether infected or not, has one of four possible immune repertoires $\emptyset$, $\{1\}$, $\{2\}$, $\{1,2\}$. We assume that an individual with immune repertoire $\emptyset$ has probability σ of acquiring immunity to strain 2 (as well as strain 1) on infection with strain 1, and the same probability σ of acquiring immunity to strain 1 on infection with strain 2. Following Gog and Grenfell (2002), we assume further that an individual with immune repertoire $\{1\}$ also has probability σ of acquiring immunity to strain 2 on contact with an individual infected with strain 1 even though infection with strain 1 is impossible, and similarly when an individual with immune repertoire $\{2\}$ comes into contact with an individual infected with strain 2. These assumptions allow us to write down a system of four equations for four classes of hosts: susceptible to strain 1, S_1 (whether with immune repertoire $\emptyset$ or $\{2\}$ and whether or not infected with strain 2); infected with strain 1, I_1; susceptible to strain 2, S_2; and infected with strain 2, I_2. Note that these classes are not mutually exclusive, and that some individuals do not belong to any of them. We assume that the recovery rate from each strain is the same and denote it by ν_0, but that each strain has a different rate of transmission denoted by β_1 and β_2. The equations are as follows

$$\begin{aligned} S_1'(t) &= \mu_0 N - \mu_0 S_1 - \beta_1 S_1 I_1 - \sigma\beta_2 S_1 I_2, \\ I_1'(t) &= \beta_1 S_1 I_1 - (\mu_0 + \nu_0) I_1, \\ S_2'(t) &= \mu_0 N - \mu_0 S_2 - \beta_2 S_2 I_2 - \sigma\beta_1 S_2 I_1, \\ I_2'(t) &= \beta_2 S_2 I_2 - (\mu_0 + \nu_0) I_2. \end{aligned} \tag{4.1.1}$$

It is assumed that there is no death from infection and the birth and death rates are the same so that the total size of population (N) is a constant. We normalise the system (4.1.1) by introducing the new variables and parameters as follows

$$s_1 = \frac{S_1}{N},\ i_1 = \frac{I_1}{N},\ s_2 = \frac{S_2}{N},\ i_2 = \frac{I_2}{N},\ T = (\mu_0 + \nu_0)t,\ \mu = \frac{\mu_0}{\mu_0 + \nu_0},$$

and the reproductive ratio of strain 1 and strain 2 respectively

$$R_1 = \frac{\beta_1 N}{\mu_0 + \nu_0} \text{ and } R_2 = \frac{\beta_2 N}{\mu_0 + \nu_0}.$$

The model becomes

$$\begin{aligned} s_1'(T) &= \mu(1 - s_1) - R_1 s_1 i_1 - \sigma R_2 s_1 i_2, \\ i_1'(T) &= R_1 s_1 i_1 - i_1, \\ s_2'(T) &= \mu(1 - s_2) - R_2 s_2 i_2 - \sigma R_1 s_2 i_1, \\ i_2'(T) &= R_2 s_2 i_2 - i_2, \end{aligned} \tag{4.1.2}$$

With isolation

Because of similar symptoms and the difficulty of clinically distinguishing a viral strain, we assume that rate at which infected individuals are detected and removed to quarantine (q_0) is the same for strain 1 and strain 2. Removing such individuals to quarantine does not change their immune status and they return to the same S_i class after recovery, so (on the assumption that there are few individuals in quarantine at any one time) the equations for S_1 and S_2 are unchanged. We assume that individuals leave the quarantined class at rate κ_0. The model takes the form

$$\begin{aligned} S_1'(t) &= \mu_0 N - \mu_0 S_1 - \beta_1 S_1 I_1 - \sigma\beta_2 S_1 I_2, \\ I_1'(t) &= \beta_1 S_1 I_1 - (\nu_0 + \mu_0 + q_0) I_1, \\ S_2'(t) &= \mu_0 N - \mu_0 S_2 - \beta_2 S_2 I_2 - \sigma\beta_1 S_2 I_1, \\ I_2'(t) &= \beta_2 S_2 I_2 - (\nu_0 + \mu_0 + q_0) I_2, \\ Q'(t) &= q_0(I_1 + I_2) - \kappa_0 Q. \end{aligned} \tag{4.1.3}$$

We normalise the system (4.1.3) by introducing the new variables and parameters as follows

$$s_1 = \frac{S_1}{N},\ i_1 = \frac{I_1}{N},\ s_2 = \frac{S_2}{N},\ i_2 = \frac{I_2}{N},\ q = \frac{Q}{N},$$

$$T = (\mu_0 + \nu_0 + q_0)t,\ \mu = \frac{\mu_0}{\mu_0 + \nu_0 + q_0},\ \theta = \frac{q_0}{\mu_0 + \nu_0 + q_0},\ \kappa = \frac{\kappa_0}{\mu_0 + \nu_0 + q_0},$$

and the two isolation basic reproductive ratios for strain 1 and strain 2,

$$R_{1q} = \frac{\beta_1 N}{\mu_0 + \nu_0 + q_0} \text{ and } R_{2q} = \frac{\beta_2 N}{\mu_0 + \nu_0 + q_0}.$$

The model is now in the form

$$\begin{aligned} s_1'(T) &= \mu(1 - s_1) - R_{1q} s_1 i_1 - \sigma R_{2q} s_1 i_2, \\ i_1'(T) &= R_{1q} s_1 i_1 - i_1, \\ s_2'(T) &= \mu(1 - s_2) - R_{2q} s_2 i_2 - \sigma R_{1q} s_2 i_1, \\ i_2'(T) &= R_{2q} s_2 i_2 - i_2, \\ q'(T) &= \theta(i_1 + i_2) - \kappa q \end{aligned} \tag{4.1.4}$$

We remark here that R_{1q} and R_{2q} can be written in terms of R_1 and R_2 as

$$R_{1q} = (1 - \theta)R_1 \text{ and } R_{2q} = (1 - \theta)R_2.$$

With vaccination

We assume that a vaccine targeted at strain 1 is given to newborns so that a fraction p of vaccinated infants acquire immunity to strain 1 and a fraction $p\tau$ acquires immunity

to strain 2; here τ is the cross-immunity coefficient induced by vaccination. Vaccination effectively protects an individual from both strains if $\tau = 1$; we assume that it is less than σ which is the cross-immunity coefficient induced by infection to the viral strain. The model is

$$\begin{aligned} S_1'(t) &= \mu_0(1-p)N - \mu_0 S_1 - \beta_1 S_1 I_1 - \sigma\beta_2 S_1 I_2, \\ I_1'(t) &= \beta_1 S_1 I_1 - (\nu_0 + \mu_0) I_1, \\ S_2'(t) &= \mu_0(1-p\tau)N - \mu_0 S_2 - \beta_2 S_2 I_2 - \sigma\beta_1 S_2 I_1, \\ I_2'(t) &= \beta_2 S_2 I_2 - (\nu_0 + \mu_0) I_2. \end{aligned} \tag{4.1.5}$$

From the model, the successfully vaccinated newborns enter the vaccination class V and

$$V'(t) = p\mu_0 N - \mu_0 V \tag{4.1.6}$$

Because vaccination gives full protection to strain 1 and cross-immunity to strain 2, only a fraction τp of newborns acquire immunity to both strains. Thus, the rest of them, a fraction $(1-\tau)p$ of newborns who acquire only immunity to strain 1 and a fraction $1-p$ of newborns who are unvaccinated and acquire no immunity to any strain, are susceptible to strain 2 and so the recruitment to the S_2 class is at rate $\mu(1-p\tau)N$. The equation (4.1.6) is decoupled from the system (4.1.5) and V can be found explicitly from the following equation

$$V(t) = pN + (V_0 - pN)e^{-\mu_0 t} \tag{4.1.7}$$

where V_0 is the initial condition of V at time $t = 0$. The system (4.1.5) is normalised by introducing a set of variables and parameters as follows

$$s_1 = \frac{S_1}{N},\ i_1 = \frac{I_1}{N},\ s_2 = \frac{S_2}{N},\ i_2 = \frac{I_2}{N},\ T = (\mu_0 + \nu_0)t,\ \mu = \frac{\mu_0}{\mu_0 + \nu_0},$$

and the model becomes

$$\begin{aligned} s_1'(T) &= \mu(1-p) - \mu s_1 - R_1 s_1 i_1 - \sigma R_2 s_1 i_2, \\ i_1'(T) &= R_1 s_1 i_1 - i_1, \\ s_2'(T) &= \mu(1-\tau p) - \mu s_2 - R_2 s_2 i_2 - \sigma R_1 s_2 i_1, \\ i_2'(T) &= R_2 s_2 i_2 - i_2, \end{aligned} \tag{4.1.8}$$

From the model, the vaccination basic reproductive ratios for strain 1 and strain 2 are

$$R_{1p} = (1-p)R_1 \text{ and } R_{2p} = (1-p\tau)R_2.$$

4.1.2 Stability analysis

By setting the right-hand sides of the system (4.1.2),(4.1.4), and (4.1.8) equal to zero, we have four steady states for each model.

Without intervention

1) The disease-free steady state

$$P^0 = (s_1^0, i_1^0, s_2^0, i_2^0) = (1, 0, 1, 0).$$

2) The single-strain steady state of strain 1

$$P^1 = (s_1^1, i_1^1, s_2^1, i_2^1) = \left(\frac{1}{R_1}, \frac{\mu}{R_1}(R_1 - 1), \frac{1}{1 + \sigma(R_1 - 1)}, 0\right)$$

which is positive if and only if

$$R_1 > 1. \tag{4.1.9}$$

3) The single-strain steady state of strain 2

$$P^2 = (s_1^2, i_1^2, s_2^2, i_2^2) = \left(\frac{1}{1 + \sigma(R_2 - 1)}, 0, \frac{1}{R_2}, \frac{\mu}{R_2}(R_2 - 1)\right)$$

which is positive if and only if

$$R_2 > 1. \tag{4.1.10}$$

4) The coexistent steady state

$$P^* = (s_1^*, i_1^*, s_2^*, i_2^*)$$

where

$$s_1^* = \frac{1}{R_1}, \;\; i_1^* = \frac{\mu}{(1 - \sigma^2)R_1}\left[(R_1 - 1) - \sigma(R_2 - 1)\right]$$

and

$$s_2^* = \frac{1}{R_2}, \;\; i_2^* = \frac{\mu}{(1 - \sigma^2)R_2}\left[(R_2 - 1) - \sigma(R_1 - 1)\right].$$

The coexistent steady state is positive if and only if both of the following conditions hold

$$(R_1 - 1) - \sigma(R_2 - 1) > 0 \tag{4.1.11}$$

and

$$(R_2 - 1) - \sigma(R_1 - 1) > 0. \tag{4.1.12}$$

With isolation

1) The disease-free steady state

$$P_q^0 = (s_{1q}^0, i_{1q}^0, s_{2q}^0, i_{2q}^0, q_q^0) = (1, 0, 1, 0, 0).$$

2) The single-strain steady state of strain 1

$$P_q^1 = (s_{1q}^1, i_{1q}^1, s_{2q}^1, i_{2q}^1, q_q^1) = \left(\frac{1}{R_{1q}}, \frac{\mu}{R_{1q}}(R_{1q}-1), \frac{1}{1+\sigma(R_{1q}-1)}, 0, \frac{\theta\mu}{\kappa R_{1q}}(R_{1q}-1)\right)$$

which is positive if and only if

$$R_{1q} > 1. \tag{4.1.13}$$

3) The single-strain steady state of strain 2

$$P_q^2 = (s_{1q}^2, i_{1q}^2, s_{2q}^2, i_{2q}^2, q_q^2) = \left(\frac{1}{1+\sigma(R_{2q}-1)}, 0, \frac{1}{R_{2q}}, \frac{\mu}{R_{2q}}(R_{2q}-1), \frac{\theta\mu}{\kappa R_{2q}}(R_{2q}-1)\right)$$

which is positive if and only if

$$R_{2q} > 1. \tag{4.1.14}$$

4) The coexistent steady state

$$P_q^* = (s_{1q}^*, i_{1q}^*, s_{2q}^*, i_{2q}^*, q_q^*)$$

where

$$s_{1q}^* = \frac{1}{R_{1q}}, \quad i_{1q}^* = \frac{\mu}{(1-\sigma^2)R_{1q}}\left[(R_{1q}-1) - \sigma(R_{2q}-1)\right],$$
$$s_{2q}^* = \frac{1}{R_{2q}}, \quad i_{2q}^* = \frac{\mu}{(1-\sigma^2)R_{2q}}\left[(R_{2q}-1) - \sigma(R_{1q}-1)\right],$$

and

$$q_q^* = \frac{\theta\mu}{(1-\sigma^2)\kappa R_{1q}R_{2q}}\left[R_{2q}(R_{1q}-1) + R_{1q}(R_{2q}-1) - \sigma\left[R_{1q}(R_{1q}-1) + R_{2q}(R_{2q}-1)\right]\right].$$

The coexistent steady state is positive if and only if both of the following conditions hold

$$(R_{1q}-1) - \sigma(R_{2q}-1) > 0 \tag{4.1.15}$$

and

$$(R_{2q}-1) - \sigma(R_{1q}-1) > 0. \tag{4.1.16}$$

With vaccination

1) The disease-free steady state

$$P_p^0 = (s_{1p}^0, i_{1p}^0, s_{2p}^0, i_{2p}^0) = (1-p, 0, 1-p\tau, 0).$$

2) The single-strain steady state of strain 1

$$P_p^1 = (s_{1p}^1, i_{1p}^1, s_{2p}^1, i_{2p}^1) = \left(\frac{1}{R_1}, \frac{\mu}{R_1}(R_{1p}-1), \frac{1-p\tau}{1+\sigma(R_{1p}-1)}, 0\right)$$

which is positive if and only if

$$R_{1p} > 1. \tag{4.1.17}$$

3) The single-strain steady state of strain 2

$$P_p^2 = (s_{1p}^2, i_{1p}^2, s_{2p}^2, i_{2p}^2) = \left(\frac{1-p}{1+\sigma(R_{2p}-1)}, 0, \frac{1}{R_2}, \frac{\mu}{R_2}(R_{2p}-1)\right)$$

which is positive if and only if

$$R_{2p} > 1. \tag{4.1.18}$$

4) The coexistent steady state

$$P_p^* = (s_{1p}^*, i_{1p}^*, s_{2p}^*, i_{2p}^*)$$

where

$$s_{1p}^* = \frac{1}{R_1}, \quad i_{1p}^* = \frac{\mu}{(1-\sigma^2)R_1}\left[(R_{1p}-1) - \sigma(R_{2p}-1)\right]$$

and

$$s_{2p}^* = \frac{1}{R_2}, \quad i_{2p}^* = \frac{\mu}{(1-\sigma^2)R_2}\left[(R_{2p}-1) - \sigma(R_{1p}-1)\right].$$

The two-strain steady state is positive if and only if both of the following conditions are hold

$$(R_{1p}-1) - \sigma(R_{2p}-1) > 0 \tag{4.1.19}$$

and

$$(R_{2p}-1) - \sigma(R_{1p}-1) > 0. \tag{4.1.20}$$

We define the stability conditions of each steady state in each model by considering the eigenvalues of the Jacobian matrix and by using the Routh-Hurwitz criteria. Each of the steady states is stable if and only if all eigenvalues of the Jacobian matrix at the steady state are negative. In case we cannot determine the eigenvalues of the Jacobian explicitly, we consider whether the coefficients of the characteristic equation satisfy the

Routh-Hurwitz criteria instead. For example if the characteristic polynomial is of order 4,

$$\lambda^4 + a_1\lambda^3 + a_2\lambda^2 + a_3\lambda + a_4,$$

the steady state is stable if and only if

$$a_1 > 0, a_3 > 0, a_4 > 0, \text{ and } a_1a_2a_3 > a_3^2 + a_1^2a_4.$$

Without intervention

The Jacobian matrix of the system (4.1.2) is

$$J = \begin{bmatrix} -\mu - R_1i_1 - \sigma R_2i_2 & -R_1s_1 & 0 & -\sigma R_2s_1 \\ R_1i_1 & R_1s_1 - 1 & 0 & 0 \\ 0 & -\sigma R_1s_2 & -\mu - R_2i_2 - \sigma R_1i_1 & -R_2s_2 \\ 0 & 0 & R_2i_2 & R_2s_2 - 1 \end{bmatrix}. \quad (4.1.21)$$

It is straightforward to determine the stability conditions of each steady state so we omit their derivation here.
1) The disease-free steady state is stable if and only if

$$R_1 < 1 \text{ and } R_2 < 1.$$

2) The stability conditions for the disease single-strain steady state of strain 1 are

$$R_1 > 1 \text{ and } (R_2 - 1) - \sigma(R_1 - 1) < 0.$$

3) Similarly, the stability conditions for the disease single-strain steady state of strain 2 are

$$R_2 > 1 \text{ and } (R_1 - 1) - \sigma(R_2 - 1) < 0.$$

4) By the Routh-Hurwitz criteria, the coexistent steady state is stable if and only if

$$i_1^* > 0 \text{ and } i_2^* > 0 \text{ or } (R_1 - 1) - \sigma(R_2 - 1) > 0 \text{ and } (R_2 - 1) - \sigma(R_1 - 1) > 0$$

A bifurcation diagram in terms of R_1 and R_2 for this case is shown in Figure 4-1 (a). Without cross-immunity, $\sigma = 0$, we have coexistence whenever $R_1 > 1$ and $R_2 > 1$. If the cross-immunity is perfect, $\sigma = 1$, there is no coexistence of the strains so that either strain 1 persists because $R_1 > R_2$ and $R_1 > 1$ or strain 2 persists when $R_2 > R_1$ and $R_2 > 1$.

With isolation

In the similar way, the stability conditions can be derived straightforwardly by considering the Jacobian matrix of the system (4.1.4) so that we omit their proofs.
1) The disease-free steady state is stable if and only if

$$R_{1q} < 1 \text{ and } R_{2q} < 1$$

or

$$\theta > 1 - \frac{1}{R_1} \text{ and } \theta > 1 - \frac{1}{R_2}.$$

2) The single-strain steady state of strain 1 is stable if and only if

$$R_{1q} > 1 \text{ and } R_{2q} - 1 - \sigma(R_{1q} - 1) < 0$$

or

$$\theta < 1 - \frac{1}{R_1} \text{ and } (R_2 - 1) - \sigma(R_1 - 1) < (R_2 - \sigma R_1)\theta.$$

3) The single-strain steady state of strain 2 is stable if and only if

$$R_{2q} > 1 \text{ and } R_{1q} - 1 - \sigma(R_{2q} - 1) < 0$$

or

$$\theta < 1 - \frac{1}{R_2} \text{ and } (R_1 - 1) - \sigma(R_2 - 1) < (R_1 - \sigma R_2)\theta.$$

4) The coexistent steady state is stable if and only if

$$R_{2q} - 1 - \sigma(R_{1q} - 1) > 0 \text{ and } R_{1q} - 1 - \sigma(R_{2q} - 1) > 0$$

or

$$(R_2 - 1) - \sigma(R_1 - 1) > (R_2 - \sigma R_1)\theta \text{ and } (R_1 - 1) - \sigma(R_2 - 1) > (R_1 - \sigma R_2)\theta.$$

A bifurcation diagram in terms of R_1 and R_2 is shown in Figure 4-1 (b).

With vaccination

The Jacobian matrix of the system (4.1.8) is in the same form with the system (4.1.2). We have the stability conditions of each steady state as follows;
1) The disease-free steady state is stable if and only if

$$R_{1p} < 1 \text{ and } R_{2p} < 1$$

or

$$p > 1 - \frac{1}{R_1} \text{ and } p > \frac{1}{\tau}\left(1 - \frac{1}{R_2}\right)$$

2) The single-strain steady state of strain 1 is stable if and only if

$$R_{1p} > 1 \text{ and } R_{2p} - 1 - \sigma(R_{1p} - 1) < 0$$

or

$$p < 1 - \frac{1}{R_1} \text{ and } (R_2 - 1) - \sigma(R_1 - 1) < (\tau R_2 - \sigma R_1)p$$

3) The single-strain steady state of strain 2 is stable if and only if

$$R_{2p} > 1 \text{ and } R_{1p} - 1 - \sigma(R_{2p} - 1) < 0$$

or

$$p < \frac{1}{\tau}\left(1 - \frac{1}{R_2}\right) \text{ and } (R_1 - 1) - \sigma(R_2 - 1) < (R_1 - \sigma\tau R_2)p$$

4) The coexistent steady state is stable if and only if

$$R_{2p} - 1 - \sigma(R_{1p} - 1) > 0 \text{ and } R_{1p} - 1 - \sigma(R_{2p} - 1) > 0$$

or

$$(R_2 - 1) - \sigma(R_1 - 1) > (\tau R_2 - \sigma R_1)p \text{ and } (R_1 - 1) - \sigma(R_2 - 1) > (R_1 - \sigma\tau R_2)p.$$

A bifurcation diagram in terms of R_1 and R_2 is shown in Figure 4-1 (c).

4.1.3 Transcritical Bifurcation Diagrams

Since all the steady states and stability conditions can be found explicitly, we can plot the bifurcation diagrams according to the characteristics of the parameters in which we are interested in each model. We remark here that all the conditions we propose are for studying the long-term behaviour of the strains.

Assume that we know the basic reproductive ratio of strain 1 and 2 when intervention is absent. It may be useful for public health if we know which rates of isolation and vaccination for both strains to die out, strain 1 to persist, strain 2 to persist, and both strains to coexist. Say, if we pick one point on the (R_1, R_2) plane, will we be able to tell what will happen when θ and p vary. To answer this question, we divide the (R_1, R_2) plane into areas corresponding to Figure 4-1(a).

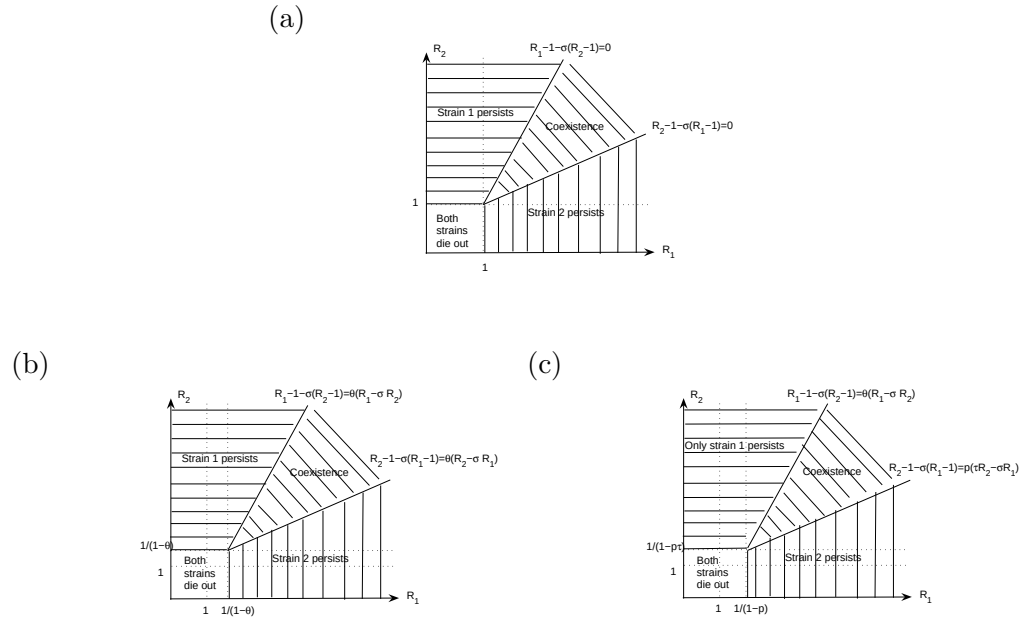

Figure 4-1: Bifurcation diagrams in terms of R_1 and R_2 for the models without intervention (a), with isolation (b), and with vaccination (c)

With isolation

We choose θ, the non-dimensionalised quarantine rate to be a bifurcation parameter. We then plot it against i_1 and i_2 at each steady state and determine the stable branches and unstable branches by the stability conditions. The bifurcations in the diagram are of the transcritical type where two steady states exchange their stability at the bifurcation point. We are interested in studying the dynamics of two co-circulating strains, so $R_1 > 1$ and $R_2 > 1$ are assumed. We separate the area of parameters R_1 and R_2 relating to Figure 4-1(a) when intervention is absent.

1. $(R_1 - 1) - \sigma(R_2 - 1) > 0$ and $(R_2 - 1) - \sigma(R_1 - 1) < 0$
   The transcritical bifurcation diagram is shown in Figure 4-2(a). Without isolation, only strain 1 persists in this case. Consequently, to eradicate the disease is to eradicate strain 1. So if $\theta < 1 - 1/R_1$, strain 1 is endemic in the population. If not, $\theta > 1 - 1/R_1$, the disease dies out.

2. $(R_1 - 1) - \sigma(R_2 - 1) > 0$ and $(R_2 - 1) - \sigma(R_1 - 1) > 0$
   According to the condition, both strains coexist in the host population when isolation is absent.

   On one hand, if $R_1 > R_2$, the bifurcation diagram is shown in Figure 4-2(b). Both strains coexist if the isolation rate is not high enough ($\theta < [(R_2 - 1) - \sigma(R_1 - 1)]/(R_2 - \sigma R_1)$). With the cross-immunity and the higher attempt of isolation ($[(R_2 - 1) - \sigma(R_1 - 1)]/(R_2 - \sigma R_1) < \theta < 1 - 1/R_1$), strain 2 becomes extinct by the advantage of strain 1 in term of transmission but strain 1 is still endemic

(a)

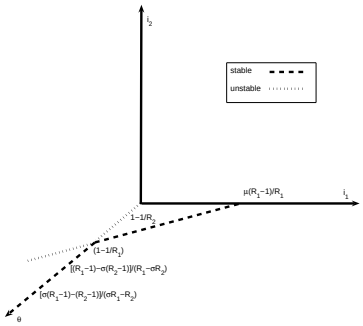

(b)

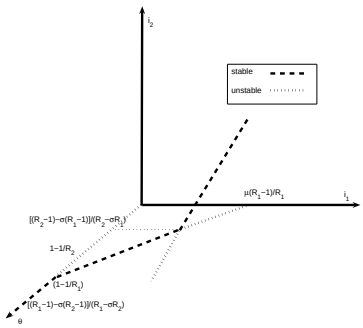

(c)

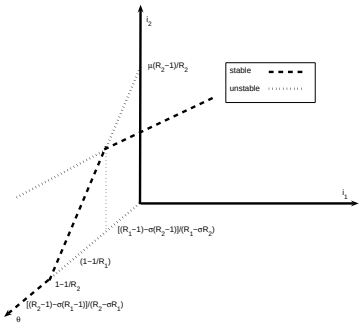

(d)

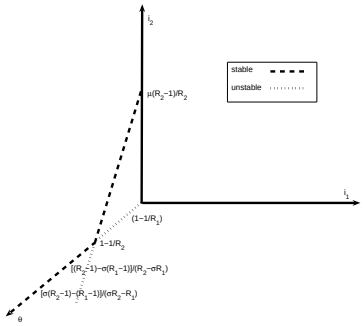

Figure 4-2: Bifurcation diagrams with a bifurcation parameter θ: (a) when strain 1 is dominant, (b) when both strains can coexist and $R_1 > R_2$, (c) when both strains can coexist and $R_2 > R_1$ and (d) when strain 2 is dominant .

in the population. If the isolation rate is high enough so that $\theta > 1 - 1/R_1$, it promises the extinction the disease.

On the other hand, if $R_2 > R1$, the bifurcation of the latter case is shown in Figure 4-2(c). Coexistence of both strains occurs at the low rate of isolation ($\theta < [(R_1 - 1) - \sigma(R_2 - 1)]/(R_1 - \sigma R_2)$). Strain 1 can be driven out from the population when isolation is more concerned ($[(R_1 - 1) - \sigma(R_2 - 1)]/(R_1 - \sigma R_2) < \theta < 1 - 1/R_2$). If the isolation rate is very high ($\theta > 1 - 1/R_2$), the disease is eradicated.

3. $(R_1 - 1) - \sigma(R_2 - 1) < 0$ and $(R_2 - 1) - \sigma(R_1 - 1) > 0$
   The bifurcation diagram can be found in Figure 4-2(d). Without isolation, strain 2 persists. To eradicate the disease from the population is to drive out strain 2. If $\theta > 1 - 1/R_2$, strain 2 can be driven out.

With vaccination

We are interested in the behaviour of the system in terms of the parameter p so we take it to be a bifurcation parameter in the model. We plot bifurcation diagrams on the axes p, i_1, and i_2 by considering the stability conditions at the steady state. Since we are interested in only the positive value of p and when $R_1 > 1$ and $R_2 > 1$, the area of parameters (R_1, R_2) is separated into three cases as follows (see Figure 4-1(a)):

1. $(R_1 - 1) - \sigma(R_2 - 1) > 0$ and $(R_2 - 1) - \sigma(R - 1) < 0$
   Without vaccination, only strain 1 persists. In this case, we separate it into two subcases according with the sign of the following term

$$R_1(R_2 - 1) - \tau R_2(R_1 - 1). \tag{4.1.22}$$

   By considering the relation between R_1 and R_2 according with the parameter τ which is the cross-immunity induced by vaccination (See Figure 4-3). If $R_1(R_2 - 1) - \tau R_2(R_1 - 1) < 0$, in the presence of vaccination, strain 1 is facilitated. It means that either strain 2 cannot invade the host population or strain 1 can persist although the vaccination rate is high. On the other hand, if $R_1(R_2 - 1) - \tau R_2(R_1 - 1) > 0$, strain 2 is better in the environment. However, by the assumption that $\tau < \sigma \leq 1$, we cannot have the case when $R_1(R_2 - 1) - \tau R_2(R_1 - 1)$ is negative in Case 2) and Case 3) when $R_2 > R_1$.

   The transcritical bifurcation diagrams are shown in Figure 4-4(a)-(b). In (a), τ plays an important role in this case. If the vaccine coverage is low ($p < [\sigma(R_1 - 1) - (R_2 - 1)]/(\sigma R_1 - \tau R_2)$), strain 1 is endemic because it has a competitive advantage

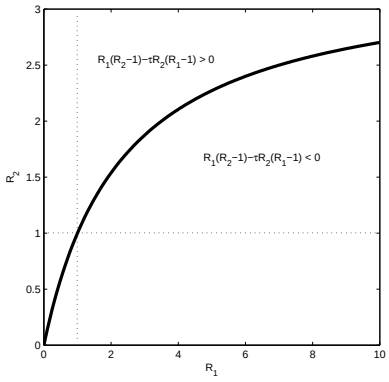

Figure 4-3: The relation between R_1 and R_2 with the presence of τ in the term $R_1(R_2-1)-\tau R_2(R_1-1)$

in the absence of vaccination. When $[\sigma(R_1-1)-(R_2-1)]/(\sigma R_1-\tau R_2) < p < [(R_1-1)-\sigma(R_2-1)]/(R_1-\sigma\tau R_2)$, the vaccination starts to affect strain 1 and by our assumption that the vaccine is targeted to strain 1 with a higher probability than strain 2, the system favors strain 2 so the coexistence of the strains occurs. With a higher vaccine coverage ($[(R_1-1)-\sigma(R_2-1)]/(R_1-\sigma\tau R_2) < p < (1-1/R_2)/\tau$), strain 1 can be eradicated while strain 2 still persists, but the number of infectious individuals to strain 2 is decreased if we increase vaccine coverage. If the fraction of vaccinating newborns is very high $p > (1-1/R_2)/\tau$), strain 2 cannot persist any more. Hence the disease dies out. In (b), strain 1 is far better than strain 2 in both of the absence and the presence of vaccination. Vaccination is very effective (τ is big) so that strain 2 is not preferred by the presence of the vaccination. If $p < (1-1/R_1)$, strain 1 persists. Otherwise, it dies out. Overall, vaccination is effective to strain 1 in this case.

2. $(R_1-1)-\sigma(R_2-1) > 0$ and $(R_2-1)-\sigma(R-1) > 0$
   In this case both strains are endemic when there is no vaccination. This case only happens when $\sigma^2 < \tau < \sigma$ since the intersection of the lines $\tau R_2-\sigma R_1 = 0$ and $(R_1-1)-\sigma(R_2-1) = 0$ is not in the positive quadrant if $\tau < \sigma^2$. By the assumption that $\tau < \sigma$, we have $R_2 > R_1$. The bifurcation diagram is shown in (See Figure 4-5). If p is small ($p < [(R_1-1)-\sigma(R_2-1)]/(R_1-\sigma\tau R_2)$), both strains coexist. If $[(R_1-1)-\sigma(R_2-1)]/(R_1-\sigma\tau R_2) < p < (1-1/R_2)/\tau$, strain 1 is driven out. If $p > (1-1/R)2)/\tau$, we can eradicate the disease.

3. $(R_1-1)-\sigma(R_2-1) < 0$ and $(R_2-1)-\sigma(R-1) > 0$
   Without vaccination, only strain 2 persists. The bifurcation diagrams are shown in Figure 4-6. Strain 2 is better than strain 1 both with and without vaccination. The disease can be driven out by eradicating strain 2. So, if $p > (1-1/R_2)/\tau$,

(a)

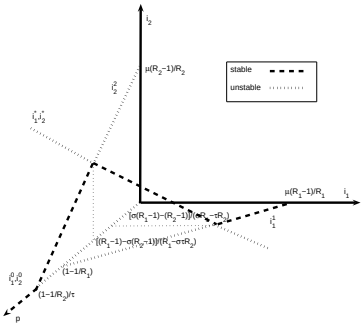

(b)

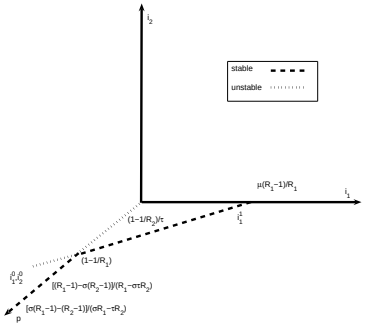

Figure 4-4: Bifurcation diagrams with a bifurcation parameter p for case 1; (a) strain 2 is dominant (b) strain 1 is dominant

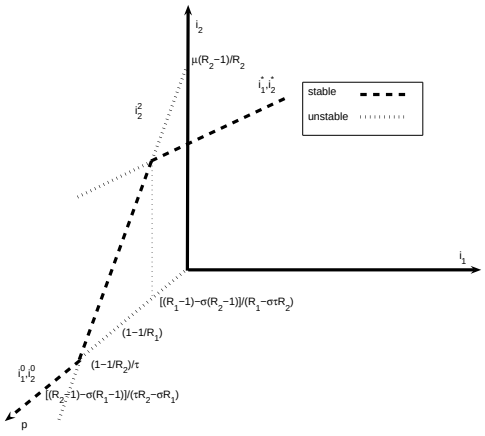

Figure 4-5: Bifurcation diagrams with a bifurcation parameter p for case 2

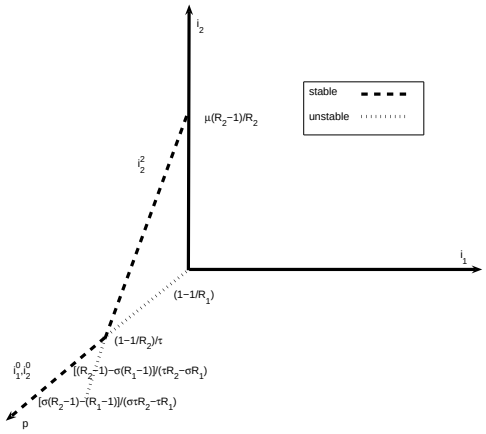

Figure 4-6: Bifurcation diagrams with a bifurcation parameter p for case 3 where strain 2 is dominant

strain 2 is extinct, otherwise it is endemic.

4.1.4 Numerical studies

An average lifetime of human $(1/\mu_0)$ is approximately 70 years. Infectious period of influenza $1/\nu_0$ is around 7 days. Both of these parameters are fixed in all of the simulations. We simulate the models without nondimensionalisation so that the simulations give us the number of infected individuals not the fraction of them. Because there are many cases according to the study of bifurcations, we only show some numerical results from the isolation model (4.1.3) when the parameters of influenza strains are corresponding to case 2.

We choose to show the numerical results of case 2 when $R_1 > R_2$ from the bifurcation analysis in section 4.1.3. If $R_1 = 3.5, R_2 = 3$, and $\sigma = 0.75$, both strains coexist when $\theta < 0.3333$; only strain 1 persists when $0.3333 < \theta < 0.7143$; and both strains die out when $\theta > 0.7143$. Figure 4-7(a) shows the numerical result when $\theta = 0.2$, so we have the coexistence of the strains. In Figure 4-7(b), $\theta = 0.5$, strain 2 is driven out by strain 1. In Figure 4-7(c), we have $\theta = 0.85$, so both strains die out from the host population.

In addition, we assume that the delay in isolation occurs for one month. Instead of starting the isolation at the beginning $(t = 0)$, we introduce it one month later and compare it with the situation that the delay does not occur. We run the simulation with $\theta = 0$ until one month and then continue running it but with $\theta = 0.5$ after that and compare it with the result that we run the simulation with $\theta = 0.5$ constantly from the beginning. The sample case that we further study here is from the previous

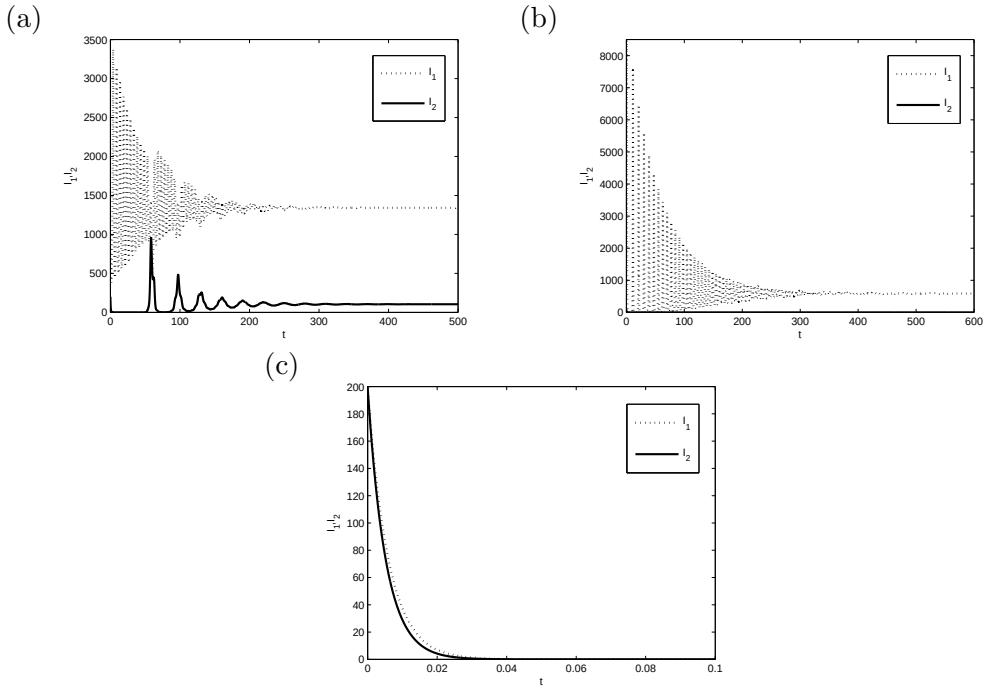

Figure 4-7: Numerical result when isolation is launched; (a) Coexistence of the two strains occurs (b) Only strain 1 is endemic (c) The disease dies out

result (See Figure 4-7(b)) where strain 1 is endemic and when $R_1 = 3.5, R_2 = 3$, and $\sigma = 0.75$. The simulations were run until $t = 5000$ in years but we only choose to show the results in some time intervals that the difference between the models are distinguished because the models are synchronized when time becomes very large. By starting with the same number of infectious individuals, we simulate the model in the situation that we have the delay in isolation to compare it with the situation that we start isolation at the beginning of the disease (See Figure 4-8). In Figure 4-8(a), we show the number of infectious individuals to strain 1 at the beginning of the disease. We can see that with the delay in isolation a high jump appears (or an outbreak) while the model without the delay produces the lower jumps. The high jumps continually appears but with the lower height when time increases (See Figure 4-8(b)) and finally the number of infectious diseases in both cases tends to $i_{1q}^1 N$. For strain 2, it dies out quickly in the absence of isolation delay while it leads to one outbreak (a high jump) and then dies out in the presence of isolation delay (See Figure 4-8(c)). From the result, we conclude that the delay in isolation leads to serious outbreaks.

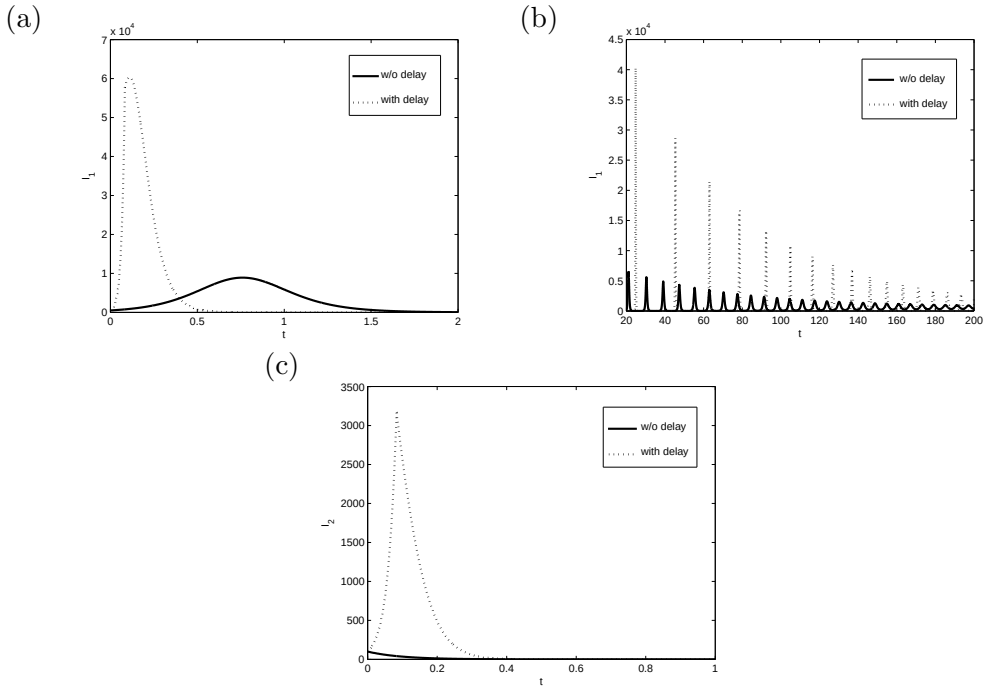

Figure 4-8: Numerical result when a delay in isolation occurs: (a) The dynamics of strain 1 at the onset of the disease: (b) The dynamics of strain 1 when $t \in [40, 200]$ (c) The dynamics of strain 2

4.1.5 Comparisons of the models

The basic reproductive ratios

We only show the comparison of R_2, R_{2q}, and R_{2p}. The comparison of R_1, R_{1q}, and R_{1p} can be studied in the similar way. Without intervention, the reproductive ratio of strain 2 is

$$R_2 = \frac{\beta_2 N}{(\mu_0 + \nu_0)}$$

We can write the isolation basic reproductive ratio and the vaccination basic reproductive ratio of strain 2 in terms of R_2 and other parameters as follows

$$R_{2q} = (1 - \theta)R_2 \text{ and } R_{2p} = (1 - p\tau)R_2$$

where $\theta = q_0/(\mu_0 + \nu_0 + q_0)$. These two reproductive ratios are not only depended on R_2 but also rate of isolation or the fraction of vaccination. By comparing R_{2q} and R_{2p} with R_2, we obviously see that for strain 2 to be able to invade the population in the presence of isolation and vaccination ($R_{2q} > 1, R_{2p} > 1$) it needs to be highly transmitted or to have a larger basic reproductive ratio than one without intervention. We show the critical values of the rate of isolation and the fraction of vaccination in

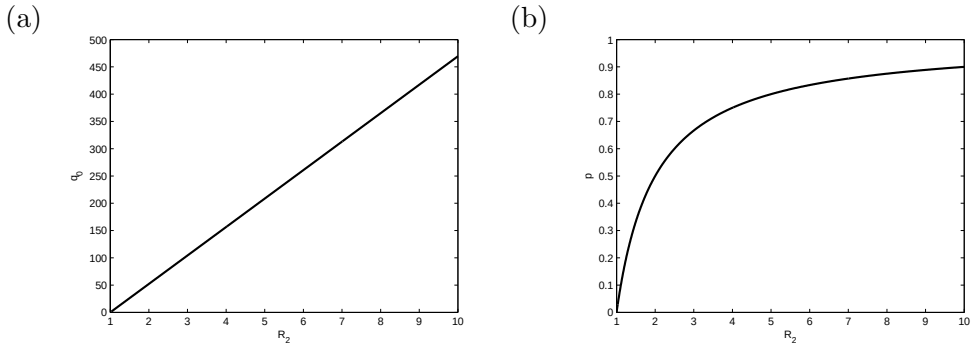

Figure 4-9: The critical rate of isolation and the critical value of the vaccine coverage (a) $q_0 = (\mu_0 + \nu_0)(R_2 - 1)$ (b) $p = (1 - 1/R_2)/\tau$

Figure 4-9.

We further study the comparison via a fixed R_1 and a varied R_2 of each strategy by considering the number of infected individuals. If $R_1 = 3.2, R_2 = 3.5, \sigma = 0.8$, and $\tau = 0.75$, the set of parameters are corresponding to Case 2 when $R_2 > R_1$ in the bifurcation analysis for the model with isolation and Case 2 in the bifurcation analysis for the model with vaccination. With isolation, the critical value of q_0 where there is a change of steady states between the coexistent steady state and the single-strain steady state of strain 2 is q_0^c which is approximately 52.2. If $q_0 < q_0^c$, coexistence of two strains occurs. On the other hand, if $q_0 > q_0^c$, only strain 2 can persists. With vaccination, the critical value of vaccination, p^c, is approximately 0.182. If $p < p^c$, there is coexistence of the strains. If not, strain 2 is endemic. We introduced both critical values so as to ensure that at some values of R_2 we can find q_0 and p that either both strains coexist or only strain 2 persists. In order to compare the difference between the strategies by the number of infected individuals we choose q_0 and p close to the critical value and plot the corresponding steady states when R_2 is varied.

First we choose $q_0 = 52.0$ while $p = 0.18$ (See Figure 4-10(a)). These two numbers roughly represent the final attempt before strain 1 is driven out from the host population when $R_2 = 3.5$. At $R_2 = 3.5$ in the graph, we see that the number of infecteds at the steady state resulting from isolation is smaller than ones resulting from vaccination and without intervention. Hence, isolation is an efficient way to control the disease when $R_1 = 3.2, R_2 = 3.5, \sigma = 0.8$, and $\tau = 0.75$ by comparing the number of infected individuals to both strains. By fixing R_1, q_0, p and varying R_2, isolation is still an efficient way to control the disease in long term.

Second, we choose $q_0 = 52.2$ while $p = 0.19$ (See Figure 4-10(b)). The two numbers estimate the initial controls that can be used to drive out strain 1 from the host population. At $R_2 = 3.5$, isolation is the better way to control the disease. By varying R_2 and

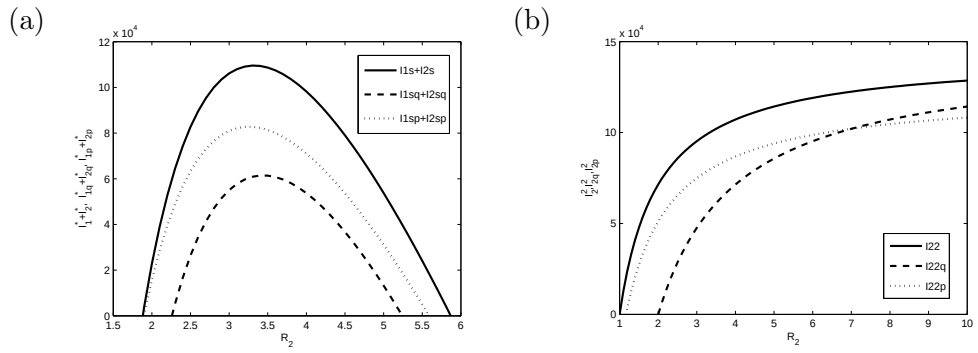

Figure 4-10: The comparison between R_2 and the number of infectious individuals (a) R_2 Vs $I_1^* + I_2^*, I_{1q}^* + I_{2q}^*, I_{1p}^* + I_{2p}^*$ (b) R_2 Vs $I_2^2, I_{2q}^2, I_{2p}^2$

comparing the number of infected individuals to strain 2, when the basic reproductive ratio of strain 2 becomes big (> 7), vaccination becomes the better way to control the disease.

The mean age of infection

We only study the mean age of infection to strain 1 here. The mean age of infection to strain 2 can be studied in the similar way. We separate the mean age of infection for each strategy into two cases:

1. in the absence of strain 2
2. in the presence of strain 2

First, without intervention and in the absence of strain 2, the mean age of infection to strain 1 is

$$A_1 = \frac{1}{\beta_1 I_1^1} = \frac{1}{\mu_0(R_1 - 1)}.$$

In the presence of strain 2, the mean age of infection to strain 1 is

$$A_2 = \frac{1}{\beta_1 I_1^*} = \frac{(1-\sigma^2)}{\mu_0((R_1 - 1) - \sigma(R_2 - 1))}.$$

By considering the ratio of A_1 and A_2, we have

$$\frac{A_2}{A_1} = \frac{(1-\sigma^2)}{1 - \sigma(R_2 - 1)/(R_1 - 1)}$$

In case $R_1 - 1 < \sigma(R_2 - 1)$, coexistence does not occur because strain 2 is dominant, so the host's mean age of infection is the mean age of infection to strain 2. If $\sigma(R_2 - 1) <$

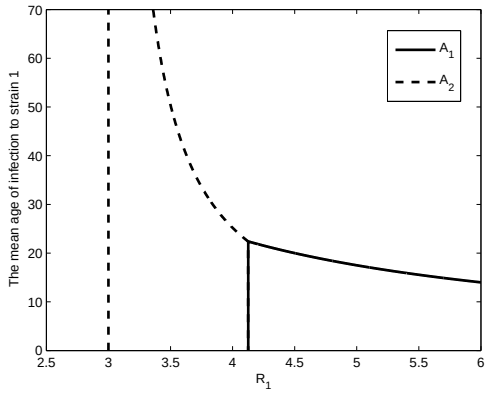

Figure 4-11: The mean age of infection to strain 1 when $R_2 = 3.5$ and $\sigma = 0.8$

$R_1 - 1 < (R_2 - 1)/\sigma$ then $A_2/A_1 > 1$. The mean age of infection to strain 1 is determined by A_2 which is when strain 2 is present. Since coexistence occurs in this case, the host's mean age of infection is the minimum of the mean age of infection to strain 1 and the mean age of infection to strain 2. By comparing A_1 and A_2, we conclude that coexistence with strain 2 increases the mean age of infection to strain 1. In case $R_1 - 1 > (R_2 - 1)/\sigma$, strain 1 is dominant and outcompetes strain 2 from the population so that the host's mean age of infection is the mean age of infection to strain 1. We remark here that all the conditions that we consider here result from the stability conditions. The mean age of infection to strain 1 in the absence of intervention when $R_2 = 3.5$ and $\sigma = 0.8$ is shown in Figure 4-11. It can be seen that when $R_1 < 4.125$ strain 2 coexists with strain 1 so the host's mean age of infection is described by A_2 and when $R_1 > 4.125$ only strain 1 persists so the host's mean age is described by A_1.

Second, with isolation, the mean age of infection to strain 1 in the absence of strain 2 is as follows

$$A_{1q} = \frac{1}{\beta_1 I_{1q}^1} = \frac{1}{\mu_0(R_1 - 1 - q_0/(\mu_0 + \nu_0))}.$$

By comparing it with A_1 we obviously obtain $A_{1q} > A_1$. The mean age of infection to strain 1 in the presence of strain 2 is

$$A_{2q} = \frac{1}{\beta_1 I_{1q}^*} = \frac{(1 - \sigma^2)}{\mu_0((R_1 - 1) - \sigma(R_2 - 1) - q_0(1 - \sigma)/(\mu_0 + \nu_0))}.$$

Clearly, by comparing it with A_2, we have $A_{2q} > A_2$. Therefore, isolation helps to increase the mean age of infection. The ratio of A_{1q} and A_{2q} is

$$\frac{A_{2q}}{A_{1q}} = \frac{(1 - \sigma^2)}{1 - \sigma(R_2 - 1 - q_0/(\mu_0 + \nu_0))/(R_1 - 1 - q_0/(\mu_0 + \nu_0))}.$$

Coexistence of the strains cannot occur and only strain 2 is endemic when $R_1 - 1 - q_0/(\mu_0 + \nu_0) < \sigma(R_2 - 1 - q_0/(\mu_0 + \nu_0))$ so that the mean age of infection to strain 1 does not exist. In case $\sigma(R_2 - 1 - q_0/(\mu_0 + \nu_0)) < R_1 - 1 - q_0/(\mu_0 + \nu_0) < (R_2 - 1 - q_0/(\mu_0 + \nu_0))/\sigma$, both strains coexist and we also have $A_{2q}/A_{1q} > 1$. The mean age of infection to strain 1 is A_{2q}. Furthermore, by comparing A_{1q} and A_{2q} we conclude that coexistence with the other strain increases the mean age of infection to strain 1. In case $R_1 - 1 - q_0/(\mu_0 + \nu_0) > (R_2 - 1 - q_0/(\mu_0 + \nu_0))/\sigma$, only strain 1 persists so that the host mean age of infection is A_{1q}.

Third, with vaccination, the mean age of infection to strain 1 in the absence of strain 2 is

$$A_{1p} = \frac{1}{\beta_1 I_{1p}^1} = \frac{1}{\mu_0((1-p)R_1 - 1)}.$$

Obviously, by comparing it with A_1, we have $A_{1p} > A_1$. So, in the absence of strain 2, the vaccination helps to delay the mean age of infection to strain 1. In the presence of strain 2 and vaccination, the mean age of infection to strain 1 is

$$A_{2p} = \frac{1}{\beta_1 I_{1p}^*} = \frac{(1-\sigma^2)}{\mu_0(R_1 - 1 - \sigma(R_2 - 1) - p(R_1 - \sigma\tau R_2))}.$$

In case $R_2/R_1 < 1/\sigma\tau$, we have $A_{2p} > A_2$ which implies that the mean age of infection to strain 1 when two strains are co-circulating is increased by vaccination. Considering the ratio of A_{1p} and A_{2p}, we have

$$\frac{A_{2p}}{A_{1p}} = \frac{(1-\sigma^2)}{1 - \sigma[(1-p\tau)R_2 - 1]/[(1-p)R_1 - 1]}.$$

Since strain 2 is dominant if $(1-p)R_1 - 1 < \sigma((1-p\tau)R_2 - 1)$, we do not have the mean age of infection to strain 1 in this case. Whenever $\sigma((1-p\tau)R_2 - 1) < (1-p)R_1 - 1 < ((1-p\tau)R_2 - 1)/\sigma$, both strains coexist and $A_{2p} > A_{1p}$. Hence, the mean age of infection to strain 1 is increased by the presence of strain 2. Lastly, if $(1-p)R_1 - 1 > ((1-p\tau)R_2 - 1)/\sigma$, strain 1 persists and the host's mean age of infection is A_{1p}.

By fixing the basic reproductive ratio of strain 2, $R_2 = 3.5, \sigma = 0.8, \tau = 0.75$ and by assuming that $p = 0.5$ and $q = 84$ so that $p > q_0/((\mu_0 + \nu_0)R_1)$(See Figure 4-12(a)), we have $\max\{1 + (R_2 - 1)/\sigma, 1 + (R_2 - 1)/\sigma - (1/\sigma - 1)q_0/(\mu_0 + \nu_0), 1 + (R_2 - 1)/\sigma + p(1-\tau)(R_2 - (1-\sigma)/(1-\tau))/(\sigma(1-p))\} = 1 + (R_2 - 1)/\sigma + p(1-\tau)(R_2 - (1-\sigma)/(1-\tau))/(\sigma(1-p)) = 4.9688$. If R_1 is higher than this, it guarantees that the host's mean age of infection is A_1, A_{1q}, or A_{1p} corresponding to the case without intervention, with isolation, or with vaccination respectively. Consequently, we can compare the host mean age of infection from each strategy. From Figure 4-12(b), vaccination and

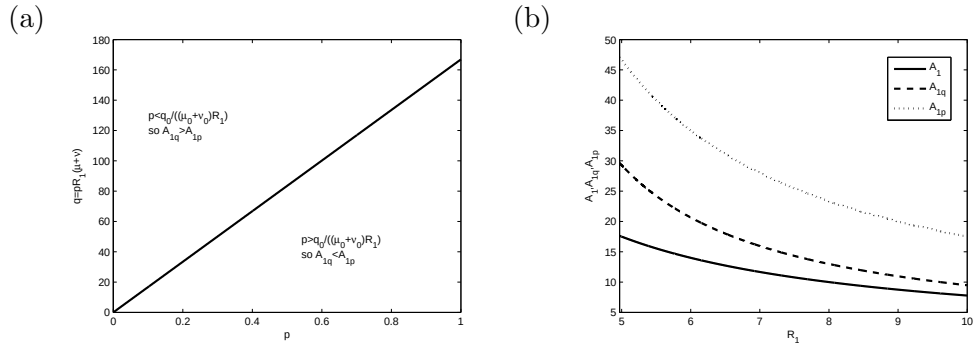

Figure 4-12: (a) The relation of q, p and R_1 that desires whether vaccination or isolation is better for the host's mean age (b) The comparison of A_1, A_{1q}, and A_{1p}

isolation extends the host's mean age of infection comparing with the system without intervention. Note that by considering the area in Figure 4-12(a), vaccination is chosen to be the better strategy to control the disease so that $A_{1p} > A_{1q}$. The comparison of A_2, A_{2q}, and A_{2p} can be studied in a similar way.

In summary, isolation and vaccination help to increase the host's mean age of infection to the strain. In the same way, coexistence with the other strain also increases the host's mean age of infection. However, without cross-immunity this does not happen.

4.1.6 Rate of invasion of the novel strain

In this section instead of assuming that we have two strains of influenza co-circulating in the host population to study the long-term dynamics, we consider the situation that strain 1 is endemic first in the presence of isolation, vaccination or in the absence of them and strain 2 is absent. Strain 1 is assumed to be at the single-strain steady state of strain 1. The invasion dynamics of strain 2 at the beginning in each strategy can be approximated by linearisation about a steady state as follows;

1. Without intervention, I_2 satisfies

$$I_2'(t) = \beta_2 S_2^1 I_2 - (\mu_0 + \nu_0) I_2$$

Since I_2 follows an exponential growth,

$$I_2(t) = C_1 e^{(\beta_2 S_2^1 - (\mu_0 + \nu_0))t} = C_1 e^{kt}$$

where C_1 is a positive constant and the invasion rate of strain 2 is

$$k = \frac{(\mu_0 + \nu_0)((R_2 - 1) - \sigma(R_1 - 1))}{(1 + \sigma(R_1 - 1))}$$

2. With isolation,

$$I_2'(t) = \beta_2 S_{2q}^1 I_2 - (\mu_0 + \nu_0 + q_0) I_2$$

so

$$I_2(t) = C_2 e^{(\beta_2 S_{2q}^1 - (\mu_0 + \nu_0 + q_0))t} = C_2 e^{k_q t}$$

where C_2 is a positive constant and the invasion rate of strain 2 in the presence of isolation is

$$k_q = \frac{(\mu_0 + \nu_0 + q_0)(R_{2q} - 1 - \sigma(R_{1q} - 1))}{(1 + \sigma(R_{1q} - 1))}$$

3. With vaccination,

$$I_2'(t) = \beta_2 S_{2p}^1 I_2 - (\mu_0 + \nu_0) I_2$$

Since I_2 follows an exponential growth, we obtain

$$I_2(t) = C_3 e^{(\beta_2 S_{2p}^1 - (\mu_0 + \nu_0))t} = C_3 e^{k_p t}$$

where C_3 is a positive constant and the invasion rate of strain 2 in the presence of vaccination is

$$k_p = \frac{(\mu_0 + \nu_0)(R_{2p} - 1 - \sigma(R_{1p} - 1))}{1 + \sigma(R_{1p} - 1)}.$$

Since the rate of invasion of strain 2 ($k,\ k_q,$ or k_p) is a linear function of R_2, by fixing R_1 and varying R_2 we can compare $k,\ k_q,$ or k_p by considering the intersection of R_2 and $k,\ k_q,$ or k_p when these three are zeros and the slopes of the lines. We define the value of R_2 that $k = 0$, $k_q = 0$, or $k_p = 0$ as R_{2k}, R_{2kq}, and R_{2kp} respectively. Also the slopes of the lines $k(R_2)$, $k_q(R_2)$, and $k_p(R_2)$ are defined as m, m_q, and m_p. First, if $k = 0$, we have $R_2 = R_{2k} = 1 + \sigma(R_1 - 1)$. The slope of k, m, is $(\mu_0 + \nu_0)/(1 + \sigma(R_1 - 1))$. Second, if $k_q = 0$, we obtain $R_2 = R_{2kq} = 1 + \sigma(R_1 - 1) + (1 - \sigma)\frac{q_0}{(\mu_0 + \nu_0)}$. The slope of k_q, m_q, is $(\mu_0 + \nu_0)/(1 + \sigma(R_1 - 1) - \sigma q_0 R_1/(\mu_0 + \nu_0 + q_0))$. We obviously see that $R_{2kq} > R_{2k}$ and $m_q > m$. Hence, the rate of invasion of strain 2 in the presence of isolation is smaller than one without any intervention when $R_2 < R_2^*$ where R_2^* is the value of R_2 that k and k_q intersect. Above this value, $k_q > k$. In words, after some value of R_2, isolation starts to facilitate strain 2 to invade with the higher rate than without intervention. Third, if $k_p = 0$, we have $R_2 = R_{2kp} = 1 + \sigma(R_1 - 1) + \frac{(1-\sigma)\tau p - \sigma(1-\tau)pR_1}{(1-p\tau)}$. The tangent of the line k_p, is $(\mu_0 + \nu_0)/(1 + \sigma(R_1 - 1) + [(1 - \sigma)\tau p - \sigma(1 - \tau)pR_1]/(1 - p\tau))$. Since strain 1 is assumed to be endemic in the population before strain 2 is introduced, $R_1 > 1$. Also, according to what we assume that the cross-immunity induced by infection is

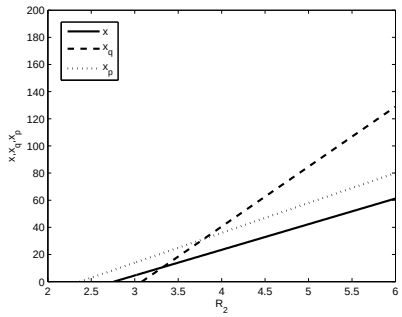

Figure 4-13: The invasion of strain 2 when $R_1 = 3.2$

always better than the cross-immunity induced by the vaccination, $\sigma > \tau$. By these two assumptions we can prove that

$$\frac{(1-\sigma)\tau p - \sigma(1-\tau)pR_1}{(1-p\tau)} < 0.$$

So, $R_{2kp} < R_{2k}$ and $m < m_p$ which implies that the two lines k and k_p never intersect and $x_p > x$, in the positive quadrant. Hence, vaccination targeted to strain 1 helps strain 2 to invade the host population with the faster rate. Note that in case $\tau = 1$, a vaccine gives protection against both strains, there are some values of R_2 that the invasion rate of strain 2 in the presence of vaccination is smaller than one without intervention. Other than that, it is larger than the invasion rate of strain 2 when there is no intervention. An example of invasion rate of strain 2 in each strategy when R_1 is 3.2 is shown in Figure 4-13.

In conclusion, if strain 1 is endemic in the population first, at some value of the basic reproductive ratio of a new strain, isolation reduces the rate of invasion of the new strain. Above that, it increases the invasion rate of the new strain. By assumption that a vaccine is against strain 1 but it might give cross-protection to the new strain, the new strain invades a population with a higher rate of invasion than one without intervention. By comparing the numbers of susceptible individuals to strain 2 when only strain 1 is endemic in the population in all three cases ($S_2^1, S_{2q}^1, S_{2p}^1$), we can see that $S_{2q}^1 > S_2^1$ and $S_{2p}^1 > S_2^1$. So it can be concluded that isolation and vaccination increase the number of susceptible individuals of the new strain so that the rate of invasion of the new strain when the intervention is present is higher than one without it. However, in isolation, when $R_2 < R_1$, isolation is effective to the new strain.

4.1.7 Economic points of view

We first study the cost of isolation and vaccination that can be used to eradicate the disease. Second we include the cost from infection to compare the loss from each strategy.

The cost of isolation during the time interval $[0, T^*]$ is $C_1 \int_0^{T^*} Q dt$ where C_1 is the cost of isolation per individual per year. We estimate the isolation cost (£3660 per week) as the summation of the hospitalisation cost, the extra fee of intensive cares from the consultation, the after-hours visits(Scuffham and West (2002); we use £1 = €1.15 as an exchange rate), and the average income lost in a week (≈£479). So, C_1 is approximately £190,320 per year. From the equation

$$Q'(t) = q_0(I_1(t) + I_2(t)) - \kappa_0 Q(t),$$

we integrate both sides of the equation to obtain

$$\int_0^{T^*} Q dt = [q_0 \int_0^{T^*} (I_1 + I_2) dt - (Q(T^*) - Q(0))]/\kappa_0.$$

The cost of vaccination during the time interval $[0, T^*]$ is $C_2 \mu p N T^*$ where C_2 is the cost of vaccination per individual. The cost of vaccination (£10) is approximated by the summation of a vaccine price and an administering cost (Scuffham and West, 2002).

We assume that $R_1 = 3.2, R_2 = 3.5, \sigma = 0.8, \kappa_0 = 365/7, \tau = 0.75$, this set of parameters is corresponding to case II of the bifurcation analysis part in both isolation and vaccination. Consequently, to control the disease by isolation we must have $\theta > 1 - 1/R_2 \approx 0.71$ (or $q_0 > 130.4$). In the vaccination case, if $p > (1 - 1/R_2)/\tau \approx 0.95$, we can control the disease. This vaccine coverage might not be able to exceed in real which implies that we cannot eliminate the disease from the population. However, we show the numerical result of the successful case here. We choose $\theta = 0.72$ and $p = 0.96$ as the initial control values that both strategies can be used to control the disease to compare the cost between two strategies. From the numerical results, the disease dies out within 1 year in both strategies so we calculate the cost of isolation and vaccination within 1 year. We start the simulations with the same initial conditions ($S_1(0) = 9000000, I_1(0) = 1000, S_2(0) = 9000000, I_2(0) = 1500, Q(0) = 0, V(0) = 0$, and $N(t) = 10000000$). Since we solve the system (4.1.2), (4.1.4), and (4.1.8) by MATLAB which uses Runge-Kutta's method to solve the differential equations, we know the values of $S_1, I_1, S_2, I_2, Q,$ and V at some values of t so to estimate the integration of those values we use the composite trapezoidal rule with different step sizes. From the simulation, the cost of isolation within 1 year is £18,270,720 and the cost of vaccination is £1,371,428. Hence, without concerning with the cost from being sick,

vaccination is cheaper.

Next, we introduce the cost from being sick C_3 (£3530 per week or £183,560 per year) which is approximated by the summation of the hospitalisation cost and the weekly income. With including the cost of being sick, the number of infected individuals $(I_1 + I_2)$ is concerned. Without intervention, the government lose £3.22e+10. With isolation, the government needs to pay £17,621,760 for the sickness of infected individuals and £18,270,720 from launching isolation programme so £35,892,480 in total. For vaccination programme, it costs the government £3.2188e+10 from citizens being sick and £1,371,428 from launching the vaccination programme so £3.2189e+10 in total. Therefore, with the sickness cost being included, the isolation is the better choice for controlling the disease. However, isolation depends on identifying infectious individuals which the symptoms can be ambiguous. In our case q_0 is 134.12 ($\theta = 0.72$) which means that it takes less than 3 days $(365 * (1/q_0))$ to identify the disease and remove the infected individuals to an isolation class. By considering the cost from applying the vaccination programme with the cost from being sick of infected individuals when there is no intervention, they are very high and close. However, the cost of sickness in the future is not included when there is no intervention so that the disease is endemic.

All in all, without considering the sickness cost, vaccination is a cheaper strategy comparing with isolation. With the sickness cost, isolation is cheaper. However, isolation needs to be under the condition that detecting and removing an infectious individual is very efficient. Furthermore, from the result, we recommend the government to use either one of the strategies to control the disease so as to reduce the loss in the future.

4.1.8 Combination of isolation and vaccination

In case isolation and vaccination are launched together, the model that describes the two circulating strains in the host population becomes

$$\begin{aligned} S_1'(t) &= \mu_0(1-p)N - \mu_0 S_1 - \beta_1 S_1 I_1 - \sigma\beta_2 S_1 I_2, \\ I_1'(t) &= \beta_1 S_1 I_1 - (\nu_0 + \mu_0 + q_0) I_1, \\ S_2'(t) &= \mu_0(1-p\tau)N - \mu_0 S_2 - \beta_2 S_2 I_2 - \sigma\beta_1 S_2 I_1, \\ I_2'(t) &= \beta_2 S_2 I_2 - (\nu_0 + \mu_0 + q_0) I_2 \\ Q'(t) &= q_0(I_1 + I_2) - \kappa_0 Q. \end{aligned} \tag{4.1.23}$$

The dynamic of the variable Q does not affect the dynamics of other variables, so the differential equation of Q can be disregarded from the system. We introduce the isolation-vaccination basic reproductive ratios of both strains here which are

$$R_{1pq} = (1-p)R_{1q} = (1-p)(1-\theta)R_1 \text{ and } R_{2pq} = (1-p\tau)R_{2q} = (1-p\tau)(1-\theta)R_2.$$

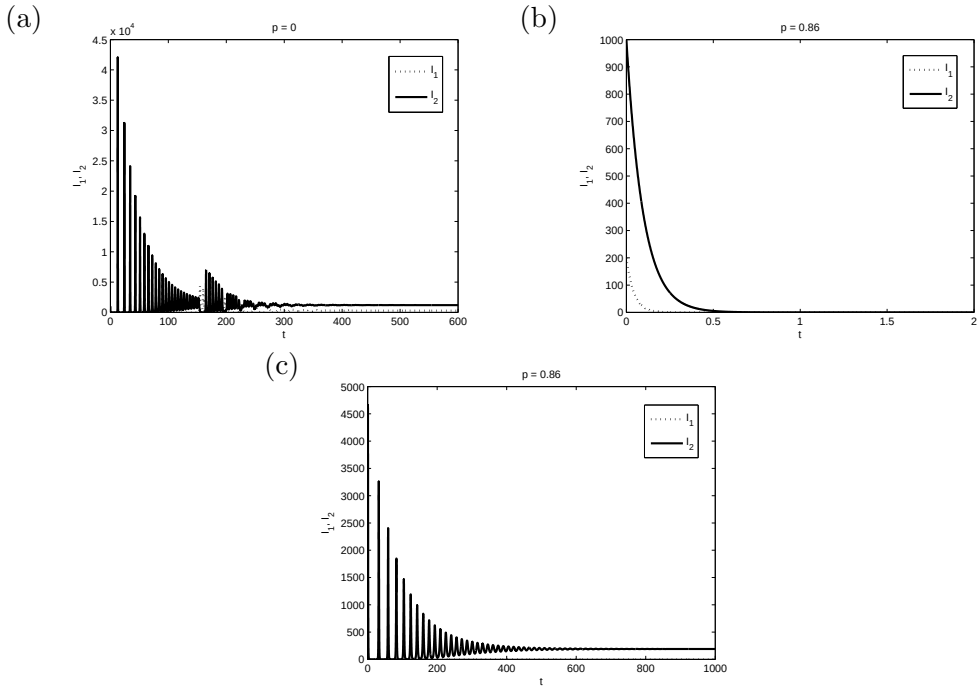

Figure 4-14: (a) $p = 0, \theta = 0.2$ (b) $p = 0.86, \theta = 0.2$ (c) $p = 0.86, \theta = 0$

By comparing the basic reproductive ratios of each strategy, we obviously see that launching two strategies at the same time is more effective than launching only one of them or none of them. We simulate the model (4.1.23) so as to study the number of infectious individuals numerically. By assuming that $R_1 = 3.2, R_2 = 3.5, \sigma = 0.8, \tau = 0.75$ and $\theta = 0.2$ ($q_0 \approx 13$), both strains coexist if vaccination is not launched and both strains die out when 0.86 of newborns are vaccinated constantly(See Figure 4-14(a) and (b) respectively). In case the isolation is not applied ($q_0 = 0$), at the same vaccine coverage ($p = 0.86$), strain 2 is endemic in the host population (See Figure 4-14(c)) and to eradicate it from the host population we need a very high vaccine coverage ($p > 0.9524$).

In conclusion, controlling the disease is more effective by applying two strategies, isolation and vaccination, together.

4.1.9 Conclusion and discussion

Firstly, we introduce three different models: (1) the model for two co-circulating strains in the absence of intervention, (2) the model with the presence of isolation, and (3) the model with the presence of vaccination. The first model is based on the status-based model by Gog and Grenfell (2002) while in the second and third models we introduce

isolation and vaccination into them.

Secondly, in each model we determine the steady states and their stability conditions. Since all the steady states and the conditions are explicit, we can study the bifurcation by drawing the bifurcation diagrams from them. Only transcritical bifurcations occur in our case. Because there are many parameters concerning with the conditions, we separate them into cases according when there is no intervention. By considering the characteristics of strains via their basic reproductive ratios, cross-immunity between them, and a value of a bifurcation parameter which is θ (relating to the isolation rate) in isolation and p (a vaccine coverage) in vaccination, we propose the conditions that help us to predict the long-term dynamics of the strains whether both strains coexist, either one of them persists, or the disease dies out.

Thirdly, we use the numerical simulations to illustrate some of the results from the bifurcation part. Some set of parameters for influenza are used. In addition, we introduce a delay in isolation. By comparing with the result without delay in it, we have found that the delay leads to high jumps of the number of infectious individuals which represent serious outbreaks.

Fourthly, we compare epidemic quantities such as a basic reproductive ratio, a mean age of infection, an invasion rate of a new strain and an economic cost in each strategy. By considering the basic reproductive ratio of each strategy, to invade the host population in the presence of isolation and vaccination, each strain needs to be more transmitted than when there is no intervention. We also compare the basic reproductive ratio from each strategy with the number of infectious individuals numerically.

We study the mean age of infection to strain 1 when either strain 2 is absent or present in each strategy. We show that the host's mean age of infection to strain 1 is extended (so hosts are unlikely to get infected) by isolation, vaccination, or coexistence with the other strain.

By assuming that strain 1 is endemic in the host population first, we can study the invasion rate of a new strain which is strain 2 in this case. We have found that isolation can either reduce the invasion rate of the new strain or support it. It depends on the basic reproductive ratio of the novel strain or how highly transmitted of the strain. By assumption that a vaccine is against strain 1 but it might give cross-immunity to strain 2, it leads to the higher rate of invasion of the new strain comparing with the situation that no intervention is applied. Hence, the new strain with higher transmission rate is more preferred in the presence of isolation or vaccination.

In term of economics, we study the cost from launching isolation or vaccination programme. Without considering the sickness cost of infectious individuals, vaccination is

an economical way to control influenza. With the sickness cost of infectious individuals, isolation is an economical way. However, isolation needs to be under the effective detecting and removing infectious individuals to quarantine. The study also suggests that launching either strategy is better than preventing nothing.

Finally, we combine two strategies in the model and study it numerically. It shows that controlling influenza by launching both strategies at the same time is very efficient. The model might be further used to study the trade-off between isolation and vaccination when the cost of interventions is restricted. Also, optimal control can be further studied.

All in all, we hope that this work might benefit the public heath and us to understand the dynamics of influenza when a control strategy is applied and to know more about the advantages and the disadvantages of the strategy.

4.2 An influenza model with optimal vaccination strategy

When the number of strains of a pathogen increases, many multi-strain models become difficult to analyse. As an alternative approach to this problem, a waning immunity of a host with time is considered. Since vaccination plays an important role to control many diseases, in this work we extend the $SIRC$ (susceptible-infected-recovered-cross-immune) model, where C represents a compartment for the cross-immune individuals who are intermediate between S and R compartments, by introducing a new compartment which represents individuals with perfect immunity including ones who are vaccinated. We use this new compartment, P, instead of the compartment R from the previous model. Then we study the dynamics of the system in order to find the ways to eradicate the disease. We propose the threshold of eradicating the disease when the vaccination rate is constant with time. We then study the optimal control of vaccination where the vaccination rate depends on time in minimizing the treatment cost of influenza.

Various multi-strain models for influenza have been formulated (Andreasen et al., 1997; Lin et al., 1999; Gog and Swinton, 2002; Gog and Grenfell, 2002). Many of them are difficult to analyze when the number n of strains increases. In this work, we study an alternative method to model influenza by considering waning of immunity with time and partial protection according to the change of circulating strains in the same cluster. Gupta et al. (1996, 1998) introduced the concept of a cluster of strains and described it as a collection of independently transmitted strains with nonoverlapping repertoires of dominant polymorphic determinants that organize themselves. Some experimental results (Gill and Murphy, 1977; Potter et al., 1977) showed that reinfection of recovered individuals from influenza linearly increases with time from the last infection. Hence

the SIRS model might not be suitable for studying influenza. To solve this problem, Gomes et al. (2004, 2005) combined temporary and partial immune protections so that individuals do not fall into extreme categories of host immune response. Alternatively, Casagrandi et al. (2006) introduced a new compartment for cross-immune individuals, C, to model a multi-strain disease like influenza, where immunity of hosts in this compartment can be boosted by infecting with new strains in the same cluster as the currently infecting strain. This paper is based on the latter work. We extend the SIRC model to study dynamical behaviours when vaccination is present.

Vaccination is one of the control strategies that are used to control influenza. The vaccination programme is set with an aim to reduce the prevalence of the disease and if possible eradicate it. The vaccines trigger the host immune system to respond and produce antibodies against the viral strains in them. They are chosen to protect individuals from strains that are most dangerous and are likely to invade the population. Highly changing the molecules on the influenza viral surface leads to the failure of vaccination. Mathematical models have been used to study the impact of the vaccination programmes (Gomes et al., 2004; Alexander et al., 2004; Restif and Grenfell, 2006*b*; Raimundo et al., 2007; Gandon and Day, 2007; Martcheva et al., 2008; Billings et al., 2008). Their goal is to help us to understand the dynamics of influenza and other multiple-strain diseases in the presence of vaccination and to determine efficient ways to control them. Likewise, the goal of this work is to try to find the way to control influenza by introducing vaccination to the SIRC model (Casagrandi et al., 2006), which is an alternative model for studying multi-strain diseases like influenza.

Influenza virus is divided into subtypes based on the major differences of the two protein molecules on its surface. In each subtype, the virus gradually and continually mutates to create new strains and with the host immune selection some strains gather together and form a cluster. Our model is based on the $SIRC$ model (Casagrandi et al., 2006) which is used for explaining the influenza strains generated by the drift process in a human population. Hosts become cross-immune when their immune memories are challenged by the new variants that mutate from the strains in the same cluster. So they either become infected again or regain perfect immunity. The total loss of host immunity is assumed to be by the change of a circulating cluster.

In our model, a host population, $\tilde{N}$, is divided into four subpopulations subject to a currently dominant cluster: susceptible ($\tilde{S}$), infected ($\tilde{I}$), perfectly immune ($\tilde{P}$), and cross-immune ($\tilde{C}$).

Susceptible individuals are recruited to the population either by birth or immigration and by loss of partial immunity to the incoming strain. The population is diminished by infection, vaccination, and natural death or emigration.

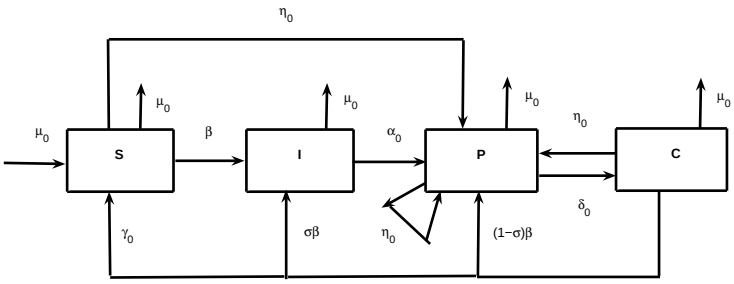

Figure 4-15: A flow diagram of the SIPC model

The infected population is increased by infection of susceptibles and reinfection of some individuals with partial cross-immunity to the new dominant strain and it is reduced by recovery and natural death.

The infected individuals enter the perfectly immune compartment by recovery. Since reinfection with other similar strains of pathogens boosts immunity, some individuals in the cross-immune state regain their total immunity so they consequently reenter the perfectly immune compartment. Since we cannot clinically distinguish between susceptible and perfectly immune or cross-immune individuals easily, we assume that vaccines are given to individuals in all three compartments. Immunity will be boosted by the vaccines if individuals are in the cross-immune compartment so that they become totally immune to the pathogen again, but nothing will happen to perfectly immune individuals because they still have perfect immunity to the disease so that the vaccination has no effect on it. The population in the perfectly immune compartment decreases by the emerging of the new strain created by the drift process and sharing the same cluster with the previous strain or by natural death.

The movement into the cross-immune compartment is by the loss of immunity to the new strain that has emerged. The movement out is by reinfection with the currently circulating strain, having no immunity to the current strain because of the difference between it and the previously infecting strain, vaccination, or natural death.

The flow diagram of the model is shown in Figure 4-15. The description of the parameters can be found in table 4.1. In the model, an average lifetime of human, $1/\mu_0$, is approximately 70 years. Infectious period of influenza, $1/\alpha_0$ is around 7 days. Since strains can be grouped as a cluster and the new dominant cluster is estimated to appear in every 1-2 year (Hay et al., 2001) and persists between 2 and 5 years (Cox and

Table 4.1: Lists of parameters for influenza

Parameter	Description	Value
μ_0	birth and death rate	1/70
α_0	rate of recovery	365/7
δ_0	rate of losing immunity of a recovered individual	1/1.5
γ_0	rate of losing immunity of a cross-immune individual	0.5
σ	probability of reinfection of a cross-immune individual	(vary)
R_0	the basic reproductive ratio	3-5
η_0	vaccination rate	(vary)

Bender, 1995; Plotkin et al., 2002), we suppose $1/\delta_0$ to be 1.5 years and $1/\gamma_0$ to be 2 years respectively. The probability σ of reinfection of a cross-immune individual is assumed to be linearly dependent with time since last infection (Pease, 1987), so

$$\sigma \approx r(1/\delta_0 + 1/\gamma_0)$$

where r is approximately 0.026 (1/year). Note that when cross-immunity is absent, $\sigma = 1$, the SIPC model is equivalent to the SIPS model. The model takes the form

$$\begin{aligned}
\tilde{S}'(t) &= \mu_0(\tilde{N} - \tilde{S}) - \beta\tilde{S}\tilde{I} - \eta_0\tilde{S} + \gamma_0\tilde{C}, \\
\tilde{I}'(t) &= \beta\tilde{S}\tilde{I} + \sigma\beta\tilde{C}\tilde{I} - (\mu_0 + \alpha_0)\tilde{I}, \\
\tilde{P}'(t) &= (1-\sigma)\beta\tilde{C}\tilde{I} + \alpha_0\tilde{I} - (\mu_0 + \delta_0)\tilde{P} + (\eta_0\tilde{P} - \eta_0\tilde{P}) + \eta_0\tilde{S} + \eta_0\tilde{C}, \\
\tilde{C}'(t) &= \delta_0\tilde{P} - \beta\tilde{C}\tilde{I} - (\mu_0 + \eta_0 + \gamma_0)\tilde{C}.
\end{aligned} \tag{4.2.1}$$

To simplify the equation, we introduce a set of new variables and parameters as follows

$$\tau = (\mu_0 + \alpha_0)t,\ R_0 = \frac{\beta N}{(\mu_0 + \alpha_0)},\ \mu = \frac{\mu_0}{(\mu_0 + \alpha_0)},\ \delta = \frac{\delta_0}{(\mu_0 + \alpha_0)},\ \eta = \frac{\eta_0}{(\mu_0 + \alpha_0)},$$

$$S = \frac{\tilde{S}}{\tilde{N}},\ I = \frac{\tilde{I}}{\tilde{N}},\ P = \frac{\tilde{P}}{\tilde{N}},\ C = \frac{\tilde{C}}{\tilde{N}},$$

where R_0 is the basic reproductive ratio of the currently invading strain (Note that other authors might have it in term of the square root of this term, and then the system 4.2.1 becomes

$$\begin{aligned}
S'(\tau) &= \mu(1 - S) - R_0SI - \eta S + \gamma C, \\
I'(\tau) &= R_0SI + \sigma R_0CI - I, \\
P'(\tau) &= (1-\sigma)R_0CI + (1-\mu)I - (\mu + \delta)P + \eta S + \eta C, \\
C'(\tau) &= \delta P - R_0CI - (\mu + \eta + \gamma)C.
\end{aligned} \tag{4.2.2}$$

We can substitute $P = 1 - S - I - C$ to make the equation for P redundant. Therefore the system that we study from now on is

$$\begin{aligned} S'(\tau) &= \mu(1-S) - R_0 SI - \eta S + \gamma C, \\ I'(\tau) &= R_0 SI + \sigma R_0 CI - I, \\ C'(\tau) &= \delta(1-S-I-C) - R_0 CI - (\mu+\eta+\gamma)C. \end{aligned} \tag{4.2.3}$$

4.2.1 Analysis of the steady states

Steady states

By setting the RHS of (4.2.3) equal to zero, we have two kinds of steady states, the disease-free steady state and the disease-present steady state as follows

1. The disease-free steady state

   $$Po^0 = (S^0, 0, C^0) = \left(\frac{\delta\gamma + \mu(\mu+\eta+\gamma+\delta)}{\delta\gamma + (\mu+\eta)(\mu+\eta+\gamma+\delta)}, 0, \frac{\delta\eta}{\delta\gamma + (\mu+\eta)(\mu+\eta+\gamma+\delta)} \right)$$

   We introduce a new quantity here to be used analytically in finding the disease-present steady state,

   $$R_v = R_0(S^0 + \sigma C^0).$$

   It will be mentioned in detail later in the stability analysis section.

2. The disease-present steady state

   $$Po^* = (S^*, I^*, C^*)$$

   where

   $$S^* = \frac{1}{R_0} - \sigma C^* \tag{4.2.4}$$

   $$C^* = \frac{\delta(R_0 - 1 - R_0 I^*)}{R_0(R_0 I^* + (\mu+\eta+\gamma+(1-\sigma)\delta))} \tag{4.2.5}$$

   and I^* satisfies the following equation

   $$f(I^*) = a(R_0 I^*)^2 + b(R_0 I^*) + c = 0 \tag{4.2.6}$$

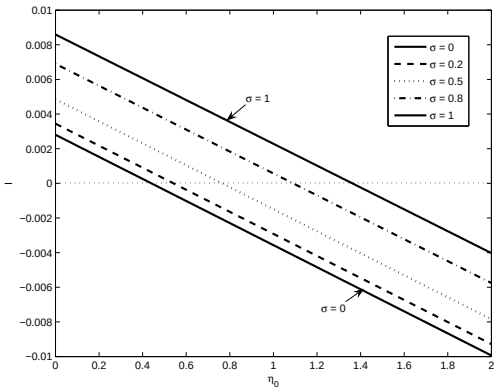

Figure 4-16: The maximum values of I^* from the polynomial $f(I^*)$ are plotted when η_0 is varying at various values of σ.

where

$$\begin{aligned} a &= 1 + \sigma\delta, \\ b &= (1 + \sigma\delta)(\mu + \eta) + (\mu + \eta + \gamma + \delta) + \delta\gamma - (\mu + \sigma\delta)R_0, \\ c &= [(\mu + \eta)(\mu + \eta + \gamma + \delta) + \delta\gamma](1 - R_v). \end{aligned}$$

If c is positive or $R_v < 1$, both of the roots have negative real parts in which we are not interested. If c is negative, we have one positive root and one negative root of I^*.

Figure 4-16 shows that when η_0 is increased, c becomes smaller and so I^* which is the largest root from the equation (4.2.6) is decreased to zero and becomes negative finally. It means that at some rates of vaccination we are able to eradicate the disease. Furthermore, the weaker the cross-immunity is, the higher is the rate of vaccination to be needed to eradicate the disease.

Stability analysis

We analyse the stability of the steady states by considering the signs of eigenvalues and by using Routh-Hurwitz criteria. From the system (4.2.3), the Jacobian matrix is

$$J = \begin{bmatrix} -(\mu + \eta + R_0 I) & -R_0 I & \gamma \\ R_0 I & R_0 S + \sigma R_0 C - 1 & \sigma R_0 I \\ -\delta & -(\delta + R_0 C) & -(\mu + \eta + \gamma + \delta + R_0 I) \end{bmatrix}$$

At the disease-free steady state, the characteristic equation of the Jacobian matrix is

$$(\lambda-(R_0S^0+\sigma R_0C^0-1))(\lambda^2+((\mu+\eta)+(\mu+\eta+\gamma+\delta))\lambda+(\mu+\eta)(\mu+\eta+\gamma+\delta)+\delta\gamma)=0.$$

Since both roots of the second-order polynomial in the characteristic equation certainly have negative real parts, the stability of the disease-free steady state depends on the sign of the first term. Therefore, the disease-free steady state is stable if and only if

$$R_v = R_0(S^0 + \sigma C^0) < 1.$$

R_v is the basic reproductive ratio of the disease when the vaccination is present and it is equal to R_0 if there is no vaccination.

At the disease-present steady state, we have the characteristic polynomial of order three as follows

$$\lambda^3 + a_1\lambda^2 + a_2\lambda^3 + a_3$$

where

$$\begin{aligned}
a_1 &= (\mu + \eta + R_0I^*) + (\mu + \eta + \gamma + \delta + R_0I^*),\\
a_2 &= (\mu + \eta + R_0I^*)(\mu + \eta + \gamma + \delta + R_0I^*) + \delta\gamma + \sigma R_0I^*(\delta + R_0C^*) + R_0^2I^*S^*,\\
a_3 &= \sigma R_0I^*(\delta + R_0C^*)(\mu + \eta + R_0I^*) + R_0^2I^*S^*(\mu + \eta + \gamma + \delta + R_0I^*) + \gamma R_0I^*(\delta + R_0C^*)\\
&\quad -\sigma\delta R_0^2I^*S^*.
\end{aligned}$$

Obviously, if (S^*, I^*, C^*) is in the positive orthant, all the coefficients of the polynomial are all positive (since $\sigma \leq 1$) and by substituting

$$\gamma C^* = R_0I^*S^* + \eta S^* + \mu S^* - \mu$$

and canceling out all the similar terms we can prove that

$$a_1a_2 > a_3.$$

On the other hand, if I^* is negative or in other words (S^*, I^*, C^*) is not in the positive orthant, a_3 is clearly negative. Therefore, by the Routh-Hurwitz criteria, the disease-free steady state is stable if and only if it is in the positive orthant.

4.2.2 Numerical Verification

The model (4.2.3) is analysed numerically to illustrate our study. Figure 4-17 illustrates the bifurcation diagram of the bifurcation parameter R_v and R_0 with the proportion of infectious individuals. The transcritical bifurcation where two steady states exchange

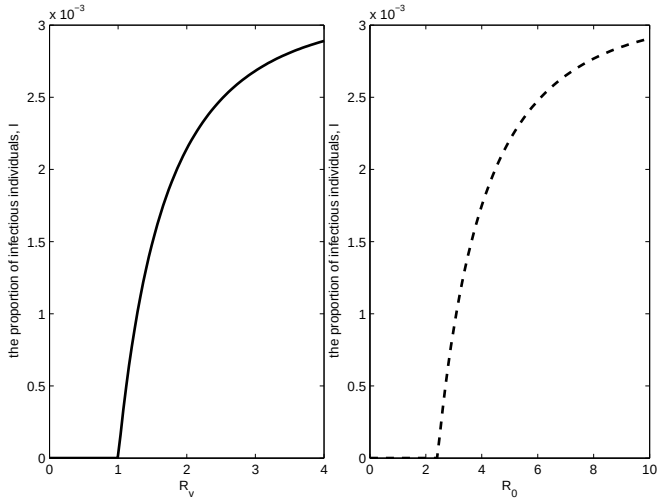

Figure 4-17: The bifurcation diagrams between R_v and I and R_0 and I when $\eta_0 = 0.4$

their stabilities occurs at $R_v = 1$ or $R_0 = 1/(S^0 + \sigma C^0)$. Next, we explore the implication of variable vaccination rates. The bifurcation diagram between η_0 and I^* is shown in Figure 4-18. Let us define η_0^* to be the value of η_0 where the graph intersects the axis $I^* = 0$. The point $(\eta_0^*, 0)$ is a transcritical bifurcation point and η_0^* is $\eta^*(\mu_0 + \alpha_0)$ where η^* is the largest root of the polynomial

$$\eta^2 + ((\mu + \gamma) + (1 - R_0)\mu + (1 - \sigma R_0)\delta)\eta + (1 - R_0)(\mu(\mu + \gamma + \delta) + \delta\gamma).$$

Influenza persists if the rate of vaccination is less than η_0^* and dies out if it is greater than η_0^*. Moreover, from the polynomial the larger R_0 is, the higher is the rate of vaccination needed to eradicate the disease.

By fixing the values of parameter indicated in Table 4.1, the value of η_0^* calculated from the second-order polynomial is approximately 0.54 and from the numerical simulation it is approximately 0.54 as well. Figure 4-19(a) shows the result when $\eta_0 = 0.25$. In this case, the rate of vaccination is below our critical rate of vaccination (η_0^*) so the influenza persists in the host population and the solutions tend to the disease-present steady state as time increases. On the other hand, if the rate of vaccination is large enough, $\eta_0 = 0.75$, the solutions tend to the disease-free steady state in long term so the influenza finally dies out (See Figure 4-19(b)).

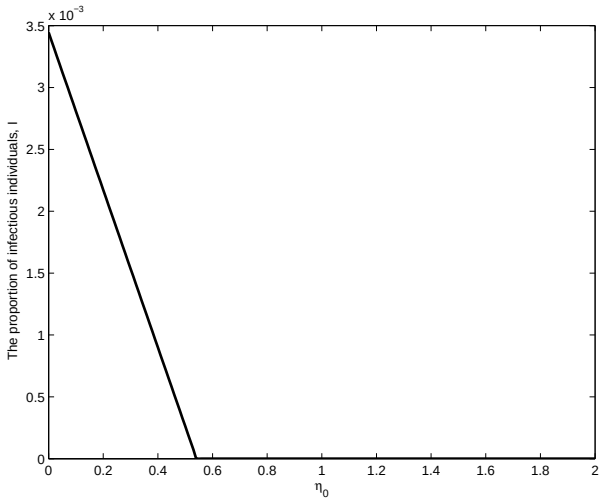

Figure 4-18: The bifurcation diagram between η_0 and $I(\infty)$ when $R_0 = 3$

(a)

(b)

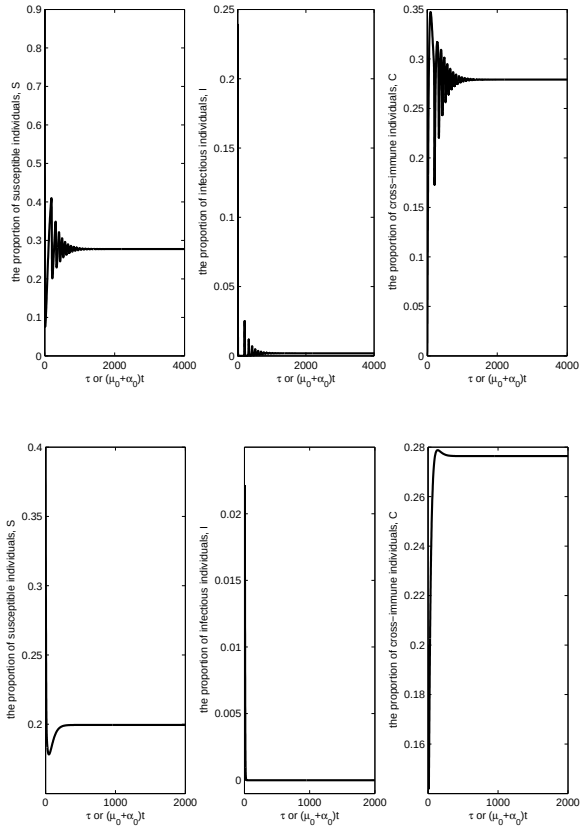

Figure 4-19: (a) $\eta_0 = 0.25$, $R_0 = 3$, $\sigma = 0.2$ (b) $\eta_0 = 0.75$, $R_0 = 3$, $\sigma = 0.2$

4.2.3 Optimal Control

In this section, we study the system (4.2.1) when the vaccination rate is allowed to vary with time ($\eta_0 = \eta_0(t)$) to minimize the cost of treatments from getting infected with influenza.

We consider an optimal control to minimize an objective functional:

$$J(\eta_0) = \int_0^T [A\tilde{I}(t) + \frac{D}{2}\eta_0^2(t)]dt$$

where A is the cost of treatments and the loss of income from influenza per individual per year. Our main goal is to minimize the total cost of treatments and the loss of income during T year of a population by introducing a vaccination control which varies with time. In general, the quadratic term of control in the objective functional is introduced for avoiding either the singularity of control or the bang-bang control (Lenhart and Workman, 2007). In here, for simplicity, we exclude the total cost of vaccination which represents by the linear control term that might lead to the bang-bang control, so the quadratic term helps to prevent the singularity of control in our case. For the coefficient $D/2$ of the quadratic term, we consider its explanation in two cases. First, $D/2$ is treated to be fairly small not to affect the other cost but not too small so that they lead to the singularity. Hence, in this case, the objective of the use of the control is to minimize the treatment cost and the income loss. Second, $D/2$ represents the waste cost of seeking vaccinated individuals to vaccinate again. So the use of the control in the latter is for minimizing the total waste cost of income, treatments, and seeks for vaccinated individuals to vaccinate again.

In mathematical speaking, the goal of this study is to find an optimal control η_0^* such that

$$J(\eta_0^*) = \min_{\Omega}\{J(\eta_0)\},$$

where $\Omega = \{\eta_0 \in L^1(0,T) | \eta_0^{\min} \leq \eta_0 \leq \eta_0^{\max}\}$ where L^1 is the space of all *Lebesgue* integrable functions. We sequently arrange the variables $\tilde{S}, \tilde{I}, \tilde{P}$, and $\tilde{C}$ as the 1st-4th state variables. By following the Pontryagin's Maximum Principle (Pontryagin et al., 1962), we introduce a Hamiltonian function for as follows

$$H = A\tilde{I}(t) + \frac{D}{2}\eta_0^2(t) + \sum_{i=1}^{4}\lambda_i g_i$$

where λ_i is the adjoint variable corresponding to the state variable i and g_i is the right hand side of the differential equation of the ith state variable. By the Pontryagin's Maximum Principle, we arrive at the necessary conditions for the existence of an op-

timal control η_0^* corresponding to the solutions of $\tilde{S}^*, \tilde{I}^*, \tilde{P}^*$, and $\tilde{C}^*$, that they must satisfy the system (4.2.1), the adjoint and transversality conditions, and the optimality condition. The adjoint conditions for the minimization of the objective functional is as follows

$$\begin{aligned}
\lambda_1'(t) &= \lambda_1(\mu_0 + \beta\tilde{I} + \eta_0) - \lambda_2\beta\tilde{I} - \lambda_3\eta_0 \\
\lambda_2'(t) &= -A + \lambda_1\beta\tilde{S} - \lambda_2(\beta\tilde{S} + \sigma\beta\tilde{C} - (\mu_0 + \alpha_0)) - \lambda_3((1-\sigma)\beta\tilde{C} + \alpha_0) + \lambda_4\beta\tilde{C} \\
\lambda_3'(t) &= \lambda_3(\mu_0 + \delta_0) - \lambda_4\delta_0 \\
\lambda_4'(t) &= -\lambda_1\gamma - \lambda_2\sigma\beta\tilde{I} - \lambda_3((1-\sigma)\beta\tilde{I} + \eta_0) + \lambda_4(\beta\tilde{I} + \mu_0 + \gamma_0 + \eta_0)
\end{aligned} \tag{4.2.7}$$

Note that the adjoint conditions are derived from the Hamiltonian function

$$\lambda_j'(t) = -\frac{\partial H}{\partial x_j}$$

where x_j is the jth state variable and $j = 1, 2, \ldots, 4$. The transversality boundary conditions are assumed to be:

$$\lambda_1(T) = \lambda_2(T) = \lambda_3(T) = \lambda_4(T) = 0.$$

Since the control is bounded, the optimality condition can be found by considering $\partial H/\partial\eta_0$ as follows

$$\eta_0^*(t) = \min\left\{\eta_0^{\max}, \max\left\{\eta_0^{\min}, \left(\frac{\lambda_1\tilde{S} - \lambda_3(\tilde{S} + \tilde{C}) + \lambda_4\tilde{C}}{D}\right)\right\}\right\}$$

The proof of necessary condition is omitted here. Further details can be found in (Pontryagin et al., 1962; Lenhart and Workman, 2007).

Estimation of costs

In the objective functional, A is the cost of being sick which is approximated by a summation of an income that an individual lose during being sick and a cost of treatment. Because influenza has an infectious period around 7 days, the income loss of an individual is estimated by the average weekly income which is £479. The cost of influenza treatment is estimated as £80 per person per week (Reisinger et al., 2004; Burls et al., 2002). This is the basic treatment cost without including the cost of hospitalisation. It is the cost of treating by treatments such as Oseltamivir or Zanamivir, a general practitioner visit, a prescription, and a test. Hence, the total cost of being sick is £559 per person per week so A is £29148 per person per year. We consider two explanations of a weight-cost factor $D/2$; (1) it is small enough not to affect the other costs but not too small so that they lead to the bang-bang control ($D/2 < 1$) and so

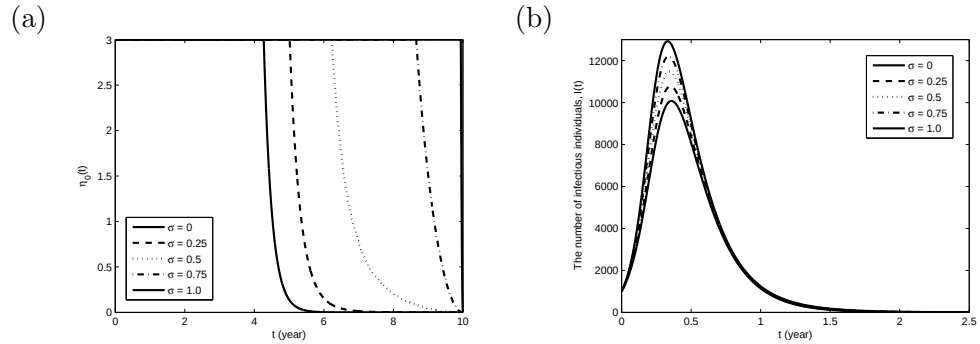

Figure 4-20: (a) An optimal control of vaccination when $R_0 = 5$, $\eta_0^{\max} = 3.0$, $\eta_0^{\min} = 0.0$, A=29148, D=0.01 (b) The number of infectious individual corresponding with the optimal control

we choose it equal to 0.01, or (2) $D/2$ represents a waste cost of seeking individuals who already vaccinated to vaccinate again. In the latter, it can be approximated by the cost of health care repeatedly making random phone calls to already-vaccinated people to persuade them to vaccinate again. So $D/2$ is $pk\tilde{N}$ where p is the probability of an individual who picks up the call is vaccinated already (≈ 0.1, for instance), k is the cost of each call including the staff cost ($\approx$£1). In the simulation, we assume that $\tilde{N}$ is 50,000. Hence $D/2$ can be approximated by £5,000. Since η_0 represents rate of vaccination and we assume that the public health can manage to vaccinate the whole population within 4 months at maximum, $\eta_0^{\max} = 3$. The minimum rate of vaccination is set at 0. Also, we study the cost within 10 years and the basic reproductive ratio is fixed at 5. Other parameters are fixed as before.

Numerical results of the optimal control

The ODE problem is solved by the forward-backward sweep method and the Runge-Kutta method of order 4. For the small value of D, by varying sigma, the vaccination control needs to be higher for eradicating influenza when σ is increased (see Figure 4-20(a)). Furthermore, in Figure 4-20(b), the disease dies out quickly within 2 years and the number of infectious individuals increases when σ increases. In Figure 4-21(a), when $D/2$ represents the waste cost of phone calls to persuade vaccinated individuals to vaccinate again, the control strategy needs to be under higher measure when σ increases. Note that when σ is big enough (less cross-immunity), the optimal control is broken and the solution blows up in this case. Figure 4-21(b) shows that the number of infectious individual is increased when σ is increased.

From both numerical results, we can conclude that no matter $D/2$ represents, cross-immunity plays an important role in controlling influenza. When cross-immunity is

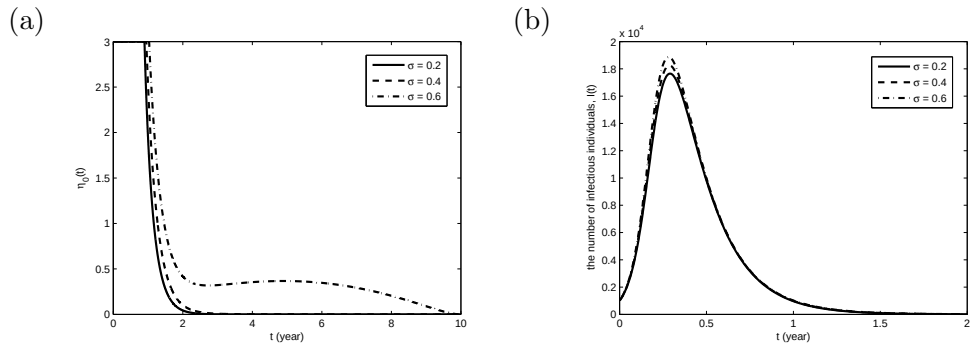

Figure 4-21: (a) An optimal control of vaccination when $R_0 = 5$, $\eta_0^{\max}$=3.0, $\eta_0^{\min}$=0.0, A=29148, D=10000 (b) The number of infectious individual corresponding with the optimal control

low in individual ($1 - \sigma$ is small), to minimize the treatment cost of the population by vaccination, public health needs a better control measure than when cross-immunity is high. Furthermore, the number of infectious individual is increased when cross-immunity is low.

4.2.4 Conclusion and discussion

We propose the vaccination model that describes the dynamics of influenza. We have shown that vaccination can be used to eradicate the disease from the host population. By applying the parameter values for influenza virus, we can find the critical vaccination rate (η_0^*) that the disease persists if the vaccination rate is below it and dies out if the vaccination rate is above it. Furthermore, the lowest rate of vaccination that eradicates the disease is reduced if the cross-immunity is very strong, $\sigma \to 0$. On the other hand, it is increased when the basic reproductive ratio of influenza becomes bigger ($R_0 >> 1$).

For example, influenza with the basic reproductive ratio equaling 3 and other parameters corresponding with values in the table 4.1, if we apply vaccines to 75% of susceptible individuals per year, all of the influenza viruses in the same cluster will completely die out from the host population within 11 months. The more we vaccinate susceptibles the quicker the influenza dies out. However the efficacy of vaccines need to be so high that the immunity acquired by them in susceptible hosts needs to be effective as the immunity that recovery hosts gain after infection. Cox and Bender (1995) and Plotkin et al. (2002) demonstrated that a dominant cluster of virus sequences is tentatively replaced by another every 2-5 years and, by phylogenetic techniques, the next season's influenza sequences can be efficiently predicted from the persistence of the circulating clusters. Hence, vaccines that match the dominant antigenic properties of circulating strains are possibly available. From our model, influenza can be eradicated at some

vaccination rates within the time that is less than the life span of the clusters. In summary, in terms of public heath, vaccination is one of the proficient ways to prevent and reduce morbidity of humans from influenza.

When the vaccination rate depends on time for minimizing the total treatment cost, we found that cross-immunity is an important key for the shape of the optimal control. The weaker of the cross-immunity is, the stronger of the vaccination control needs. The number of infectious individuals corresponding to the optimal control is higher, when cross-immunity is weak.

In conclusion, from both studies either a control is constant or varying with time, cross-immunity plays an important role in controlling influenza. If the cross-immunity is weak, the better control strategy is needed than when it is strong. All in all, there are variable factors concerning with controlling influenza, we hope that our work is one of the studies that gives public health an insight in eradicating influenza.

The model can be further studied by introducing seasonality, modelling different suptypes of pathogens, introducing control strategies depending on time for other objectives in controlling influenza. It may also be extended to study the vector-borne diseases.

4.3 A vaccination model for two-cocirculating strains of malaria

We consider two strategies of vaccination and propose two models based on the host-vector model with polarized immunity in Section 3.1, Chapter 3. First, vaccination is applied in the homogeneous human population with the vaccination rate u. Second, host age is important so we separate the human population into two age classes, juvenile and adult. Children are vaccinated at rate u.

4.3.1 A vaccination model with no age classes

We start with introducing vaccination into the system (3.1.3) and then reduce the number of equations in the similar way with the previous study. Based on the status-

based framework, our primary model is:

$$\begin{aligned}
\dot{S}_{\emptyset}(t) &= \mu N_h - \mu S_{\emptyset} - C(\emptyset,\{1\},1)\beta_1 V_1 S_{\emptyset} - C(\emptyset,\{1,2\},1)\beta_1 V_1 S_{\emptyset} - \\
&\quad C(\emptyset,\{2\},2)\beta_2 V_2 S_{\emptyset} - C(\emptyset,\{1,2\},2)\beta_2 V_2 S_{\emptyset} - uS_{\phi}, \\
\dot{S}_{\{1\}}(t) &= C(\emptyset,\{1\},1)\beta_1 V_1 S_{\emptyset} - C(\{1\},\{1,2\},2)\beta_2 V_2 S_{\{1\}} - \\
&\quad C(\{1\},\{1,2\},1)\beta_1 V_1 S_{\{1\}} - \mu S_{\{1\}} + \tau u S_{\emptyset} - uS_{\{1\}} + \tau u S_{\{1\}}, \\
\dot{S}_{\{2\}}(t) &= C(\emptyset,\{2\},2)\beta_2 V_2 S_{\emptyset} - C(\{2\},\{1,2\},1)\beta_1 V_1 S_{\{2\}} - \\
&\quad C(\{2\},\{1,2\},2)\beta_2 V_2 S_{\{2\}} - \mu S_{\{2\}} - uS_{\{2\}}, \\
\dot{S}_{\{1,2\}}(t) &= C(\emptyset,\{1,2\},1)\beta_1 V_1 S_{\emptyset} + C(\emptyset,\{1,2\},2)\beta_2 V_2 S_{\emptyset} + \\
&\quad C(\{1\},\{1,2\},2)\beta_2 V_2 S_{\{1\}} + C(\{2\},\{1,2\},1)\beta_1 V_1 S_{\{2\}} - \mu S_{\{1,2\}} + \\
&\quad (1-\tau)uS_{\emptyset} + (1-\tau)uS_{\{1\}} + uS_{\{2\}} - uS_{\{1,2\}} + uS_{\{1,2\}}, \\
\dot{I}_1(t) &= \beta_1 V_1 (S_{\emptyset} + S_{\{2\}}) - (\mu + \nu_1) I_{\{1\}}, \\
\dot{I}_2(t) &= \beta_2 V_2 (S_{\emptyset} + S_{\{1\}}) - (\mu + \nu_2) I_{\{2\}}, \\
\dot{U}(t) &= B - \eta U - \alpha_1 I_1 U - \alpha_2 I_2 U, \\
\dot{V}_1(t) &= \alpha_1 I_1 U - \eta V_1, \\
\dot{V}_2(t) &= \alpha_2 I_2 U - \eta V_2.
\end{aligned} \tag{4.3.1}$$

In this model, we vaccinate a whole human population with rate u. We assume that the vaccine protects completely against strain 1, but partially against strain 2 with the fraction $1-\tau$. The vaccinated individuals move between immune classes. First, naive individuals move out from the naive compartment at rate $uS_{\emptyset}$. Only a fraction τ of these enter the $S_{\{1\}}$ class and the rest of them (a fraction $(1-\tau)$) enter the $S_{\{1,2\}}$ class. Second, individuals who are already immune to strain 1 move out of the compartment by vaccination at rate $uS_{\{1\}}$ but a fraction τ of these still have only immunity to strain 1 so they reenter the same class. The rest of them (a fraction $(1-\tau)$) have immunity to both strain and enter the $S_{\{1,2\}}$ class. Third, individuals who are already immune to strain 2 are vaccinated at rate $uS_{\{2\}}$ and enter the $S_{\{1,2\}}$ class. Finally, individuals of the $S_{\{1,2\}}$ remain in that class on vaccination. Because $C(\emptyset,\{1\},1)+C(\emptyset,\{1,2\},1)=1$ and $C(\{2\},\{1,2\},1)=1$,

$$\dot{S}_1 = \mu N_h - \mu S_1 - \beta_1 V_1 S_1 - C(\emptyset,\{1,2\},2)\beta_2 V_2 S_{\emptyset} - C(2,\{1,2\},2)\beta_2 V_2 S_{\{2\}} - uS_1.$$

By the assumption that the probabilities of acquiring further immune memory to the other strain of the naive individual and the infectious individual with the current strain are equivalent, $C(\emptyset,\{1,2\},2) = C(\{2\},\{1,2\},2) = \sigma_{12}$, we obtain

$$\dot{S}_1 = \mu N_h - \mu S_1 - \beta_1 V_1 S_1 - \sigma_{12}\beta_2 V_2 S_1 - uS_1.$$

Similarly, because $C(\emptyset,\{2\},2)+C(\emptyset,\{1,2\},2)=1$, $C(\{1\},\{1,2\},2)=1$, and $C(\emptyset,\{1,2\},1)=C(\{1\},\{1,2\},1)=\sigma_{21}$), we have

$$\dot{S}_2=\mu N_h-\mu S_2-\beta_2 V_2 S_2-\sigma_{21}\beta_1 V_1 S_2-(1-\tau)uS_2.$$

Hence, the model takes the following form:

$$\begin{aligned}
\dot{S}_1(t) &= \mu N_h-\mu S_1-\beta_1 V_1 S_1-\sigma\beta_2 V_2 S_1-uS_1,\\
\dot{I}_1(t) &= \beta_1 V_1 S_1-(\mu+\nu)I_1,\\
\dot{S}_2(t) &= \mu N_h-\mu S_2-\beta_2 V_2 S_2-\sigma\beta_1 V_1 S_2-(1-\tau)uS_2,\\
\dot{I}_2(t) &= \beta_2 V_2 S_2-(\mu+\nu)I_2,\\
\dot{M}(t) &= B_v-\alpha_1 I_1 M-\alpha_2 I_2 M-\gamma M,\\
\dot{V}_1(t) &= \alpha_1 I_1 M-\gamma V_1,\\
\dot{V}_2(t) &= \alpha_2 I_2 M-\gamma V_2.
\end{aligned} \tag{4.3.2}$$

In this model, we assume that $\sigma_{21}=\sigma_{12}$. In the similar way with the system (3.1.4), linear stability of the disease-free steady state of this system can be investigated by using the next-generation matrix. By ordering the infected variables as I_1, I_2, V_1, V_2, the matrix of new infections F is given by

$$F=\begin{bmatrix} \underline{0} & F_{12}\\ F_{21} & \underline{0}\end{bmatrix},$$

where

$$F_{12}=\begin{bmatrix} \beta_1\mu N_h/(\mu+u) & 0\\ 0 & \beta_2\mu N_h/(\mu+(1-\tau)u)\end{bmatrix}, F_{21}=\begin{bmatrix} \alpha_1 N_v & 0\\ 0 & \alpha_2 N_v\end{bmatrix},$$

and $\underline{0}=[0]_{2\times 2}$. The matrix of transfer between classes is

$$V=\mathrm{diag}\{\mu+\nu,\mu+\nu,\gamma,\gamma\}.$$

The characteristic equation of the next generation matrix (FV^{-1}) is

$$\left(\lambda^2-\frac{\mu\alpha_1\beta_1 N_h N_v}{\gamma(\mu+u)(\mu+\nu)}\right)\left(\lambda^2-\frac{\mu\alpha_2\beta_2 N_h N_v}{\gamma(\mu+(1-\tau u)(\mu+\nu)}\right)=0.$$

Hence the threshold condition is

$$R_{0vac}<1$$

where

$$R_{0vac}=\max\{R_{01vac},R_{02vac}\},$$

(a) (b)

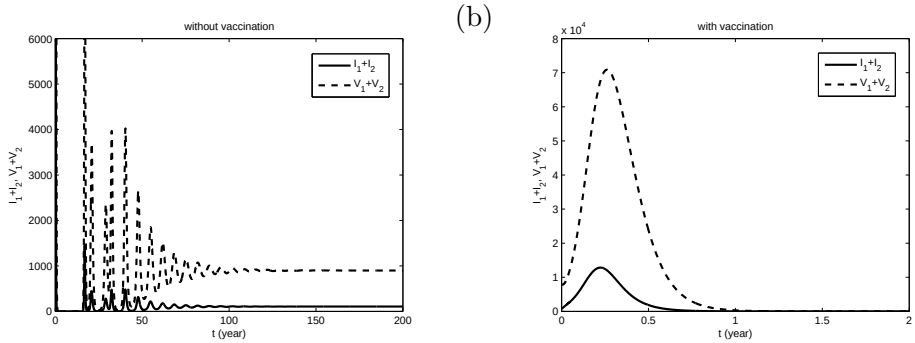

Figure 4-22: (a) A numerical result of the number of infectious human to both strains and the number of infectious mosquitoes when $R_{01}^2 = 7$, $R_{02}^2 = 6.5$, and the vaccination is absent: both strains coexist in the human population. (b) A numerical result when $R_{01}^2 = 7$, $R_{02}^2 = 6.5$, and the vaccination is present at rate $u = 0.3$ with the partial immunity to strain 2 $\tau = 0.7$: both strains die out quickly.

$$R_{01vac} = \sqrt{\frac{\mu\alpha_1\beta_1 N_h N_v}{\gamma(\mu+u)(\mu+\nu)}} = \sqrt{\frac{\mu}{(\mu+u)}}R_{01}, \text{ and}$$

$$R_{02vac} = \sqrt{\frac{\mu\alpha_2\beta_2 N_h N_v}{\gamma(\mu+(1-\tau)u)(\mu+\nu)}} = \sqrt{\frac{\mu}{(\mu+(1-\tau)u)}}R_{02}.$$

Since considering $R_{0vac}, R_{01vac}, R_{02vac}$ and $R_{0vac}^2, R_{01vac}^2, R_{02vac}^2$ whether they are less than 1 or greater than 1 are equivalent, we instead study the latter for the better scale. Consequently, the critical value of the vaccination rate to eradicate both strains from the host population is

$$u_c = \max\left\{\mu(R_{01}^2 - 1), \frac{\mu(R_{02}^2 - 1)}{(1-\tau)}\right\}.$$

We study the system for the numerical results. In case there are two strains of malaria co-circulating with $R_{01}^2 = 7$, $R_{02}^2 = 6.5$, and $\sigma = 0.35$, both strains coexist when the vaccination is absent (see Figure 4-22(a)). However, when the vaccination is present and the parameter of cross-protection induced by vaccination $1 - \tau = 0.3$, the disease is eradicated when $u > u_c = 0.26$ where u is taken to be 0.3 (see Figure 4-22(b)). A bifurcation diagram of a parameter u and the asymptotic solutions of I_1 and I_2 when τ is fixed at 0.7 is shown in Figure 4-23(a). It can be seen that when $u > 0.26$, both strains dies out in the the host population. In Figure 4-23(b), we fix $u = 0.26$ and vary the parameter τ for the bifurcation diagram of τ and the asymptotic solutions I_1 and I_2. The disease dies out when $\tau < 0.7$. The number of infectious individuals is increased when cross-immunity is weak (τ is big). From the bifurcation diagrams, we conclude that high rate of vaccination and strong cross-immunity induced by vaccination can

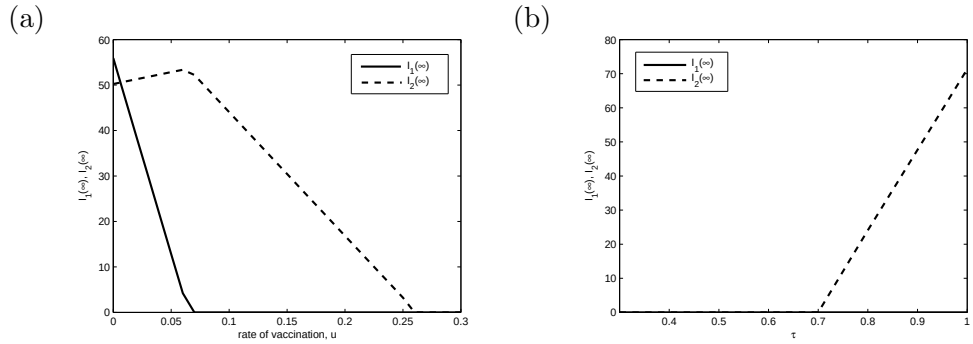

Figure 4-23: (a) A bifurcation diagram of vaccination rate u, and the asymptotic solutions of infectious individuals to strain 1 and 2 ($R_{01}^2 = 7, R_{02}^2 = 6.5, \sigma = 0.35, \tau = 0.7$) (b) A bifurcation diagram of τ, $I_1(\infty)$, and $I_2(\infty)$ ($u = 0.26$)

guarantee extinction of the strains.

4.3.2 A vaccination model with age classes

Because the morbidity between children and adults infected with malaria can be different, it might be economical to vaccinate only children. Hence, we propose the model with age classes here to study whether the disease can be eradicated by just vaccinating children and how realistic it is to do that. We divide the human population into two age classes, children and adults. The juvenile and adult groups are described by the superscript 1 and 2, respectively. In each age class, an individual belongs to one of the immune classes described in the previous models. There is only a recruitment in the juvenile group and there is no vertical transmission, so the individuals are born disease-free. The transmission rate from infectious mosquitoes with strain i to susceptible humans in group j is described by β_{ij} for $i = 1, 2, j = 1, 2$ and the transmission rate from infectious humans with strain i in group j to susceptible mosquitoes is described by α_{ij}. We assume that the recovery rate is different according to age but not with the strain. The death rate μ is the same for all groups. An individual moving out of the juvenile into adult is described by the maturation rate ω. Vaccination is applied to children only. It is also applied in both susceptible and infectious children because the symptoms can be asymptomatic but individuals are infectious.

$$
\begin{aligned}
\dot{S}_1^1(t) &= \mu N_h - \mu S_1^1 - \omega S_1^1 - \beta_{11} V_1 S_1^1 - \sigma \beta_{21} V_2 S_1^1 - u S_1^1, \\
\dot{I}_1^1(t) &= \beta_{11} V_1 S_1^1 - (\mu + \nu_1) I_1^1, \\
\dot{S}_1^2(t) &= \omega S_1^1 - \beta_{12} V_1 S_1^2 - \sigma \beta_{22} V_2 S_1^2 - \mu S_1^2, \\
\dot{I}_1^2(t) &= \beta_{12} V_1 S_1^2 - (\mu + \nu_2) I_1^2, \\
\dot{S}_2^1(t) &= \mu N_h - \mu S_2^1 - \omega S_2^1 - \beta_{21} V_2 S_2^1 - \sigma \beta_{11} V_1 S_2^1 - (1-\tau) u S_2^1, \\
\dot{I}_2^1(t) &= \beta_{21} V_2 S_2^1 - (\mu + \nu_1) I_2^1, \\
\dot{S}_2^2(t) &= \omega S_2^1 - \beta_{22} V_2 S_2^2 - \sigma \beta_{12} V_1 S_2^2 - \mu S_2^2, \\
\dot{I}_2^2(t) &= \beta_{22} V_2 S_2^2 - (\mu + \nu_2) I_2^2, \\
\dot{M}(t) &= B_v - \alpha_{11} I_1^1 M - \alpha_{12} I_1^2 M - \alpha_{21} I_2^1 M - \alpha_{22} I_2^2 M - \gamma M, \\
\dot{V}_1(t) &= \alpha_{11} I_1^1 M + \alpha_{12} I_1^2 M - \gamma V_1, \\
\dot{V}_2(t) &= \alpha_{21} I_2^1 M + \alpha_{22} I_2^2 M - \gamma V_2,
\end{aligned}
\tag{4.3.3}
$$

where N_h is the total number of host population, N_j the total number of juvenile population, N_a the total number of adult population, and $N_h = N_j + N_a$. For the system to have a constant total number of population, $N_j = \frac{\mu}{\omega} N_a$ is assumed.

Linear stability of the disease-free steady state of this system can be investigated by using the next generation matrix. By ordering the infected variables as $I_1^1, I_1^2, I_2^1, I_2^2, V_1, V_2$, the matrix of new infections F is given by

$$
F = \begin{bmatrix} \underline{0} & \underline{0} & F_{13} \\ \underline{0} & \underline{0} & F_{23} \\ F_{31} & F_{32} & \underline{0} \end{bmatrix},
$$

where

$$
F_{13} = \begin{bmatrix} \beta_{11} & 0 \\ \beta_{12} S_1^{20} & 0 \end{bmatrix}, F_{23} = \begin{bmatrix} 0 & \beta_{21} S_2^{10} \\ 0 & \beta_{22} S_2^{20} \end{bmatrix},
$$

$$
F_{31} = \begin{bmatrix} \alpha_{11} M^0 & \alpha_{12} M^0 \\ 0 & 0 \end{bmatrix}, F_{32} = \begin{bmatrix} 0 & 0 \\ \alpha_{21} M^0 & \alpha_{22} M^0 \end{bmatrix},
$$

and $\underline{0} = [0]_{2\times 2}$. Also, $S_1^{10}, S_1^{20}, S_2^{10}, S_2^{20}$, and M^0 are values of the variables at the disease-free steady state. The matrix of transfer between classes is

$$
V = \mathrm{diag}\{\mu + \nu_1, \mu + \nu_2, \mu + \nu_1, \mu + \nu_2, \gamma, \gamma\}.
$$

The characteristic equation of the next-generation matrix (FV^{-1}) is

$$
\lambda^2 \left(\lambda^2 - \left(\frac{\alpha_{11}\beta_{11} M^0 S_1^{10}}{\gamma(\mu+\nu_1)} + \frac{\alpha_{12}\beta_{12} M^0 S_1^{20}}{\gamma(\mu+\nu_2)} \right) \right) \left(\lambda^2 - \left(\frac{\alpha_{21}\beta_{21} M^0 S_2^{10}}{\gamma(\mu+\nu_1)} + \frac{\alpha_{22}\beta_{22} M^0 S_2^{20}}{\gamma(\mu+\nu_2)} \right) \right) = 0.
$$

Hence, the threshold condition is

$$
R_{age-vac} < 1 \tag{4.3.4}
$$

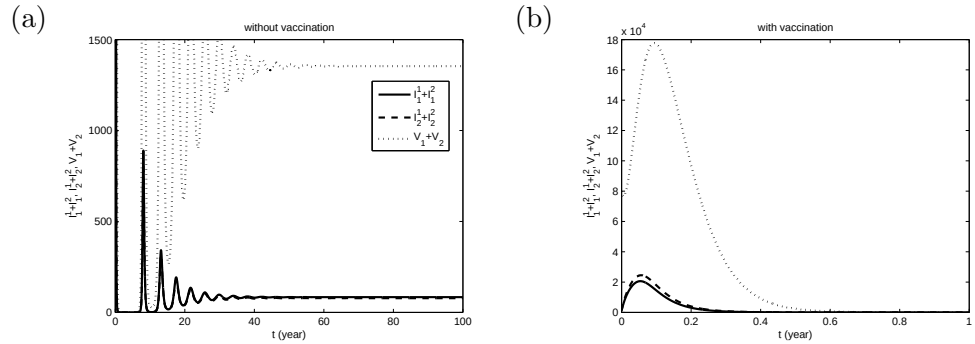

Figure 4-24: In the simulation, $\omega = 1/15, \nu_1 = 365/20, \nu_2 = 365/14, \gamma = 365/20, b = 0.5 * 365, p_1^v = p_2^v = 0.85, \alpha_{11}N_v = \alpha_{12}N_v = \alpha_{21}N_v = \alpha_{22}N_v = bp_1^v = 155, p_{11}^h = 0.25, p_{12}^h = 0.15, p_{21}^h = 0.22, p_{22}^h = 0.13$ (p_{ij} is the probability of successful infection with strain i in group j), $\beta_{11}N_h = bp_{11}^h = 45, \beta_{12}N_h = bp_{12}^h = 27, \beta_{21}N_h = bp_{21}^h = 40, \beta_{22}N_h = bp_{22}^h = 24, \tau = 0.7$, and $\sigma = 0.35$: (a) both strains coexists with $R^2_{vac-age(1)} = 5.3, R^2_{vac-age(2)} = 4.7$, (b) both strains die out by vaccination at rate $u = 3$.

where

$$R_{age-vac} = \max\left\{R_{age-vac(1)}, R_{age-vac(2)}\right\},$$

$$R_{age-vac(1)} = \sqrt{\frac{\alpha_{11}\beta_{11}\mu N_h N_v}{\gamma(\mu+\nu_1)(\mu+\omega+u)} + \frac{\alpha_{12}\beta_{12}\mu N_h N_v}{\gamma(\mu+\nu_2)(\mu+\omega+u)}}$$

and

$$R_{age-vac(2)} = \sqrt{\frac{\alpha_{21}\beta_{21}\mu N_h N_v}{\gamma(\mu+\nu_1)(\mu+\omega+(1-\tau)u)} + \frac{\alpha_{22}\beta_{22}\mu N_h N_v}{\gamma(\mu+\nu_2)(\mu+\omega+(1-\tau)u)}}.$$

The critical vaccination rate to eliminate both strains from the population can be derived from the threshold condition. The system is unwieldy to analyse, so here we show numerically that by applying a vaccination rate that satisfies the threshold condition (4.3.4), we can eradicate both strains of the diseases (see Figure 4-24). We assume that the transmission rate of infectious human to susceptible mosquitoes are equal for both strains. Children group is different from adult in the transmission rate of infectious mosquitoes to susceptible humans and the recovery rate from each strain. Without vaccination and $R_{01} = 5.32$ and $R_{02} = 4.66$, both strains coexist (see Figure 4-24(a)). With the vaccination rate $u > 2.6$, in the simulation $u = 3$ is chosen, both strains go extinct (see Figure 4-24(b)). It means that a vaccination campaign must be effective enough to vaccinate a whole children population within six months.

4.3.3 Conclusion and discussion

In case vaccination for malaria is available, it is important to study the transmission dynamics of it to gain an insight and to find the effective way to eliminate the disease. We propose two different models to study the protozoan dynamics in host population when vaccination is present. The first models considers the homogeneous population of humans while the second model takes account for the human population with two age classes, children and adults. Only the juvenile group is vaccinated instead of a whole human population. The second model captures the idea that immune response in children might be less efficient than adults. In each model we propose the threshold condition for eradicating both strains/species of malaria. We also verify our result numerically.

Assume that the transmission rates of both strains are the same in both groups ($\alpha_{11} = \alpha_{12} = \alpha_1$ and $\alpha_{21} = \alpha_{22} = \alpha_2$). Now, we would like to compare critical rates of vaccination to eliminate strain 1 from the population (rate of vaccination for strain 2 or both strains can be considered in the similar way) in both models, with and without age-classes. Because it takes longer for juveniles to recover, recovery rate of adults are always bigger, $\nu_1 < \nu_2$. By comparing these two recovery rates with one in the homogeneous population model (ν), $\nu_1 < \nu < \nu_2$. The critical rate of vaccination to eliminate strain 1 from the host population in the non age-class model is

$$u_c = \mu(R_{01}^2 - 1).$$

The critical rate of vaccination for strain 1 in the age-class model is

$$u_{c-age} = \mu R_{01}^2 \left(\frac{(\mu+\nu)}{(\mu+\nu_1)} + \frac{(\mu+\nu)}{(\mu+\nu_2)} \right) - (\mu+\omega).$$

Note that we write u_{c-age} in terms of R_{01} which is the basic reproductive ratio of strain 1 in the absence of vaccination in the non age-class model. By our parameter range, individuals stay in the juvenile class until they are 15 year old (the maturation rate, ω, is 1/15) and they die at age 70 year old ($\mu = 1/70$). We assume that the infectious periods of juveniles and adults are 20 and 14 days. Hence, we assume that $\nu_1 = 365/20 < \nu = 365/17 < \nu_2 = 365/14$. In the non age-class model, we vaccinate a whole population while we vaccinate only juveniles in the age-class model. If $R_{01}^2 = 8$ and $N = 200,000$, we have

$$u_c N = 20000 \text{ and } u_{c-age} N_j = u_{c-age} \frac{\mu}{(\mu+\omega)} N = 5,210$$

as the total number of individuals whom we need to vaccinate within 1 year to eradicate strain 1 when there are no age classes and when there are age classes, respectively. We

find that public heath only needs to vaccinate at least 5,210 juveniles per year to control strain 1 while they need to vaccinate at least 20,000 of random individuals to be able to drive out strain 1. From this result, we suggest that vaccinating only juveniles is more effective than random individuals.

4.4 Controlling mosquitoes

Another effective way of controlling malaria is by controlling mosquitoes (Takken and Knols, 2005). Several means affect mosquitoes differently. For example, destroying the mosquito's habitat and breeding sites, the use of larvicide, and introducing sterile mosquitoes help to reduce the number of new coming mosquitoes (Fillinger and Lindsay, 2006; Fillinger et al., 2009; Scott et al., 2002). The use of repellents and bed nets does not kill mosquitoes but helps to decrease the biting rate (Bradley et al., 1986). By spraying the walls and ceilings of the house with insecticide, the survival of adult mosquitoes resting indoors is reduced (Pates et al., 2005). Recent reports show improvement of the study that could lead to introducing genetically modified mosquitoes, that could kill 100 per cent of parasites in their guts, to replace wild mosquitoes (Ito et al., 2002; Povelones et al., 2009) so that the transmission of malaria to humans is reduced by reducing the probability of successful infection in a human who gets bitten by an infectious mosquito

Referring to the basic reproductive ratio of strain i (for $i = 1, 2$) of the system (3.1.4),

$$R_{0i} = \sqrt{\frac{\alpha_i \beta_i NM}{(\mu + \nu)\eta}}.$$

Because the use of mosquito repellents and bed nets reduces the biting rate which is described in the model via the transmission rate of infection to humans and mosquitoes (β_i, α_i) such that $\beta_i N = bp_{h_i}$ and $\alpha_i M = bp_{m_i}$ respectively where; b is the biting rate of mosquitoes (bites/human/year); p_{h_i} is the probability of successful infection with strain i in human, and p_{m_i} is the probability of successful infection with strain i in mosquito, the basic reproductive ratio of the strain in the system (3.1.4) is reduced by the effect of reducing the biting rate. Furthermore, if the biting rate is effectively reduced such that R_{0i} becomes less than 1, the strain is eradicated from the host population. Although reducing biting rate of mosquitoes can reduce the basic reproductive ratios of both strains at the same time, here we only show the result of it in strain 1 when

$$R_{01}^2 = \frac{b^2 p_{h_1} p_{m_1}}{(\mu + \nu)\eta}$$

The study of it in strain 2 can be done in the similar way. The study of the effect of

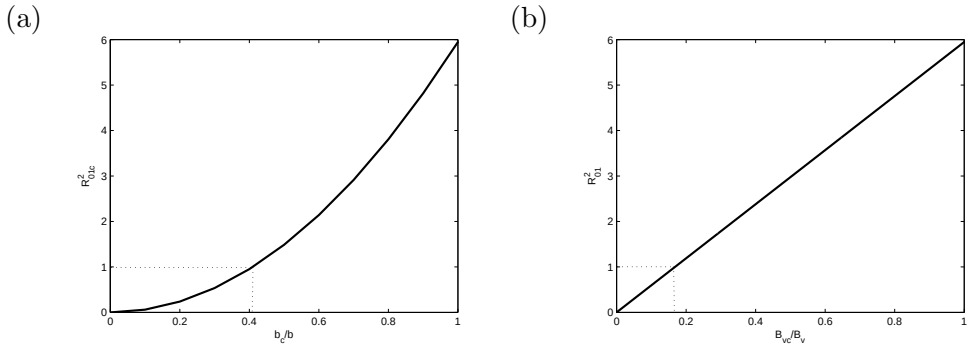

Figure 4-25: (a) A relation between the ratio of the biting rate which is reduced by applying control via bed nets and repellents (b_c) comparing with the biting rate at the beginning when a control is not applied yet (b) and the square of the basic reproductive ratio of strain 1 ($b = 0.5 * 365, p_{h_1} = 0.1, p_{m_1} = 0.85$) (b) A relation between the recruitment rate which is reduced by control via destroying mosquito habitat (B_c) comparing with the recruitment rate at the beginning when a control is not yet used (B) and the square of the basic reproductive ratio of strain 1 ($B = M * \eta = 4.2\text{e+}6$, $b = 0.5 * 365$)

reducing biting rate to both strains at the same time is consequently the result of those two studies. In Figure 4-25(a), we show that the basic reproductive ratio of strain 1 is reduced by decreasing biting rate of mosquitoes at the beginning. At $b_c/b = 1$, it is before the control is launched where $R^2_{01} = 5.95$, b_c represents the new biting rate when the control is present, and $b_c = b = 0.5 * 365$ bites/human/year. After the biting rate is reduced so that $b_c/b < 1$, the basic reproductive ratio of strain 1 $\left(R^2_{01c} = \frac{b_c^2 p_{h_1} p_{m_1}}{(\mu+\nu)\eta}\right)$ is decreased. If the biting rate b_c is below 0.2 (or $b_c/b < 0.41$), strain 1 dies out.

By destroying the mosquito's habitat,applying the larvicides, or introducing the sterile mosquitoes, we reduce the parameter B which is the recruitment rate of mosquitoes in the basic reproductive ratio. Again, here we only consider the effect of it in strain 1. Figure 4-25(b) shows that reducing prevalence of strain 1 can be done by decreasing the recruitment rate of mosquitoes via destroying the mosquito's habitat or breeding sites. At $B_c/B = 1$ where B_c is the new recruitment rate when the control is present, we begin with $R^2_1 = 5.95$ and $B_c = B = 4.2\text{e+}6$ numbers of mosquitoes per year. After the recruitment rate is reduced by the control so that $B_c/B < 1$, the basic reproductive ratio of strain 1 $\left(R^2_{1c} = \frac{B_c b p_{h_1} b p_{m_1} M}{\eta^2(\mu+\nu)}\right)$, where M is 231000 without any control, is decreased. In case the recruitment B_c is below 7e+5 mosquitoes/year (or $B_c/B < 0.17$), strain 1 is extinct.

By considering the possibility of replacing the wild mosquitoes by genetically modified mosquitoes that could kill the malaria parasites in their guts, we might be able to reduce the prevalence of malaria by reducing the probability of infection in human

(p_{h_1}). When p_{h_1} is reduced, the basic reproductive ratio R^2_{01c} becomes smaller (see Figure 4-26(a)). At $p_{hc}/p_{h_1} = 1$, the control is absent. When the control is applied, the ratio becomes less than 1 and when p_{h_1} is below 0.01 (or $p_{h_1c}/p_{h_1} < 1/R^2_{01} \approx 0.13$), malaria is eradicated.

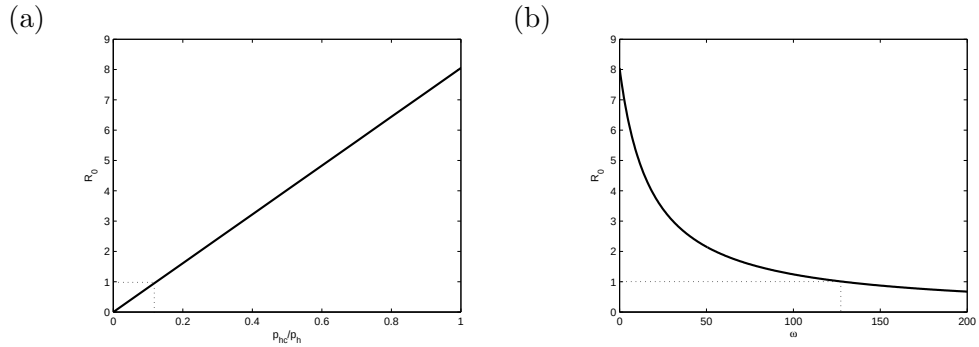

Figure 4-26: (a) A relation between the ratio of the probability of successful infection in human when the control is applied (p_{hc}) and when it is not applied (p_h) with R^2_{01} (b) A plot between rate of killing mosquitoes by the insecticide (ω) and the basic reproductive ratio (R_{01})

Finally, by launching the insecticide programme to control the mosquitoes, some adult mosquitoes die in the sprayed areas. We can describe this strategy in the model (3.1.4) by removing both susceptible and infectious mosquitoes at rate ω. Hence, the terms $-\omega U$, $-\omega V_1$, and $-\omega V_2$ are added to the right hand side of the differential equations for U, V_1, and V_2 in the system (3.1.4). The total size of mosquito population is now time-dependent. The basic reproductive ratio becomes $R^2_{01c} = \frac{b^2 p_{h_1} p_{m_1} q}{(\eta+\omega)(\mu+\nu)}$. In Figure 4-26(b), we show the relation between rate of decreasing mosquitoes by the insecticide and the basic reproductive ratio. In case, we start with $R^2_{01} = 8$ in the absence of the insecticide programme, the basic reproductive ratio is reduced when the insecticide programme is effective. To eradicate malaria, we need $\omega = 129$ or in other words we need to shorten mosquito's lifetime to be approximately 3 days on average by the insecticide.

In conclusion, we suggest that all the control measures should be launched together to efficiently find the way to reduce the loss from malaria or hopefully eradicate it. The optimal strategy should be further studied.

Conclusion and discussion

We discuss the control measures in mosquitoes. This is done by considering the basic reproductive ratios, how the controls affect parameters in the model and consequently affect the basic reproductive ratios, and how to eradicate the disease accord-

ing to the threshold condition. Several ways of controlling mosquitoes are discussed. For example, destroying mosquito's habitats, applying larvicides, and releasing sterile mosquitoes reduce the number of new coming mosquitoes, which is described by the recruitment rate in the model. To eradicate the disease, the controls must be applied until $\left(R_0 = \frac{Bb^2 p_h p_m}{\eta^2(\mu+\nu)N} < 1\right)$ where B is the recruitment rate and other parameters are fixed. Other controls such as the use of bed nets, releasing genetically modified mosquitoes that could not transmit malaria, the use of insecticides, are also discussed in the similar way.

4.5 Conclusions and discussion

We first study a status-based model based on Gog and Grenfell (2002) for two strains of influenza when isolation and vaccination are present. The goal of this study is to try to understand how isolation and vaccination help with controlling influenza. We propose critical isolation rate and vaccination coverage in terms of the parameters when there is no intervention. These sets of critical values help to predict what the result in long term should be when isolation and vaccination are applied. This may be useful in term of controlling influenza. Numerically, we assume a delay in isolation. We find that the delay leads to serious outbreaks through the time space. Hence, we recommend public health to start isolation programme since the beginning to reduce loss as much as possible. We next consider the epidemic quantities: the basic reproductive ratio, the mean age at infection, the invasion rate of new strain, and the economic cost. By comparing the basic reproductive ratios, we find that strains should be more virulent when isolation or vaccination are present to be able to invade the host population. We find that the host mean age at infection is extended by isolation, vaccination, or coexistence with the other strain. Interestingly, isolation and vaccination lead to higher rate of invasion comparing with when there is no intervention. We suggest that a new strain needs to have a higher rate of invasion to be able to establish in the population not only to compete with the endemic strain but also in the situation that controls are applied. We find that isolation and vaccination help to reduce the total cost of loss from hospitalization and individual income.

Second, we study a vaccination model of influenza with waning of immunity and cross-immunity with time. This model is used to study influenza strains in the same cluster. In this work, we first introduce a constant rate vaccination and propose a critical rate of vaccination to eliminate influenza from the population. We next introduce a time-dependent rate of vaccination to minimize the treatment cost for influenza. We find the optimal control that helps to eliminate influenza and minimize the treatment cost. From our optimal control shape, a high rate of vaccination is needed at the

beginning but it can be reduced after certain time later. Moreover, we also find that cross-immunity help to strictness of control measure.

Third, in this section, we introduce vaccination into the malaria model in Chapter 3. We consider two types of vaccination models: with no age classes and without age classes. We propose critical vaccination rates for eliminating both strains of malaria for both models. By comparing the minimum number of individuals whom we need to vaccinate within one year to eradicate malaria strain from the human population, we find that vaccination only in juveniles is more effective than vaccination in both juveniles and adults.

We finally end this chapter by discussing about controlling mosquitoes. This is one of the most important way to control diseases such as malaria. We consider four different means of controlling mosquitoes: 1) by using bed nets and repellents to reduce bitting rate of mosquitoes, 2) by using larvicides, destroying mosquito's habitat, and introducing sterile mosquitoes, to reduce mosquito newcomers, 3) by replacing wild mosquitoes by genetically modified mosquitoes that do not transmit malaria to reduce the probability of infection, and 4) by applying insecticide to increase the death rate of adult mosquitoes. To eliminate malaria, we introduce a critical value of a controlled variable in each means.

Chapter 5

Conclusion and further work

For decades, the world has been challenged by the reemergence of multi-strain infectious diseases such as influenza, malaria, HIV, and hepatitis. In this work, we are particularly interested in influenza and malaria which are endemic in many areas of the world. We use mathematical models to study the dynamics of the diseases in order to try to understand and gain insights when various factors are taken into account. In some diseases, for instance influenza, cross-immunity plays an important role in reducing the prevalence and spread of the disease. Hence, we here concentrate on the presence of cross-immunity in the model. In chapter 2, we use a real line to represent antigenic space where each point on the real line represents each strain of influenza. The system of n ordinary differential equations based on the status-based framework by Gog and Grenfell (2002) becomes a system of two integro-differential equations. When mutation in the virus is introduced, we find that a travelling wave occurs and represents an antigenic drift process with strains present in the population dying out and being replaced by new ones at new points in the antigenic space. We also find that the presence of cross-immunity might not affect a wave speed of travelling wave. In the case that cross-immunity is only conferred on two neighbouring strains, we show that a travelling wave always occurs whenever mutation is present and we furthermore calculate the minimum wave speed which is independent of the cross-immunity value. This model can be further investigated in a two-dimensional antigenic space. In the second section, we propose a metapopulation model to study spatial heterogeneity in two subpopulations. We introduce the basic reproductive ratio of the system and show numerically that the threshold conditions are satisfied. This metapopulation model should be further investigated when controls such as vaccination and vaccination are present or when stochastic effects are included.

We devote chapter 3 to study a multi-strain vector-borne disease like malaria. In the first section, we introduce a status-based framework where an individual is categorized

by its immune status and cross-immunity is conferred by exposure to the disease via an infective mosquito, rather than developing the full infection itself, the model becomes tractable with only one immune variable to describe host immunity to each strain. The model is studied analytically and numerically for threshold conditions for a strain. In the second section, we introduce single-species models for *P. falciparum* and *P. vivax* with acquired immunity allowed to wane with time. We then introduce a coinfection model that captures interactions between both species by including suppression of both species to each other during coinfection. We further investigate whether *P. vivax* avoids encountering *P. falciparum* which is more harmful by introducing seasonality in transmission rate of *P. falciparum* as a sinusoidal function under the assumption that there is a season in each year that *P. falciparum* is highly transmitted. We find that the prevalence of *P. vivax* is high between every two peaks of *P. falciparum* which suggests that during high transmission of *P. falciparum*, *P. vivax* may maintain lower transmission and it may become highly transmitted later when the prevalence of *P. falciparum* is low. By omitting coinfection between *P. falciparum* and *P. vivax*, we propose a cross-immunity model by assuming that cross-species immunity is present and acts in the similar way with suppression during subsequent infection in the coinfection model. We study the relation between cross-immunity values, cross-immunity of *P. falciparum* to reduce transmission of *P. vivax* and cross-immunity of *P. vivax* to reduce complication of *P. falciparum*. We find that when the former is very high, *P. vivax* may die out while both coexist no matter how large the latter is unless the former is very high. Moreover, we further investigate the mean age of infection. We find that the latter helps to increase the mean age at infection while the former reduces it.

In addition, we study a single species or strain model with waning immunity based on the SIRS model for human population and the SI model for mosquito population. We individualy incoporate seasonality, incubation time in mosquitoes, and vector-bias to infectious humans. In case there are three seasons (hot, rainy, winter) in each year, by introducing seasonality in the recruitment and transmission rates, malaria might be highly transmitted between hot and rainy season. By incorporating incubation time in mosquitoes, the prevalence of malaria is reduced when malaria parasites take longer to incubate in mosquitoes. By including manipulation of malaria parasites that infectious humans might be more attractive to mosquitoes than susceptible or recovered humans, a diffusion term to represent mosquito movement, and a chemotactic term toward chemical such as breath or sweat, travelling waves from infected population to uninfected population occurs. We also find that the more attractive infectious humans are, the faster the disease travels and spreads. The minimum wave speed is calculated analytically. We next study a vector-bias bias model in detail. However, the model for humans is based on the SIS model which is another type of model that has been used to study malaria and is in more simplistic form. We show that transcritical bifurcation

occurs at the basic reproductive ratio of the system equaling 1 by projecting the fold onto the extended centre manifold. We introduce incabation time in mosquitoes into the vector-bias model and find that the longer incubation time reduces the prevalence of malaria. We then incorporate a random movement of mosquitoes and a chemotactic terms toward humans, both of which result in the occurence of travelling waves. Its speed is estimated numerically and the minimum wave speed is calculated analytically.

In chapter 4, we study multi-strain models in the presence of controls. We introduce isolation and vaccination into the status-based model for influenza based on Gog and Grenfell (2002) in the first section. In the isolation model, infectious individuals are removed to isolation. A fraction of newborns is vaccinated with two possibilities, acquiring immunity to strain 1 only or acquiring complete immunity to both strains, in the vaccination model. We determine steady states and their stability conditions. We plot transcritical bifurcation diagrams with isolation rate and vaccination rate as bifurcation parameters. We then illustrate some of numerical results that satisfy with the diagrams. We compare epidemic quantities, the mean age at infection, the invasion rate of a new strain, and the economic cost. For example, we show that the host's mean age at infection is increased by isolation, vaccination, and the presence of the other strain. By considering the invasion rate of strain 2, we find that the new strain with higher transmission rate is preferred in the presence of isolation and vaccination. In the second section, we study controls in influenza based on the SIRC model with waning of immunity in recovered and cross-immune individuals (Casagrandi et al., 2006). We consider constant and time-dependent rate of vaccination in the model. We propose a critical rate of vaccination to eradicate the disease. In case the goal of vacccination campaign is to eradicate influenza with minimizing the treatment cost, we find that cross-immunity is an important key for the shape of the optimal control. The weaker cross-immunity is, the stronger vaccination control needs and the more number of infectious individuals is.

For malaria, controls can be applied in either humans or mosquitoes. Here, we assume that vaccination is available and study two types of models, with and without age-classes. The model is based on a status-based framework in Section 3.1, Chapter 3. The first model considers the homogeneous population of humans while the second model takes into account the less immune response in children than adults. For both models, we propose the threshold conditions to eradicate malaria and verify them numerically. In controlling mosquitoes, there are various means such as destroying mosquito's breeding sites, applying larvicide, using bed nets and repellents, using insecticide, and possibly introducing genetically modified mosquitoes. Several means affect mosquitoes differently. Here, we consider how controls affect parameters in the model via the basic reproductive ratio of the system, since eradication follows if con-

trols are applied until the basic reproductive ratio becomes less than 1. This work can be further investigated by introducing multiple controls in a host-vector model for malaria for optimal control strategies.

Bibliography

Abu-Raddad, L. J. and Ferguson, N. M. (2004), 'The impact of cross-immunity, mutation and stochastic extinction on pathogen diversity', *Proc. R. Soc. Lond. B* **271**, 2431–2438.

Adams, B., Holmes, E. C., Zhang, C., Jr., M. P. M., Nimmannitya, S., Kalayanarooj, S. and Boots, M. (2006), 'Cross-protective immunity can account for the alternating epidemic pattern of dengue virus serotypes circulating in Bangkok', *PNAS* **103**, 14234–14239.

Adams, B. and Sasaki, A. (2007), 'Cross-immunity, invasion and coexistence of pathogen strains in epidemiological models with one-dimensional antigenic space', *Math. Biosci.* **210**, 680–699.

Adams, B. and Sasaki, A. (2009), 'Antigenic distance and cross-immunity, invasibility and coexistence of pathogen strains in an epidemiological model with discrete antigenic space', *Theor. Popul. Biol.* **76**, 157–167.

Alexander, M. E., Bowman, C., Moghadas, S. M., Summers, R., Gumel, A. B. and Sahai, B. M. (2004), 'A vaccination model for transmission dynamics of influenza', *SIADS* **3**, 503–524.

Anderson, R. M. and May, R. M. (1991), 'Infectious Diseases of Humans: Dynamics and Control', *Oxford University Press* .

Andreasen, V. (2003), 'Dynamics of annual influenza A epidemics with immuno-selection', *J. Math. Biol.* **46**, 504–536.

Andreasen, V., Lin, J. and Levin, S. A. (1997), 'The dynamics of cocirculating influenza strains conferring partial cross-immunity', *J. Math. Biol.* **35**, 825–842.

Anstey, N. M., Russell, B., Yeo, T. W. and Price, R. N. (2009), 'The pathophysiology of *vivax* malaria', *Cell* **25**, 220–227.

Aron, J. L. (1988), 'Mathematical modeling of immunity to malaria', *Math. Biosci.* **90**, 385–396.

Bailey, N. J. T. (1975), *The Mathematical Theory of Infectious Diseases and Its Application*, Griffin, London.

Becker, N. (1978), 'The use of epidemic models', *Biometrics* **35**, 295–305.

Beier, J. C. (1998), 'Malaria parasites development in mosquitoes', *Annu. Rev. Entomol.* **43**, 519–543.

Belshe, R. B. (2005), 'The origins of pandemic influenza: Lessions from the 1918 virus', *N. Engl. J. Med.* **353**, 2209–2211.

Billings, L., Fiorillo, A. and Schwartz, I. B. (2008), 'Vaccination in disease models with antibody-dependent enhancement', *Proc. R. Soc. Interface* **211**, 265–281.

Boldin, B. and Diekmann, O. (2008), 'Superinfections can induce evolutionarily stable coexistence of pathogens', *J. Math. Biol.* **56**, 635–672.

Boni, M. F., Gog, J. R., Andreasen, V. and Christiansen, F. B. (2004), 'Influenza drift and epidemic size: the race between generating and escaping immunity', *Theor. Popu. Biol.* **65**, 179–191.

Bradley, A. K., Greenwood, A. M., Byass, P., Greenwood, B. M., Marsh, K., Tulloch, S. and Hayes, R. (1986), 'Bed-nets (mosquito-nets) and morbidity from malaria', *Lancet* **2**, 204–207.

Bremermann, H. J. and Thieme, H. R. (1989), 'A competitive exclusion principle for pathogen virulence', *J. Math. Biol.* **27**, 179–190.

Bruce, M. C. and Day, K. P. (2002), 'Cross-species regulation of malaria parasitaemia in the human host', *Curr. Opin. Microbiol.* **5**, 431–437.

Bruce, M. C., Donnelly, C. A., Alpers, M. P., Galanski, M. R., Barnwell, J. W., Walliker, D. and Day, K. P. (2000), 'Cross-species interactions between malaria parasites in humans', *Science* **287**, 845–848.

Burattini, M. N., Massad, E. and Coutinho, F. A. B. (1993), 'Malaria transmission rates estimated from serological data', *Epidemiol. Infect.* **111**, 503–523.

Burls, A., Clark, W., Stewart, T., Preston, C., Bryan, S., Jefferson, T. and Fry-smith, A. (2002), 'Zanamivir for the treatment of influenza in adults: a systematic review and economic evaluation', *Health Technology Assessment* **6**.

Calvez, V., Korobeinikov, A. and Maini, P. K. (2005), 'Cluster formation for multi-strain infections with cross-immunity', *J. Theor. Biol.* **233**, 75–83.

Carlton, J. (2003), 'The *Plasmodium vivax* genome sequencing project', *Trends Parasitol.* **19**, 227–231.

Carman, W. F., Zannetti, A. R., Karayiannis, P., Waters, J., Manzillo, G., Tanzi, E., Zuckermann, A. J. and Thomas, H. C. (1990), 'Vaccine-induced escape mutant of hepatitis B virus', *Lancet* **336**, 325–329.

Carrat, F. and Flahault, A. (2007), 'Influenza vaccine: The challenge of antigenic drift', *Vaccine* **25**, 6852–6862.

Casagrandi, R., Bolzoni, L., Levin, S. A. and Andreasen, V. (2006), 'The SIRC model and influenza A', *Math. Biosci* **200**, 152–169.

Cassiday, P. K., Sanden, G. N., Heuvelman, K., Mooi, F. R., Bisgard, K. M. and Popovic, T. (2000), 'Polymorphism in *Bordetella pertussis* pertactin and pertussis toxin virulence factors in the United States', *J. Infect. Dis.* **182**, 1402–1408.

Castillo-Chavez, C., Hethcote, H. W., Andreasen, V., Levin, S. A. and Liu, W. M. (1989), 'Epidemiological models with age structure, proportionate mixing, and cross-immunity', *J. Math. Biol.* **27**, 233–258.

Castillo-Chavez, C., Huang, W. and Li, J. (1996), 'Competitive exclusion in gonorrhea models and other sexually transmitted diseases', *SIAM. J. Appl. Math.* **56**, 494–508.

Castillo-Chavez, C., Huang, W. and Li, J. (1997), 'The effects of female's susceptibility on the coexistence of multiple pathogen strains of sexually transmitted diseases', *J. Math. Biol.* **35**, 1432–1416.

Castillo-Chavez, C., Huang, W. and Li, J. (1999), 'Competitive exclusion and coexistence of multiple strains in an SIS STD model', *SIAM J. Appl. Math.* **59**, 1790–1811.

Cattaneo, R., Schmid, A., Eschle, D., Baczko, K., Meulen, V. T. and Billeter, M. A. (1988), 'Biased hypermutation and other genetic changes in defective measles viruses in human brain infections', *Cell* **55**, 255–265.

Chamchod, F. (2006), 'MSc project: Modelling Dutch Elm Disease'.

Chen, W. N. and Oon, C. J. (2000), 'Hepatitis B virus surface antigen (HBsAg) mutants in Singapore adult and vaccinated children with high anti-hepatitis B virus antibody levels but negative for HBsAg', *J. Clin. Microbiol.* **38**, 2793–2794.

Chiyaka, C., Garira, W. and Dube, S. (2007*a*), 'Mathematical modelling of the impact of vaccination on malaria epidemiology', *Qual. Theor. Diff. Equat. Anal.* **1**, 28–58.

Chiyaka, C., Garira, W. and Dube, S. (2007*b*), 'Transmission model of endemic human malaria in a partially immune population', *Math. Comput. Model.* **46**, 806–822.

Chiyaka, C., Tchuenche, J. M., Garira, W. and Dube, S. (2008), 'A mathematical analysis of the effects of control strategies on the transmission dynamics of malaria', *Appl. Math. Comput.* **195**, 641–662.

Coetzee, M., Craig, M. and Sueur, D. L. (2000), 'Distribution of African malaria mosquitoes belonging to the *Anopheles gambiae* complex', *Parasitol Today* **16**, 74–77.

Cogswell, F. B. (1992), 'The hypnozoite and relapse in primate malaria', *Clin. Microbiol. Rev.* **5**, 26–35.

Collins, W. E., Skinner, J. C. and Jeffery, G. M. (1968), 'Studies on the persistence of malarial antibody response', *Am. J. Epidemiol.* **87**, 592–598.

Contacos, P. G., Collins, W. E., Jeffery, G. M., Krotoski, W. A. and Howard, W. A. (1972), 'Studies on characterization of *Plasmodium-vivax* strains from Central-America', *Am. J. Trop. Med. Hyg.* **31**, 707.

Costantini, C., Gibson, G., Sagnon, N., Torre, A. D., Brady, J. and Coluzzi, M. (1996), 'Mosquito responses to carbon dioxide in a West African Sudan savanna', *Med. Vet. Entomol.* **10**, 220–227.

Cowman, A. I. and Crabb, B. S. (2006), 'Invasion of red blood cells by malaria parasites', *Cell* **124**, 755–766.

Cox, N. and Bender, C. A. (1995), 'The molecular epidemiology of influenza viruses', *Sem. Virol.* **6**, 359–370.

Cox-Singh, J., Davis, T. M., Lee, K. S., Shamsul, S. S., Matusop, A., Ratnam, S., Rahman, H. A., Conway, D. J. and Singh, B. (2008), '*Plasmodium knowlesi* malaria in humans is widely distributed and potentially life threatening', *Clin. Infect. Dis.* **46**, 165–171.

Cox-Singh, J. and Singh, B. (2008), '*Knowlesi* malaria: newly emergent and of public health importance?', *Trends. Parasitol.* **24**, 406–410.

Cui, L., Escalante, A. A., Imwong, M. and Snounou, G. (2003), 'The genetic diversity of *Plasmodium vivax* populations', *Trends Parasitol.* **19**, 220–226.

Davies, J., Grilli, E. and Smith, A. (1984), 'Influenza A: infection and reinfection', *J. Hyg.(Cambridge)* **92**, 125.

Dawes, J. H. P. and Gog, J. R. (2002), 'The onset of oscillatory dynamics in models of multiple disease strain', *J. Math. Biol.* **45**, 471–510.

Day, K. P. and Marsh, K. (1991), 'Natually acquired immunity to *Plasmodium falciparum*', *Immunol. Today* **12**, A68–71.

Diekmann, O. and Heesterbeek, J. A. P. (2000), *Mathematical Epidemiology of Infectious Diseases, Model Building, Analysis and Interpretation*, Wiley.

Dietz, K., Molineaux, L. and Thomas, A. (1974), 'A malaria model tested in the African savannah', *Bull. World Health Organ.* **50**, 347–357.

Doolan, D. L., Dobano, C. and Baird, J. K. (2009), 'Acquired immunity to malaria', *Clin. Microbiol. Rev.* **22**, 13–36.

Drakeley, C., Sutherland, C., Bousema, J. T., Sauerwein, R. W. and Targett., G. A. (2006), 'The epidemiology of *Plasmodium falciparum* gametocytes: weapons of mass dispersion', *Trends. Parasitol.* **22**, 424–430.

Ebel, G. D., Dupuis, A. P., Ngo, K., Nicholas, D., Kauffman, E., Jones, S. A., Young, D., Maffei, J., Shi, P. Y., Bernard, K. and Kramer, L. D. (2001), 'Partial genetic characterization of West Nile virus strains, New York State, 2000', *Emerg. Infec. Dis.* **7**, 650–653.

Eron, J. J., Vernazza, P. L., Johnston, D. M., Seillier-Moiseiwitsch, F., Alcorn, T. M., Fiscus, S. A. and Cohen, M. S. (1998), 'Resistance of HIV-1 to antiretroviral agents in blood and seminal plasma: Implications for transmission', *AIDS* **15**, 181–189.

Esteva, L. and Vargas, C. (2003), 'Coexistence of different serotypes of dengue virus', *J. Math. Biol.* **46**, 31–47.

Feng, Z. and Velasco-Hernandez, J. X. (1997), 'Competitive exclusion in a vector-host model for the dengue fever', *J. Math. Biol.* **35**, 523–544.

Ferguson, N., Anderson, R. and Gupta, S. (1999), 'The effect of antibody-dependent enhancement on the transmission dynamics and persistence of multiple-strain pathogens', *Proc. Natl. Acad. Sci. USA* **96**, 790–794.

Fillinger, U. and Lindsay, S. W. (2006), 'Suppression of exposure to malaria vectors by an order of magnitude using microbial larvicides in rural Kenya', *Trop. Med. Int. Health* **11**, 1629–1642.

Fillinger, U., Sombroek, H., Majambere, S., van Loon, E., Takken, W. and Lindsay, S. W. (2009), 'Identifying the most productive breeding sites for malaria mosquitoes in The Gambia', *Malaria J.* **8**, 62.

Fillipe, J. A. N., Riley, E. M., Drakeley, C. J., Sutherland, C. J. and Ghani, A. C. (2007), 'Determination of the processes driving the acquisition of immunity to malaria using a mathematical transmission', *PLOS Comput. Biol.* **3**, e255.

Frank, A. L., Taber, L. H. and Wells, J. M. (1983), 'Individuals infected with two subtypes of influenza A virus in the same season', *J. Infect. Dis.* **147**, 120–124.

Gandon, S. and Day, T. (2007), 'The evolutionary epidemiology of vaccination', *J. R. Soc. Interface* **4**, 803–817.

Gandon, S., Jansen, V. A. A. and van Baalen, M. (2001), 'Host life history and the evolution of parasite virulence', *Evolution* **55**, 1056–1062.

Gandon, S., van Baalen, M. and Jansen, V. A. A. (2002), 'The evolution of parasite virulence, superinfection, and host resistance', *Am. Nat.* **159**, 658–669.

Gardner, M. J., Hall, N., Fung, E., White, O., Berriman, M., Hyman, R. W., Carlton, J. M., Pain, A., Nelson, K. E., Bowman, S., Paulsen, I. T., James, K., Eisen, J. A., Rutherford, K., Salzberg, S. L., Craig, A., Kyes, S., Chan, M. S., Nene, V., Shallom, S. J., Suh, B., Peterson, J., Angiuoli, S., Pertea, M., Allen, J., Selengut, J., Haft, D., Mather, M. W., Vaidya, A. B., Martin, D. M. A., Fairlamb, A. H., Fraunholz, M. J., Roos, D. S., Ralph, S. A., McFadden, G. I., Cummings, L. M., Subramanian, G. M., Mungall, C., Venter, J. C., Carucci, D. J., Hoffman, S. L., Newbold, C., Davis, R. W., Fraser, C. M. and Barrell, B. (2002), 'Genome sequence of the human malaria parasite *Plasmodium falciparum*', *Nature* **419**, 498–511.

Gaudart, J., Toure, O., Dessay, N., Dicko, A., Ranque, S., Forest, L., Demongeot, J. and Doumbo, O. K. (2009), 'Modelling malaria incidence with environmental dependency in a locality of Sudanese savannah area, Mali', *Malaria J.* **8**, 61.

Gill, P. and Murphy, A. (1977), 'Naturally acquired immunity to influenza type A: a further prospective study', *Med. J. Austr.* **2**, 761–765.

Githeko, A. K., Lindsay, S. W., Confalonieri, U. E. and Patz, J. A. (2000), 'Climate change and vector-borne diseases: a regional analysis', *Bull. WHO* **78**, 1136–1147.

Githeko, A. K., Service, M. W., Mbogo, C. M., Atieli, F. K. and Juma, F. O. (1994), 'Origin of blood meals in indoor and outdoor resting malaria vectors', *Acta Trop.* **58**, 307–316.

Glendinning, P. (1999), *Stability, Instability and Chaos: an introduction to the thery of nonlinear differential equations*, Cambridge University Press.

Gog, J. R. and Grenfell, B. T. (2002), 'Dynamics and selection of many-strain pathogens', *PNAS* **99**, 17209–17214.

Gog, J. R. and Swinton, J. (2002), 'A status-based approach to multiple strain dynamics', *J. Math. Biol.* **44**, 169–184.

Gomes, M. G. M., Margheri, A., Medley, G. F. and Rebelo, C. (2005), 'Dynamical behaviour of epidemiological models with sub-optimal immunity and nonlinear incidence', *J. Math. Biol.* **51**, 414–430.

Gomes, M. G. M., White, L. J. and Medley, G. F. (2004), 'Infection, reinfection, and vaccination under suboptimal immune protection: epidemiological perspectives', *J. Theor. Biol.* **228**, 539–549.

Grenfell, B. T., Bjornstad, O. N. and Kappey, J. (2001), 'Travelling waves and spatial hierarchies in measles epidemics', *Nature* **414**, 716–723.

Grenfell, B. T., Pybus, O. G., Gog, J. R., Wood, J. L. N., Daly, J. M., Mumford, J. A. and Holmes, E. C. (2004), 'Unifying the epidemiological and evolutionary dynamics of pathogens', *Science* **303**, 327–332.

Guerra, C. A., Snow, R. W. and Hay, S. I. (2006), 'Mapping the global extent of malaria in 2005', *Trends Parasitol.* **22**, 353–359.

Gupta, S. and Day, K. P. (1994), 'A strain theory of malaria transmission', *Parasitol. Today* **10**, 476–481.

Gupta, S., Ferguson, N. and Anderson, R. M. (1998), 'Chaos, persistence, and evolution of strain structure in antigenically diverse infectious agents', *Science* **280**, 912–915.

Gupta, S., Maiden, M. C. J., Feavers, I. M., Nee, S., May, R. M. and Anderson, R. M. (1996), 'The maintenance of strain structure in populations of recombining infectious agents', *Nature Medicine* **2**, 437–442.

Gupta, S., Snow, R. W., Donnelly, C. A., Marsh, K. and Newbold, C. (1999), 'Immunity to non-cerebral severe malaria is acquired after one or two infections', *Nat. Med.* **5**, 340–343.

Gupta, S., Swinton, J. and Anderson, R. M. (1994), 'Theoretical studies of the effects of heterogeneity in the parasite population on the transmission dynamics of malaria', *Proc. R. Soc. Lond. B* **256**, 231–238.

Gupta, S., Trenholme, K., Anderson, R. M. and Day, K. P. (1994), 'Antigenic diversity and the transmission dynamics of *Plasmodium falciparum*', *Science* **263**, 961–963.

Hay, A. J., Gregory, V., Dougas, A. R. and Lin, Y. P. (2001), 'The evolution of human influenza viruses', *Proc. Roy. Soc. Lond. B* **356**, 1861–1870.

Herbert, W. H. (2000), 'The mathematics of infectious diseases', *SIAM Rev.* **42**, 599–653.

Holmes, E. C., Ghedin, E., Miller, N., Taylor, J., Ba, Y. and George, S. K. (2005), 'Whole-genome analysis of human influenza A virus revels multiple persistent lineages and reassortment among recent H3N2 viruses', *PLoS Biol* **3**, 300.

Hosack, G. R., Rossignol, P. A. and van den Driessche, P. (2008), 'The control of vector-borne disease epidemics', *J. Theor. Biol.* **255**, 16–25.

Hoshen, M. and Morse, A. (2004), 'A weather-driven model of malaria transmission', *Malaria J.* **3**, 32–46.

Hulden, L., Hulden, L. and Heliovaara, K. (2008), 'Natural relapse in *vivax* malaria induced by *Anopheles* mosquitoes', *Malaria J.* **7**, 1–11.

Hviid, L. (2005), 'Naturally acquired immunity to *Plasmodium falciparum* malaria in Africa', *Acta Trop.* **95**, 270–275.

Iannelli, M., Martcheva, M. and Li, X. (2005), 'Strain replacement in an epidemic model with super-infection and perfect vaccination', *Math. Biosci.* **195**, 23–46.

Ishikawa, H., Ishii, A. and Nagai, N. (2003), 'A mathematical model for the transmission of *Plasmodium vivax* malaria', *Parasitol. Int.* **52**, 81–93.

Ito, J., Ghosh, A., Moreira, L. A., Wimmer, E. A. and Jacobs-Lorena, M. (2002), 'Transgenic anopheline mosquitoes impaired in transmission of malaria parasites', *Nature* **417**, 452–455.

Kamo, M. and Sasaki, A. (2002), 'The effect of cross-immunity and seasonal forcing in a multi-strain epidemic model', *Physica D* **165**, 228–241.

Keeling, M. J. and Rohani, P. (2008), *Modeling infectious diseases in humans and animals*, Princeton University Press.

Kent, R. J., Thuma, P. E., Mharakurwa, S. and Norris, D. E. (2007), 'Seasonality, blood feeding behaviour, and transmisson of *Plasmodium falciparum* by *Anopheles Arabiensis* after an extended drought in Southern Zambia', *Am. J. Trop. Med. Hyg.* **76**, 267–274.

Kermack, W. O. and McKendrick, A. G. (1927), 'A contribution to the mathematical theory of epidemics', *Proc. R. Soc. A* **115**, 700–721.

Kingsolver, J. G. (1987), 'Mosquito host choice and the epidemiology of malaria', *Am. Nat.* **130**, 811–827.

Koella, J. C. (1991), 'On the use of mathematical models of malaria transmission', *Acta Trop.* **49**, 1–25.

Koella, J. C. and Antia, R. (2003), 'Epidemiological models for the spread of anti malarial resistance', *Malaria J.* **2**, 3.

Koella, J. C. and Boete, C. (2003), 'A model for the coevolution of immunity and immune evasion in vector-borne diseases with implications for the epidemiology of malaria', *Am. Nat.* **161**, 698–707.

Koelle, K., Cobey, S., Grenfell, B. and Pascual, M. (2006), 'Epochal evolution shapes the phylodynamics of interpandemic influenza A (H3N2) in humans', *Science* **314**, 1898–1903.

Lacroix, R., Mukabana, W. R., Gouagna, L. C. and Koella, J. C. (2005), 'Malaria infection increases attractiveness of humans to mosquitoes', *PLOS Biol.* **3**, e298.

Larson, H., Tyrrell, D., Bowker, C., Potter, C. and Schild, G. (1978), 'Immunity to challenge in volunteers vaccinated with an inactivated current or earlier strain of influenza A(H3N2)', *J. Hyg. (Cambridge)* **80**, 243.

Lenhart, S. and Workman, J. T. (2007), *Optimal Control Applied to Biological Models*, Chapman & Hall/CRC, London.

Li, J., Ma, Z., Blythe, S. P. and Castillo-Chavez, C. (2003), 'Coexistence of pathogens in sexually-transmitted disease model', *J. Math. Biol.* **47**, 547–568.

Lin, J., Andreasen, V., Casagrandi, R. and Levin, S. A. (2003), 'Travelling waves in a model of influenza A drift', *J. Theoret. Biol.* **222**, 437–445.

Lin, J., Andreason, V. and Levin, S. A. (1999), 'Dynamics of influenza A drift: the linear three-strain model', *Math. Biosci.* **162**, 33–51.

Looareesuwan, S., White, N. J., Bunnag, D. and et al. (1987), 'High-rate of *Plasmodium vivax* relapse following treatment of *falciparum*-malaria in thailand', *Lancet* **2**, 1052–1055.

Macdonald, G. (1952), 'The analysis of equilibrium in malaria', *Trop. Dis. Bull.* **49**, 813–829.

Macdonald, G. (1957), *The Epidemiology and Control of Malaria*, Oxford University Press.

Maitland, K., Williams, T. N. and Newbold, C. I. (1997), 'Plasmodium vivax and P-falciparum: Biological interactions and the possibility of cross-species immunity', *Parasitology Today* **13**, 227–231.

Martcheva, M., Bolker, B. M. and Holt, R. D. (2008), 'Vaccine-induced pathogen strain replacement: what are the mechanisms?', *Proc. R. Soc. Interface* **5**, 3–13.

May, R. M. and Nowak, M. A. (1995), 'Coinfection and the evolution of parasite virulence', *Proc. R. Soc. Lond. B* **261**, 209–215.

Mendis, K., Sina, B. J., Marchesini, P. and Carter, R. (2001), 'The neglected burden of *Plasmodium vivax* malaria', *Am. J. Trop. Med. Hyg.* **64**, 97–106.

Mosquera, J. and Adler, F. R. (1998), 'Evolution of virulence: a unified framework for coinfection and superinfection', *J. Theor. Biol.* **195**, 293–313.

Mota, M. M., Hafalla, J. C. and Rodriguez, A. (2002), 'Migration through host cells activates *Plasmodium* sporozoites for infection', *Nat. Med.* **8**, 1318–1322.

Muir, D. (1988), Anopheline mosquitoes: vector-reproduction, life cycle and biotope, *in* W. Wernsdorfer and I. McGregor, eds, 'Malaria: Principles and Practice of Malariology', Churchill Livingstone, pp. 431–451.

Mukabana, W. R., Takken, W., Killeen, G. I. and Knols, B. G. J. (2004), 'Allomonal effect of breath contributes to differential attractiveness of humans to the African malaria vector *Anopheles gambiae*', *Malaria J.* **3**, 1–8.

Murray, J. D. (1993), *Mathematical Biology*, Springer.

Nelson, M. I. and Holmes, E. C. (2007), 'The evolution of epidemic influenza', *Nat Rev Genet* **8**, 196–205.

Ngwa, G. A. (2004), 'Modelling the dynamics of endemic malaria in growing population', *Discrete Contin. Dyn. Syst. Ser. B* **4**, 1173–1202.

Nowak, M. A. and May, R. M. (1994), 'Superinfection and the evolution of parasite virulence', *Proc. R. Soc. Lond. B* **255**, 81–89.

Nuno, M., Chowell, G., Wang, X. and Castillo-Chavez, C. (2007), 'On the role of cross-immunity and vaccines on the survival of less fit flu-strains', *Theoret. Popul. Biol.* **71**, 20–29.

Nuno, M., Feng, Z., Martcheva, M. and Castillo-Chavez, C. (2005), 'Dynamics of two-strain influenza with isolation and partial cross-immunity', *SIAM J. Appl. Math.* **65**, 964–982.

Okello, P. E., Bortel, W. V., Byaruhanga, A. M., Correwyn, A., Roelants, P., Talisuna, A., D'Alessandro, U. and Coosemans, M. (2006), 'Variation in malaria transmission intensity in seven sites throughout Uganda', *Am. J. Trop. Med. Hyg.* **75**, 219–225.

Ord, R. L., Tami, A. and Sutherland, C. J. (2008), 'Ama1 genes of sympatric *Plasmodium vivax* and *P. falciparum* from Venezuela differ significantly in genetic diversity and recombination frequency', *PLOS One* **3**, e3366.

Palese, P. and Young, J. F. (1982), 'Variation of influenza A, B, and C viruses', *Science* **215**, 1486–1474.

Pascual, M., Ahumada, J. A., Chaves, L. F., Rodo, X. and Bouma, M. (2006), 'Malaria resurgence in the East African highlands: temperature trends revisited', *PNAS* **103**, 58295834.

Pates, H. V., Takken, W., Curtis, C. F. and Huisman, P. W. (2005), 'Mosquito behaviour and vector control', *Annu. Rev. Entomol.* **50**, 53–70.

Patz, J. A. and Olson, S. H. (2006), 'Malaria risk and temperature: Influences from global climate change and local land use practices', *PNAS* **103**, 56355636.

Pease, C. (1987), 'An evolutionary epidemiological mechanism, with applications to type A influenza', *Theoret. Populat. Biol* **31**, 422–452.

Plotkin, J. B., Dushoff, J. and Levin, S. A. (2002), 'Hemagglutinin sequence clusters and the antigenic evolution of ifluenza A virus', *Proc. Nat. Acad. Sci USA* **99**, 6263–6268.

Pongsumpun, P. and Tang, I. M. (2007), 'Transmission model for plasmodium vivax malaria', *Ele. Com. Eng.* pp. 276–281.

Pontryagin, L. S., Boltyanskii, V. G., Gamkrelidze, R. V. and Mishchenko, E. F. (1962), *The Mathematical Theory of Opimal Processes*, Wiley, New York.

Potter, C., Jennings, R., Nicholson, K., Tyrrel, D. and Dickinson, K. (1977), 'Immunity to attenuated influenza virus WRL 105 infection induced by hetrologous inactivated influenza A virus vaccines', *J. Hyg. (Cambridge)* **79**, 321–332.

Povelones, M., Waterhouse, R. M., Kafatos, F. C. and Christophides, G. K. (2009), 'Leucine-rich repeat protein complex activates mosquito complement in defense against *Plasmodium* parasites', *Science* **324**, 258–261.

Raimundo, S. M., Yang, H. M. and Engel, A. B. (2007), 'Modelling the effects of temporary immune protection and vaccination against infectious dieases', *Appl. Math. Comput.* **189**, 1723–1736.

Recker, M. and Gupta, S. (2005), 'A model for pathogen population structure with cross-protection depending on the extent of overlap in antigenic variant repertoires', *J. Theoreti. Biol.* **232**, 363–373.

Reisinger, K., Greene, G., Aultman, R., Sander, B. and Gyldmark, M. (2004), 'Effect of influenza treatment with Oseltamivir on health outcome and costs in otherwise healthy children', *Clin. Drug Invest.* pp. 395–407.

Restif, O. and Grenfell, B. T. (2006*a*), 'Integrating life history and cross-immunity into the evolutionary dynamics of pathogens', *Proc. R. Soc. B* **273**, 409–416.

Restif, O. and Grenfell, B. T. (2006*b*), 'Vaccination and the dynamics of immune evasion', *Proc. R. Soc. Interface* **4**, 143–153.

Rosenberg, R., Wirtz, R. A., Schneider, I. and Burge, R. (1990), 'An estimation of the number of malaria sporozoites ejected by a feeding mosquito', *Trans. R. Soc. Trop. Med. Hyg.* **84**, 209–212.

Ross, R. (1911), *The Prevention of Malaria*, John Murray.

Ross, R. (1916), 'An application of the theory of probabilities to the study of a priori pathometry', *Proc. R. Soc. Lond. A* **92**, 204–230.

Ruan, S., Wang, W. and Levin, S. A. (2006), 'The effect of global travel on the spread of SARS', *Math. Biosci. Eng.* **3**, 205–218.

Ruan, S., Xiao, D. and Beier, J. C. (2008), 'On the delayed Ross-Macdonald model for malaria transmission', *Bull. Math. Biol.* **70**, 1098–1114.

Saldana, J., Elena, S. F. and Sole, R. V. (2003), 'Coinfection and superinfection in RNA virus populations: a selection-mutation model', *Math. Biosci.* **183**, 135–160.

Sani, A. and Kroese, D. P. (2008), 'Controlling the number of HIV infectives in a mobile population', *Math. Biosci.* **213**, 103–112.

Sato, S., Suzuki, K., Akahane, Y., Akiyama, K., Yunomura, K., Tsuda, F., Tanaka, T., Okamoto, H., Miyakawa, Y. and Mayumi, M. (1995), 'Hepatitis B virus strains with mutations in the core promoter in patients with fulminant hepatitis', *Ann. Internal Medicine* **122**, 241–248.

Scott, T. W., Takken, W., Knols, B. G. J. and Boete, C. (2002), 'The ecology of genetically modified mosquitoes', *Science* **298**, 117–119.

Scuffham, P. A. and West, P. A. (2002), 'Economic evaluation of strategies for the control and management of influenza in Europe', *Vaccine* **20**, 2562–2578.

Skinner, W., Tong, H., Pearson, T., Strauss, W. and Maibach, H. (1965), 'Human sweat components attractive to mosquitoes', *Nature* **207**, 661–662.

Smith, D. J., Lapedes, A. S., de Jong, J. C., Bestebroer, T. M., Rimmelzwaan, G. F., Osterhaus, A. D. M. E. and Fouchier, R. A. M. (2004), 'Mapping the antigenic and genetic evolution of influenza virus', *Science* **305**, 371–376.

Smith, D. L., Dushoff, J., Snow, R. W. and Hay, S. I. (2005), 'The entomological inoculation rate and *Plasmodium falciparum* infection in African children', *Nature* **438**, 493–495.

Smith, G. J., Vijaykrishna, D., Bahl, J., Lycett, S. J., Worobey, M., Pybus, O. G., Ma, S. K., Cheung, C. L., Raghwani, J., Bhatt, S., Peiris, J. S., Guan, Y. and Rambaut, A. (2009), 'Origins and evolutionary genomics of the 2009 swine-origin H1N1 influenza A epidemic', *Nature* **459**, 1122–1125.

Snounou, G. and White, N. J. (2004), 'The coexistence of plasmodium: sidelights from *falciparum* and *vivax* malaria in Thailand', *Trends Parasitol.* **20**, 333–339.

Snow, R. W., Guerra, C. A., Noor, A. M., Myint, H. Y. and Hay, S. I. (2005), 'The global distribution of clinical episodes of *Plasmodium falciparum* malaria', *Nature* **434**, 214–217.

Sonoguchi, T., Naito, H., Hara, M., Takeuchi, Y. and Fukumi, H. (1985), 'Cross-subtype protection in humans during sequential, overlapping and/or concurrent epidemics caused by H3N2 and H1N1 influenza viruses', *J. Infect. Dis.* **151**, 81–88.

Supriatna, A. K., Soewono, E. and van Gils, S. A. (2008), 'A two-age-classes dengue transmission model', *Math. Biosci.* **216**, 114–121.

Syafruddin, D., Krisin, abd Sekartuti, P. A., Dewi, R. M., Coutrier, F., Rozy, I. E., Susanti, A. I., Elyazar, I. R. F., Sutamihardja, A., Rahmat, A., Kinzer, M. and Rogers, W. O. (2009), 'Seasonal prevalence of malaria in West Sumba district, Indonesia', *Malar. J.* **8**, 8.

Takken, W. and Knols, B. G. J. (1999), 'Odor-mediated behaviour of Afrotropical malaria mosquitoes', *Annu. Rev. Entomol.* **44**, 131–157.

Takken, W. and Knols, B. G. J. (2005), 'Malaria vector control: current and future strategies', *Trends Parasitol.* **25**, 101–104.

van den Driessche, P. and Watmough, J. (2002), 'Reproduction numbers and sub-threshold endemic equilibria for compartmental models of disease transmission', *Math. Biosci.* **285**, 29–48.

Weber, C., Boursaux-Eude, C., Coralie, G., Caro, V. and Guiso, N. (2001), 'Polymorphism of *Bordetella pertussis* isolates circulating for the last 10 years in France, where a single effective whole-cell vaccine has been used for more than 30 years', *J. Clin. Microbiol.* pp. 4396–4403.

Webster, R., Bean, W., Gorman, O., Chambers, T. and Kawaoka, Y. (1992), 'Evolution and ecology of influenza A viruses', *Microbiol. Rev.* **56**, 152–179.

Webster, R. G. (1998), 'Influenza: An emerging disease', *Emerg. Infec. Dis.* **4**, 436–441.

Wei, H. M., Li, X. Z. and Martcheva, M. (2008), 'An epidemic model of a vector-borne disease with direct transmission and time delay', *J. Math. Anal. Appl.* **342**, 895–908.

White, N. J. (2008), '*Plasmodium knowlesi*: The fifth human malaria parasite', *Clin. Infect. Dis* **46**, 172–173.

William, T. N., Maitland, K., Bennett, S., Ganczakowski, M., Peto, T. E., Newbold, C. I., Bowden, D. K., Weatherall, D. J. and Clegg, J. B. (1996), 'Cross-species immunity (High incidence of malaria in alpha-thalassaemic children)', *Nature* **383**, 522–525.

Yamauchi, L. M., Coppi, A., Snounou, G. and Sinnis, P. (2007), 'Plasmodium sporozoites trickle out the injection site', *Cell. Microbiol.* **9**, 1215–1222.

Yang, H. M. (2000), 'Malaria transmission model for different levels of acquired immunity and temperature dependent parameter (vector)', *J. Public Health* **34**, 223–231.

Yang, H. M. and Ferreira, C. P. (2008), 'Assessing the effects of vector control on dengue transmission', *Appl. Math. Comput.* **198**, 401–413.